REMOTE SENSING APPLICATIONS TO CLIMATE RISKS MANAGEMENT IN FOREST CONSERVATION

DOCTORAL THESIS 2023

SUPERVISORS: ANTONIO FLORES MOYA, ÁNGEL ENRIQUE SALVO TIERRA Y JOSE ANTONIO CARREIRA DE LA FUENTE

ÁLVARO CORTÉS MOLINO

FACULTY OF SCIENCES - PHD PROGRAM OF BIOLOGICAL DIVERSITY AND ENVIRONMENT
DEPARTMENT OF BOTANY AND PLANT PHYSIOLOGY - UNIVERSITY OF MALAGA

2023

ÁLVARO CORTÉS MOLINO

TESIS DOCTORAL

DECLARACIÓN DE AUTORÍA Y ORIGINALIDAD DE LA TESIS PRESENTADA PARA OBTENER EL TÍTULO DE DOCTOR

D./Dña Álvaro Cortés Molino
Estudiante del programa de doctorado Diversidad biológica y medio ambiente de la Universidad de Málaga, autor/a de la tesis, presentada para la obtención del título de doctor por la Universidad de Málaga, titulada:
Remote sensing applications to climate risks management
Realizada bajo la tutorización de y dirección de (si tuviera varios directores deberá hacer constar el nombre de todos)
Antonio Flores Moya, Enrique Salvo Tierra y Jose Antonio Carreira de la Fuente

DECLARO QUE:

La tesis presentada es una obra original que no infringe los derechos de propiedad intelectual ni los derechos de propiedad industrial u otros, conforme al ordenamiento jurídico vigente (Real Decreto Legislativo 1/1996, de 12 de abril, por el que se aprueba el texto refundido de la Ley de Propiedad Intelectual, regularizando, aclarando y armonizando las disposiciones legales vigentes sobre la materia), modificado por la Ley 2/2019, de 1 de marzo.

Igualmente asumo, ante a la Universidad de Málaga y ante cualquier otra instancia, la responsabilidad que pudiera derivarse en caso de plagio de contenidos en la tesis presentada, conforme al ordenamiento jurídico vigente.

En Málaga, a de de

UNIVERSIDAD
DE MÁLAGA

Autor: Álvaro Cortés Molino

https://orcid.org/0000-0001-5350-9028

EDITA: Publicaciones y Divulgación Científica. Universidad de Málaga
Portada e ilustraciones: Jaime de la Torre Naharro

UNIVERSIDAD DE MÁLAGA

FACULTAD DE CIENCIAS

DEPARTAMENTO DE BOTÁNICA Y FISIOLOGÍA VEGETAL

Área de Botánica

Remote sensing applications to climate risks management in forest conservation

Memoria presentada para optar al grado de Doctor por la Universidad de Málaga

por Álvaro Cortés Molino

Dirigida por A. Enrique Salvo Tierra, y José A. Carreira de la Fuente
Tutorizada por Antonio Flores Moya

UNIVERSIDAD DE MÁLAGA

FACULTAD DE CIENCIAS

DEPARTAMENTO DE BOTÁNICA Y FISIOLOGÍA VEGETAL

Área de Botánica

Visado en Málaga a 14 de junio de 2023

Los directores

Fdo. Á. Enrique Salvo Tierra
Profesor titular del Área de Botánica.
Universidad de Málaga

Fdo. José A. Carreira de la Fuente
Profesor titular del Área de Ecología
Universidad de Jaén

El tutor
Fdo. Antonio Flores Moya
Catedrático del Área de Botánica
Universidad de Málaga

Memoria presentada para optar al Grado de Doctor por la Universidad de Málaga

UNIVERSIDAD DE MÁLAGA

FACULTAD DE CIENCIAS

DEPARTAMENTO DE BOTÁNICA Y FISIOLOGÍA VEGETAL

Área de Botánica

D. Á. Enrique Salvo Tierra, Profesor Titular del Departamento de Botánica y Fisiología Vegetal (Área Botánica) de la Universidad de Málaga, D. José A. Carreira de la Fuente, Profesor Titular del Departamento de Biología Animal, Biología Vegetal y Ecología (Área Ecología) de la Universidad de Jaén, y D. Antonio Flores Moya Catedrático del Departamento de Botánica y Fisiología Vegetal (Área Botánica) de la Universidad de Málaga

CERTIFICAN:

Que la presente memoria titulada "**Remote sensing applications to climate risks management in forest conservation**" presentada por el Licenciado en Ciencias Ambientales, Álvaro Cortés Molino, ha sido realizada bajo nuestra dirección y tutorización, y que el trabajo presentado y las publicaciones que lo avalan no han sido utilizadas en tesis anteriores. Y considerando que representa el trabajo de Tesis Doctoral, autorizamos su exposición y defensa para optar al Grado de Doctor por la Universidad de Málaga.

Y para que así conste, a los efectos oportunos, firma el presente en Málaga 14 de junio de 2023

Fdo. Á. Enrique Salvo Tierra
Profesor Titular del Área de Botánica
Universidad de Málaga

Fdo. José A. Carreira de la Fuente
Profesor Titular del Área de Ecología
Universidad de Jaén

Fdo. Antonio Flores Moya
Catedrático del Área de Botánica
Universidad de Málaga

"*You may be able to fool the voters, but not the atmosphere.*"

— Donella Meadows

Financial support

This PhD Project has been financially supported by the following institutions and projects:

- Project: 'Urban green spaces management with Unmanned Aerial Vehicles (UAV)' Andalusian Technological Corporation (2018-2020).

- Project: 'Modulating role of LITHOlogy in the response of Mediterranean FORest ecosystems to climate change: tree growth, soil processes and future projections (LITHOFOR)'. Project code: RTI2018-095345-B-C21. Funding: Spanish Ministry of Science, Innovation and Universities; State Program for R+D+i Oriented to the Challenges of Society (2021-2022).

- Grant for the achievement of international mention in doctoral thesis by University of Málaga (2022).

- The study of Chapter 2 was financially supported by the Deutsche Forschungsgemeinschaft (DFG; CRC990, Sub-project A02).

This work has been developed in:

- The Research Group of Biodiversity, Conservation, and Natural Resources (P.A.I. RNM-115, Junta de Andalucía), of the Department of Botany and Plant Physiology of the University of Málaga.
- The Research Group of Forest Ecology and Landscape Dynamics (P.A.I. RNM-296, Junta de Andalucía), of the Department of Animal Biology, Vegetal Biology and Ecology of the University of Jaén.
- Tropical Silviculture and Forest Ecology, University of Göttingen, Germany.

Resumen

La presente tesis doctoral tiene como objetivo desarrollar diferentes estudios en los que se aplican diferentes técnicas de teledetección para explorar las potencialidades de este campo dentro de la conservación de sistemas forestales en un contexto de riesgos asociados al cambio climático.

Los tres estudios se desarrollan en dos ecosistemas forestales diferentes. El primero se ubica en la selva de Harapan, en la provincia de Jambi, en Sumatra (Indonesia). Se trata pues, de un área caracterizada por un clima tropical húmedo, con una precipitación media anual que supera los 2000 mm·año^{-1}, una temperatura media anual por encima de 25 ºC y suelos formados por acrisoles. El bosque de Harapan ha experimentado un periodo importante de talas y extracción de madera que ha dado lugar a una gran deforestación en la mayor parte del territorio, siendo el lugar de estudio un reducto de selva existente gracias al hecho de ser un espacio natural protegido de administración gubernamental. El origen de la deforestación ha sido principalmente cambio de usos del suelo, de forestal a agrícola. Así, el bosque de Harapan actualmente cuenta con alrededor de 45000 ha y se encuentra rodeado de explotaciones de aceite de palma y cultivos de caucho.

Por otro lado, los capítulos 3 y 4 tienen lugar en la población de *Abies pinsapo* Boiss. más extensa existente, localizada en el municipio de Yunquera (Málaga, España) y formando parte del Parque Nacional Sierra de las Nieves. Este bosque se caracteriza por abarcar un rango altitudinal de 800-1550 m.s.n.m. Las precipitaciones anuales se distribuyen entre los meses de octubre y mayo en torno a 1500 mm·año^{-1}, seguido de un periodo estival seco. La temperatura media anual es de 14.7 ºC. La especie predominante es *Abies pinsapo*, un abeto relicto procedente del terciario que actualmente se distribuye principalmente en las Sierras de Grazalema (Cádiz), Bermeja (Málaga), Sierra de las Nieves (Málaga). El pinsapo se encuentra estrechamente emparentado con otros abetos circunmediterráneos como *A. marocana* Trab., *A. numidica* de Lannoy ex Carrière o *A. cephalonica* Loud. Durante la década de 1960 se tomaron medidas de protección para la regeneración de esta población de *A. pinsapo* en Yunquera, tras un periodo de uso intensivo del territorio que se tradujo en una elevada carga ganadera y cortas sin regulación. Actualmente la masa se ha recuperado notablemente, regenerando en masas principalmente puras. Sin embargo, en el pinsapar de Yunquera, acompañando a *A. pinsapo* también está presente *Pinus halepensis* Mill., de carácter más termófilo, formando en ocasiones masas mixtas junto a otras pertenecientes al género *Quercus* sp. y *Juniperus* sp. Sin embargo, en las últimas décadas se ha evidenciado síntomas de estancamiento de la masa y un aumento de fenómenos de mortalidad asociado a eventos de sequía.

Ambos ecosistemas forestales, pese a pertenecer a regiones climáticamente distantes –tropical húmedo en Sumatra y mesomediterráneo en la Península Ibérica– tienen elementos comunes que son de interés a destacar. En primer lugar, se caracterizan por una elevada presión antrópica en el pasado que conllevó usos intensivos del territorio en ambos casos; ya sea para la conversión de tierras y desaparición del bosque o la sobreexplotación desregulada de los recursos agroforestales. En segundo lugar, ambos ecosistemas son de un alto grado de interés ecológico y conservacionista. En el caso del bosque de Harapan, se trata de un núcleo que concentra todo un *hotspot* de biodiversidad, siendo el hábitat de más de 300 especies de aves y especies en peligro crítico como *Panthera tigris sumatrae* Pocock o *Elephas maximus sumatranus* Temminck. Mientras que en el caso del pinsapar de Yunquera, se trata de la población más grande existente de esta especie endémica, un abeto relicto procedente del terciario y circunscrito a pequeñas poblaciones amenazadas. La pluvisilva tropical permite estudiar en detalle variables bioclimáticas de interés en gestión de riesgos como es la evapotranspiración. La evapotranspiración en bosques tropicales supone una importante contribución al clima global y a la cantidad de precipictaciones que tienen lugar a nivel global. Modelizando, por tanto, el funcionamiento de la evapotranspiración a escala de detalle en este tipo de ecosistemas permite generar conocimiento que puede ser aplicado en bosques de otras regiones climáticas. Conocimiento que será de especial interés para monitorizar el consumo de agua del dosel forestal en un escenario de aumento de riesgos climáticos tales como la sequía.

La conservación de estos ecosistemas requiere de ofrecer oportunidades y garantías a la población que vive en ellos, además de aplicar todo el conocimiento científico-tecnológico disponible. En este sentido, el auge de tecnologías de captura de información masiva del territorio supone multiplicar la cantidad de datos disponible bajo demanda. De esta manera, es posible obtener información sobre las características del terreno, registros climáticos, fisiológicos o datos de estructura de la vegetación a muy alta resolución y cada vez a un menor coste en tiempo y recursos. Dentro de estas tecnologías, podemos diferenciar principalmente dos tipos: aquellas basadas en sensores fijos en el territorio y que permiten obtener información en tiempo real. Un ejemplo son los sensores de flujo de savia para monitorizar la actividad hidráulica a escala de árbol en masas forestales, o también estaciones meteorológicas para registrar la evolución de variables como la humedad, temperatura, viento, radiación o evapotranspiración para estudiar condiciones microclimáticas bajo el dosel forestal. El otro grupo de tecnologías corresponden a toma de información por parte de sensores diseñados para estar a bordo de dispositivos móviles aéreos —satélites, aviones, drones— o terrestres. El primer grupo es conocido como detección próxima y se ve beneficiada del auge de nuevas tendencias como el internet de las cosas (IoT) al poder tomar y procesar datos en tiempo real, abriendo la puerta a automatizaciones en la agricultura y selvicultura. El uso de sensores sobre

plataformas móviles corresponde a la disciplina conocida como teledetección, puesto que implica la captura de información a cierta distancia de la superficie vegetal.

Ambas tecnologías pueden integrarse, existiendo un gran potencial de sinergias que faciliten la toma de decisiones en la gestión del territorio. Sin embargo, esta tesis doctoral se centra en el empleo de diferentes técnicas de teledetección para la obtención y procesamiento de información de los dos ecosistemas descritos. La razón es sencilla: mientras que las tecnologías IoT aún están explorando todo su potencial para su aplicación en gestión y conservación forestal, la teledetección es una disciplina lo suficientemente desarrollada como para ser implementada y apoyar proyectos de estudio, conservación y gestión ambiental a un coste asequible. Si bien la literatura científica es abundante en cuanto a las aplicaciones de la teledetección en gestión forestal, existe la necesidad de mayor número de estudios que hilen desde una perspectiva multi-enfoque cómo la teledetección puede ser empleada en la gestión forestal adaptativa en un contexto de cambio climático. Una perspectiva que integre de manera conjunta, y no sectorial, los principales riesgos asociados al cambio climático y que amenazan los bosques del planeta: sequías, incendios y cómo pueden interactuar entre sí ambos riesgos.

De esta manera, los objetivos de esta tesis doctoral pasan por el desarrollo de tres estudios que pretenden profundizar en una aplicación multienfoque de la teledetección a la gestión de riesgos climáticos en conservación forestal mediante: (i) La modelización de la evapotranspiración de un dosel forestal; (ii) La monitorización de los efectos provocados por eventos de sequía y brotes de plagas; y (iii) La simulación del riesgo de incendio asociado a dinámicas de mortalidad y recuperación forestal.

El **capítulo 1** consiste en una introducción que describe el contexto en el cual se desarrolla tesis doctoral. El primer apartado hace un resumen de los fundamentos ecológicos que implican las principales perturbaciones en sistemas forestales. Comienza con una breve revisión crítica de las diferentes teorías que pretenden explicar el funcionamiento de la dinámica de ecosistemas forestales. Se destaca la importancia de las perturbaciones de intensidad baja o media en los ecosistemas y cómo la teoría clásica ha obviado o infravalorado la relevancia de estos fenómenos a favor de una perspectiva más determinista. A continuación, se realiza una revisión de las diferentes perturbaciones asociadas a riesgos climáticos, empezando por los eventos de sequía. Se mencionan las variadas estrategias de los árboles para hacer frente a la escasez de agua y se detallan los impactos que produce la sequía en los principales bosques del planeta. También se desarrolla brevemente el impacto provocado por brotes de plagas forestales y la influencia que las oscilaciones climáticas pudieran tener en esta perturbación. Además, hay un apartado que detalla los efectos del fuego en los

ecosistemas forestales, analizando en qué consiste el riesgo de incendio y la existencia de mecanismos ecológicos de respuesta al fuego para garantizar la supervivencia de las especies vegetales. El segundo apartado de este capítulo hace repaso por las diferentes técnicas que pueden aplicarse para una gestión forestal adaptativa en un contexto de cambio climático. Se resumen las estrategias de gestión para promover una respuesta resiliente de los bosques frente al riesgo de sequías e incendios; además de algunos métodos para minimizar la intensidad de estos fenómenos. Finalmente, se profundiza en cómo la teledetección puede servir de apoyo a esta gestión forestal adaptativa. Se detallan las diferentes tecnologías existentes y sus aplicaciones, desde los diferentes sensores (fotogramétricos, multiespectrales, LIDAR, etc.). hasta las plataformas empleadas (drones, satélites, vehículos, etc.). Por último, hay un epígrafe sobre evaluación de riesgos y otro en el que se establecen los objetivos de la tesis.

El **capítulo 2** se corresponde al primer estudio: "*Combining UAV thermography, point cloud analysis and machine learning for assessing small-scale evapotranspiration patterns in a tropical rainforest*". El propósito de este trabajo es contribuir al entendimiento de los factores que pueden influir en la evapotranspiración (ET) en un dosel forestal tropical a escala de píxel con datos de muy alta resolución (10 cm) procedentes de sensores fotogramétrico y termográfico embarcados en un vehículo aéreo no tripulado (UAV). Concretamente, se usaron datos fotogramétricos para modelizar la ET con el objeto de poder analizar si las microvariaciones procedentes de datos RGB del dosel pueden explicar la varianza de la ET. Los vuelos se realizaron a lo largo de cuatro parcelas de 50 x 50 m en el bosque tropical de Harapan durante una campaña de muestreo en agosto de 2017. Con las imágenes térmicas se generaron mapas de evapotranspiración, procesándolas con datos de temperatura y radiación para cada una de las parcelas mediante el modelo DATTUTDUT. Mientras que con las imágenes fotogramétricas se aplicaron las técnicas Structure from Motion (SfM) para dar lugar a ortoimágenes RGB y nubes de puntos 3D del dosel forestal. Con los datos fotogramétricos se obtuvieron un total de 16 variables a escala de píxel. Posteriormente, se empleó un procedimiento de aprendizaje automático con el total de variables obtenidas consistente, en primer lugar, en una técnica de selección de variables conocida como Forward Feature Selection (FFS) que tiene en cuenta la autocorrelación espacial y el riesgo de sobreajuste de los modelos. En segundo lugar, se realizaron modelos de correlación con la técnica Random Forest (RF). Todo este proceso se hizo para cada parcela y en cada paso se empleó la validación cruzada de tipo "dejando uno fuera" (LLO-CV). Los resultados de este estudio arrojaron una alta variabilidad espacial de la ET, e indicaron que las variables relacionadas con la altura y la estructura del dosel, estudiadas inicialmente, no fueron capaces de explicar de forma individual dicha variabilidad de la ET ($R^2 <$ 0.01). Sin embargo, el procedimiento de aprendizaje automático empleado dio lugar de nueve a

diez variables seleccionadas y los modelos RF resultaron en un RMSE entre 0.04 y 0.09 $mm \cdot h^{-1}$ y un R^2 que varía entre 0.56-0.65. No obstante, no se observó que ninguna variable estuviese presente en el 100% de los modelos de todas las parcelas. Además, la importancia de cada variable en la modelización de cada parcela no era constante, cambiando incluso la presencia o ausencia de alguna de ellas. Las conclusiones que se extrae de este estudio son: (i) Existe una gran variabilidad espacial de la transpiración a escala de píxel; (ii) los atributos del dosel forestal siguen teniendo capacidad de influir en la ET a muy pequeña escala; (iii) Las relaciones observadas entre la ET y las variables predictoras son de carácter no lineal y, además, no existe ningún predictor que predomine claramente sobre las demás; y por tanto (iv) la ET no se ve directamente influenciada por ninguno de los predictores utilizados de forma individual, si no a través de una compleja interrelación entre un conjunto de ellos.

El **capítulo 3** se corresponde con el segundo estudio: "*Unexpected resilience in relict* Abies pinsapo *Boiss. Forests to dieback and mortality induced by climate change*". El propósito de este trabajo fue realizar un estudio multitemporal sobre el bosque de pinsapos de Yunquera (Málaga, España) con el objeto de evaluar la resiliencia en esta población (capacidad adaptativa; respuesta post-mortalidad) tras los efectos de eventos de sequía que se evidenciaron en estudios anteriores en forma de fenómenos de decaimiento forestal en dicha masa. Para ello se emplearon datos procedentes de satélites, ortoimágenes y muestreos de campo para analizar la evolución del decaimiento del pinsapar en los últimos 36 años (1985-2020). El muestreo de campo se llevó a cabo a lo largo de treinta y una parcelas en 2003 y 2020 para caracterizar cambios en la estructura de la masa a lo largo de tres rangos altitudinales: bajo (880-1150 m.s.n.m.), medio (1150-1350 m) y alto (1350-1550 m). En este muestreo se tomaron datos de diámetro a la altura del pecho (DBH), área basal y se clasificaron los individuos en base a su estado de decaimiento. Por otro lado, se emplearon imágenes de satélite Landsat 5 y 7 para calcular el índice NDVI al final del periodo estival y realizar un análisis factorial dinámico (DFA) para detectar tendencias comunes en las series temporales a lo largo de los rangos altitudinales y un gradiente de incidencia solar topográfica (SI). También se realizaron modelos lineales mixtos (LMEM) para modelizar el comportamiento del NDVI con relación a variables climáticas como temperatura y radiación en diferentes estaciones, además del Índice Estandarizado de Precipitación y Evapotranspiración (SPEI). Cambios históricos en la cobertura forestal asociada al pinsapo fueron analizados a través de la clasificación de ortoimágenes procedentes del Plan Nacional de Ortofotografía Aérea (PNOA). Los resultados de este trabajo contrastan con las evidencias en estudios previos en los que se constata un proceso de decaimiento y mortalidad de la masa forestal, puesto que durante 17 años no ha habido cambios en las proporciones de áreas basales correspondientes a las diferentes clases de decaimiento; así como se ha

experimentado un aumento consistente de la actividad fotosintética estimada con el NDVI desde mitad de la década de los 2000; además de un incremento de la cobertura forestal asociada al pinsapar en las bandas altitudinales medias y altas. En consecuencia, en este estudio se proveen suficientes evidencias para concluir que los bosques de *A. pinsapo* están mostrando una resiliencia a los eventos de decaimiento y mortalidad inducidos por el cambio climático mayor de la esperada, que contradice las proyecciones de extinciones locales y cambios altitudinales que arrojaban los modelos predictivos desarrollados en estudios anteriores. Esta inesperada resiliencia podría explicarse por el concurso de mecanismos de compensación tales como: (i) un efecto de liberación del crecimiento de los pinsapos supervivientes a los eventos de mortalidad por sequía, que entonces pueden prosperar con menos competencia por los recursos, (ii) el reclutamiento exitoso de nuevos individuos de pinsapo a partir de los adultos supervivientes, y (iii) efectos de facilitación mediados por la revegetación, con otras especies más heliófilas propias del bosque y sotobosque mediterráneo, de los huecos de mortalidad de pinsapo de mayor superficie, que favorecerían el establecimiento en los mismos del nuevo reclutado de pinsapo, muy tolerante a la sombra.

El **capítulo 4** se corresponde con el tercer estudio: "*Using ForeStereo and LIDAR data to assess fire and canopy structure-related risks in relict* Abies pinsapo *Boiss. forests*". El propósito de este trabajo fue el de combinar el uso de LIDAR aéreo e imágenes hemisféricas obtenidas con ForeStereo —un dispositivo de inventario forestal— para evaluar tanto el riesgo de incendio en el pinsapar de Yunquera como la variabilidad espacial de la estructura del dosel forestal. Se establecieron 49 parcelas de muestreo a lo largo del área de estudio. Las variables estructurales de la masa (altura, DBH, estructura de copa, densidad, área basal, etc.) se calcularon con las imágenes hemisféricas obtenidas con ForeStereo. Estos datos fueron empleados para calcular modelos de regresión con datos de LIDAR aéreo (0.5 puntos·m^{-2}). Posteriormente, las parcelas fueron ajustadas a seis modelos de combustible, basados en el criterio de clasificación UCO40, y el total del área de estudio se clasificó con el algoritmo Nearest Neighbor sobre imágenes de satélite Sentinel con una precisión de 0.56. Posteriormente, el software FlamMap se empleó para simular escenarios de fuego basados en modelos de combustible, estructura de la masa y datos derivados del relieve topográfico. Además, se analizó la estructura del dosel con el objeto de detectar el estatus de la masa y vulnerabilidades asociadas. Los resultados mostraron un bosque de crecimiento secundario que tiene una creciente presencia de modelos de combustible con potencial para una alta tasa de propagación del fuego (50 m·min^{-1}), además de una alta cobertura forestal (CC > 80% en casi un 25% del territorio) y una alta densidad de copa (> 0.1 kg·m^{-3} en > 60% del territorio). Las conclusiones de este trabajo señalan: (i) un alto riesgo de propagación de incendio, con modelos de combustible que agravarían la severidad del fuego; (ii) este riesgo de incendio es promovido por el sobrecrecimiento de matorral

denso en los huecos de mortalidad provocados por el fenómeno de decaimiento que experimenta la masa, que se mezcla con un acúmulo de combustible muerto; (iii) la necesidad de establecer políticas de gestión proactiva que incentiven el control de modelos de combustible que puedan generar peores comportamientos de un hipotético fuego y que promuevan una mejora en la diversidad estructural del pinsapar para contrarrestar el fenómeno de decaimiento.

El **capítulo 5** desarrolla la discusión global y conclusiones generales de la Tesis doctoral. Este trabajo profundizó en la integración de diferentes fuentes de datos de teledetección a través de procedimientos multienfoque que demostraron gran potencial para agilizar y aumentar la precisión en la adquisición e interpretación de información aplicada a la gestión forestal. Los riesgos asociados al cambio climático, tales como la sequía y los incendios, requieren de este tipo de procedimientos multienfoque para dar respuesta a los crecientes desafíos que plantean. Con este propósito, se han desarrollado tres estudios para contribuir al campo de la gestión de riesgos climáticos en la conservación forestal. Cada estudio empleó tecnologías que en conjunto abarcan de forma complementaria las principales ramas de la teledetección. Debido a la gran cantidad de información obtenida se emplearon técnicas de ciencia de datos y aprendizaje automático para los análisis posteriores. Toda la metodología en este trabajo tiene un gran potencial para: (i) Asistir en el diseño e implementación de un régimen de perturbaciones de baja intensidad que permita diversificar y dinamizar los procesos ecológicos; (ii) Apoyar la gestión de riesgos de incendios mediante el cartografiado y la simulación del riesgo para desarrollar estrategias de actuación sobre el combustible; (iii) Monitorizar la evapotranspiración y la actividad fotosintética para realizar un seguimiento de las respuestas del bosque frente a perturbaciones y para diseñar sistemas de alerta temprana frente a fenómenos de sequía y decaimiento.

Abbreviations

AIC	Akaike Information Criterion
AICc	Corrected Akaike Information Criterion
ALS	Aerial Laser Scanning
ANOVA	Analysis of Variance
BAI	Basal Area Index
CC	Canopy Cover
CBD	Canopy Bulk Density
CBH	Canopy Base Height
CHM	Canopy Height Model
Cover10	Canopy cover of a given pixel above 10 m
CRR	Canopy Relief Ratio
CV	Coefficient of Variation
CWSI	Crop Water Stress Index
DATTUTDUT	Deriving Atmosphere Turbulent Transport Useful To Dummies Using Temperature
DBH	Diameter at Breast Height
DEM	Digital Elevation Model
DTM	Digital Terrain Model
DFA	Dynamic Factor Analysis

ESA	European Space Agency
ET	Evapotranspiration
FFS	Forward Feature Selection
G	Basal area
GLI	Green Leaf Area Index
GNDVI	Green Normalized Difference Vegetation Index
GNSS	Global Navigation Satellite System
Height_abs_max	Maximum canopy height
Height_abs_min	Minimum canopy height
Height_abs_sm	Absolute canopy height
Height_rel	Relative canopy height
Ho	Stand height
IoT	Internet of Things
KIA	Kappa Index of Agreement
LAI	Leaf Area Index
LAD	Leaf Area Density
LIDAR	Light Detection And Ranging
LMEM	Linear Mixed Effect Models
LLO-CV	Leave-Location-Out Cross Validation
MMT	Minimum Travel Time

m.a.s.l.	Meters above sea level
NA	No data
NASA	National Aeronautics and Space Administration
NBR	Normalized Burn Ratio index
NDVI	Normalized Difference Vegetation Index
NIR	Near Infrared band
NDRE	Normalized Difference Red Edge index
OBIA	Object-Based Image Analysis
P25	25th percentile
P50	50th percentile
P75	75th percentile
P90	90th percentile
PCD	Point Cloud Density
PET	Potential Evapotranspiration
PNOA	Plan Nacional de Ortofotografía Aérea
Raup	Radiation of prior autumn
RF	Random Forest
RMSE	Root-mean-square error
Rsp	Radiation of spring
Rsu	Radiation of summer

Rwi	Radiation of winter
SAR	Synthetic Aperture Radar
SD	Standard Deviation
SI	Solar Incidence
SfM	Structure from Motion
SLAM	Simultaneous Location and Mapping
SPEI	Standardised Precipitation-Evapotranspiration-Index
Ssp	SPEI of spring
Ssu	SPEI of summer
T	Transpiration
TLS	Terrestrial Laser Scanning
Tsp	Temperature of spring
Tsu	Temperature of summer
UAV	Unmanned Aerial Vehicle
VARI	Visual Atmospheric Resistance Index
VLS	Vehicle Laser Scanning
VTOL	Vertical Take-Off Landing

Contents

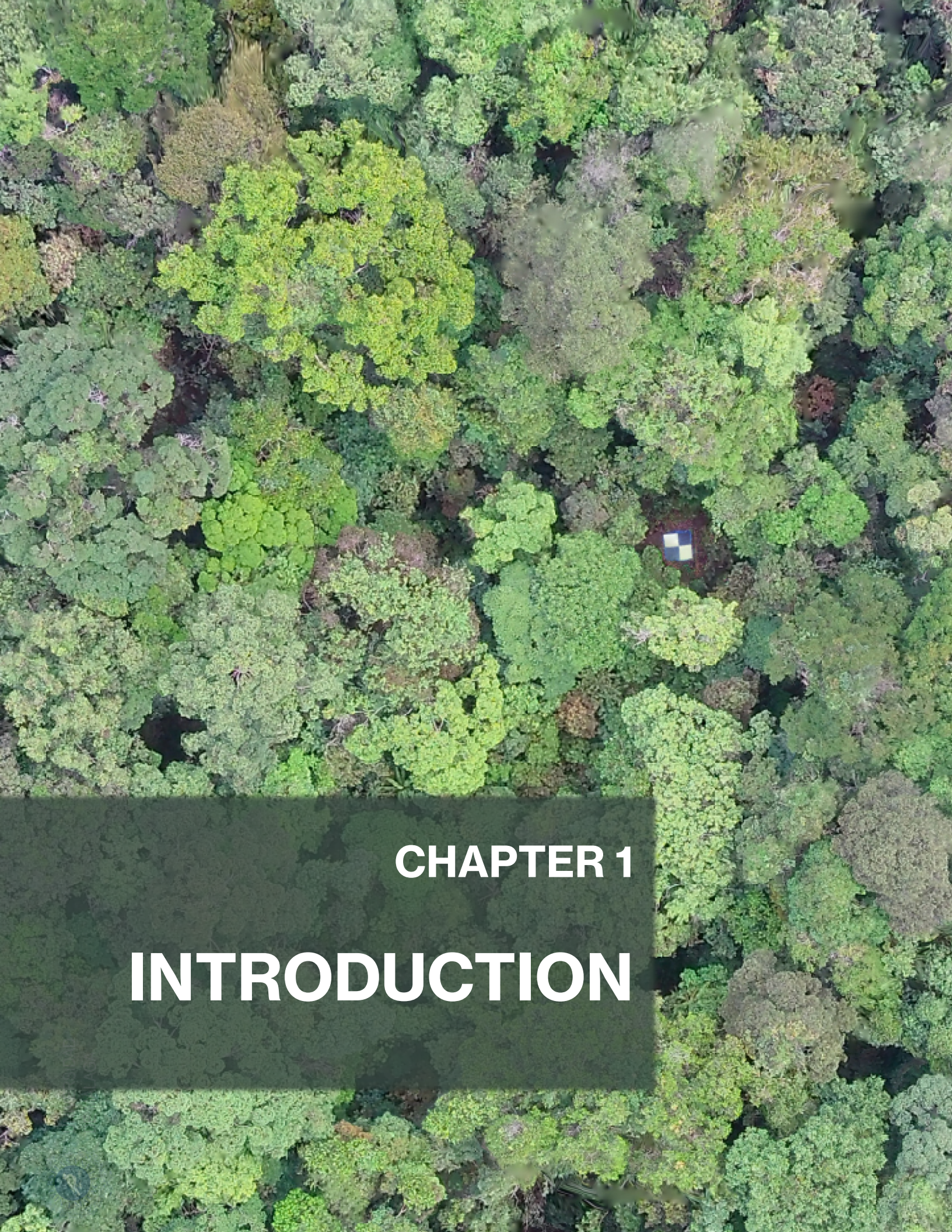

CHAPTER 1

INTRODUCTION

Introduction 1

1.1. Forest ecosystems and climate risks

Fighting climate change is a harsh challenge that involves economic planification policies and all the best science and technology available to be applied. Environmental science is crucial to understand socioeconomic implications and ecosystems impacts due to climate change effects. Environmental scientists should lead the provision of technical solutions and build scientifically and economically feasible paths toward decarbonized societies. Forests are one of the most relevant ecosystems threatened by global change. They are home to almost 25% of the world's population and 80% of world's terrestrial biodiversity (IUCN, 2021). Stopping deforestation and promoting restoration are highly significant components for climate change mitigation. Global forest restoration could add more than 25% of global forest increase with the potential to store an equivalent of 25% of the 2019 atmospheric carbon pool (Bastin *et al.*, 2019).

Dealing with climate change impacts on forests requires an understanding of vegetation dynamics for a science-based forest management. Clements (1916) proposed a model to describe vegetation succession, based on a deterministic final stage termed as 'climax'. This model was further developed by other authors such as Tansley (1935), who proposed the 'polyclimax', the chance for multiple possible climax stages; and Whittaker (1953), who modified the polyclimax concept to hypothesize the 'climax-pattern', based on local environmental gradients. Nevertheless, even with all the revisions that the climax model received, all these authors fell in the idea of a deterministic steady-state community which depends on environmental gradients, obviating other influences (Pickett & McDonnell, 1989). According to Gibson (1996), there are enough reasons to conceive the climax concept as an unrealistic ideal: (i) disturbance is always present in ecosystems, (ii) many plant communities do not keep pace with changes in current weather conditions and climate, and (iii) the time required for some species to dominate ecological communities may be longer than the recurrence interval of a given disturbance. Nowadays, the climax concept is disused in modern ecology and plant science in favor of conceptual models of disturbance-recovery cycles and patch dynamics. Although there is still a significant influence of the climax concept in vegetation management and science (and climax will remain useful in some contexts), alternative theories are increasingly spreading (Gibson, 1996; Gunderson & Holling, 2002; Niering, 1987; Picket & White, 1985; Pickett & McDonnell, 1989; Seidl & Turner, 2022).

If the old paradigm associate disturbance to degradation, modern ecology incorporates the disturbance regime as a relevant driver to understand both unsustainable and sustainable ecosystem dynamics and functionality (Chapin *et al.*, 1991). Low or medium-intensity disturbances release nutrients previously retained in biomass structure, allow switching of dominating species, activate resilience mechanisms against future disturbance events of higher intensity, and foster species composition change during the ecological succession (Franklin *et al.*, 2007; Picket & White, 1985).

Understanding post-disturbance responses, and a clear definition of resilience are key to comprehend forest dynamics and future ecosystem trajectories. In this respect, Seidl & Turner (2022) proposed a conceptual framework, in which they developed four possible reorganization pathways following disturbance (Fig.1.1). They also stated that many forest ecologists focus their studies expecting regime shifts, but this only happens when disturbance reach a threshold or tipping point in which vegetation structure, function and composition is profoundly altered. Focusing only on regime shifts could ignore relevant processes taking place during the post-disturbance reorganization phase. The model proposed by Seidl & Turner (2022) is based on the 'panarchy' theory stated by Gunderson & Holling (2002), with special attention on the reorganization phase.

In forest systems, natural disturbances are commonly forest fires, pests outbreaks, windthrows, floods, overgrazing or droughts. Climate change is causing an increase on wildfire risks (An *et al.*, 2015; Bowman *et al.*, 2020), drought events (Allen *et al.*, 2010, 2015), and pests outbreaks (Logan *et al.*, 2003; Pureswaran *et al.*, 2018) in several forest ecosystems across the planet. However, there is still uncertainty in particular systems, e.g., boreal treeline could move poleward, but bog formation from permafrost melt has the potential to hinder this process and even promote a regression of the treeline (Crawford, 2008; Walvoord & Kurylyk, 2016).

1.1.1. The impacts of drought events on forests

Organisms exhibit two main differentiated strategies in their response to environmental stress: avoidance (e.g., go dormant or migrate during periods of stress that occur on a regular basis) or tolerance (behavioral, morphological, physiological, and metabolic changes that allow coping with stress). Trees are big and long-living organisms, and thus exhibit mechanisms of tolerance against water stress such as: dehydration strain avoidance or postponement through water storage

or leaf abscission, developing deep and wide root systems, reducing flow resistance between roots and leaves, reducing the capacity

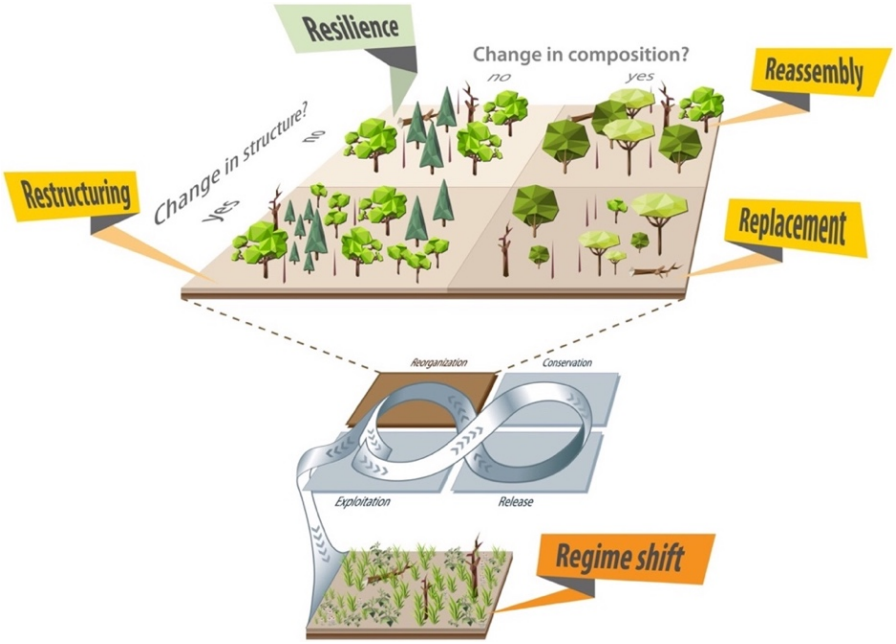

Figure 1.1 Forest post-disturbance possible pathways within a panarchic dynamic, obtained from Seidl & Turner (2022). Ecosystem succession is controlled by four processes: *exploitation*, in which colonization of disturbed areas takes place; *conservation*, characterized by biomass accumulation and storage; *release*, in which nutrients are suddenly liberated by disturbances (Gunderson & Holling, 2002). After disturbance, the system enters into the *reorganization* phase, in which it can transit through five possible pathways: *resilience*, when there is no change in structure and composition; *restructuring*, when there are changes in structure but not in species composition; *reassembly*, when there are changes in composition but not in structure; *replacement*, when there are changes in structure and species composition; and *Regime shift*, when the system jumps to a non-forest configuration.

for growth rates, increasing tissue elasticity, minimizing transpiration rates by leaf morphological changes (such as smaller leaf sizes, trichomes development or thicker cuticula), or stomatal control (Pallardy & Kozlowski, 2008). In ecophysiological terms, because of trade-off between carbon and water use, there are 'isohydric' plant species, which 'avoid' drought by closing stomata (keeping relatively stable xylem water potentials but risking carbon starvation); and 'anisohydric' plant species, which 'tolerate' drought by decreasing xylem water potential (keeping stomata open but risking hydraulic failure).

Conifers can better deal with water deficits than hardwoods since they can store water in their sapwood (Woodward, 1987). Also, internal damages caused by cavitation are confined in just individual tracheids (Gregory & Petty, 1973). This storage can provide enough water for transpiration during several days (Waring *et al.*, 1979; Waring & Running, 1978).

Drought decreases net primary production and net carbon exchange in worldwide forests (Wu *et al.*, 2011). Under this circumstance, carbon sequestration is minimized (Schlesinger *et al.*, 2016). Thus, severe drought in rainforests could compromise the forest carbon sink and turn to a net source, with the subsequent feedback to climate change emissions (Bonal *et al.*, 2016; Phillips *et al.*, 2009). These droughts evidenced that water stress can easily trigger tree mortality, revealing that 'tropical forest trees operate within very narrow hydraulic safety margins' (Corlett, 2016).

However, droughts are relevant in forest dynamics —including tropical rainforests— and their post-disturbance responses are highly complex (Bonal *et al.*, 2016). Thus, forest stands may turn from a resistance behavior under low disturbance conditions to a resilience response, such as facilitating post-drought recovery. As drought severity increases, forests become more vulnerable to growth reduction, diebacks, and pests outbreaks (Schlesinger *et al.*, 2016). Furthermore, this vulnerability is exacerbated with higher wildfires risks and changes in management policies. Yet, there is still a relevant knowledge gap that make drought-derived dieback hard to predict. Physiological approaches only provide specific tree data over a short period of time, and this does not include sufficient information about the complex tree-environment interactions over a longer period (Trugman *et al.*, 2021). Mortality threshold resulting from a high loss of xylem conductivity appears to be specifically dependent on species and context (Camarero *et al.*, 2021a). For instance, *Pinus halepensis* Mill. has been reported to recover after a conductivity fall of 80% (Klein *et al.*, 2012). Functional traits (e.g., wood density and leaf morphology) are also highly dependent on species strategies, drought characteristics or soil water storing capacity (McDowell *et al.*, 2008). Even tree-ring stable isotopes, despite their importance to understand how dieback happened after a drought, have relevant limitations. Pest outbreaks, abundant water consumption from fast-

growing trees or rapid drought due to structural overshoot from previous climatic conditions could interfere in isotope signals interpretation (Camarero *et al.*, 2021a; Jump *et al.*, 2017). Furthermore, there is contradictory information regarding the influence of a tree's height on hydraulic failure. McDowell & Allen (2015) and Bennett *et al.*, (2015) hypothesized that tall trees have greater dying risks to water stress, while other authors found a lack of consistent evidence for this statement (Colangelo *et al.*, 2017, Camarero 2021b). They reported that larger trees might show greater capacity to accumulate water or develop efficient root systems to better access deep soil water storage.

The considerable variability in drought responses, both between and within species (e.g., local individual adaptations), as observed from physiological and functional traits approaches, might hinder the prediction of general drought-induced dieback in forests.

1.1.2. The impacts of pest outbreaks on forests

Forest pests are mainly composed by invertebrates (i.e., insects and nematodes) and fungus species that usually causes roots rotting, defoliation, bark perforation or transpiration interruption. Many pest's species are not only integrated into the regular activity of a healthy forest but are also specific to the genus of dominant tree species (Doğmuş-Lehtijärvi, *et al.*, 2006; Jactel *et al.*, 2015). In these cases, pests contribute to forest health by removing weak trees, releasing nutrients, and facilitating ecological succession (Hobbie & Villeger, 2015). Insects that feed on wood —xylophagus— can also serve as vectors for fungal species. This is of particular concern with invasive alien species, which are spreading and causing high impacts in their new locations (Choi & Park, 2019; Hulcr & Dunn, 2011; Ramsfield *et al.*, 2016). Although bacterial diseases are less abundant than insects or fungal outbreaks, they can cause significant impacts in forests. For instance, some bacterial species like *Xylella fastidiosa* or *Gibbsiella quercinecans* are spreading in Central Europe oaks (Tkaczyk, 2022).

Pest spreading can differ across forest systems. In temperate forests, it has been reported that pests frequently kill trees, which could cause widespread dieback and subsequent gap opening. In contrast, outbreaks in tropical forests tends to be spatially limited (Gely *et al.*, 2020). Periods of very low temperature cause high mortality in many pest species, so hard winters is a natural agent of pest control (Kausrud *et al.*, 2012). Then, climate change can promote thermal requirements for insects and fungus pests, shortening diapauses. This situation can lead to an intensification in outbreaks (Logan *et al.*, 2003). Nevertheless, it is still little known how thermal stress and heat waves could impact forest insects (Jactel *et al.*, 2019). Previously stressed trees are more vulnerable to pest

attacks, so post-disturbance stages —after wildfires or droughts— are pest outbreaks route of entry (Gely *et al.*, 2020).

1.1.3. The impacts of wildfires on forests

Traditionally, biogeography has little appreciated the influence of fire on vegetation, emphasizing mostly climate and soil as the main drivers in the shaping and distribution of plant species populations and terrestrial ecosystems (Pausas & Keeley, 2009). However, some authors have been studying fire as a relevant biogeographical factor for more than 35 years. Minnich, (1988) described the relationships among fire, vegetation, and land use occurred in California over centuries. Also, Stott, (1988) conducted an exhaustive examination to understand the role of fire in Southeast Asian forests, were dry season burns take place every 1-3 years. Both concluded that fire is a natural component of forest ecosystem dynamics and should be accounted in management policies. As concern about fires has increased over the last decades, the 'pyrogeography' concept —time and space distribution of wildfires— is growing in scientific usage (Bowman *et al.*, 2013; Krawchuk *et al.*, 2009; Pausas, 2022; Sannikov, 1994).

Fire history on Earth is narrowly tied to plant evolution (Keeley *et al.*, 2011). Photosynthetic activity allowed sufficient atmospheric oxygen, and terrestrial plants provided fuel, both the components required for combustion. Before plants, fire did not exist on Earth (Pausas & Keeley, 2009). A higher oxygen proportion in past atmosphere (> 30%) could had promoted spontaneous combustion, even on humid areas (Lenton, 2001). The expanse of fire on Earth might have facilitated the colonization of C_4 grasses across the planet, stimulating a feedback process in which they spread over burned areas while they increased fire risk (Keeley & Rundel, 2005).

Bradstock, (2010) proposed a model that integrates fire in biogeography, describing how climate effects conditionate the pyrogeography. This model shows that fire happens under four circumstances:

- **Enough biomass to provide fuel**. In dry ecosystems, biomass production depends on previous wet years.
- **Biomass availability to burn**. This is conditioned by dry seasons or drought events when fuel moisture is minimized. In dry ecosystems fuel could be available to burn the whole year.

- **Capacity to spread.** This behavior is controlled by fuel structure, topography, and weather conditions: high temperature, low humidity, and strong winds.
- **Presence of ignitions**. Ignitions are provoked mostly by humans and lightning. Other ignition sources, such as volcanic activity, sparks from rock falls or meteorite impact are less common (Belcher, 2013). Spontaneous combustion can happen when plant litter generates heat internally, due to microbial activity (> 70ºC), faster than it is dissipated, and then chemical oxidation occurs in low moisture conditions with a good supply of oxygen (Scott, 2000).

Fires can be classified by the type of fuel in which combustion is spread. When it mainly burns dead litter, shrubs and herbaceous, is known as surface fires. They burn at low temperature (< 350°C) and produce great amount of charcoal (Scott, 2000). Crown fires happen when combustion reach the forest canopy (through torching) and are the most virulent ones (McGranahan & Wonkka, 2021). Soils with elevated organic matter content (e. g. humus or peat) can burn in ground fires at low temperature, but that can last for weeks or even years (Scott, 2000). This is especially striking in Taiga ecosystem due to permafrost melting, promoting persistent 'zombie fires', smoldering below ground during long time (Kuklina *et al*., 2022).

The quantification of fire impact and risk have three relevant components: Fire *intensity* is the energy released by the combustion of the vegetation fuel; *frequency* is the temporal distribution of wildfire events, while *severity* defines biological and physical impacts (McGranahan & Wonkka, 2021).

The requisite of dry seasons for fuel available to burn make tropical savannas and Mediterranean-type ecosystems —except Chilean matorral— the most fire-prone ecosystems, where most species have fire adaptation traits or even include it as part of their biological cycles (McGranahan & Wonkka, 2021; Scott *et al.*, 2014). Nevertheless, there is a high variability in flammable ecosystems in terms of structure, composition, and dynamics. There are two possible explanations, based on how the role of fire is understood: One hypothesis assumes that climate is the major control of growth forms and fire is just a consequence of these forms. The alternative premise postulates that climate selects which growth forms could take place in a region and fire is a second layer filter in which it selects which of these growth forms could dominate in flammable ecosystems (McGranahan & Wonkka, 2021).

Many fire plant traits consist in resprouting from isolating structures that protect living tissues from heat. Bark thickness provides effective protection for epicormic buds that are activated

after fire. These buds can be dormant deep under the bark, even in the wood. Resprouting can also take place from roots, with clonal expansion. Some species can even develop below-ground carbohydrate reserves —many are lignotubers or rhizomes— that can provide enough energy to maintain the roots while re-building the canopy after fire. The ability to store seeds above ground for its germination after fire is known as serotiny (serotinuos seeders) or *pyriscence* (Scott *et al.*, 2014), and it is very common in conifers (e.g., *Cupressus*, *Pinus*, *Sequoiadendron* or *Callitris*) and some angiosperm families (i.e., Asteraceae, Ericaceae, Myrtaceae, Casuarinaceae). Although there are plenty of fire plant traits, these are mostly present in fire-prone environments, such as Mediterranean vegetation —except Chilean matorral— and savannas. It has been documented a total of 1345 serotinous species across these ecosystems in Australia, South Africa, the Mediterranean Basin, North America, and Asia (Lamont *et al.*, 2020). The concept of serotiny can also be extended to all plant parts, as it refers a later development, and it is opposed to coetaneous growth (Goodrich, 1983). For instance, some species flower after burn (Scott *et al.*, 2014). One extreme case of rapid flowering is *Bulbostylis paradoxa* (Spreng.) Lindm. in the Brazilian Cerrado ecosystem (Fig. 1.2), it can respond to fire in just 24 hours (Fidelis *et al.*, 2017). Serotinous responses after fire are key strategies for recolonization and vegetation spread in the ecological succession (Kelly, 1994). In some cases, germination can even be triggered by smoke (Keeley *et al.*, 2011).

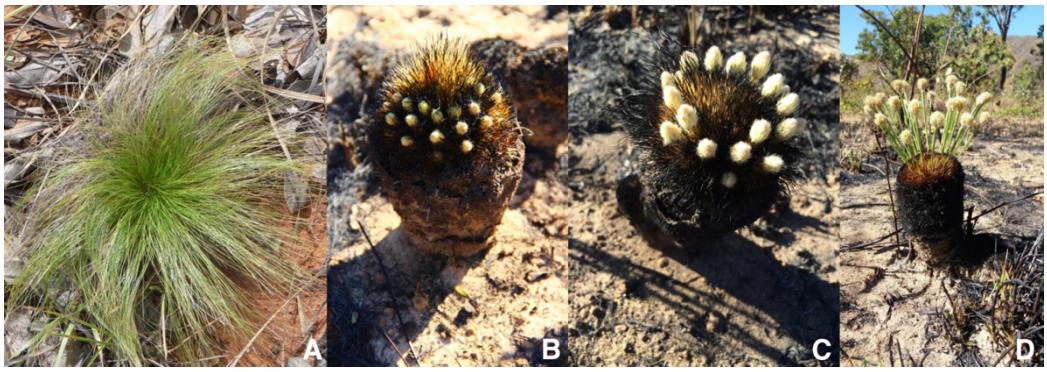

Figure 1.2. *Bulbostylis paradoxa* (Spreng.) Lindm. flowering 24 h after fire. Images obtained from Fidelis *et al.* (2017). This species constitutes one example of extreme fire adaptation in the Brazilian Cerrado ecosystem. **A**: Plant before fire; **B**: 24 h after fire; **C**: 48 h after fire; and **D**: 15 days after fire.

Fire suppression in flammable ecosystems, a consequence of changes in management policies, has led to the disappearance of their main natural disturbance in North American, European, and Australian forests (Sanderson, 1974). Suppression involves cumulative effects over time, leading to an increase of future wildfire intensity and severity due to natural fuel accumulation (Davis *et al.*, 2010; Steel *et al.*, 2015). There is an increasing trend to shift from fire suppression to management, which includes controlled and prescribed burnings, (Eloy *et al.*, 2019; see 1.2 section). The combination of fire suppression, subsequent forest densification and fuel accumulation, along with climate change, is promoting larger wildfires of high intensity and severity.

Climate change can extend fire spread potential and provide more fuel available to burn in ecosystems previously developed under humid or cold climate conditions (Flannigan *et al.*, 2000). Fire is present in almost all Earth ecosystems, but climate change may alter the frequency and intensity of these fires (Jones *et al.*, 2022). Even in flammable systems, an intensification of frequency and severity could exhaust fire adaptations (Nolan *et al.*, 2021) and promote non-forested vegetation areas, favoring shrublands or grasslands.

1.1.4. Other threats and their influence on climate change vulnerability

Worldwide forests have additional issues that aggravate climate impacts such as deforestation in tropical areas (Chakravarty *et al.*, 2012; Guo *et al.*, 2018; O'Brien, 1996) or, the opposite, rural abandonment, particularly in China and the Mediterranean Basin (Ustaoglu & Collier, 2018; Weissteiner *et al.*, 2011; Zhou *et al.*, 2020). The consequences of deforesting the whole tropics 'could result in global warming equivalent to that caused by burning of fossil fuels since 1850, with more warming and considerable drying in the tropics' (Lawrence & Vandecar, 2015). Also, tropical deforestation could imply the loss of at least two-thirds of the world's biodiversity (Raven, 1988). However, impacts on rainforests are heterogeneous. Despite fragmentation caused by the spread of small-scale agriculture in the Congo Basin, biodiversity remains relatively intact. The Amazon region holds the rainforest most vulnerable to climate change and land use stressors, while Congo Basin shows more resilience. The vulnerability of Asian rainforests is mainly led by land use change, as rainfall is not expected to decrease significantly (Saatchi *et al.*, 2021). Land use change can have a greater influence on ecological variables than climate change, leading to rapid biodiversity loss, soil erosion, or reduced habitat availability. Additionally, new land use and management changes are expected as a result of new climate adaptation policies (Dale, 1997). When large regions are

deforested, a decrease in transpiration leads to less cloud formation, less rainfall and local temperature increases (McAlpine *et al.*, 2018; Smith *et al.*, 2023).

Meanwhile, in China and the Mediterranean region, rural abandonment deprives their cultural landscapes of their spatial dynamics, creating vegetation homogeneity across the landscape and non-forest biodiversity loss (Uchida & Ushimaru, 2014). Eventually, this homogeneity can lead to higher fire risk and worse fire scenarios (Ursino & Romano, 2014). Rural abandonment and rainforest loss are a consequence of complex economic and demographic processes which results in land use changes that require social sciences approaches (K. Brown & Pearce, 1994; Quintas-Soriano *et al.*, 2022).

In addition to land cover change, alien species invasions are also an increasing risk to worldwide forests since they tend to homogenize biodiversity and simplify ecosystems functions (Morri *et al.*, 2019). Invasive alien species are spread by human activity (Hulme, 2009), and they can cause new forest pest outbreaks —with subsequent large diebacks—, species substitution or impede ecological succession (Gurevitch & Padilla, 2004).

1.2. Adaptive forest management for new climate scenarios

Since climate change is intensifying the frequency and severity of forest disturbances (Schelhaas *et al.*, 2003), there is a need to actuate before tipping points are reached and regime shifts take place during the reorganization phase (Seidl & Turner, 2022). Restoration and adaptation must focus on future scenarios, avoiding approaches based on how landscape 'should be' according to past environments which might differ of future conditions. In this respect, adaptive forest management is an integrated approach that aims to protect and develop forest functionality as a key for future forest ecosystem services provision under a global change context (Spathelf *et al.*, 2018). The purpose of adaptive forest management is to anticipate or avoid the worst effects of high intensity disturbances by assisting dynamics responses to climate impacts (Bolte *et al.*, 2009). These management practices are relevant in this doctoral thesis, since remote sensing techniques are a powerful tool to provide insights about the evolution of ecological attributes across several spatial and time scales; and to assess the effectiveness of handling with forest disturbances (Camarretta *et al.*, 2020).

There are silvicultural practices that can stimulate resilience responses to disturbance. Thinning is one of the most employed treatments to improve general forest status. Reducing tree competition increases resources availability to persisting trees (D'Amato *et al.*, 2013). Thinning can increase net precipitation (reducing canopy interception and later evaporation), soil moisture, tree water use efficiency and benefits growth; although a decrease in stemflow and transpiration have also been reported (del Campo *et al.*, 2022). Even so, the application of thinning has contrasting effects depending on its intensity, spatial arrangement, post-thinning climate and forest types. Law *et al.*, (2013) reported that thinning can result in a significantly reduction of net primary production, needing a longer time for recovery than that from fire itself in North-West Pacific forests. Nevertheless, there is strong evidence showing that thinning treatments are effective to ensure that remaining trees can better cope with increasing fire and droughts events (del Campo *et al.*, 2022; Manrique-Alba *et al.*, 2022; Sohn *et al.*, 2016).

Changes in landscape management over the last century have led to wildfire suppression. This has resulted in greater fuel accumulation which currently promotes higher fire intensity. During the 19th and early 20th centuries a 'let burn' policy was assumed, as local communities were unable to control wildfires (Sanderson, 1974). However, traditional knowledge from indigenous people was reported to be of interest in fire management since they are a consequence of a long experimentation, and they could be implemented in modern forest management practices (Kimmerer & Lake, 2001). In this respect, prescribed burning is a powerful management tool with increasing acceptance in countries with fire-prone environments. Prescribed burning consists of creating ignition points across a delimited area to drive a low-intensity fire over a vegetation surface. The main idea behind this practice is to implement low-disturbance regimes in forest ecosystems, with the aim of minimizing the risk of higher severity and larger fires by reducing vegetation fuel load (Burrows & McCaw, 2013; Fernandes, 2015; Penman *et al.*, 2011). However, this technique is underused in Southern Europe due to many policy barriers to implement it (Fernandes *et al.*, 2013) and there is still relevant knowledge gap to cope with (Fernandes, 2015).

Adaptive forest management could also imply new thermophile species selection or favoring present species in the forest which are already drought tolerant (Albert *et al.*, 2017; Bolte *et al.*, 2009). In addition, transgenically altered trees could be key to cope with drier environments and to fight against desertification (Marchin *et al.*, 2017; Polle *et al.*, 2019). However, to be effective, genetic modification needs to be aligned with the conservation and enhancement of ecosystems functionality goals.

Increasing tree diversity and promoting mixed stands, could stimulate higher resistance and resilience responses to disturbance (Bolte *et al.*, 2009). The outcomes of adaptive management are still uncertain, and some impacts may result from its implementation. It could compromise biodiversity conservation and old-growth forests protection, since landscape might change and differ from the original ecosystem (Law *et al.*, 2013). However, in the absence of adaptive management, stronger impacts might arise in the long term, such as forest substitution or regime shifts (Bolte *et al.*, 2009; Hörl *et al.* 2020; Jandlt *et al.* 2019).

1.3. Remote sensing technologies for forest management

Remote sensing was born as a science to study landscape patterns for military purposes. Today, it is a powerful tool which benefits from the rise of new technologies such as big data processing or the Internet of Things (Dey *et al.*, 2019; Din *et al.*, 2015; Liu *et al.*, 2021). The capabilities of remote sensing and its applications allowed these techniques to grow and spread within several fields. Forestry is one of the main sciences that broadly apply remote sensing, since it can reduce the time required for sampling and inventories. The results obtained from the derived large datasets are employed to improve the monitoring and decision making in forest management (Wulder *et al.*, 2008; Wulder & Franklin, 2003).

1.3.1. Remote sensors

Resolution determines the nature of data acquisition that a sensor can capture. Temporal resolution is the time frequency in which the data is obtained of a specific observation area (e.g., time needed for a satellite to complete an orbit and return to the same point), spectral resolution is the precision of a sensor to distinguish wavelengths and its fluctuations, spatial resolution refers to the pixel size, and radiometric resolution is the amount of data stored in a pixel expressed by bits. The quality of the data obtained is determined by how accurately it can represent the feature of interest (Chuvieco, 2010).

Remote sensors can be classified by how the data is captured. Passive sensors include radiometers and spectrometers that capture in the visible, infrared, and thermal infrared ranges from the electromagnetic spectrum. These sensors just record the reflectance of Earth surface objects, and they cannot obtain surface data in cloudy conditions. Each surface object has a specific

reflectance in the electromagnetic spectrum. Hyperspectral sensors obtain reflectance data through several bands, allowing to record the whole spectral signature. Meanwhile, multispectral sensors data have less number of bands and they are used through spectral indices (Joseph, 2011). Spectral sensors are useful in precision agriculture, where it is possible to monitor crop health and vigor deficiencies for improving management (Kent Shannon *et al.*, 2018).

Thermal sensors capture temperature surface from the thermal infrared spectrum (8-14 μm) and are highly employed for monitoring industrial activities, military purposes, civil security and emergencies, energy management and environmental monitoring (Prakash, 2000).

Passive sensors that only record the visible spectrum data are known as RGB or photogrammetric cameras. They are employed to obtain orthoimages and 3D data through Structure from motion photogrammetry (SfM). These techniques allow high precision geometric calculations, with subsequent outputs such as surface contours, object dimensions, surface areas or distances (Westoby *et al.*, 2012).

Active sensors are those which can emit and record data through radio detection and ranging or scanners. These sensors can capture data in most atmospheric conditions and produce 3D precise data. Light Detection and Ranging (LIDAR) is the most widely employed technology. They consist of scanners with a laser pulse that can measure the distance between the device and the object, calculating the time between the laser pulse and its reflectance detection (Chuvieco, 2010). The output is a 3D point cloud data, similar to photogrammetry. Notwithstanding, LIDAR can penetrate canopy vegetation and capture ground returns (Means *et al.*, 2000). However, photogrammetry can produce high quality data at very low cost and its deployment is more versatile and agile for aerial platforms (Westoby *et al.*, 2012).

Synthetic Aperture Radar (SAR) is another established system with increasing applications. This technology consists of several radar consecutive pulses of a small antenna that combined can broad the signal similar to a bigger antenna. SAR technology have two main techniques: polarimetry, when the data capture is based on the polarization of the radar waves; or interferometry when there is a comparison between the interference wave phase pattern from two SAR images (Flores *et al.*, 2019). This system has potential applications in agriculture (Liu *et al.*, 2019), forestry (Flores *et al.*, 2019) and oceanography (Gens, 2008).

1.3.2. Platforms for remote sensing

Hot air balloons were the first platforms employed to obtain aerial images during the XIX century. During the first half of XX century, airplanes started to obtain landscape data capture with aerial black and white images for military research. In the second half of the century, the potential of aerial images for landscape management were studied with several airplane flights. The rise of spatial technologies during the end of the Cold War developed multiple technologies that amplified the amount of data able to capture of Earth surface at different scales. The deployment of consolidated satellites for landscape observation started in the early 70s with the Landsat program launched by NASA (Moore, 1979). The European Spatial Agency (ESA) were created in 1975 and founded the Copernicus program by 2014. Copernicus developed the Sentinel satellite constellation, providing high temporal and spatial resolution images from Earth surface (Saunier *et al.*, 2017).

The commercial use of Unmanned Aerial Vehicles (UAV), also called 'drones', started in 2010 decade, due to the miniaturization of flight stabilization components. The rise of UAVs meant a relevant leap to remote data capture. They are flexible and highly increased the temporal and spatial resolution since flights can be performed at user demand and at closer surface than satellites (Ehsani & Mari Maja, 2013). There are two common UAV models: fixed-wings and multirotor. Fixed-wing UAVs are light and have enough autonomy to fly over an hour, covering a high spatial area. However, most of the current models cannot carry heavy payload yet, such as LIDAR or hyperspectral cameras. Multirotor models are more versatile than fixed-wing UAVs, they can fly in narrow spaces, and carry a heavier payload, although the autonomy barely reach an hour of battery use in current devices (Boon *et al.*, 2017). In addition, there are hybrid models (i.e., fixed-wing UAV and Vertical Take-Off and Landing; VTOL) which are an emerging option that attempt to combine the best of the two technologies (Saeed *et al.*, 2015).

Terrestrial platforms are also employed for LIDAR (Terrestrial Laser Scanning, TLS) and hemispherical photogrammetric devices. They are carried on backpacks, tripods, or vehicles to record the whole sampling area at very high precision and low cost. The most relevant advantages of these systems are that they can capture data under covered areas (i.e., canopies) or inside buildings (Dassot *et al.*, 2011). Scanning with tripods require multiple scans to cover the same area due to obstacles shading, while vehicles (Vehicles Laser Scanning, VLS) or backpacks are based on Simultaneous Localization and Mapping (SLAM), as an alternative method to GNSS-denied environments (Su *et al.*, 2021).

1.3.3. Processing the sensor's outputs

Remote sensors reduce the amount of fieldwork required and the time employed for monitoring large study areas. With the increasing precision and resolution of remote sensors the amount of data for processing is enormous. Professional users require high computing power and specific software to analyze the big data generated. Data science techniques are crucial for managing and studying large datasets (Dey *et al.*, 2019). Remote sensing provides information that can be used for predictive models, image classification, multitemporal analysis through time series, and regression analysis. Field data is commonly used to validate sensor's outputs and the performance of predictive models. Machine learning algorithms, such as random forests, support vector machine or neuronal networks are the most common techniques to model and predict the main variable of interest (Maxwell *et al.*, 2018).

The whole process of data capture and processing is increasingly efficient. Other technologies are being employed combined with remote sensing, such as Internet of Things (IoT) that allow to amplify the data sources with wireless real time data capturing. The application of remote sensing, IoT and machine learning algorithms to agriculture originated the precision agriculture field, also known as digital agriculture (Din *et al.*, 2015). The application of remote sensing for a similar approach in forestry is discussed in next section.

1.3.4. Remote sensing and forest management

Reflectance of vegetation cover is a direct consequence of Leaf Area Index (LAI) and the photosynthetic activity. Chlorophyll pigments absorb in the blue (0.45-0.51 μm) and red (0.62-0.7 μm) spectral bands, while there is a high reflectance in the Near Infrared (NIR; 0.75-2.5 μm) band due to leaf mesophyll structure and water content (Chuvieco, 2010). Multispectral derived data are used to study the reflectance through indices. Normalized Difference Vegetation Index (NDVI) is the most employed index to study vegetation cover, with more than fifty years of usage (Anyamba & Tucker, 2012). This index ranges from -1 to +1, but 0.2-0.9 are values related to vegetation cover reflectance. The main use of NDVI is as proxy of photosynthetic performance since the index values are directly proportional with plant health status. When the slope originated due to the difference between red absorbance and NIR reflectance flattens, the plant is under stress conditions (Kent Shannon *et al.*, 2018). Normalized Difference Red Edge (NDRE) is another index based on the Red Edge band (0.68-0.73 μm) which show the rapid change between red absorbance and NIR

reflectance and it is more precise for estimating photosynthesis performance or chlorophyll content (Hunt *et al.*, 2011). GNDVI is another index that study the 'greenness' of a vegetation cover and it is employed to study the water and nitrogen uptake of crops (Schmidt *et al.*, 2009).
NDVI have been widely employed from satellite images to obtain forest cover changes across different time series (Othman *et al.*, 2018). Tropical deforestation rates have been monitored with land cover classification and multitemporal analysis of satellite images (Schultz *et al.*, 2016). NDVI calculation through satellites sensors are also a powerful tool to detect forest biomass and impacts at regional scale, such as pest outbreaks, dieback events or wildfire severity (Escuin *et al.*, 2008; González-Alonso *et al.*, 2006; Huang *et al.*, 2021a; Lovelock *et al.*, 2017). However, NDVI shows significant limitations to consider. There is a lack of sensitivity to detect plant vitality or biomass changes when they are at high levels. NDVI index shows better performance at low LAI values or when there is a certain vegetation stress (e.g., low rainfalls; Gu *et al.*, 2013; Huang *et al.*, 2021b). In general, working with spectral indices at pixel level to monitor plant vitality in multilayered canopies might involve understory interferences to detect top-canopy damage signals.

Additional multispectral indices were developed to detect specific surface objects such as water bodies with the Normalized Difference Water Index (NDWI; McFeeters, 1995); or to delimitate severity in burnt areas with Normalized Burn Ratio (NBR; Escuin *et al.*, 2008).

Hyperspectral cameras are an emerging technology with the potential to map tree species composition within a forest, and it is sensible to detect changes in canopy chemistry. They can be a relevant device to map forest biomass and composition if combined with LIDAR sensors (Fig 1.3; Dalponte *et al.*, 2008; Shen & Cao, 2017).

Thermal cameras have a relevant potential for studying plant water stress. Leaf temperature is directly related with stomatal conductance and the amount of water contained in mesophyll structure (Chuvieco, 2010). Based on this concept, it was developed the Crop Water Stress Index (CWSI) to study water stress in agriculture (Nielsen, 1990). Thermal sensors are common in satellite's payload, they provide surface temperature which can be employed to estimate tropical rainforests evapotranspiration (Prakash, 2000; Timmermans *et al.*, 2015) or the cooling effects of forests within a city in urban heat islands (García, 2022).

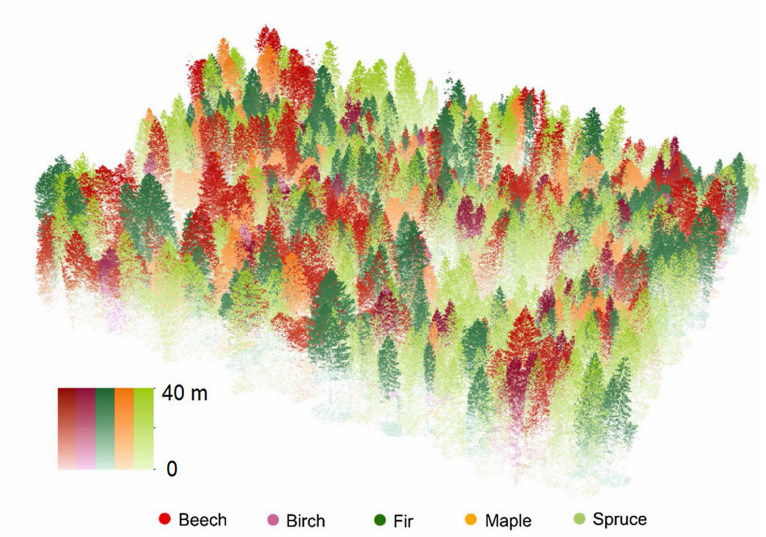

Figure 1.3. Tree species classification from LIDAR and hyperspectral data in a mixed temperate forest, obtained from (Shi *et al.*, 2018).

New satellite launches are improving their sensors resolution and quality, although UAV systems are becoming more efficient and more affordable choices. UAVs are one of the key devices in new forestry, since flights can be performed at demand, capturing several variables of interest in forest management. Multispectral, hyperspectral, and thermal cameras can be miniaturized and obtain similar data as satellites but with higher resolution (Torresan *et al.*, 2017). However, what makes UAVs essential in forestry is the potential to obtain aerial 3D data at very low cost: canopy cover, crown heights, LAI and multistory structure can be calculated with Structure from Motion photogrammetry (Iglhaut *et al.*, 2019). Also, they have been used to detect lianas in rainforests (Fig. 1.4; Waite *et al.*, 2019), invasive plant species (Hill *et al.*, 2017), and quantify gap formations (Gaulton & Malthus, 2010). Photogrammetry can provide similar data as Aerial LIDAR Scanning (ALS). However, SfM photogrammetry generates 3D point clouds from RGB images, so it is limited to capture only top of the canopy data; whereas ALS can reach the ground since laser can penetrate tree crowns and receive below canopy returns (Lim *et al.*, 2003). In these LIDAR systems, data quality is expressed in points·m^{-2}. Many government administrations have scanned their territory with an ALS boarded in airplanes to provide free 3D point cloud data for civil purposes. The point cloud quality ranges 0.5-4 points·m^{-2}. There is no relevant increase in the quality of the point cloud

above 1 points·m^{-2}, due to the filter effect of vegetation canopy to the laser pulses reaching ground. ALS data is employed to obtain Digital Elevation Models (DEMs) with the classification of the point clouds (Garcia *et al.*, 2017). Ground points allow to generate Digital Terrain Models (DTM), which consists of topographical 3D bare ground data, whereas Canopy Height Models (CHM) are points corresponding to vegetation that are normalized to obtain relative heights of the forest. With CHM files is possible to obtain canopy structural metrics and statistical distribution of points within voxels (Lim *et al.*, 2003; McGaughey, 2018; Means *et al.*, 2000).

Although ALS pulses can penetrate canopies, the quality of these point clouds are indirectly proportional to the closeness to the ground. This is critical in high-dense forests. On the opposite, Terrestrial Laser Scanning (TLS) devices have less resolution reaching top of the canopy, while they are highly precise measuring understory forest metrics (e.g., stem diameters, shrubs and bush biomass or canopy base height; Hilker *et al.*, 2012).

The most efficient techniques combination to scan a whole forest is to perform photogrammetric UAV flights (with the possibility to carry other sensors simultaneously on the payload such as thermal or multispectral) and ground LIDAR data capture through TLS or SLAM (Dassot *et al.*, 2011; Garcia *et al.*, 2017; Iglhaut *et al.*, 2019). This combined workflow —TLS/SLAM + UAV flights— results in entire forest vertical structure data with additional thermal or multispectral data at lower costs and time consumption than the combination of ALS + TLS.

Figure 1.4. UAV liana detection over a rainforest canopy, obtained from (Waite *et al.*, 2019). (a) show a liana free and (b) liana-infested tree crown.

SAR technologies have also been employed to estimate forest biomass across large areas, but currently, there are fewer case studies with SAR applications comparing to LIDAR systems (Flores *et al.*, 2019). However, SAR systems exhibit greater advantages because they are insensitive to weather variations and show better performance in biomass estimation, since they can penetrate deeper into the canopy (Sun & Liu, 2020). In precision agriculture remote sensing is combined with other technologies such as Internet of Things (IoT) permanent sensors to constitute a whole ecosystem management, the digital agriculture or agriculture 4.0 (Basso & Antle, 2020). In 'forestry 4.0' remote sensing techniques can be combined with IoT devices (Singh *et al.*, 2022), such as sap flux or soil moisture sensors and microclimatic stations to monitor forest structure and physiology (Li *et al.*, 2019).

1.4 Climate risk assessment and management

Remote sensing has been widely reported to be a relevant tool to risk assessment and management. Fire risk is composed by a set of driving factors: topography, meteorology, and vegetation fuel. From this set, only vegetation fuel can be directly manageable, hence surveying fuel models is the keystone of fire risk assessment. Fuel models are classifications of vegetation structure, based mostly on (i) the main component that address fire spread: litter, grass, shrubs, bushes, dead wood and their mixed possibilities; (ii) the moisture of living and dead fuel, (iii) the surface/volume ratio of vegetation structure, and (iv) vertical and horizontal continuity of vegetation structure (Anderson, 1982; Scott & Burgan, 2005). Fire prevention practices are based on minimizing risk of ignitions and high severity scenarios through fuel management. Structures dominated by dense and thin formations provokes a rapid-fire expansion, while coarser fuels slowdown fire but increase severity, due to surface-volume ratios (McGranahan & Wonkka, 2021). The main goal in prevention is to avoid crown fires by reducing ladder fuels, opening overstorey canopies, and create shrubs-cleared patches (Brown *et al.*, 2004). Eventually, management results in new fuel models which consists in heterogenous landscapes with less vegetation density and continuity, enhancing response to fire and minimizing severity (Coop *et al.*, 2020). Remote sensing technologies provide a relevant tool for surveying fuel models and moisture levels estimation through satellite or UAV imagery (Yebra *et al.*, 2018). Also, forest and terrain structure data (i.e., slope, aspect, altitude, tree heights, CBH, CBD, canopy cover) can be obtained through LIDAR point cloud processing (Botequim *et al.*, 2019; Khani *et al.*, 2018). All the integrated information is employed to

perform fire risk simulations through fire behavior mapping software such as FlamMap (Finney, 2006).

Drought periods can be assessed through climatic indexes based on evapotranspiration data, such as the Standardized Precipitation-Evapotranspiration Index (SPEI). SPEI allow to monitor the duration and intensity of droughts in specific regions (Beguería *et al.*, 2014). Evapotranspiration (ET) is a key component of SPEI, since it is a variable closely related to physiological water management in plants. Evapotranspiration and sap flux information are the most employed data to assess plant hydraulics in drought events, allowing to analyze forest vulnerability to water scarcity (Granier & Breda, 1996; Waring *et al.*, 1979). UAV and satellite imagery are usually employed to map ET, validated with ground data stations (Aguilos *et al.*, 2018; Baker *et al.*, 2021). Mapping ET have the potential to detect differences in forest water usage, and, subsequently, vulnerable areas to droughts. Detecting vulnerable areas to drought are relevant to determine where to apply adaptive forest management practices.

Objectives of the Doctoral Thesis

The main objective of this Doctoral Thesis is to study the applications of remote sensing techniques in endangered forests for assessing risks and vulnerabilities against climate change to be applied in adaptive management. For this purpose, three studies were conducted in which they aimed:

1. **To study canopy evapotranspiration in a forest using RGB and thermal imagery from an Unmanned Aerial Vehicle (UAV).** This objective is detailed in Chapter 2 and its sub-objectives were:
    a. To study small-scale canopy evapotranspiration patterns in a rainforest through the combination of UAV thermography, point cloud analysis, and machine learning.
    b. To evaluate whether evapotranspiration can be predicted reliably from multiple canopy variables with a Random Forest approach.
2. **To monitor the ecological responses of a forest to post-drought dieback and mortality induced by climate change.** This objective is developed in Chapter 3 and aims to assess the conservation status of *Abies pinsapo* forests in its largest population located in the National Park of Sierra de las Nieves (Yunquera, province of Málaga, Spain). The sub-objectives were:
    a. To analyze the spatio-temporal dynamics of forest productivity at landscape level using Landsat NDVI time series.
    b. To characterize the spatio-temporal balance of canopy gaining/loss through aerial orthoimages.
    c. To assess changes in *A. pinsapo* tree status and mortality at the forest stand level through two field sampling campaigns separated in time by almost two decades.
3. **To assess fire and canopy structure-related risks using ForeStereo and LIDAR data.** This objective is detailed in Chapter 4 and its sub-objectives were:
    a. To analyze fire risk in *A. pinsapo* forests and its possible connection to post-drought mortality dynamics.
    b. To analyze canopy structure variability and its potential association to previously reported declining growth symptoms in *A. pinsapo* forests.

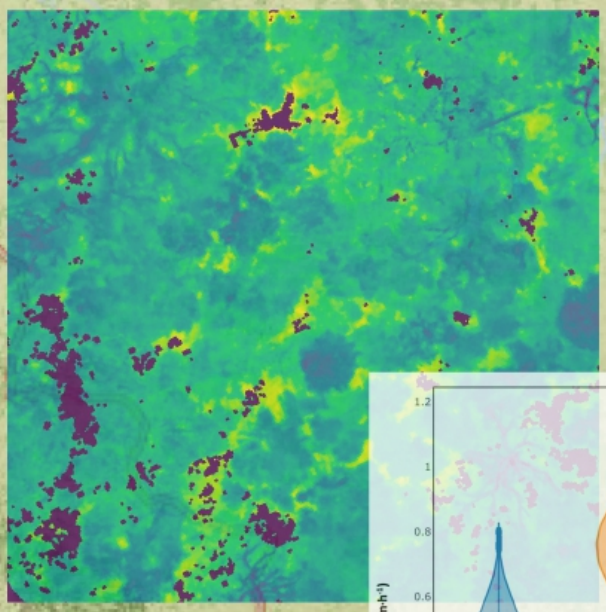

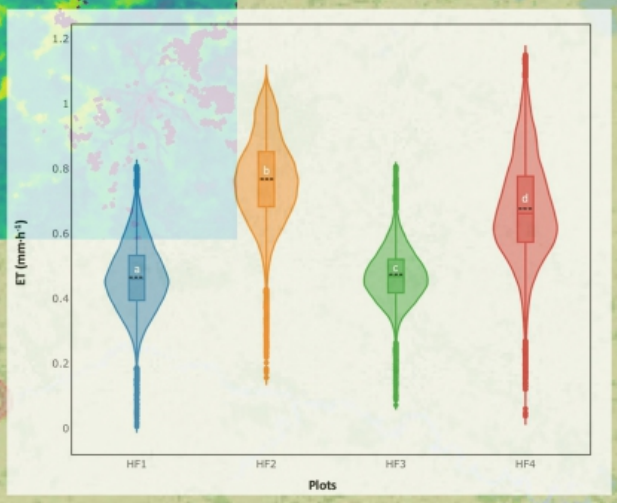

CHAPTER 2

STUDY 1

Combining UAV thermography, point cloud analysis and machine learning for assessing small-scale evapotranspiration patterns in a tropical rainforest

2

Abstract

Microclimate and vegetation structure control evapotranspiration (ET) from land surfaces at stand and landscape scale. Tropical rainforests are among the most diverse and complex terrestrial ecosystems, harboring vast plant and animal species throughout their dense multistory canopy. They contribute substantially to global precipitation through their high ET. However, there is little information about ET influences at very small spatial scales under given climatic conditions. In a tropical rainforest on Sumatra, we studied the relationship between pixel-level ET as derived from high-resolution (~10 cm), near-surface thermography from an unmanned aerial vehicle (UAV) and canopy structure as derived from RGB image and 3D point cloud analyses. The 16 derived potential predictors encompassed vegetation height, height variability, vegetation density and reflectance variables. Using regression models, several of the studied variables had a significant linear relationship with ET, but the explained variance was only marginal. However, applying a random forest algorithm including forward feature selection and target oriented cross validation explained substantial parts of the pixel-level variance in ET (R^2 = 0.56 – 0.65), thus indicating multiple non-linear relationships with interactions among predictor variables. Therein, green leaf index, leaf area density and vegetation height were often the most important variables for the prediction outcome, but their sequence varied among the four study plots. Overall, combining canopy structure variables derived from RGB photogrammetry explained relatively large parts of spatial ET variations. Our study thus indicates the large potential of combining UAV-based thermography and photogrammetry techniques with machine learning approaches to better understand ET, but also suggests that more work remains to be done in explaining ET pattern at very small spatial scales.

Cortés-Molino, A., Valdés-Uribe, A., Elläßer, F., Bulusu, M., Ahongshangbam, J., Hendrayanto, Hölscher, D., Röll, A. (2023). Combining UAV thermography, point cloud analysis and machine learning for assessing small-scale evapotranspiration patterns in a tropical rainforest. *Ecohydrology* https://doi.org/10.3389/fpls.2022.991720

2.1. Introduction

Climate change is projected to lead to an intensification of the hydrological cycle (Allan *et al.*, 2020; Yeh & Wu, 2018) and to increases in frequency and severity of extreme meteorological events such as droughts or floods (Barichivich *et al.*, 2018; Donat *et al.*, 2019; Kundzewicz, 2008; Trenberth, 1999). Terrestrial evapotranspiration (ET) as a key component in the hydrological cycle accounts for approximately 40% of global precipitation (Schlesinger & Jasechko, 2014). ET is the combination of water evaporation from surfaces and transpiration from plants. The contribution of transpiration to ET varies across biomes, around 50% in drylands and up to 70% in tropical rainforests (Schlesinger & Jasechko, 2014). Assessments of ET in tropical rainforests are generally very challenging due to the remoteness and high topographical and structural complexity of the ecosystem.

ET dynamics are driven by micrometeorological variables including solar radiation, vapor pressure deficit and wind speed. The combination of these variables can be expressed in the maximum possible ET rate under ideal conditions, the potential evapotranspiration (PET, Allen *et al.*, 1998). PET assumes an unlimited supply of water while actual ET is strongly governed by water availability, i.e., precipitation and soil moisture, and further strongly influence by topographical and physiological aspects (Dimitriadou & Nikolakopoulos, 2021). The transpiration component of ET largely depends on leaf surface and canopy properties. Crown leaf density and vertical vegetation structure (e.g., tree or crown height) have been proposed as key regional controls of ET (Coronel *et al.*, 2011), while studies at the local level also report strong influences of canopy conductance and plant health (e.g., Nazarbakhsh *et al.*, 2020; Marques *et al.*, 2020). While ET controls at larger spatial scales thus are relatively well studied (e.g., Williams *et al.*, 2012; Nelson *et al.*, 2020), small-scale controls of ET have received less attention, particularly in tropical rainforests. Studies at the tree level indicate a dominant influence of tree and crown size on per-tree transpiration (Ahongshangbam *et al.*, 2020; Kotowska *et al.*, 2021; Meinzer *et al.*, 2005). Local differences in tree density and sizes and the associated differences in local 'canopy packing' were reported to lead to considerable small-scale variability in transpiration patterns at eight lowland rainforest sites (Ahongshangbam *et al.*, 2020). Assessments of rainforest ET at even higher spatial resolution (i.e., in cm- or dm-scales) are to our knowledge not yet available. From the studies at larger spatial scales, one may speculate that key variables such as vegetation height and its variability and vegetation and leaf density may also influence ET at smaller spatial scales under given micrometeorological conditions.

A widely used method to measure ET fluxes is the eddy covariance technique, where ET is measured at very high temporal resolution and over long periods of time. However, the technique

averages ET in a single value over a footprint of typically a few hectares around the measurement tower (Baldocchi, 2020). At larger spatial scales, ET is often assessed via thermography from satellites, but even modern products such as ECOSTRESS have only moderate spatial and temporal resolution, i.e., 70 m and one overflight a day (Fisher *et al.*, 2020). A further major constraint of passive satellite methods is cloud cover, which can result in only few usable images per year for a given (tropical) region. A promising method for the assessment of ET, at landscape scale and with high temporal (e.g., hourly) and very high spatial resolution (i.e., cm-scale), is thermography from unmanned aerial vehicles (UAV), also referred to as drones (Rauneker & Lischeid, 2012). While establishing high-resolution temporal ET time series from multiple UAV flights is logistically more challenging, spatial ET patterns at a given sites can often be assessed from a single flight, e.g., carried out close to noon under conditions of relatively high solar irradiance. To derive ET from land surface temperatures, energy balance models with varying levels of complexity can be applied. Timmermans *et al.* (2015) developed the 'Deriving Atmosphere Turbulent Transport Useful To Dummies Using Temperature' (DATTUTDUT) model, a simplified one-source energy balance model that requires only surface temperature data and few auxiliary variables such as time and location as input. The DATTUTDUT model was implemented in the QGIS plugin QWaterModel (Ellsäßer *et al.*, 2020b) to provide a simple-to-use graphical interface for ET assessments. The approach showed high agreement with reference ground methods across spatial scale from leaf to ecosystem when tested in a in tropical oil palm plantation (Ellsäßer *et al.*, 2020b, 2021) and in a tropical agroforest (Ellsäßer *et al.*, 2020a).

Using the structure from motion (SfM) technique, the images recorded with UAVs can be used to calculate high-density 3D point clouds and orthomosaic maps (Westoby *et al.*, 2012). Commonly, this is carried out with UAV-recorded red-green-blue (RGB) images. In analogy to point clouds derived from the typically much more expensive LiDAR technology, forest structure variables and crown and canopy metrics can be extracted from the photogrammetrically derived point clouds (Iglhaut *et al.*, 2019). Previous studies at the tree-level showed that crown metrics derived from RGB 3D point cloud analysis were better predictors of per-tree and per-palm transpiration than conventionally applied variables like stem diameter (Ahongshangbam *et al.*, 2019; 2020). We are not aware of any previous studies connecting ecohydrological forest functions such as transpiration or ET to forest structure at even smaller spatial scales. Potential variables of interest derived from RGB images and point clouds in the context of small-scale ET patterns include simple indices such as the green leaf index (GLI; Louhaichi *et al.*, 2001) and visual atmospherically resistance index (VARI; Gitelson *et al.*, 2002), point cloud variables related to e.g., voxel density or height distribution (McGaughey & Carson, 2003) as well as classic ecological variables such as the leaf area index or leaf area density (Kricher, 2011).

High-resolution UAV imagery produces large datasets with potentially millions of georeferenced pixels and multiple variables derived from different sensors, with complex, often non-linear relationships and variable interactions. For analyzing such large datasets, machine learning techniques are widely employed across the ecological sciences because of their typically much better model performance and prediction accuracy compared to conventional methods (e.g., Camps-Valls, 2009; Maxwell *et al.*, 2018; Meyer & Pebesma, 2022). Regardless of the applied algorithm, spatial predictions via machine learning are time-consuming and computationally intensive, limiting the application of multiple algorithms at the same time and highlighting the importance of the choice of an appropriate algorithm for the given study context. For spatial predictions in ecological studies, random forest stands out among the available algorithms as particularly well-performing (Ahmad *et al.*, 2017; Fernandez-Delgado *et al.*, 2014), e.g., when applied to predict reference ET (Dias *et al.*, 2021; Feng *et al.*, 2017), ET of tropical mountain forests (Valdés-Uribe *et al.*, 2023), water stress (Virnodkar *et al.*, 2020) , sap flux and leaf stomatal conductance (Ellsäßer, et al., 2020a), net ecosystem exchange (Reitz *et al.*, 2021) or land-cover change (Aide *et al.*, 2013). Recent studies have proposed solutions to previous autocorrelation and overfitting issues in spatial predictions via forward feature selection and target oriented cross validation, thus minimizing the risk of spatial overfitting with random forests and showing realistic overall model performances (Gasch *et al.*, 2015; Meyer *et al.*, 2018, 2019).

In our study, we used an UAV to capture high-resolution, close-to-surface thermal and RGB images of the canopy at four study plots in a lowland rainforest in Sumatra, Indonesia. We applied the DATTUTDUT model to assess pixel-level ET and derived spatially matching structural canopy variables from RGB image and point cloud analysis. The objectives were to further explore small-scale patterns in ET, with a focus on (i) assessing the relationship between ET and single structural variables and (ii) evaluating whether ET can be predicted reliably from multiple canopy variables with a random forest machine learning approach.

2.2. Materials & Methods

2.2.1. Study region and plots

The study area was in the Harapan rainforest in Jambi province (Sumatra, Indonesia) (Fig.2.1). The climate is tropical humid with mean annual precipitation of 2.235 mm·year^{-1} and average annual temperature of 26.7ºC, with two peak rainy seasons in March and December, and a drier period from June to September. The soils in this area are loamy Acrisols (Drescher *et al.*, 2016). The Harapan rainforest is a tropical lowland rainforest that has a legacy of selective logging and wood extraction (Harrison & Swinfield, 2015). Today, the region almost has no natural forest left and has largely been converted to agricultural land including large proportions of oil palm and rubber plantations (Clough *et al.*, 2016). The Harapan rainforest is a protected area managed by the governmental PT REKI company.

Our study plots (plot codes: HF1, HF2, HF3, HF4, Drescher *et al.*, 2016, Fig. 2.1) were upland rainforest sites located inside the Harapan rainforest. The plots were 50 x 50 m2 in size, with a mean elevation of 65 m a.m.s.l. (for more details see Drescher *et al.*, 2016; Ahongshangbam *et al.*, 2020). A previous assessment found over 200 tree species with a diameter at breast height (DBH) of more than 10 cm across the four plots (Rembold *et al.*, 2017). Stand densities and average DBH were similar among the plots, ranging from 616 to 728 trees·ha^{-1} and 19.5 to 22.0 cm, respectively (Kotowska *et al.*, 2015).

2.2.2. Thermal and RGB image acquisition and processing

At each of the four study plots, an octocopter UAV (MK EASY Okto V3, HiSystems, Germany) was used for data acquisition. The UAV was equipped with a radiometric thermal sensor FLIR Tau 2 640 (FLIR Systems, USA) and a RGB camera with an Omnivision OV12890 CMOS sensor (Omnivision, USA). Both cameras were simultaneously mounted in a stereo configuration and on a gimbal to ensure nadir view. GPS location was recorded with an onboard GPS device (MKBNSS V3 GPS/Glonass/Beidou, HiSystems, Germany). Flight planning was conducted using the Mikro-Kopter-Tool V2.14b software. Flight paths were designed as a series of overlapping circular and grid patterns to ensure high overlap (> 80%) between images. Flight altitude was set to 80 m above ground, which corresponds to approximately 30 to 40 m above the canopy. One flight was carried out over each plot in August 2017, always close to noon and preferably during clear-sky conditions.

At the respective times of the data capture, air temperature ranged from 31°C to 38°C, and short-wave radiation from 700 W·m^{-2} to 935 W·m^{-2} (Stiegler, 2021; Table S2.1).

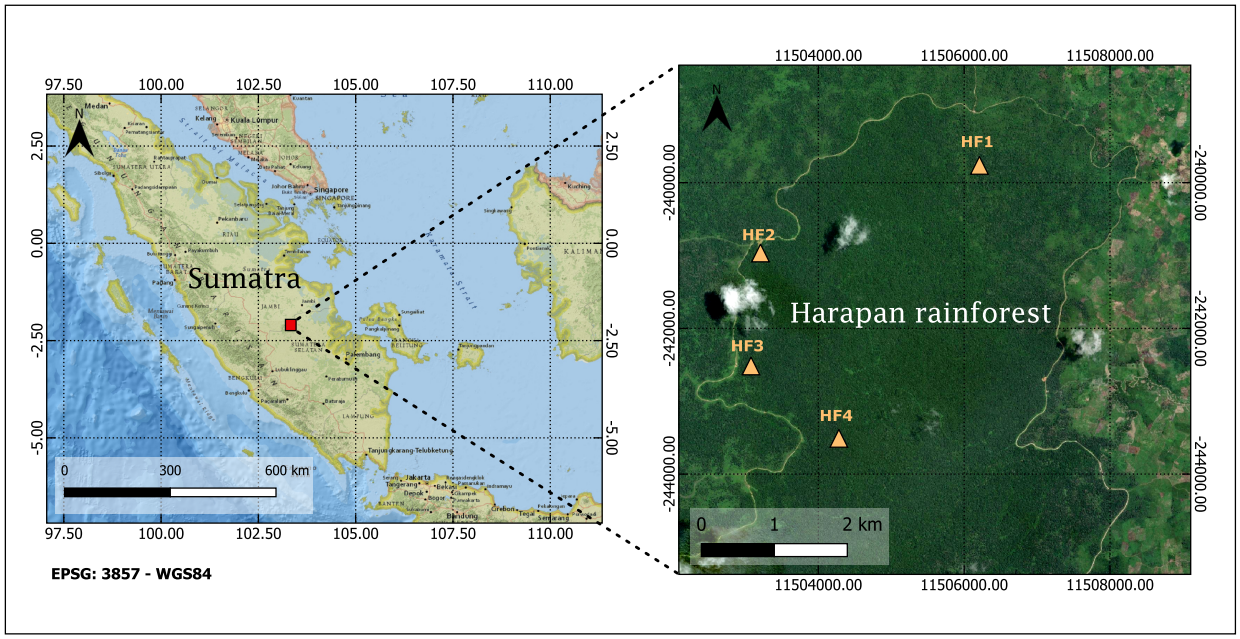

Figure 2.1. Study region in Jambi province, Sumatra, Indonesia and location of the four lowland rainforest study plots (HF1, HF2, HF3, HF4) in the Harapan rainforest.

The ThermoViewer 3.0.7 software (TeAX Technology, 2021) was used to delete blurry or non-relevant thermal images, to export the images to TIFF format and to convert the data to degrees Kelvin. To process the individual georeferenced RGB images (220 to 300 per site) and thermal images (330 – 370 images per site) to orthomosaic maps, AgiSoft MetaShape 1.8.2 (Agisoft LLC, 2021) was used. It applies the Structure from Motion (SfM) technique (Westoby *et al.*, 2012) and further outputs digital elevation models (DEM) and RGB point clouds. We then used QGIS 3.16 (QGIS Development Team, 2020) to resample all RGB-derived raster layers to match the native 10 cm resolution of the thermal orthomosaics, and to clip all layers to the respective plot boundaries (coordinates from Ahongshangbam *et al.*, 2020).

2.2.3. Evapotranspiration assessment via thermography

From the thermal orthomosaic maps of each of the four plots, ET was modeled with the QGIS plugin QWaterModel (Ellsäßer *et al.*, 2020b), which bases on the one-source energy balance model DATTUTDUT (Timmermans *et al.*, 2015). We used the default settings of QWaterModel (version 1.3) in deriving ET. We used a previously established and tested modelling workflow to incorporate measured short-wave irradiance data into the modelling process (Ellsäßer *et al.*, 2020b; Ellsäßer *et al.*, 2021) and also included measured air temperature data. For all four plots, we used in-situ measured data from a nearby microclimatic station operated by the EFForTS project (Stiegler, 2021) where short-wave irradiance was measured in an open area (at 3 m height) with a CMP3 Pyranometer (Kipp & Zonen, The Netherlands) in 10 min intervals and air temperature was measured (at 2 m height) with a thermohygrometer (type 1.1025.55.000, Thies Clima, Göttingen, Germany); therein, we used the climate data that matched the time stamp of the respective UAV flight at each plot. From the thermal orthomosaic maps of the study plots and the shortwave radiation and air temperature data QWaterModel then processes ET maps.

2.2.4. Structural variables derived from photogrammetry

From the RGB orthomosaics and point clouds of each plot, several canopy-related variables were derived at the pixel level, in alignment with the 10 cm resolution of the thermal orthomosaics. From the RGB orthomosaics, we obtained the visual atmospherically resistance index (VARI, García-Martínez *et al.*, 2020; Gitelson *et al.*, 2002; eq. 1) and the green leaf index (GLI, Louhaichi *et al.*, 2001; Raymond Hunt *et al.*, 2011; eq. 2), which are measures of vegetation fraction based on normalized RGB bands.

VARI = (Green - Red) / (Green +Red - Blue) (eq.1)

GLI = (2 x (Green - Red – Blue / (2 x (Green + Red +Blue) (eq.2)

From the RGB 3D point clouds, we obtained several height-related metrics (Table 2.1) at the pixel-level with the Gridmetrics algorithm from the Fusion software (McGaughey, 2018), i.e., the 'relative height' (Height_rel, the maximum z value among all voxels belonging to a given pixel in the 2D plane, divided by the mean z value observed in the respective plot), the absolute minimum (Height_abs_min) and maximum z values (Height_abs_max) within a given pixel, the percentiles 25 (P25), 50 (P50), 75 (P75) and 90 (P90) of the z-value distribution within a given pixel as well as their coefficient of variation (CV_Height) and the percentage of points above mean height (PM).

Further outputs of the algorithm include the canopy cover of a given pixel above 10 m (Cover10), the canopy relief ratio (CRR), which characterizes canopy shape (McGaughey, 2018) as well as point cloud density (PCD) per pixel. Pixel-level leaf area density (LAD) was estimated with the leafR package (Almeida *et al.*, 2019)

2.2.5. Data analysis

Due to the non-simultaneous nature of the data acquisition and the therewith associated varying climatic conditions that can potentially affect ET, the analysis was carried out separately for the four study plots. The dataset for each plot consisted of up to 226,000 pixels, with information on the target variable ET and the 16 potential explanatory variables (Table 2.1) for each 10 cm-pixel. We first examined the ET distributions at the four plots in violin plots.

For subsequent analysis, all pixels were removed from the according datasets that had at least one no data (NA) entry among the 17 variables. As an initial step, we computed correlation matrices among all variables with the R package corrplot (Wei & Simko, 2021). To examine the influence of single variables on pixel-level ET, we applied linear regressions between ET and each of the 16 potential predictor variables, separately for each study plot. For visualization in scatterplots, we selected the variables leaf area density (LAD) and maximum vegetation height (Height_abs_max) due to their importance for modelling forest structure (Andersen *et al.*, 2005; McGaughey, 2018; Mutlu, 2006) and their reported strong influence on ET in studies at larger spatial scales (Coronel *et al.*, 2011).

Table 2.1. Variables from thermography, RGB orthomosaics, 3D point clouds and Digital Elevation Models (DEM) at each of the study plots.

Abbreviation	Units	Variable	Source	Reference
ET	$mm \cdot h^{-1}$	Evapotranspiration	Thermal orthomosaic	Timmermans et al., 2015
GLI	Dimensionless	Green Leaf Index	RGB orthomosaic	Louhaichi et al., 2001
VARI	Dimensionless	Visual Atmospherically Resistance Index	RGB orthomosaic	Gitelson et al., 2002
Height_abs_max	m	Maximum canopy height	Point cloud	McGaughey, 2018
Height_abs_min	m	Minimum canopy height	Point cloud	McGaughey, 2018
Height_abs_sm	m	Absolute canopy height obtained from the smoothed Digital Elevation Model (DEM)	DEM	McGaughey, 2018
Height_rel	Dimensionless	Relative canopy height	Point cloud	McGaughey, 2018
P25	m	25^{th} percentile	Point cloud	McGaughey, 2018
P50	m	50^{th} percentile	Point cloud	McGaughey, 2018
P75	m	75^{th} percentile	Point cloud	McGaughey, 2018
P90	m	90^{th} percentile	Point cloud	McGaughey, 2018
CRR	Dimensionless	Canopy Relief Ratio calculated as: (mean (h) - min (h)) / (max (h) - min (h))	Point cloud	McGaughey, 2018
CV_height	%	Coefficient of Variance of height distribution	Point cloud	McGaughey, 2018
Cover10	%	Canopy Cover of a given pixel above 10 m	Point cloud	McGaughey, 2018
LAD	$m^2 \cdot m^{-3}$	Leaf Area Density	Point cloud	Almeida et al., 2019
PCD	points	Point Cloud Density: number of points in each pixel	Point cloud	McGaughey, 2018
PM	%	Percentage of points above mean height	Point cloud	McGaughey, 2018

For predicting pixel-level ET from multiple variables, we applied a random forest approach, therein closely following best-practice methodology as outlined in previous studies (e.g., Valdes-Uribe *et al.*, 2023). To consider spatial autocorrelation and avoid overfitting, we implemented the following approach: (i) The assignation of spatial ID to 1x1 m blocks (Roberts *et al.*, 2017), (ii) The random selection of spatial predictors through forward feature selection (FFS) and k-fold leave-location-out cross validation (LLO-CV; Meyer *et al.*, 2018, 2019) with the CAST R package (Meyer *et al.*, 2023) and (iii) random forest modelling and k-fold LLO-CV with the caret package (Kuhn, 2021).

First, using the Rpackage 'blockCV' (Valavi *et al.*, 2019), we partitioned each plot into spatial blocks of 1 m^2 (the minimum area accepted by the function). For every pixel inside that block, a distinct ID number between 1 to 5 was allocated, which corresponds to the desired number of cross-validation folds (set to 5 by default; Roberts *et al.*, 2017). Then, each dataset was split randomly into 60% training and 40% model validation data before feature selection. To reduce computation times for the FFS, we subsampled 50,000 pixels from the training datasets through stratified random sampling (Ludwig *et al.*, 2019). The subsamples were divided by k-fold = 5 for spatial cross validation (Roberts *et al.*, 2017). At each split, the maximum combination of predictor variables (*mtry*) was set to two. The FFS algorithm is based on pairing feature combinations, wherein it saves the best initial model and adds additional features through LLO-CV improvement detection. Thus, the model improves incrementally until no further decreases in root mean square errors (RMSE) are detected (Meyer *et al.*, 2018). For each plot the combination of features selected by the FFS were used as input for the final random forest with k-fold LLO-CV and 1000 trees (following Valdes-Uribe *et al.*, 2023). We performed model validation by predicting over the 40% testing dataset. To evaluate model performance, we calculated root mean square error (RMSE) and R2 as an indicator of the variance explained by each model. We examined variable importance (in % of contribution to final model outcome) to assess the contribution of each feature at each plot using the varImp wrapper function from caret R package (Kuhn, 2021). For all statistical analyses, R 4.3.0 (R Core Team, 2023) was used.

2.3. Results

2.3.1. Spatial ET patterns

ET was highly variable among the pixels of a given plot and among the four study plots. At similar times of day, pixel-level ET varied from 0.0 to 1.2 mm·h^{-1} across the plots. Pixel-level minima of ET were below 0.1 mm·h^{-1} at all four plots, while the respective maxima were larger than 1.0 mm·h^{-1}, resulting in at least 15-fold within-plot variations in ET (Fig. 2.2, Fig. S2.1). The within-plot variation of ET expressed as the coefficient of variation (CV) was similar among the plots, ranging from 16.2% to 18.9%. Mean ET values among the four plots varied 1.7-fold, ranging from 0.5 to 0.8 mm·h^{-1} (Fig. S2.2). The higher ET values at the plots HF2 and HF4 correspond to higher air temperature and short-wave radiation at the time of overflight than at HF1 and HF3 (Table S2.1).

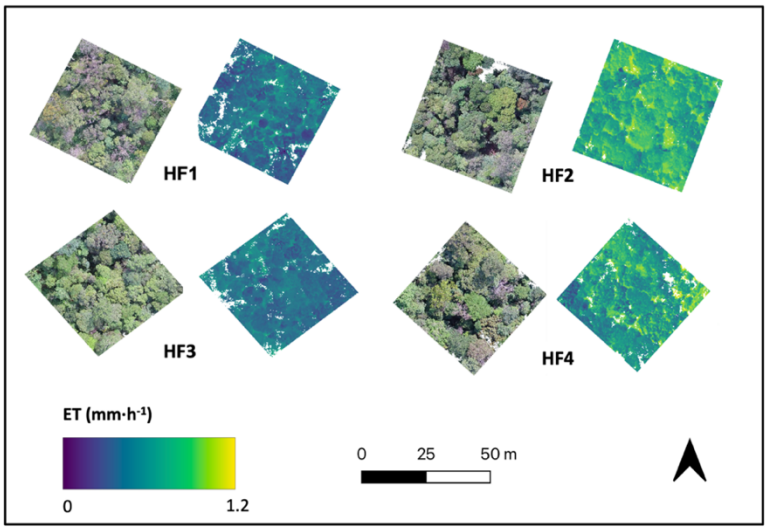

Figure 2.2. RGB (left) and evapotranspiration (ET) orthomosaics (right) for the four study plots. Hourly ET (mm·h^{-1}) as indicated in the legend was derived from UAV-based thermal images with the plugin QWaterModel (Ellsäßer, *et al.*, 2020b). The flights were carried out close to noon on successive days in August 2017. Air temperatures at the respective times of flight were 31.5°C (HF1), 36.5°C (HF2), 32.2°C (HF3) and 38.4°C (HF4), short-wave radiation was at 704 W m^{-2} (HF1), 936 W m^{-2} (HF2), 858 W·m^{-2} (HF3) and 893 W·m^{-2} (HF4).

2.3.2. Prediction of ET

Among the 16 canopy variables derived from RGB orthomosaics and point clouds, correlations with the target variable ET were very weak across all plots (R = -0.21 -0.21, Fig S2.2). Initial speculations that pixel-level variations of ET may be largely driven by vegetation height, its variability or vegetation density (incl. leaf density) were not confirmed at the level of single variables when applying linear regressions. Therein, although often significant ($p < 0.05$), the models explained only marginal amounts of the observed variance in pixel-level ET ($R^2 < 0.05$, Table S2.2), i.e., there was no suitable single predictor of pixel-level ET among the studied variables.

The forward feature selection approach for the random forest modelling resulted in the selection of nine to ten out of the 16 available variables per plot. The selection differed across plots (see Fig. 2.3), but five variables related to vegetation height (P25, P50, P75, P90, Height_abs_min) were consistently present as predictors in all plots. Three further variables related to vegetation height (Height_abs_max), height variability (CV_Height) and reflectance (GLI) were present in three out of the four models. Using the final sets of variables for each plot for pixel-level ET prediction with a random forest approach resulted in fair to good model performance, with RMSE between 0.04 and 0.09 $mm \cdot h^{-1}$ and 56% (HF1), 64% (HF3 and HF4) and 65% (HF2) of the observed variance in ET explained by the prediction models. Model performance was similar for training and prediction datasets across all plots (Table 2.2), indicating that spatial overfitting did not occur and that the models can predict ET for pixels that were not part of the respective training data.

Variable importance for the random forest model outcome differed substantially across the four plots (Fig. 2.3), with no clear dominance of any variable or variable category but some observed common patterns. One to three variables per plot were of very high importance (>75%), and another one to four variables of high importance (50 – 75%). Variables of high or very high importance came from all categories, i.e., vegetation height, height variability, vegetation density and reflectance. Specifically, the variables GLI (in three plots), CV_Height (two plots) and Height_abs_min, LAD, VARI and P75 (one plot each) were of very high importance for model outcome, and further variables of high importance in at least one of the plots included P50, P90 and Height_abs_max.

Table 2.2. Performance of random forest models at the four study plots. The variables as selected with the forward feature selection approach were applied. The total amount of pixels at a given site was randomly split into training (60%) and prediction (40%) datasets. RMSE = Root Mean Square Error. Note: The number of pixels varied across plots and differs from the presented ET pixel numbers in Fig. S2.1 because of no data value removal (7% – 23% of pixels removed).

Plot	Total number of pixels	Training models		Prediction models	
		RMSE	R^2	RMSE	R^2
HF1	169,248	0.03	0.56	0.06	0.56
HF2	167,857	0.04	0.65	0.07	0.65
HF3	211,345	0.02	0.64	0.04	0.64
HF4	169,887	0.05	0.65	0.09	0.64

2.4. Discussion

2.4.1. Spatial ET patterns

We assessed pixel-level ET patterns across four study plots in a tropical lowland rainforest with a UAV-based thermography approach and subsequent energy balance modelling. The therein applied energy balance model DATTUTDUT (Timmermans *et al.*, 2015) and the associated workflow from image acquisition to high-resolution ET orthomosaic maps had previously been established and validated against ground-based reference measurements such as eddy covariance and sap flux measurements across different land-use systems in the same study region (Ellsäßer *et al.* 2020a, Ellsäßer *et al.* 2020b, Ellsäßer *et al.* 2021) and including study sites in lowland rainforest (Bulusu *et al.*, 2023). The mean mid-day hourly ET rates for our lowland rainforest study plots under mostly cloud-free conditions (0.5 - 0.8 $mm \cdot h^{-1}$) are similar to values from a nearby commercial, mature oil palm plantation, with mean ET of 0.4 $mm \cdot h^{-1}$ and peaks up to 0.9 $mm \cdot h^{-1}$ (Ellsäßer *et al.*, 2021).This is in line with previous findings that stand-scale (evapo)transpiration of oil palm plantations can match or even surpass rates observed in (previously logged) lowland rainforests (Röll *et al.*, 2019;

Tarigan *et al.*, 2020). Somewhat lower diurnal ET peak values (around 0.5 $mm \cdot h^{-1}$) than in our study were e.g., reported for temperate ecosystems such as grasslands and coniferous forests (Kelliher *et al.*, 1993). Overall, the mean ET values in our study are within expectation, giving credibility to the applied methods and to the observed spatial ET patterns.

At the coarsest spatial scale in our study, i.e., when looking at plot-to-plot differences in ET, mean ET was approx. 50% higher in the study plots HF2 and HF4 than in HF1 and HF2. The higher ET values for HF2 and HF4 are partially driven by the climatic conditions at the time of data recording, i.e., air temperature was on average 18% higher and short-wave radiation was 17% higher than for HF1 and HF3 (Table S2.1). However, the site-to-site differences in ET are higher than the differences in temperature and radiation, thus indicating spatial variability in mean ET after accounting for the non-simultaneous nature of the measurements and the associated climatic differences. Therein, while our results are consistent with previous sap flux-based transpiration assessments at the same four study sites in terms of substantial observed plot-to-plot variability (Röll *et al.*, 2019, Ahongshangbam *et al.* 2021), they do not match the previous reports of lower transpiration rates at HF4. However, HF4 has higher stand basal area, stand structural complexity, canopy cover and total biomass compared to the other three study plots (Drescher *et al.*, 2016; Kotowska *et al.*, 2015, Röll *et al.*, 2019), which is in line with the observed high ET at the plot in our study. Correspondingly, an enhanced UAV-based sap-flux scaling method suggests the highest stand transpiration rates at HF4, with 7% to 13% lower transpiration at the other three plots (Ahongshangbam *et al.*, 2020). Magnitude and patterns of plot-to-plot variability in ET in our study thus are mostly in line with previous studies, with some divergences. Those may be due to inaccuracies and uncertainties associated with all applied methods, which were reported to be 30% to 57% for estimating transpiration in tropical rainforests with ground-based sap-flux scaling schemes (Ahongshangbam *et al.*, 2020; Granier & Breda., 1996; Röll *et al.*, 2019) and to be around 20% when scaling sap flux via UAV data-derived crown assessments (Ahongshangbam *et al.*, 2020). While the uncertainties of the applied UAV-based ET method have not yet been quantified specifically for lowland rainforests, in a nearby oil palm plantation a comparison to eddy covariance reference measurements indicated high agreement between the two methods (Ellsäßer *et al.* 2021).

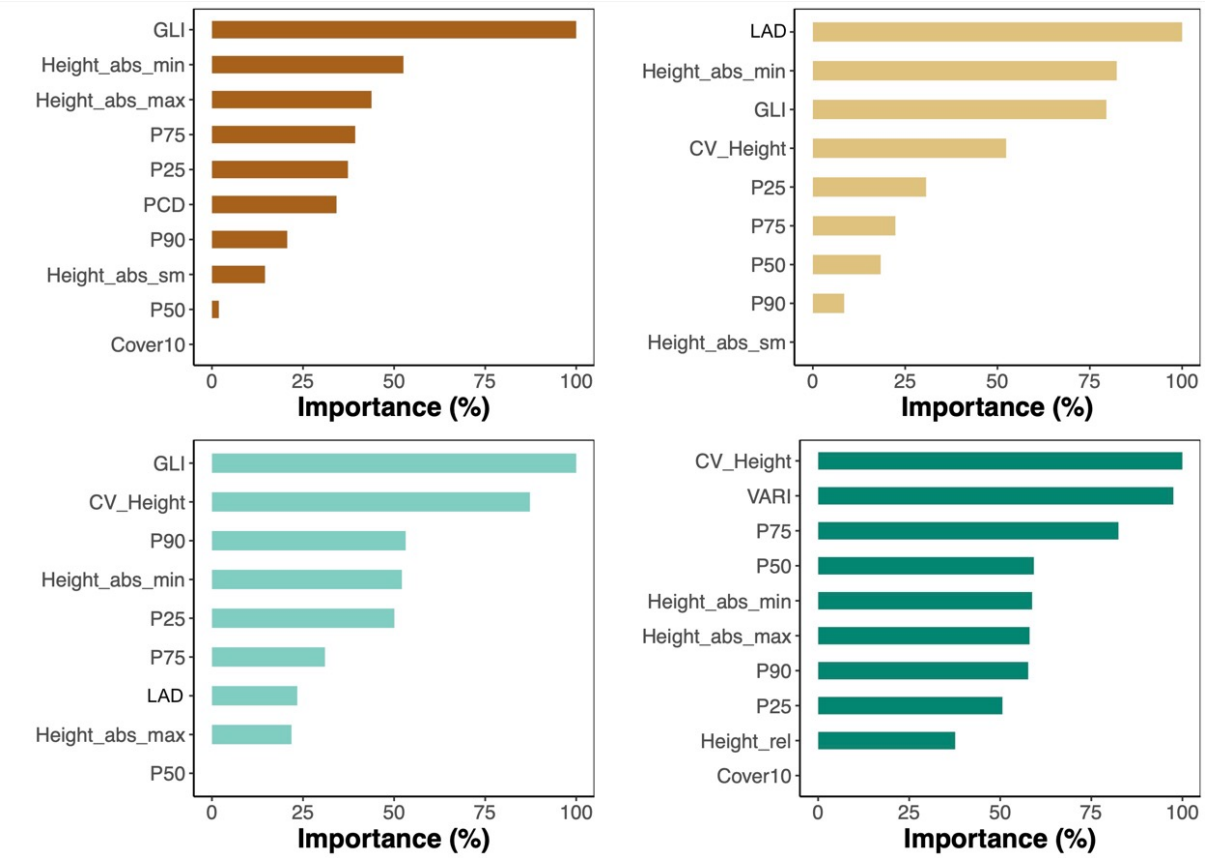

Figure 2.3. Variable importance (%) for the random forest model outcome at the four study plots. Hourly ET (mm·h^{-1}) as indicated in the legend was derived from UAV-based thermal images with the plugin QWaterModel (Ellsäßer, *et al.*, 2020b). The flights were carried out close to noon on successive days in August 2017. Air temperatures at the respective times of flight were 31.5°C (HF1), 36.5°C (HF2), 32.2°C (HF3) and 38.4°C (HF4), short-wave radiation was at 704 W m^{-2} (HF1), 936 W m^{-2} (HF2), 858 W m^{-2} (HF3) and 893 W m^{-2} (HF4).

At very fine spatial resolution (~10 cm), we also found substantial differences in ET. At all four plots, pixel-level minima of ET were below 0.1 mm·h^{-1}, while the respective maxima were larger than 1.0 mm·h^{-1}. Taking the CV as a measure of within-plot variability in ET, we obtained values of 18.9% (HF1), 16.2% (HF2), 16.4% (HF3) and 16.9% (HF4). These values are lower than the reported within-plot variability of canopy transpiration (31% CV) at the same study plots,

notably at a much coarser spatial resolution of 3 m (Ahongshangbam *et al.*, 2020). Interestingly, when exemplarily resampling our ET maps to 3 m resolution, within-plot variability of ET remains lower (10.9% to 22.0% CV) than reported for transpiration by Ahongshangbam *et al.* (2020). We are not aware of any further studies assessing rainforest (evapo)transpiration at such fine spatial resolution, i.e., at the sub-canopy scale. At the level of individual trees, several studies also point to substantial spatial variability in tree-to-tree transpiration patterns due to differences in tree size (e.g., Kotowska *et al.*, 2021; Meinzer *et al.*, 2005), which introduces spatial variability in stand-scale (evapo)transpiration patterns in dependence of stand density, tree sizes and associated local canopy packing (Ahongshangbam *et al.*, 2020). Overall, we consider the applied UAV-thermography based scheme a powerful tool for the spatially explicit, high-resolution analysis and prediction of ET within and across sites. New generations of UAVs and imaging technology allow for further enhanced spatial resolutions over increasingly large areas, synchronized multi-site campaigns and fully integrated cameras that reduce operation effort and thereby contribute to better temporal coverage.

2.4.2. Prediction of ET

We extracted 16 potential predictor variables via RGB image and point cloud analysis to further examine the drivers of small-scale ET patterns under given climatic conditions. The UAV-based image acquisition and the processing to georeferenced orthomosaics and 3D point clouds followed previously established and tested workflows (Ahongshangbam *et al.*, 2020; Ahongshangbam *et al.*, 2021). In correlation and regression analyses, we found no clear influence of the studied predictors on pixel-level ET across the variable categories vegetation height, height variability, vegetation density and reflectance in any of the four study plots. While many of the studied variables had a significant linear relationship with ET (p <0.05), the models explained less than 5% of the observed variance and thus are not suitable as single predictors of pixel-level ET. To our knowledge, there are no studies available for comparison that examine the influence of forest structural variables on (rain)forest ET patterns at very small, sub-canopy spatial scales. A related UAV-based study in a tropical oil palm agroforest showed an important influence of canopy characteristics on pixel-level predictions of sap flux and stomatal conductance, but the role of structural variables for small-scale patterns was not further assessed (Ellsäßer *et al.*, 2020b).

From results of previous studies at larger spatial scales, i.e., examining tree-to-tree and site-to-site patterns in rainforest (evapo)transpiration, one could well speculate that forest structural

variables may also influence ET under given climatic conditions at very small spatial scales. As such, given previous results that tree-level transpiration mainly scales with tree size (e.g., Meinzer *et al.*, 2005; Kotowska *et al.*, 2021) and that taller vegetation generally has access to windier and more turbulent atmospheric exchange layers (Kricher, 2011), a pattern of increasing ET with increasing vegetation height would seem reasonable. However, the relationships between several available vegetation height variables and pixel-level ET instead suggested no clear influence of vegetation height variables on ET. Likewise, height variability variables such as the canopy relief ratio or the CV_Height had no clear influence on pixel-level ET, despite evidence from studies at larger spatial scales that increasing canopy heterogeneity (as e.g., characterized by the variable canopy roughness length) leads to enhanced (evapo)transpiration (Bauerle *et al.*, 2004; Lawrence *et al.*, 2022; Tan *et al.*, 2019). Similarly, the lack of a clear influence of vegetation density variables such as point cloud density and specifically the derived variable leaf area density on pixel-level ET stands out, with further studies at larger spatial scales reporting enhanced (evapo)transpiration at higher biomass and higher crown leaf density (Ruhoff *et al.*, 2013; Tian *et al.*, 2015).

Reasons for a lack of relationships between small-scale (pixel level) ET and structural canopy variables could be of ecological nature, due to methodological limitations, or a combination of both. From an ecohydrological point of view it is well conceivable that a complex process such as rainforest ET, which is influenced by and interacting with a multitude of micrometeorological, pedological and forest structural processes, among others, is not explained by single structural variables, particularly at such small spatial scales as in our study. Possibly, the heterogeneity and dynamics within the rainforest canopy regarding micrometeorological conditions, tree species and age and associated biomass and leaf area (density), among other factors, are too large and influences of the direct and indirect pixel-level 3D environment (e.g., understory, neighboring pixels) are too prominent to see clear relationships between pixel-level ET and single structural variables. From a methods point of view, the applied UAV-based thermography method is limited to recording the uppermost canopy surface temperature of a given pixel, from which ET is subsequently modeled. It remains unclear how or to what degree ET of the multiple lower canopy strata microclimatically affects land surface temperatures of the recorded upper canopy, and what levels of uncertainty this introduces into remotely sensed ET maps. It also remains disputed how high the contribution of lower canopy strata to (evapo)transpiration in tropical rainforests is in general, with estimates ranging from as low as 20% to as high as 35% (Iida *et al.*, 2020). While the problem is common to all above-canopy thermography methods, studies across several different ecosystems reported high congruence of UAV-derived ET estimates with ground-based reference measurements such as the eddy covariance technique (Aboutalebi *et al.*, 2019; Brenner *et al.*, 2017; Ellsäßer, *et al.*, , 2020a), thus indicating the reliability of the method. Despite such methodological limitations, our study

demonstrates the large potential of bringing together UAV-based thermography and photogrammetry methods for examining the relationship between ecosystem function (ET) and forest structure at very small spatial scales.

The lack of clear linear relationships between pixel-level ET and any of the studied canopy structural variables across all four study plots, point to complex controls potentially involving non-linear relationships and interactions among multiple variables. Indeed, some previous studies reported nonlinearity in ET relationships (e.g., Zhou, 2011; Boers *et al.*, 2015) and one recent study examining remotely sensed ET across 100,000s of pixels also found no clear influences of single topographic, climatic or forest structure variables on ET across a large tropical forest region, concluding that accurate ET prediction is too complex for conventional statistical methods such as linear regressions (Valdés-Uribe *et al.*, 2023). Machine learning approaches are a powerful tool to analyze such large datasets with complex relationships. Machine learning algorithms can be trained to predict ET (or other ecosystem processes) from available ancillary variables, therein often yielding much better prediction performance than conventional prediction methods (e.g., Camps-Valls, 2009; Maxwell *et al.*, 2018; Meyer & Pebesma, 2022). Unlike conventional methods, machine learning models do not give information on predictor significance, effect direction or size; however, an analysis of model feature importance shows the importance of each variable for the overall prediction outcome. There are several machine learning algorithms that are widely applied throughout the environmental sciences (Dou & Yang, 2018; Kanevski, 2009; Lary *et al.*, 2016). Random forest is one of the most popular algorithms and often performs well in ecological contexts (Ahmad *et al.*, 2017; Fernandez-Delgado *et al.*, 2014), e.g., when predicting reference ET, water stress, sap flux, leaf stomatal conductance, net ecosystem exchange or land-cover change (Aide *et al.*, 2013; Dias *et al.*, 2021; Ellsäßer, *et al.*, 2020a; Feng *et al.*, 2017; Reitz *et al.*, 2021; Virnodkar *et al.*, 2020). The random forest algorithm is particularly suitable for spatial predictions and was thus the machine learning algorithm of choice in our study. We applied state-of-the-art techniques such as forward feature selection and target-oriented cross validation to reduce the risk of spatial overfitting (Gasch *et al.*, 2015; Ludwig *et al.*, 2019; Meyer *et al.*, 2018, 2019; Roberts *et al.*, 2017), therein achieving an overall realistic model performance.

In our study, the forward feature selection reduced the dataset for pixel-level ET prediction from the original 16 variables to a final set of 9 to 10 variables per plot, with a relatively high consistency of selection, i.e., eight variables (mostly related to vegetation height) occurred in at least three out of the four models. The similar model performance between training and testing (prediction) outcomes in the subsequent random forest modelling suggests that spatial overfitting did not occur in the models and that they thus can reliably predict ET for locations (i.e., pixels) that were

not part of the model training. Overall, the performance of the random forest models was fair for HF1 and good for the other three study plots (HF2, HF3, HF4), with RMSE between 0.03 (HF1) and 0.05 (HF4) and model prediction accuracies (R^2) between 0.56 (HF1) and 0.65 (HF4).These accuracy metrics are comparable to other studies applying random forest modelling for predictions of ecological target variables such as reference ET (R^2 = 0.91; Dias *et al.*, 2021), daily ET (R^2 = 0.63; Yang *et al.*, 2021), sap flux (R^2 = 0.80) and stomatal conductance (R^2 = 0.50; Ellsäßer, *et al.*, 2020a) as well as actual ET across a large tropical forest region (R^2 = 0.64; Valdés-Uribe *et al.*, 2023).

Variable importance for the random forest model outcome differed across the four study plots, with no clear dominance of any variable or variable category. One to three variables per plot were of very high importance (>75% feature importance for final model outcome), and another one to four variables of high importance (50 – 75%). Therein, variables of high or very high importance came from all variable categories (vegetation height, height variability, vegetation density, reflectance). The most prominently occurring variables of very high importance were GLI (reflectance) followed by CV_height (height variability) followed by Height_abs_min and P75 (vegetation height), LAD (vegetation density) and VARI (reflectance). To our knowledge, there are no studies available for comparison involving such a set of structural canopy variables for predicting ET under given climatic conditions at such small spatial scales. A random forest study predicting ET at much larger spatial scales (70 m pixel size) found a dominant influence of topographic variables, and to a lesser extent of forest structure variables such as the leaf area index, on spatial predictions of ET (Valdes-Uribe, 2023); while climatic variables were found to be of relatively minor importance in that study, some further previous studies, also at much larger spatial scales, successfully applied machine learning techniques to model ET (dynamics) from climatic datasets (Tikhamarine *et al.*, 2019; Granata , 2019). Both the random forest ET study by Valdés-Uribe (2023) and our study show varying variable importance across different studies days in tropical forests, which may (partially) be related to differences in the given climatic conditions. While in our study the reflectance variable GLI was for example of much high variable importance on days receiving less solar irradiance (flights of plots HF1 and HF3) than on sunnier days (HF2 and HF4), the underlying mechanisms of vastly varying variable importance are not yet understood. We consider our study only a first step in understanding and modelling pixel-level ET patterns, with many challenges remaining for future studies on the way to holistic spatial ET models that perform well across all spatial and temporal scales.

We conclude that combining multiple canopy structure variables that can relatively easily be derived from RGB photogrammetry explain substantial parts of the observed variance in pixel-level ET across four lowland rainforest plots in our study, but that much work remains to be done. With

36% to 44% of ET variance remaining unexplained, future studies could further improve our understanding of small-scale (rain)forest ET controls by e.g., including more sophisticated indices characterizing vegetation greenness and plant health (e.g., NDVI) derived from simultaneous high-resolution multi-or hyperspectral UAV imaging. Overall, our study adds to the available knowledge on ET and its drivers that small-scale ET patterns under given climatic conditions can well be predicted from structural variables alone when accounting for complex multiple non-linear relationships.

2.5. Conclusions of the study

At such small spatial scales as in our study (~10 cm pixel size), single ecological variables such as vegetation height or leaf area density still influenced ET but explained very little of the large observed ET variance. In contrast, multiple structural canopy variables together explained large parts of the variance in ET when applying a random forest machine learning approach, wherein no clear prevalence in importance of any single variable or variable category for the ET prediction outcome was found.

References

Aboutalebi, M., Torres-Rua, A. F., McKee, M., Kustas, W. P., Nieto, H., Alsina, M. M., White, A., Prueger, J. H., McKee, L., Alfieri, J., Hipps, L., Coopmans, C., & Dokoozlian, N. (2019). Incorporation of Unmanned Aerial Vehicle (UAV) Point Cloud Products into Remote Sensing Evapotranspiration Models. *Remote Sensing*, 12(1), 50. https://doi.org/10.3390/rs12010050

Agisoft LLC. (2021). *Agisoft Metashape*. Version 1.8. Software retrieved from https://www.agisoft.com/downloads/installer/

Ahmad, M. W., Mourshed, M., & Rezgui, Y. (2017). Trees vs Neurons: Comparison between random forest and ANN for high-resolution prediction of building energy consumption. *Energy and Buildings*, 147, 77-89. https://doi.org/10.1016/j.enbuild.2017.04.038

Ahongshangbam, J., Röll, A., Ellsäßer, F., Hendrayanto, & Hölscher, D. (2020). Airborne tree crown detection for predicting spatial heterogeneity of canopy transpiration in a tropical rainforest. *Remote Sensing*, 12(4). https://doi.org/10.3390/rs12040651

Aide, T. M., Clark, M. L., Grau, H. R., López-Carr, D., Levy, M. A., Redo, D., Bonilla-Moheno, M., Riner, G., Andrade-Núñez, M. J., & Muñiz, M. (2013). Deforestation and Reforestation of Latin America and the Caribbean (2001-2010). *Biotropica*, 45(2), 262-271. https://doi.org/10.1111/j.1744-7429.2012.00908.x

Allan, R. P., Barlow, M., Byrne, M. P., Cherchi, A., Douville, H., Fowler, H. J., Gan, T. Y., Pendergrass, A. G., Rosenfeld, D., Swann, A. L. S., Wilcox, L. J., & Zolina, O. (2020). Advances in understanding large-scale responses of the water cycle to climate change. Annals of the New York *Academy of Sciences*, 1472(1), 49-75. https://doi.org/10.1111/nyas.14337

Almeida, D. R. A. de, Stark, S. C., Shao, G., Schietti, J., Nelson, B. W., Silva, C. A., Gorgens, E. B., Valbuena, R., Papa, D. de A., & Brancalion, P. H. S. (2019). Optimizing the Remote Detection of Tropical Rainforest Structure with Airborne Lidar: Leaf Area Profile Sensitivity to Pulse Density and Spatial Sampling. *Remote Sensing*, 11(1), 92. https://doi.org/10.3390/rs11010092

Andersen, H. E., McGaughey, R. J., & Reutebuch, S. E. (2005). Estimating forest canopy fuel parameters using LIDAR data. *Remote Sensing of Environment*, 94(4), 441-449. https://doi.org/10.1016/j.rse.2004.10.013

Baldocchi, D. D. (2020). How eddy covariance flux measurements have contributed to our understanding of Global Change Biology. *Global Change Biology*, 26(1), 242-260. https://doi.org/10.1111/gcb.14807

Barichivich, J., Gloor, E., Peylin, P., Brienen, R. J. W., Schöngart, J., Espinoza, J. C., & Pattnayak, K. C. (2018). Recent intensification of Amazon flooding extremes driven by strengthened Walker circulation. *Science Advances*, 4(9), eaat8785. https://doi.org/10.1126/sciadv.aat8785

Bauerle, W. L., Bowden, J. D., McLeod, M. F., & Toler, J. E. (2004). Modelling intra-crown and intra-canopy interactions in red maple: Assessment of light transfer on carbon dioxide and water vapor exchange. *Tree Physiology*, 24(5), 589-597. https://doi.org/10.1093/treephys/24.5.589

Boers, N., Marwan, N., Barbosa, H., & Kurths, J. (2015). *How Amazonian deforestation can alter the South American circulation regime: Insights from a non-linear moisture transport model.* 10922. https://ui.adsabs.harvard.edu/abs/2015EGUGA..1710922B

Brenner, C., Thiem, C. E., Wizemann, H.-D., Bernhardt, M., & Schulz, K. (2017). Estimating spatially distributed turbulent heat fluxes from high-resolution thermal imagery acquired with a UAV system. *International Journal of Remote Sensing,* 38(8-10), 3003-3026. https://doi.org/10.1080/01431161.2017.1280202

Bulusu, M., Ellsäßer, F., Ahongshangbam, J., Marquese, I., Hendrayanto, Röll, A., & Hölscher, D. (Under review). UAV-based thermography reveals spatial and temporal variability of evapotranspiration from a tropical rainforest. *Remote Sensing of Environment*.

Camps-Valls, G. (2009). *Machine learning in remote sensing data processing.* IEEE International Workshop on Machine Learning for Signal Processing, 1-6. https://doi.org/10.1109/MLSP.2009.5306233

Clough, Y., Krishna, V. V., Corre, M. D., Darras, K., Denmead, L. H., Meijide, A., Moser, S., Musshoff, O., Steinebach, S., Veldkamp, E., Allen, K., Barnes, A. D., Breidenbach, N., Brose, U., Buchori, D., Daniel, R., Finkeldey, R., Harahap, I., Hertel, D., … Scheu, S.

(2016). Land-use choices follow profitability at the expense of ecological functions in Indonesian smallholder landscapes. *Nature Communications*, 7(1), 13137. https://doi.org/10.1038/ncomms13137

Coronel, C., Tapia Silva, O., Hernández, G., Madrigal, J. M., Rosales, E., Toledo, A., Galeana, M., López Caloca, A., & Silvan, J. L. (2011). Conceptual Elements and Heuristics from Complexity Paradigm Suitable to the Study of Evapotranspiration at the Landscape level. En L. Łabędzki (Ed.), Evapotranspiration. InTechOpen. https://doi.org/10.5772/14056

Dias, S. H. B., Filgueiras, R., Fernandes Filho, E. I., Arcanjo, G. S., Silva, G. H. D., Mantovani, E. C., & Cunha, F. F. D. (2021). Reference evapotranspiration of Brazil modeled with machine learning techniques and remote sensing. *PLOS ONE*, 16(2), e0245834. https://doi.org/10.1371/journal.pone.0245834

Dimitriadou, S., & Nikolakopoulos, K. G. (2021). Evapotranspiration trends and interactions in light of the anthropogenic footprint and the climate crisis: A review. *Hydrology*, 8(4). https://doi.org/10.3390/hydrology8040163

Donat, M. G., Angélil, O., & Ukkola, A. M. (2019). Intensification of precipitation extremes in the world's humid and water-limited regions. *Environmental Research Letters*, 14(6), 065003. https://doi.org/10.1088/1748-9326/ab1c8e

Dou, X., & Yang, Y. (2018). Evapotranspiration estimation using four different machine learning approaches in different terrestrial ecosystems. *Computers and Electronics in Agriculture*, 148, 95-106. https://doi.org/10.1016/j.compag.2018.03.010

Drescher, J., Rembold, K., Allen, K., Beckschäfer, P., Buchori, D., Clough, Y., Faust, H., Fauzi, A. M., Gunawan, D., Hertel, D., Irawan, B., Jaya, I. N. S., Klarner, B., Kleinn, C., Knohl, A., Kotowska, M. M., Krashevska, V., Krishna, V., Leuschner, C., … Scheu, S. (2016). Ecological and socio-economic functions across tropical land use systems after rainforest conversion. *Philosophical Transactions of the Royal Society B: Biological* Sciences, 371(1694), 20150275. https://doi.org/10.1098/rstb.2015.0275

Ellsäßer, F., Röll, A., Ahongshangbam, J., Waite, P. A., Hendrayanto, Schuldt, B., & Hölscher, D. (2020). Predicting tree sap flux and stomatal conductance from drone-recorded surface temperatures in a mixed agroforestry system-a machine learning approach. *Remote Sensing*, 12(24), 1-20. https://doi.org/10.3390/rs12244070

Ellsäßer, F., Röll, A., Stiegler, C., Hendrayanto, & Hölscher, D. (2020). Introducing QWater-Model, a QGIS plugin for predicting evapotranspiration from land surface temperatures. *Environmental Modelling & Software*, 130, 104739. https://doi.org/10.1016/j.envsoft.2020.104739

Ellsäßer, F., Stiegler, C., Röll, A., June, T., Hendrayanto, Knohl, A., & Hölscher, D. (2021). Predicting evapotranspiration from drone-based thermography-a method comparison in a tropical oil palm plantation. *Biogeosciences*, 18(3), 861-872. https://doi.org/10.5194/bg-18-861-2021

Feng, Y., Cui, N., Gong, D., Zhang, Q., & Zhao, L. (2017). Evaluation of random forests and generalized regression neural networks for daily reference evapotranspiration modelling. *Agricultural Water Management*, 193, 163-173. https://doi.org/10.1016/j.agwat.2017.08.003

Fernandez-Delgado, M., Cernadas, E., Barro, S., & Amorim, D. (2014). Do we Need Hundreds of Classifiers to Solve Real World Classification Problems? *Journal of Machine Learning Research*, 15, 3133-3181.

Fisher, J. B., Lee, B., Purdy, A. J., Halverson, G. H., Dohlen, M. B., Cawse-Nicholson, K., Wang, A., Anderson, R. G., Aragon, B., Arain, M. A., Baldocchi, D. D., Baker, J. M., Barral, H., Bernacchi, C. J., Bernhofer, C., Braudy, S. C., Bohrer, G., Brunsell, N., Cappelaere, B., … Hook, S. (2020). ECOSTRESS: NASA's Next Generation Mission to Measure Evapotranspiration From the International Space Station. *Water Resources Research*, 56(4). https://doi.org/10.1029/2019WR026058

García-Martínez, H., Flores-Magdaleno, H., Ascencio-Hernández, R., Khalil-Gardezi, A., Tijerina-Chávez, L., Mancilla-Villa, O. R., & Vázquez-Peña, M. A. (2020). Corn grain yield estimation from vegetation indices, canopy cover, plant density, and a neural network using multispectral and rgb images acquired with unmanned aerial vehicles. *Agriculture* (Switzerland), 10(7), 1-24. https://doi.org/10.3390/agriculture10070277

Gasch, C. K., Hengl, T., Gräler, B., Meyer, H., Magney, T. S., & Brown, D. J. (2015). Spatio-temporal interpolation of soil water, temperature, and electrical conductivity in 3D + T: The Cook Agronomy Farm data set. *Spatial Statistics*, 14, 70-90. https://doi.org/10.1016/j.spasta.2015.04.001

Gitelson, A. A., Kaufman, Y. J., Stark, R., & Rundquist, D. (2002). *Novel Algorithms for Remote Estimation of Vegetation Fraction.* https://digitalcommons.unl.edu/natrespapers/149

Granata, F. (2019). Evapotranspiration evaluation models based on machine learning algorithms—A comparative study. *Agricultural Water Management*, 217, 303-315. https://doi.org/10.1016/j.agwat.2019.03.015

Granier, A., Biron, P., Breda, N., Pontailler, J.-Y., & Saugier, B. (1996). Transpiration of trees and forest stands: Short and long-term monitoring using sapflow methods. *Global Change Biology*, 2(3), 265-274. https://doi.org/10.1111/j.1365-2486.1996.tb00078.x

Harrison, R. D., & Swinfield, T. (2015). Restoration of Logged Humid Tropical Forests: An Experimental Programme at Harapan Rainforest, Indonesia. *Tropical Conservation Science*, 8(1), 4-16. https://doi.org/10.1177/194008291500800103

Iglhaut, J., Cabo, C., Puliti, S., Piermattei, L., O'Connor, J., & Rosette, J. (2019). Structure from Motion Photogrammetry in Forestry: A Review. *Current Forestry Reports*, 5(3), 155-168. https://doi.org/10.1007/s40725-019-00094-3

Iida, S., Shimizu, T., Tamai, K., Kabeya, N., Shimizu, A., Ito, E., Ohnuki, Y., Chann, S., & Levia, D. F. (2020). Evapotranspiration from the understory of a tropical dry deciduous forest in Cambodia. *Agricultural and Forest Meteorology*, 295, 108170. https://doi.org/10.1016/j.agrformet.2020.108170

Kanevski, M. (2009). Machine Learning for Spatial Environmental Data: Theory, Applications, and Software (0 ed.). EPFL Press. https://doi.org/10.1201/9781439808085

Kelliher, F. M., Leuning, R., & Schulze, E. D. (1993). Evaporation and canopy characteristics of coniferous forests and grasslands. *Oecologia*, 95(2), 153-163. https://doi.org/10.1007/BF00323485

Kotowska, M. M., Leuschner, C., Triadiati, T., Meriem, S., & Hertel, D. (2015). Quantifying above- and belowground biomass carbon loss with forest conversion in tropical lowlands of Sumatra (Indonesia). *Global Change Biology*, 21(10), 3620-3634. https://doi.org/10.1111/gcb.12979

Kotowska, M. M., Link, R. M., Röll, A., Hertel, D., Hölscher, D., Waite, P.-A., Moser, G., Tjoa, A., Leuschner, C., & Schuldt, B. (2021). Effects of Wood Hydraulic Properties on Water Use

and Productivity of Tropical Rainforest Trees. *Frontiers in Forests and Global Change*, 3, 598759. https://doi.org/10.3389/ffgc.2020.598759

Kricher, J. (2011). *Tropical Ecology* (Princeton University Press).

Kuhn, M. (2021). *caret: Classification and Regression Training*.

Kundzewicz, Z. W. (2008). Climate change impacts on the hydrological cycle. Ecohydrology & *Hydrobiology*, 8(2-4), 195-203. https://doi.org/10.2478/v10104-009-0015-y

Lary, D. J., Alavi, A. H., Gandomi, A. H., & Walker, A. L. (2016). Machine learning in geosciences and remote sensing. *Geoscience Frontiers*, 7(1), 3-10. https://doi.org/10.1016/j.gsf.2015.07.003

Lawrence, D., Coe, M., Walker, W., Verchot, L., & Vandecar, K. (2022). The Unseen Effects of Deforestation: Biophysical Effects on Climate. *Frontiers in Forests and Global Change*, 5, 756115. https://doi.org/10.3389/ffgc.2022.756115

Louhaichi, M., Borman, M. M., & Johnson, D. E. (2001). Spatially located platform and aerial photography for documentation of grazing impacts on wheat. *Geocarto International*, 16(1), 65-70. https://doi.org/10.1080/10106040108542184

Ludwig, M., Morgenthal, T., Detsch, F., Higginbottom, T.P., Lezama Valdes, M., Nauß, T., & Meyer, H. (2019). Machine learning and multi-sensor-based modelling of woody vegetation in the Molopo Area, South Africa. *Remote Sensing of Environment*, 222, 195-203. https://doi.org/10.1016/j.rse.2018.12.019

Maxwell, A. E., Warner, T. A., & Fang, F. (2018). Implementation of machine-learning classification in remote sensing: An applied review. *International Journal of Remote Sensing,* 39(9), 2784-2817. https://doi.org/10.1080/01431161.2018.1433343

McGaughey, R. (2018). *FUSION/LDV: software for LIDAR data analysis and visualization*.

McGaughey, R. J., & Carson, W. W. (2003). Fusing LIDAR data, photographs and other data using 2D and 4D visutalization techniques. *Proceedings of Terrain Data: Applications and Visualization-Making the Connection*, 16-24.

Meinzer, F. C., Bond, B. J., Warren, J. M., & Woodruff, D. R. (2005). Does water transport scale universally with tree size? *Functional Ecology*, 19(4), 558-565. https://doi.org/10.1111/j.1365-2435.2005.01017.x

Meyer, H., Reudenbach, C., Hengl, T., Katurji, M., & Nauss, T. (2018). Improving performance of spatio-temporal machine learning models using forward feature selection and target-oriented validation. *Environmental Modelling & Software*, 101, 1-9. https://doi.org/10.1016/j.envsoft.2017.12.001

Meyer, H., Reudenbach, C., Wöllauer, S., & Nauss, T. (2019). Importance of spatial predictor variable selection in machine learning applications – Moving from data reproduction to spatial prediction. *Ecological Modelling*, 411, 108815. https://doi.org/10.1016/j.ecolmodel.2019.108815

Mutlu, M. (2006). *Mapping surface fuels using lidar and multispectral data fusion for fire behavior modelling* (Número December). Texas A&M University.

Nelson, J. A., Pérez-Priego, O., Zhou, S., Poyatos, R., Zhang, Y., Blanken, P. D., Gimeno, T. E., Wohlfahrt, G., Desai, A. R., Gioli, B., Limousin, J., Bonal, D., Paul-Limoges, E., Scott, R. L., Varlagin, A., Fuchs, K., Montagnani, L., Wolf, S., Delpierre, N., … Jung, M. (2020). Ecosystem transpiration and evaporation: Insights from three water flux partitioning methods across FLUXNET sites. *Global Change Biology*, 26(12), 6916-6930. https://doi.org/10.1111/gcb.15314

QGIS Development Team. (2020). *QGIS Geographical Information System*. Open-Source Geospatial Foundation Project.

Rauneker, P., & Lischeid, G. (2012). *Spatial distribution of water stress and evapotranspiration estimates using an unmanned aerial vehicle (UAV)*. 10477. https://ui.adsabs.harvard.edu/abs/2012EGUGA..1410477R

Raymond Hunt, E., Daughtry, C. S. T., Eitel, J. U. H., & Long, D. S. (2011). Remote sensing leaf chlorophyll content using a visible band index. *Agronomy Journal*, 103(4), 1090-1099. https://doi.org/10.2134/agronj2010.0395

Reitz, O., Graf, A., Schmidt, M., Ketzler, G., & Leuchner, M. (2021). Upscaling Net Ecosystem Exchange Over Heterogeneous Landscapes With Machine Learning. Journal of Geophysical Research: *Biogeosciences*, 126(2). https://doi.org/10.1029/2020JG005814

Rembold, K., Mangopo, H., Tjitrosoedirdjo, S. S., & Kreft, H. (2017). Plant diversity, forest dependency, and alien plant invasions in tropical agricultural landscapes. *Biological Conservation*, 213, 234-242. https://doi.org/10.1016/j.biocon.2017.07.020

Roberts, D. R., Bahn, V., Ciuti, S., Boyce, M. S., Elith, J., Guillera-Arroita, G., Hauenstein, S., Lahoz-Monfort, J. J., Schröder, B., Thuiller, W., Warton, D. I., Wintle, B. A., Hartig, F., & Dormann, C. F. (2017). Cross-validation strategies for data with temporal, spatial, hierarchical, or phylogenetic structure. *Ecography*, 40(8), 913-929. https://doi.org/10.1111/ecog.02881

Röll, A., Niu, F., Meijide, A., Ahongshangbam, J., Ehbrecht, M., Guillaume, T., Gunawan, D., Hardanto, A., Hendrayanto, Hertel, D., Kotowska, M. M., Kreft, H., Kuzyakov, Y., Leuschner, C., Nomura, M., Polle, A., Rembold, K., Sahner, J., Seidel, D., … Hölscher, D. (2019). Transpiration on the rebound in lowland Sumatra. *Agricultural and Forest Meteorology*, 274, 160-171. https://doi.org/10.1016/j.agrformet.2019.04.017

Ruhoff, A. L., Paz, A. R., Aragao, L. E. O. C., Mu, Q., Malhi, Y., Collischonn, W., Rocha, H. R., & Running, S. W. (2013). Assessment of the MODIS global evapotranspiration algorithm using eddy covariance measurements and hydrological modelling in the Rio Grande basin. *Hydrological Sciences Journal*, 58(8), 1658-1676. https://doi.org/10.1080/02626667.2013.837578

Schlesinger, W. H., & Jasechko, S. (2014). Transpiration in the global water cycle. *Agricultural and Forest Meteorology*, 189-190, 115-117. https://doi.org/10.1016/j.agrformet.2014.01.011

Stiegler, C. (2021). A03_Reki Meteo Data 2017 (2) [Data set]. Göttingen Research Online / Data. https://doi.org/10.25625/CXMO3O

Tan, Z.-H., Zhao, J.-F., Wang, G.-Z., Chen, M.-P., Yang, L.-Y., He, C.-S., Restrepo-Coupe, N., Peng, S.-S., Liu, X.-Y., Da Rocha, H. R., Kosugi, Y., Hirano, T., Saleska, S. R., Goulden, M. L., Zeng, J., Ding, F.-J., Gao, F., & Song, L. (2019). Surface conductance for evapotranspiration of tropical forests: Calculations, variations, and controls. *Agricultural and Forest Meteorology*, 275, 317-328. https://doi.org/10.1016/j.agrformet.2019.06.006

Tarigan, S., Stiegler, C., Wiegand, K., Knohl, A., & Murtilaksono, K. (2020). Relative contribution of evapotranspiration and soil compaction to the fluctuation of catchment discharge:

Case study from a plantation landscape. *Hydrological Sciences Journal*, 65(7), 1239-1248. https://doi.org/10.1080/02626667.2020.1739287

TeAX Technology. (2021). *ThermalCapture.*

Tian, X., Van Der Tol, C., Su, Z., Li, Z., Chen, E., Li, X., Yan, M., Chen, X., Wang, X., Pan, X., Ling, F., Li, C., Fan, W., & Li, L. (2015). Simulation of Forest Evapotranspiration Using Time-Series Parameterization of the Surface Energy Balance System (SEBS) over the Qilian Mountains. *Remote Sensing*, 7(12), 15822-15843. https://doi.org/10.3390/rs71215806

Tikhamarine, Y., Malik, A., Kumar, A., Souag-Gamane, D., & Kisi, O. (2019). Estimation of monthly reference evapotranspiration using novel hybrid machine learning approaches. *Hydrological Sciences Journal*, 64(15), 1824-1842. https://doi.org/10.1080/02626667.2019.1678750

Timmermans, W. J., Kustas, W. P., & Andreu, A. (2015). Utility of an Automated Thermal-Based Approach for Monitoring Evapotranspiration. *Acta Geophysica*, 63(6), 1571-1608. https://doi.org/10.1515/acgeo-2015-0016

Torres, A. F., Walker, W. R., & McKee, M. (2011). Forecasting daily potential evapotranspiration using machine learning and limited climatic data. *Agricultural Water Management*, 98(4), 553-562. https://doi.org/10.1016/j.agwat.2010.10.012

Trenberth, K. E. (1999). *Conceptual Framework for Changes of Extremes of the Hydrological Cycle With Climate Change.* En Weather and Climate Extremes (pp. 327-339). Springer Netherlands. https://doi.org/10.1007/978-94-015-9265-9_18

Valavi, R., Elith, J., Lahoz-Monfort, J.J., Guillera-Arroita, G. (2018). blockCV: An r package for generating spatially or environmentally separated folds for k-fold cross-validation of species distribution models. *Methods in Ecology and Evolution* 10:225-232.

Valdés-Uribe, A., Hölscher, D., & Röll, A. (2023). ECOSTRESS reveals the importance of topography and forest structure for evapotranspiration from a tropical region of the Andes. *Remote Sensing.*

Virnodkar, S. S., Pachghare, V. K., Patil, V. C., & Jha, S. K. (2020). Remote sensing and machine learning for crop water stress determination in various crops: A critical review. *Precision Agriculture*, 21(5), 1121-1155. https://doi.org/10.1007/s11119-020-09711-9

Wei, T., & Simko, V. (2021). *R package «corrplot»: Visualization of a Correlation Matrix.*

Westoby, M. J., Brasington, J., Glasser, N. F., Hambrey, M. J., & Reynolds, J. M. (2012). 'Structure-from-Motion' photogrammetry: A low-cost, effective tool for geoscience applications. *Geomorphology*, 179, 300-314. https://doi.org/10.1016/j.geomorph.2012.08.021

Williams, C. A., Reichstein, M., Buchmann, N., Baldocchi, D., Beer, C., Schwalm, C., Wohlfahrt, G., Hasler, N., Bernhofer, C., Foken, T., Papale, D., Schymanski, S., & Schaefer, K. (2012). Climate and vegetation controls on the surface water balance: Synthesis of evapotranspiration measured across a global network of flux towers. *Water Resources Research*, 48(6). https://doi.org/10.1029/2011WR011586

Yang, Y., Sun, H., Xue, J., Liu, Y., Liu, L., Yan, D., & Gui, D. (2021). Estimating evapotranspiration by coupling Bayesian model averaging methods with machine learning algorithms. *Environmental Monitoring and Assessment*, 193(3), 156. https://doi.org/10.1007/s10661-021-08934-1

Yeh, P. J. -F., & Wu, C. (2018). Recent Acceleration of the Terrestrial Hydrologic Cycle in the U.S. Midwest. *Journal of Geophysical Research: Atmospheres*, 123(6), 2993-3008. https://doi.org/10.1002/2017JD027706

Zhou, M. (2011). Estimates of Evapotranspiration and Their Implication in the Mekong and Yellow River Basins. En L. Łabędzki (Ed.), *Evapotranspiration*. InTechOpen. https://doi.org/10.5772/14791

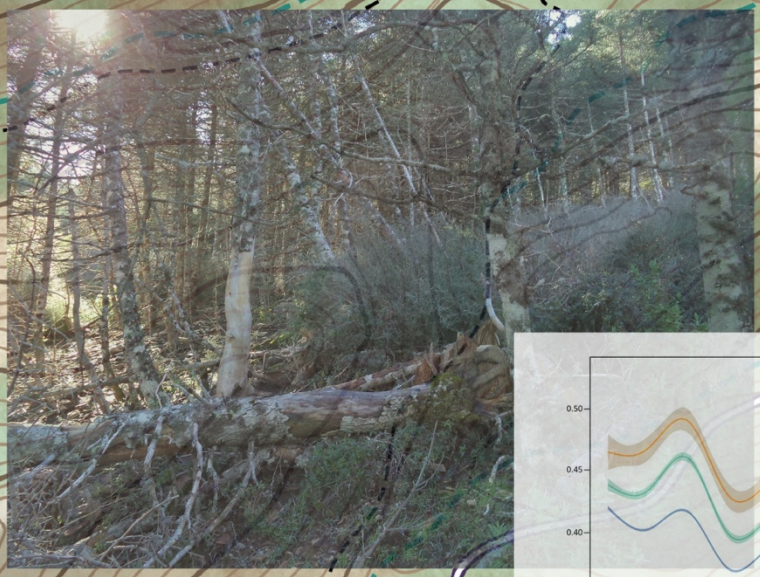

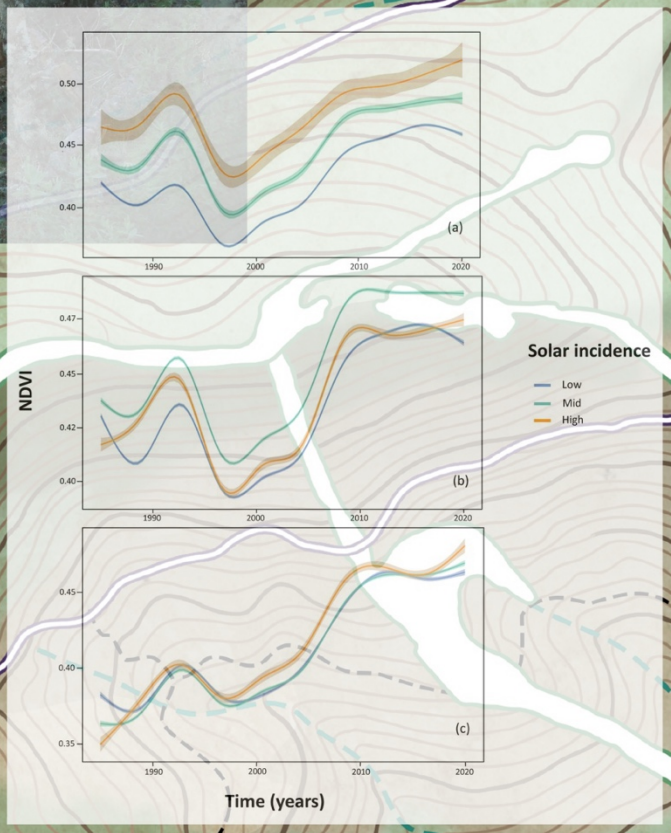

CHAPTER 3

STUDY 2

Unexpected resilience in relict *Abies pinsapo* Boiss. forests to dieback and mortality induced by climate change

3

Abstract

Acute and early symptoms of forest dieback linked to climate warning and drought episodes have been reported for relict *Abies pinsapo* Boiss. fir forests from Southern Spain, particularly at their lower ecotone. Satellite, orthoimages, and field data were used to assess forest decline, tree mortality, and gap formation and recolonization in the lower half of the altitudinal range of *A. pinsapo* forests (850-1550 m) for the last 36 years (1985-2020). Field surveys were carried out in 2003 and 2020 to characterize changes in stand canopy structure and mortality rates across the altitudinal range. Time series of the Normalized Difference Vegetation Index (NDVI) at the end of the dry season (derived from Landsat 5 and 7 imagery) were used for a Dynamic Factor Analysis to detect common trends across altitudinal bands and topographic solar incidence gradients (SI). Historical canopy cover changes were analyzed through aerial orthoimages classification. Here we show that extensive decline and mortality contrast to the almost steady alive basal area for 17 years, as well as the rising photosynthetic activity derived from NDVI since the mid-2000s and an increase in the forest canopy cover in the late years at mid and high altitudes. We hypothesized that these results suggest an unexpected resilience in *A. pinsapo* forests to climate change-induced dieback, that might be promoted by compensation mechanisms such as (i) recruitment of new *A. pinsapo* individuals; (ii) facilitative effects on such recruitment mediated by revegetation with other species; and (iii) a 'release effect' in which surviving trees can thrive with fewer resource competition. Future research is needed to understand these compensation mechanisms and their scope in future climate change scenarios.

Cortés-Molino Á., Linares J.C., Viñegla B., Lechuga V., Salvo-Tierra A.E., Flores-Moya A., Fernández-Luque I., and Carreira, J.A. (2022) Unexpected resilience in relict *Abies pinsapo* Boiss. forests to dieback and mortality induced by climate change. *Frontiers in Plant Science* 13:991720. https://doi.org/10.3389/fpls.2022.991720

3.1. Introduction

Extreme climate events such as severe droughts and heat waves are expected to increase due to climate change (Jentsch & Beierkuhnlein, 2008; Swain *et al.*, 2020), thus challenging the adaptive capacity of forests worldwide to these new scenarios (Lindner *et al.*, 2010). Disturbances are an essential component of forest ecosystem dynamics (Attiwill, 1994) that plays an important role in tree recruitment and turnover, and in stand canopy structure and compositional changes (Seidl *et al.*, 2011; Kuuluvainen *et al.*, 2021). Minor disturbances at the local scale promote forest gap opening and subsequent closing processes which, due to spatio-temporal asynchronies, results in landscape diversification and shifting-mosaic and patch dynamics at the landscape meta-scale (Picket & White, 1985). However, the increasing occurrence and severity of climate extreme events might threaten these natural disturbance dynamics and compromise both forest resistance and resilience capabilities (Gazol *et al.*, 2018a).

Resistance has been defined as the ability of ecological systems to persist or minimize damage through a disturbance event (Connell & Ghedini, 2015; Sánchez-Pinillos *et al.*, 2019). Once disturbance drivers are alleviated, the ecosystem's capacity and speed of recovery, or resilience (Gunderson, 2000), has been assessed through three approaches: from an engineering point of view, which considers a single stability state; from an ecological perspective based on the existence of multiple stabilities; and under a social-ecological criterion which assumes the maintenance of the current state (Nikinmaa *et al.*, 2020). Resistance and resilience are key concepts to understanding ubiquitous forest dieback processes currently observed at the global scale (Allen *et al.*, 2010), and to assess an increasing vulnerability to tree mortality and forest die-off from hotter drought in the Anthropocene (Allen *et al.*, 2015). Climate-driven forest decline and its consequences in terms of reduced tree- growth, increased mortality, and forecasted distributional shifts at lower ecotones have been intensively studied in the last decades (e.g., Linares *et al.*, 2009a; Camarero *et al.*, 2015; Restaino *et al.*, 2019). However, much less attention has been paid to the resilience component following drought-induced dieback events, including recovery processes at the individual (tree-growth responses; Gazol *et al.*, 2018b; DeSoto *et al.*, 2020) and community (forest vegetation recovery; Lloret *et al.*, 2004, Lloret *et al.*, 2012) levels. This is surprising since it is well known that the post-mortality phase following other types of disturbances, such as wildfires and land-use change, is key to understanding the mid-to long-term consequences in terms of species abundance changes and compositional shifts (Guo *et al.*, 2018; Yu *et al.*, 2019; Coop *et al.*, 2020).

Post-mortality dynamics may just result in minor changes in the spectrum of functional traits at the community level, but with the persistence of the main structure of the system; that is, the previously dominant tree species maintains its dominant/co- dominant status through the growth of survivor adults and regeneration (Suarez & Lloret, 2018). Or it may lead to local extinctions of more drought-vulnerable species, replacement by drought-resistant ones, and thus to state shifts if the forest ecosystem is forced beyond its resistance and resilience limits (Anderegg *et al.*, 2013). Under recurrent extreme climate events, the whole landscape structure can change, even turning forests into shrublands, as has been reported, among others, for Mediterranean cork oak (*Quercus suber* L.) forests turning to *Cistus ladanifer* L. shrub formations under persistent drought scenarios and recurrent wildfires in South Portugal (Acácio *et al.*, 2009). All these consequences may be especially detrimental for relict and endangered tree species, whose current distribution areas usually hold environmental conditions near their tolerance limits (Hampe & Jump, 2011).

Assessing post-mortality forest recovery and compositional shifts is hampered by the fact that mortality events tend to be patchy and regeneration trajectories heterogeneous across a range of spatio-temporal scales (Breshears *et al.*, 2009). Thus, to achieve a comprehensive characterization of post-drought forest resilience, a combination of methodological approaches, including both field plot-based and remotely sensed data, is needed (Dorman *et al.*, 2015; Gazol *et al.*, 2018b). The spatial resolution of available long-term satellite data (e.g., 30m pixel size for Landsat data) is coarser than needed to account for detailed canopy structural changes (e.g., gap dynamics, canopy height) and demographics processes (e.g., regeneration) at the stand level. Thus, multi-temporal aerial photographs combined with sequential field sampling are also used to gather both spatially extensive information and detailed plot-based data which together inform on changes in gap dynamics, mortality rates, tree status, forest density, and basal area (Vilà-Cabrera *et al.*, 2012; Bagus-kas *et al.*, 2014). These complementary measures can help answer if drought-induced mortality and subsequent tree growth and regeneration of the dominant tree species, and gap colonization by other species, scale up or not too persistent changes in vegetation composition and productivity.

Abies pinsapo Boiss. is a climate-relict fir species, endemic to the SW of the Iberian Peninsula, which is currently subjected to a Mediterranean-type climate seasonality. Its relict and endemic nature together with its climatic sensitivity render *A. pinsapo* the most vulnerable tree species of the Iberian Peninsula (Arista *et al.*, 2011), and as one of the most vulnerable fir species among the group of Circum-Mediterranean firs, to drought-induced growth decline and mortality (Sánchez-Salguero *et al.*, 2015). As early as the beginning of the 1990s, severe decline and extensive dieback symptoms were reported in the largest of the remaining *A. pinsapo* populations (Yunquera Forest,

Sierra de las Nieves National Park) (Linares *et al.*, 2009a), which have been associated to recurrent droughts and long-term warming trends (Linares *et al.*, 2011). Recurrent dieback events, observationally showing complex spatio-temporal dynamics, have taken place since then and continue today (Navarro-Cerrillo *et al.*, 2022). Therefore, this forest provides a unique opportunity to study the resilience component of vulnerability throughout a three-decade-long process of dieback events and post-mortality dynamics affecting a highly drought-sensitive tree species.

This work focuses on the study case of *A. pinsapo* at the Yunquera forest and aims to assess its conservation status by (i) characterizing the spatio-temporal dynamics of forest productivity at the landscape level using Landsat NDVI time series, (ii) characterizing the spatio-temporal balance of canopy gaining/loss through aerial orthoimages, and (iii) assessing changes in *A. pinsapo* tree status and mortality at the forest stand level through two field sampling campaigns separated in time by almost two decades.

3.2. Materials & methods

3.2.1. Study site and field survey

The study site was placed in the Yunquera pinsapo forest, the largest remaining forest patch of the Spanish fir (*A. pinsapo*). We chose this location because (i) it hosts most of the current *A. pinsapo* populations; (ii) it was the first one where conservation measures were adopted because of public ownership of the forest; and (iii) acute episodes of decline and stand stagnation have been observed there since 1994 (Linares *et al.*, 2009b; Navarro-Cerrillo *et al.*, 2022).

At present, *A. pinsapo* total distribution area is approx. 4000 ha in north-facing slopes above 900 m a.s.l. at coastal mountains of the Baetic Range, including somewhat continuous *A. pinsapo* forest patches (accounting for approx. 2000 ha) as well as the presence of isolated trees and small stands. This tree species is included on the IUCN Red List of Threatened Species as 'Endangered' (Arista *et al.*, 2011) and is declared as 'At risk of extinction' under regional government law (Boletín Oficial de la Junta de Andalucía, 2011).

The annual mean temperature is 14.7 ºC and annual precipitation ranges from 800 – 1600 mm in the Yunquera forest. Rainfall patterns are distinctly Mediterranean, with approx. 80% of annual precipitation falling from October to May, followed by a long summer drought.

The study area was delimited as the masks within the Yunquera forest defined as 'dominantly or pure and well- structured *A. pinsapo* forests' (70-100% of *A. pinsapo* cover; Navarro Cerrillo *et al.*, 2013) in the GIS of the Programme for the Recovery of *Abies pinsapo* (Andalusian regional government: https://www.juntadeandalucia.es/medioambiente/portal/). Areas with mixed stands (with *Quercus sp* and *Pinus halepensis* Mill.) and scattered *A. pinsapo* trees within the Yunquera forest were thus excluded from the study to avoid confusing results. Overall, the studied forest stands comprise over 300 ha and an 800 – 1550 m altitudinal gradient (Fig. 1).

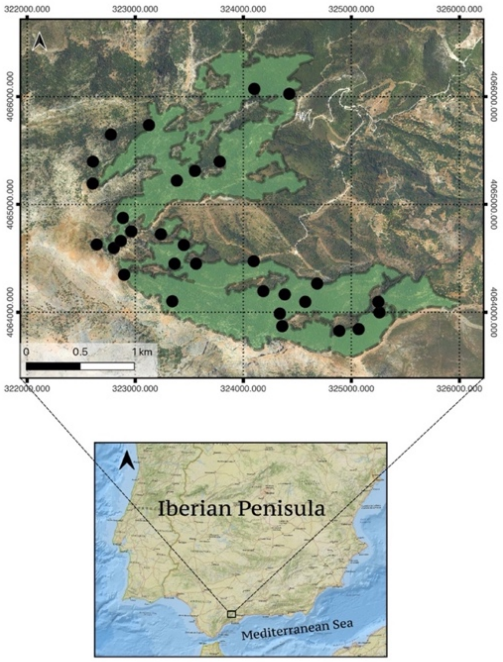

Figure 3.1. Study site location, Sierra de las Nieves National Park (Andalusia, Spain). Green color patches show the areas of pure *Abies pinsapo* stands in the Yunquera forest (ca. 300 ha) used for both the Landsat and orthomosaic multitemporal analyses (resulting from the application of a -30m buffer to the pure *Abies pinsapo* mask to preclude the problem of mixed pixels; see 2.2 section). Black dots denote the location of the 31 plots used in the 2003 and 2020 field surveys. Since the 'grain' component of the study scale in the remote sensing approach -30mx30m for Landsat imagery- is coarser than that applied in the field-survey approach, some small pure stands included in the field-survey were excluded after applying the -30m buffer and are not accounted for in the Landsat imagery analysis. Therefore, a few black dots in the Figure are outside the green area. The coordinate system employed was EPSG:25830 - ETRS89/UTM zone 30N.

The field surveys were performed in 2003 and 2020. The plots were selected using an extensive, stratified random sampling, in equifrequent classes every 200 m in elevation. We sampled the same thirty-one *A. pinsapo* plots (150 m^2) both in 2003 (Linares & Carreira, 2009) and 2020. Due to technical limitations in 2003 survey, we measured different trees for both surveys through random sampling within plots. We recorded tree diameter (considering only trees with diameter at breast height DBH > 3 cm), basal area, and recent mortality. In both surveys, environmental variables (elevation, aspect, soil type, topography, structure, overstorey, and understory types) and biotic variables (basal area of *A. pinsapo* stumps, living and dead trees) were recorded. Data on dead trees refer to those which had died recently, i.e., since the late 1990s according to dendrochronological estimates based on a previous work that correlated visual wood decay status with dendrochronological death date (Linares *et al.*, 2010b). Declining and dead trees were classified according to dieback (defoliation, needles brownness) and bark/wood decay symptoms: Class 1 for > 2/3 of the crown green and retaining needles, Class 2 for defoliation in 1/3 of the crown, Class 3 for severe defoliation and brown needles, Class 4 for a total loss of needles and thin branches, Class 5 for a total loss of medium branches and almost absent bark, and Class 6 for stumps (Fig. S3.1). Two ANOVAs were performed: one to detect BAI tree classes changes in both field surveys and another to study BAI per altitudinal bands. In this second one, tree classes were grouped by Alive, Dead, and Stumps.

3.2.2. Climatic and radiation data

To quantify climate-growth relationships, monthly mean temperature (T, units in °C; 0.25° resolution) and radiation (R, units in $W \cdot m^{-2}$) were downloaded from the EOBS database v23.1e for the period 1985–2020 (Haylock *et al.*, 2008) using the Climate Explorer webpage (https://climexp.knmi.nl/). To quantify drought severity, we used the Standardized Evapotranspiration Precipitation Index (SPEI; Beguería *et al.*, 2014). SPEI is a powerful tool for supporting drought tolerance monitoring since it is built on a climatic water balance (Vicente- Serrano *et al.*, 2010). Xu *et al.* (2018) applied SPEI to study severe drought responses in southwestern USA forests, based on several canopy traits. This index is a multi-scalar index that quantifies drought intensity based on the difference between precipitation and atmospheric evaporative demand for different periods, with negative values indicating drier-than-average conditions, and positive figures for wetter-than-average conditions. SPEI data were also obtained from the Climate Explorer webpage and downloaded at 0.5° resolution. All the variables were averaged at the seasonal time scale: prior autumn ('aup'; including September, October, and November of the previous year), winter ('wi';

December of the previous year, January, and February), spring ('sp'; March, April, and May) and summer ('su'; June, July, and August). Autumn of the current year was not included as NDVI data were obtained for August-September (see below).

3.2.3. Dynamic factor analysis of Landsat data series (1985 – 2020)

The Normalized Difference Vegetation Index (NDVI) has been used as a proxy of vegetation biomass and forest physiological performance (Wang & Tenhunen, 2004), that is sensitive to drought and changes in forest structure (Gazol *et al.*, 2018b), and allows capturing post-disturbance recovery by time series analysis (Kennedy *et al.*, 2010). The behavior of time series can be reported through the estimation of common trends, which are patterns in data that highlight relevant changes along the series.

We run Semiautomatic Classification Plugin (SCP) from QGIS software to obtain the satellite images, acquired from Landsat 5 and 7 for 36 years (1985-2020). We employed red (0.63 - 0.69 μm) and near-infrared (0.77 - 0.90 μm) spectra data with 30m spatial resolution. For each year, we obtained the first free cloud image available from the mid-August to mid- September period, since it corresponds to the end of the dry season, when biomass and NDVI are better correlated (González-Alonso *et al.*, 2006; Vaglio Laurin *et al.*, 2016). The data were radiometrically normalized, stacked, clipped with the *A. pinsapo* 'pure and well-structured forests' vector layer, and then the normalized difference vegetation index-NDVI was calculated. To minimize the edge effect in the satellite images caused by a 30 m pixel size, the layer mask was buffered -30m, and excluded perimetral pixels, so we were theoretically able to ensure dense *A. pinsapo* forest pixels.

Altitude and solar incidence (monthly sunshine levels at each pixel corrected by slope, facing, and relief shadowing effects, expressed in hours; 'SI' hereafter; Guerrero *et al.*, 2014) have been reported as the main factors conditioning *A. pinsapo* presence according to niche distribution models (Navarro-Cerrillo *et al.*, 2021). Thus, the pixels of the final satellite layers were further assigned to three altitudinal bands and three solar radiation incidence value ranges. For this, we first created a precise Digital Terrain Model (DTM) of the area using aerial LIDAR point cloud data with 0.5 points·m^{-2} resolution, obtained in 2015 by the PNOA project of the Spanish National Geographic Institute (https://centrodedescargas.cnig.es/CentroDescargas/catalogo.do?Serie=LIDAR). FUSION software was employed for point cloud processing, following the guidelines of McGaughey & Carson (2003). We extracted bare ground point cloud to create the DTM, and Landsat pixels

were clipped into three elevation bands: 880-1150 m, 1150-1350 m, and 1350-1550 m (hereafter denoted as the 1150 m, 1350 m, and 1550 m altitudinal bands). Then, we used SI data extracted from a raster layer generated by the Andalusian Digital Solar Incidence Model (REDIAM website of the Andalusian Regional Government; https://portalrediam.cica.es/geonetwork/srv/api /records/cb75e8c3eb1bcca6df28f57809d652736fad7572). We selected November data since correlation with *Abies pinsapo* distribution is the highest for this month, even to correctly predict the presence of a few isolated trees in small patches (i.e, shady gullies) within extensive areas with no *A. pinsapo* fir (personal communication; J.B. López-Quintanilla, *A. pinsapo* regional coordinator). SI data files were also ranged into three values intervals (0-46 h, 46-130 h, 130-175 h; hereafter denoted as the 46 h, 130 h, and 175 h SI ranges) to mask the elevation bands and create layers to finally clip the satellite data along the 36 years by the altitudinal bands and SI range.

A total of 324 Landsat images were processed; they were stacked, converted to data frames, and extracted the mean and standard deviation for every year of each vegetation index. The final output (NDVI time series for each pixel by SI and altitudinal values) was subjected to Dynamic Factor Analysis (DFA), both on raw and on standardized NDVI data, to find common temporal trends by running Brodgar software (Zuur *et al.*, 2007). DFA is a robust procedure to find common trends in time series and has been widely used in fisheries (Zuur *et al.*, 2003; Ogle, 2018) and landscape monitoring (Campo-Bescós *et al.*, 2013). Finally, to assess the effects of SI and altitude on NDVI time series we used repeated measures ANOVA with its subsequent Bonferroni pairwise comparison test.

3.2.4. Linear mixed effect models

We fitted linear mixed-effects models (LMEM, thereafter) using the nlme package in R software (R Development Core Team 2021) for *A. pinsapo*-dominated forests NDVI along three elevation bands: low elevation (880-1150 m a.s.l.), mid elevation (1150-1350 m a.s.l.) and high elevation (1350-1550 m a.s.l.). In order to test for heteroscedasticity, residuals were tested against observed values, predicted values, time calendar, elevation, and first-order autocorrelation. Climate variables such as seasonal data of temperature, radiation and SPEI (see section 2.2) were included as fixed factors, and each NDVI pixel from the elevation bands was included as a random factor. The covariance parameters were estimated using the restricted maximum likelihood method, which makes estimates of parameters by minimizing the likelihood of residuals from the fitting of the fixed effects portion of the model (see further details in Zuur *et al.*, 2009). For both DFA and LMEM

analyses, we used an information-theoretic approach for multi-model selection, based on the Akaike Information Criterion (AIC) corrected for small sample sizes (AICc). DAICc represents the difference between the lowest AICc observed (best fitting model) and those of each sequent model tested, being the model with DAICc = 0 the best model observed. However, all the models with DAICc < 2 have similar substantial support. Therefore, the models among them with a smaller number of explanatory variables were finally selected, following the maximum parsimony criteria (Burnham & Anderson, 2002). Residuals pattern (correlation) was tested for observed values, model predictions, time (calendar year), elevation, and first-order autocorrelation (i.e., the correlation between model residuals for the year i and the observed NDVI in the year i-1). Temporal trends of the residuals were modelled by the Loess smoothing method using a polynomial weight function of degree 3.

3.2.5. Spatio-temporal dynamics of canopy loss and gap opening

We used historical orthoimages (obtained by aircraft through the PNOA project), masked with the *A. pinsapo* distribution vector layer, to study the spatio-temporal dynamics of *A. pinsapo* cover changes (gap opening and recovery) along the study area. Due to limitations in the number of years of data capture and varying image qualities among the available years, the final set of images was limited to the ten years 1977, 1984, 1998, 2002, 2004, 2007, 2010, 2013, 2016, and 2019. All the orthoimages were resampled to 1 m of pixel size. The SegOptim R package (Gonçalves *et al.*, 2019) was applied to run a segmentation and turn the pixels into objects using Object Based Image Analysis (OBIA) technique, and then to classify the orthoimages through a random forests algorithm, with mean, standard deviation and first and third quartiles as classification features. Each orthoimage was classified into three cover classes: Shrubs (Class 1), forest canopies (Class 2), and bare ground or grasslands (Class 3). A minimum of 70 training plots per cover class and per year were selected by photointerpretation and used to assess classification accuracy (confusion matrices) using the SegOptim package. The time series of classified orthoimages were used to quantify cover changes (rate of canopy loss and recovery) through time at each of the three defined altitudinal bands.

3.3. Results

3.3.1. Climatic data and field survey

Both mean temperature and radiation data have shown a rising tendency in the last decades, especially since the 1970s (Fig. S3.2A, B). Drought intensity has also increased, especially after 2002. The last four years of the time series (2017-2020) had the lowest SPEI values, indicating a recent tendency to even more intense drought spells (Fig. S3.2C).

Across altitudinal bands, the average total *A. pinsapo* basal area was 36.0 $m^2 \cdot ha^{-1}$ in the 2003 field survey, and still alive trees (dieback classes 1, and 2), dead trees (classes 3, 4, and 5) and stumps (class 6) accounted for 79.7, 10.0, and 10.3% of the total basal area (Fig. S3.2). The basal area accounted for each tree-class had not significantly changed almost two decades later ($p > 0.05$, Table S3.1). In 2020, dead trees and stumps still accounted for more than 20% of the total basal area. Alive trees (classes 1 and 2) together remained the dominant ones in the population, and the basal area of more recently dead trees (classes 3-4) showed values like those observed in 2003 (Fig. 3.2). Alive trees showed a higher basal area at mid than at low and high altitudes both in 2003 and 2020 (Fig. 3.3). Meanwhile, declining, and dead trees had also not changed between these two sampling years (Table S3.2). Mortality only was higher in the 2020 mid elevation compared to the 2003 high elevation band.

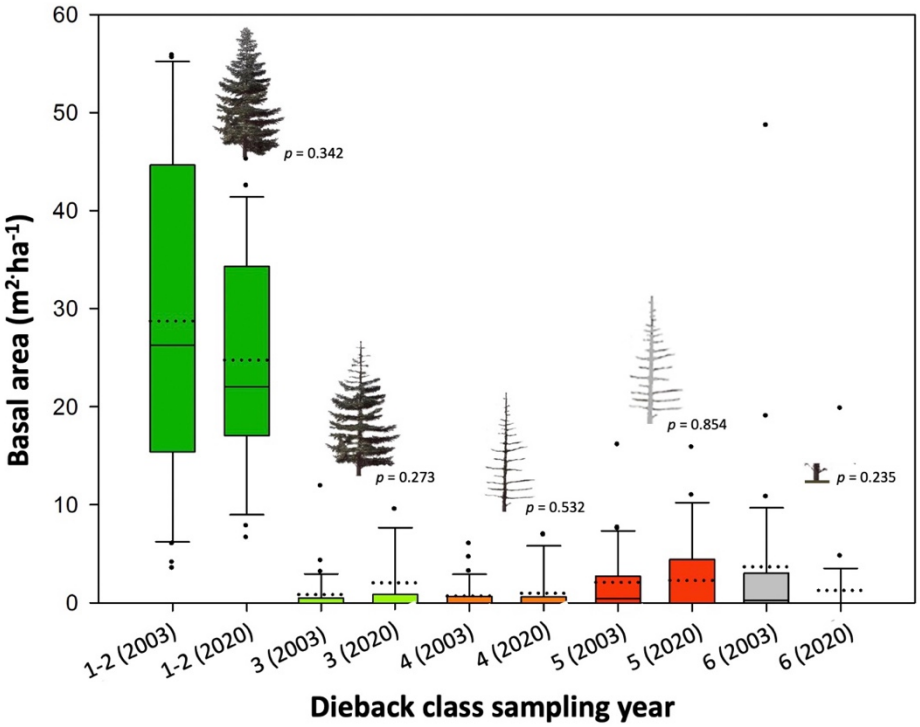

Figure 3.2. Total basal areas for the different tree classes, as obtained in the 2003 and 2020 field surveys performed on thirty-one *A. pinsapo* stands. Alive (tree-class 1); declining (class 2); and dead trees (classes 3 to 6) were classified according to canopy dieback (defoliation, needles brownness) and bark/wood decay symptoms (see also Fig. S3.1). An ANOVA was performed to compare the basal areas between years within damage class. *p*-values are indicated for each comparison (see also Table S3.1).

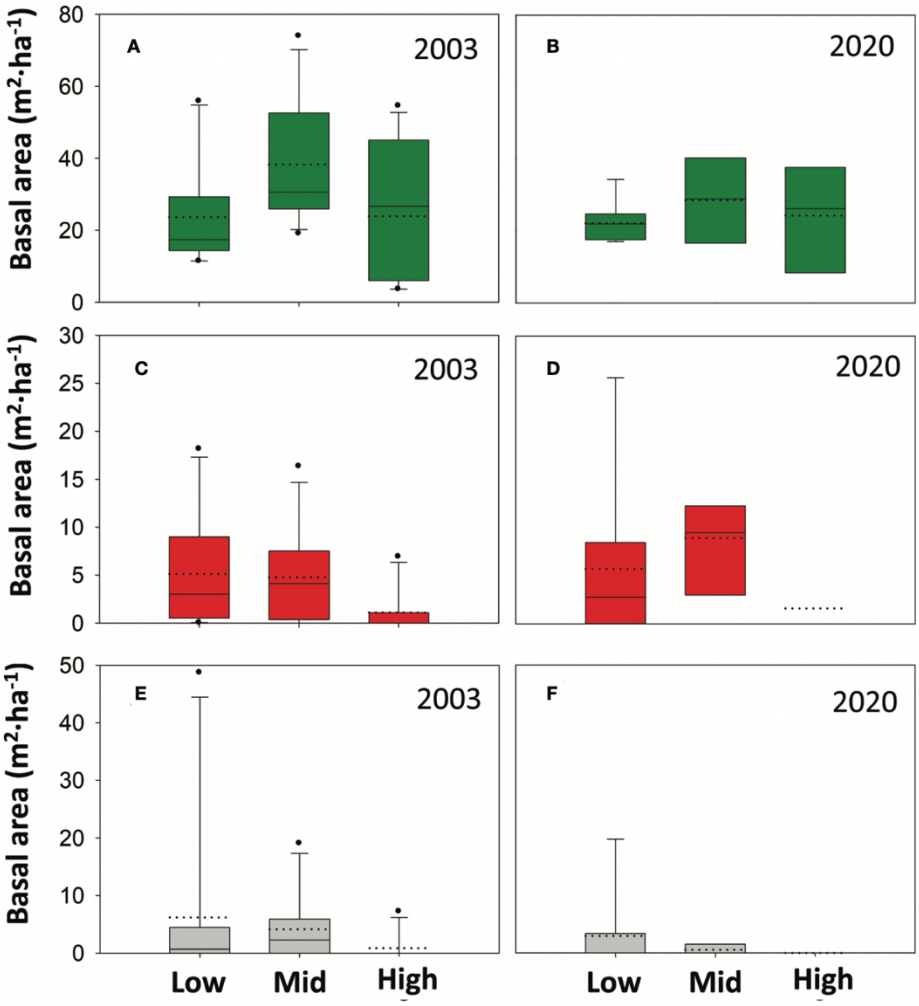

Figure 3.3 Altitudinal distribution in 2003 and 2020 of the basal area of *A. pinsapo* tree classes. Altitudinal bands: Low (880-1150 m a.s.l.), Mid (1150-1350 m), and High (1350-1550 m). Tree classes: alive trees (in green, **A** and **B**), dead trees (in red, **C** and **D**), and stumps (in grey, **E** and **F**). The ANOVA tests only showed significant increase in mortality between the 2003 high altitude band and the 2020 mid altitude band (Table S3.2).

3.3.2. Dynamic factor analysis

NDVI values for the different altitudinal bands and SI (solar radiation incidence) levels were mainly comprised between 0.4 and 0.5 (Fig. 3.4). The repeated measures ANOVA indicated significant effects ($p < 0.05$). of altitude and solar incidence on absolute NDVI values (Table S3.3), although the effect sizes were small. A Bonferroni test confirmed significant differences between all levels of both factors ($p < 0.05$). The SI value range with the least number of pixels was the one corresponding to high solar incidence (130-175 h; 1080 pixels). Pixels with a low solar incidence (0-46 h) were the most abundant (10949 pixels). Mid altitude belt (1150-1350 m) was the most abundant in the NDVI data (15678 pixels).

The temporal pattern of change in NDVI values differed depending on altitude and SI (Fig. S3.5). In the low altitudinal band (880-1150 m), NDVI becomes modulated by SI: the higher the SI range pixels belong to, the higher their NDVI values, irrespective of the considered year. However, at mid altitudes (1150-1350 m), higher NDVI values were found in areas subjected to intermediate levels of SI (46-130 h) in all years. The highest altitudinal belt (1350-1550 m) showed no distinct patterns of NDVI dynamics among SI value ranges.

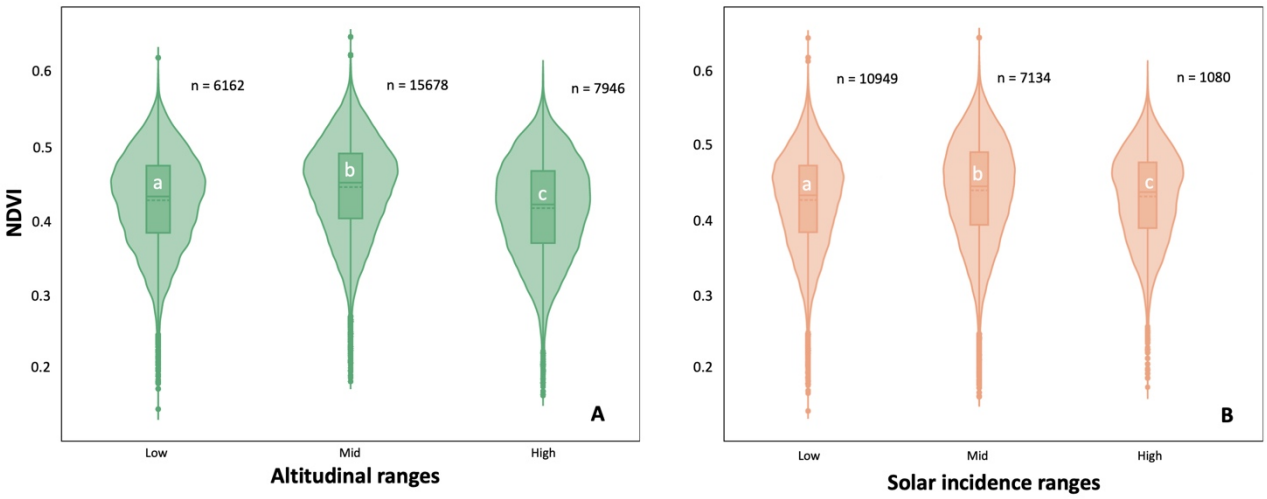

Figure 3.4. NDVI of altitudinal bands (A) and solar incidence value ranges (B). Different letters indicate differences between altitude or solar incidence levels ($p < 0.05$; Bonferroni post-hoc tests following repeated measures ANOVA; see Table S3.3). N values correspond to the number of pixels for each band.

Dynamic Factor Analysis (DFA) performed on NDVI time series expressed in absolute value revealed just one single significant common temporal trend (AIC = -2050.05) between the nine altitudes by SI combinations (Fig. S3.6A; Table S3.4). Such a common trend highlights the generality over the studied area (i) a drop in NDVI values from the mid-1990s; (ii) a subsequent rapid recovery along the 2000s (but with a partial drop by the end of this decade) that reaches NDVI levels similar to those observed at the beginning of the time series; (iii) a further increasing trend from 2010 but at a lower rate; and (iv) a trend of stabilization in the last years at NDVI levels that are the highest of the whole time series.

Two common trends (AIC = 324.298) were obtained from the DFA applied to normalized NDVI values. This analysis reveals the patterns of high frequency (successive up and down pulses) in detrended NDVI time series (Fig. S3.6B). The common trend 1 was correlated with summer and annual radiation (Rsu = 0.65, Rye = 0.54, respectively) and describes an undulating increasing tendency which tends to stabilize in the last decade of the time series. The common trend 2 showed no correlation with climate variables, and no long-term trend but mid frequency ample pulses. Contrary to the case of the DFA on absolute NDVI values, the different 'altitude by SI' combinations do show varying contributions to the two common trends extracted from normalized NDVI series. The high altitude and SI NDVI time series shows a high and positive factor loading on the first common trend, whereas the times series 'NDVI_1150_175', 'NDVI_1350_130', and 'NDVI_1550_46' are the ones with more contribution on common trend 2 (Table S3.4).

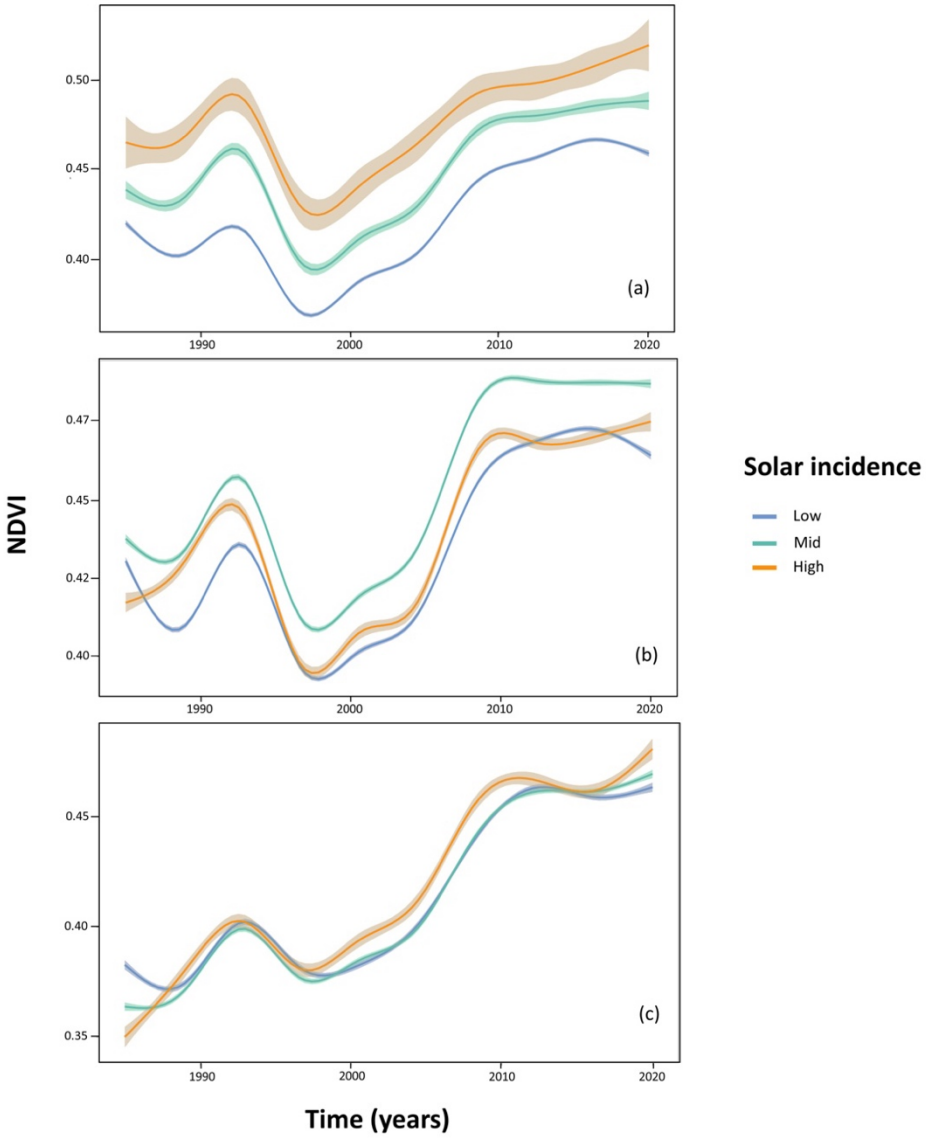

Figure 3.5. LIDAR NDVI dynamics at the low (880 – 1150 m; graph A), mid (1150 – 1350 m; graph B, and high (1350 – 1550 m; graph C) altitudinal bands, depending on November solar radiation incidence-SI levels ('Low' level: in blue 0-46 hours of solar incidence, 'Mid': in green, 46-130 hours; 'High': in red, 130-175 hours). GAM smoothing was applied to NDVI curves, and shaded areas represent the amount of variation in NDVI values (95% confidence intervals).

3.3.3. Linear mixed effect models

Low —and high— elevation showed similar contributions to the variance (33% and 36%), while the explained variance was lower at mid elevation (24%). At low-elevation, the total radiation of the autumn of the previous year was the most significant variable (positive correlation, 29% of relative weight), followed by SI (positive correlation, 23% of relative weight).

At mid elevation, the total radiation of the autumn of the previous year was also the most significant variable (positive correlation, 31% of relative weight in the model), followed by the spring drought index (positive correlation, 20% of relative weight in the model) and the summer drought index (negative correlation, 19% of relative weight in the model). The SI also showed a significant effect, as well as the temperatures of spring and summer (all of them with positive correlations with NDVI).

Contrasting to low and mid, the high elevation belt did not show a significant effect on the SI. The total radiation of the autumn of the previous year and the spring drought index were significant (both with positive correlation, 25% of relative weight, Tables 3.1, 3.2).

The residuals of the models were not related to elevation (Fig. 3.3) and did not show time autocorrelation. However, the residuals were markedly negative (that is, the predictions are systematically above the observations) between the years 1995-2006 at low and middle elevations, and between the years 1995-2004 at higher elevations (Fig. 3.7; Fig.3.4).

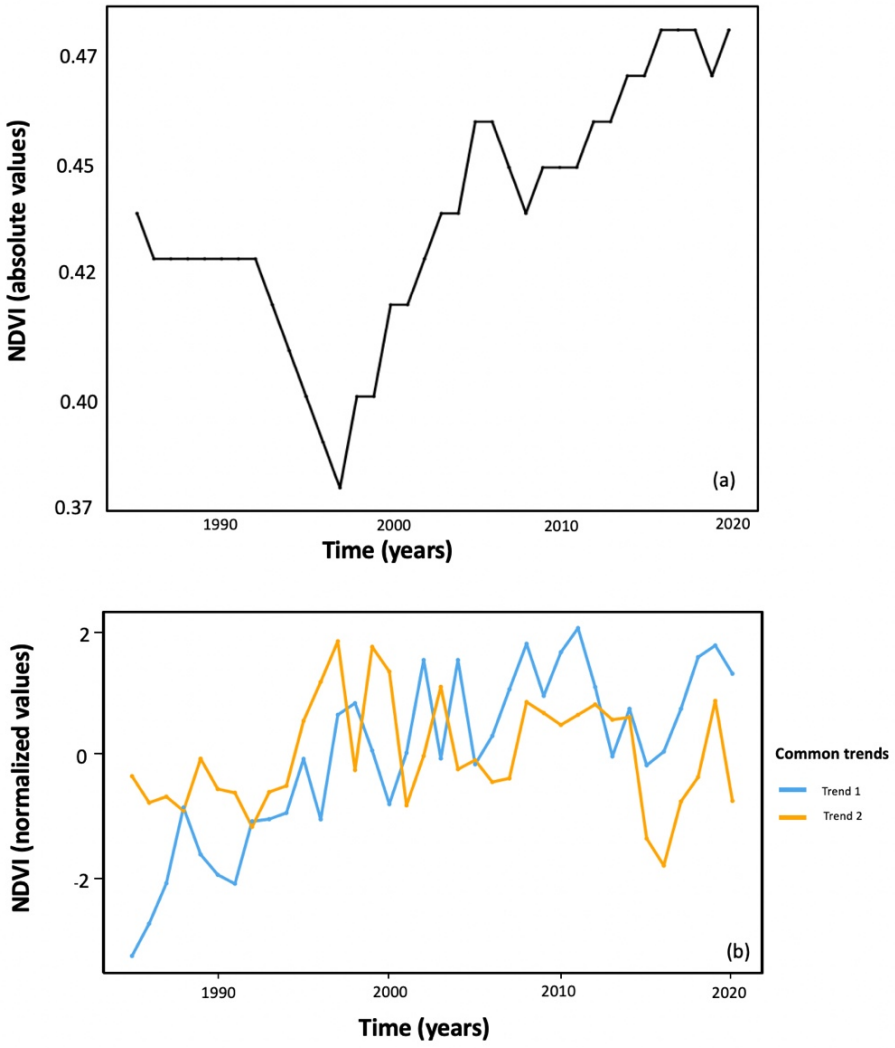

Figure 3.6. Common temporal trends among the nine NDVI time series corresponding to the different altitude by solar incidence combinations as revealed by Dynamic Factor Analysis (DFA) performed both on absolute (graph A) and on normalized (graph B) data.

3.3.4. Canopy loss evolution

The classification of orthoimages into three land-cover classes (shrubs, forest canopy, bare ground-grasslands) achieved an accuracy between 0.8-0.9 and the Kappa index ranged from 0.56-0.86 (Table S3.5). The percentage of pixels classified as canopy (Fig. S3.5) showed a drop in the 1998 orthoimage, while it strongly rose in the 2002 and 2004 images. Since then, the forest canopy coverage has remained stable except for a moderate fall in the 2013 orthoimage.

Table 3.1. Model selection criteria for *Abies pinsapo*-dominated forests NDVI along three elevation belts: low elevation (880-1150 m a.s.l.), mid elevation (1150-1350 m a.s.l.) and high elevation (1350-1550 m a.s.l.). Seasonal data of temperature (T), Radiation (R) and SPEI (S), as well as site solar incidence (SI), were tested as fixed factors, while sampling points were included as random factors. Seasons are noted as: aup, prior autumn; wi, winter; sp, spring; su, summer; autumn of the current year were not included as the NDVI data were obtained for August-September. A null model assuming NDVI constant was also tested. The K column represents the number of parameters included in the model, that is, the number of explaining variables plus one constant plus the error. Models in bold correspond to models with substantial support. ΔAICc is the difference Akaike information criterion with respect to the best model. L is the likelihood of a model given the observed NDVI data. *W*i is the relative probability that the model i is the best model for the observed data, given the candidate set of models. *W*1/*Wi* is the evidence ratio percentage for each model with each other model. N is the number of sampling points.

Fixed factors	K	ΔAICc	*L*	*Wi*	*W1/Wi*
Low Elevation (n=193)					
SI+Raup+Rsu+Rwi+Tsp+Tsu+Ssp+Ssu	10	0.00	1.00	0.26	
SI+Raup+Rsu+Tsp+Tsu+Ssp+Ssu	9	0.04	0.98	0.25	98.17
SI+Raup+Rsu+Tsu+Ssp+Ssu	8	0.21	0.90	0.23	91.70
SI+Raup+Tsu+Ssp+Ssu	7	0.55	0.76	0.20	84.53
SI+Raup+Ssp+Ssu	6	3.27	0.19	0.05	25.60
SI+Raup+Ssu	5	6.76	0.03	0.01	17.45
Raup+Ssu	4	11.56	0.00	0.00	9.10
Raup	3	19.38	0.00	0.00	2.01
null model	2	27.50	0.00	0.00	1.72
Sum			3.87		
Mid Elevation (n=210)					
SI+Raup+Rsu+Rwi+Tsp+Tsu+Ssp+Ssu	10	0.00	1.00	0.37	
SI+Raup+Rsu+Tsp+Tsu+Ssp+Ssu	9	0.17	0.92	0.34	92.04
SI+Raup+Tsp+Tsu+Ssp+Ssu	8	0.74	0.69	0.26	75.02
SI+Raup+Ssp+Ssu	6	5.28	0.07	0.03	10.32
Raup+Ssp+Ssu	5	9.02	0.01	0.00	15.47
Raup+Ssu	4	18.46	0.00	0.00	0.89
Raup	3	43.27	0.00	0.00	0.00
Mid Elevation (n=210)					
null model	2	69.75	0.00	0.00	0.00
SI+Raup+Tsu+Ssp+Ssu	7	715.95	0.00	0.00	0.00
Sum			2.69		
High Elevation (n=133)					
SI+Raup+Rsp+Rwi+Tsp+Tsu+Ssp+Ssu	10	0.00	1.00	0.31	
SI+Raup+Rsp+Tsp+Tsu+Ssp+Ssu	9	0.07	0.97	0.30	96.54
Raup+Rsp+Tsp+Tsu+Ssp+Ssu	8	0.46	0.79	0.24	82.24
Raup+Rsp+Tsp+Ssp+Ssu	7	1.73	0.42	0.13	53.01

Table 3.2. Outputs of the best-supported models showed in Table 3.1

Model		Variable	Value	Std. Error	t-value	Relative weight (%)
Model_L_NDVI=lme(NDVI~si+Raup+Tsu+Ssp+Ssu, method='REML', random=~1|x)		Intercept	-0.33	$7.99 \cdot 10^{-3}$	-41.8	
		SI	$5.07 \cdot 10^{-4}$	$7.01 \cdot 10^{-6}$	72.4	23.3
		Raup	$7.39 \cdot 10^{-4}$	$8.21 \cdot 10^{-6}$	90.0	28.9
		Tsu	0.02	$3.88 \cdot 10^{-4}$	52.7	16.9
AIC	BIC	Ssp	$8.48 \cdot 10^{-3}$	$1.58 \cdot 10^{-4}$	53.4	17.2
-314825.5	-314749.2	Ssu	$-7.40 \cdot 10^{-3}$	$1.74 \cdot 10^{-4}$	-42.7	13.7
Model_M_NDVI=lme(NDVI~si+Raup+Tsp+Tsu+Ssp+Ssu, method= 'REML', random=~1|x))		Intercept	-0.21	$4.60 \cdot 10^{-2}$	-46.0	
		SI	$1.54 \cdot 10^{-4}$	$2.50 \cdot 10^{-6}$	61.8	13.1
		Raup	$7.31 \cdot 10^{-4}$	$4.91 \cdot 10^{-6}$	148.8	31.4
		Tsp	$8.62 \cdot 10^{-3}$	$3.18 \cdot 10^{-4}$	27.0	5.7
		Tsu	$1.19 \cdot 10^{-3}$	$2.35 \cdot 10^{-4}$	50.4	10.6
AIC	BIC	Ssp	$9.18 \cdot 10^{-3}$	$9.74 \cdot 10^{-5}$	94.2	19.9
-1030031.0	-1029934.0	Ssu	$-9.31 \cdot 10^{-3}$	$1.01 \cdot 10^{-4}$	-91.5	19.3
Model_H_NDVI=lme(NDVI~Raup+Rsp+Tsp+Ssp+Ssu, method="REML", random=~1|x)		Intercept	-0.54	$5.96 \cdot 10^{-3}$	-91.1	
		Raup	$7.80 \cdot 10^{-4}$	$7.64 \cdot 10^{-6}$	102.0	23.6
		Rsp	$4.50 \cdot 10^{-4}$	$7.92 \cdot 10^{-6}$	56.9	13.2
		Tsp	0.03	$4.50 \cdot 10^{-4}$	67.3	15.5
AIC	BIC	Ssp	0.02	$1.75 \cdot 10^{-4}$	114.6	26.5
-465951.5	-465872.0	Ssu	-0.01	$1.4 \cdot 10^{-4}$	-92.1	21.3

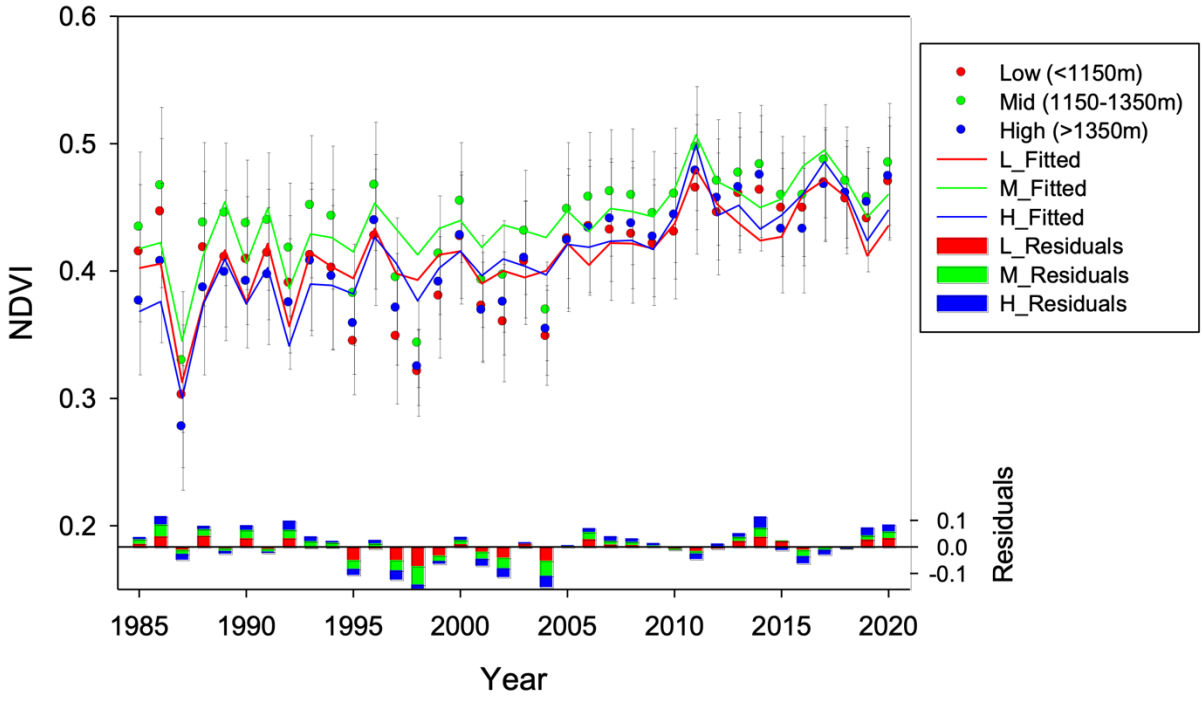

Figure 3.7. Predicted NDVI obtained by linear mixed effect models (LMEM) using climate and physiography as predictors. NDVI was fitted for low (880-1150 m a.s.l.; L_Fitted in red), mid (1150-1350 m a.s.l.; M_Fitted in green), and high (1350-1550 m a.s.l.; H_Fitted in blue) altitudinal bands. The residuals of the models (bottom bars) were computed as the difference between observed and predicted NDVI; positive bars denote years where observed NDVI values were higher than expected based on climate, while negative bars denote years where observed NDVI values were lower than expected based on climate.

Rates of forest cover change showing canopy loss (transitions from forest to shrubs or bare ground/grassland covers) between two orthoimages were the highest at the mid altitudinal band (1150-1350 m) during 2007-2010 and 2013-2016 (> 7 ha·year^{-1}). However, this band is the most abundant in the study area (>150 ha), so it also was the band that experienced the highest recovery rate (Fig. 3.8). All bands coincide in a negative net balance for the period (1984-98), with the mid band being the one least affected. The highest canopy recovery rate was dated for the 1998-2004 period in all altitudes (6-9 ha·year^{-1}). Later on (2004-2019), acute peaks of canopy loss (3-8 ha·year^{-1}) showed asynchrony across elevations. This loss was subsequently compensated by events of

canopy gaining. However, in the last years (2016-2019 comparison), all bands coincided with an increase in the canopy gain.

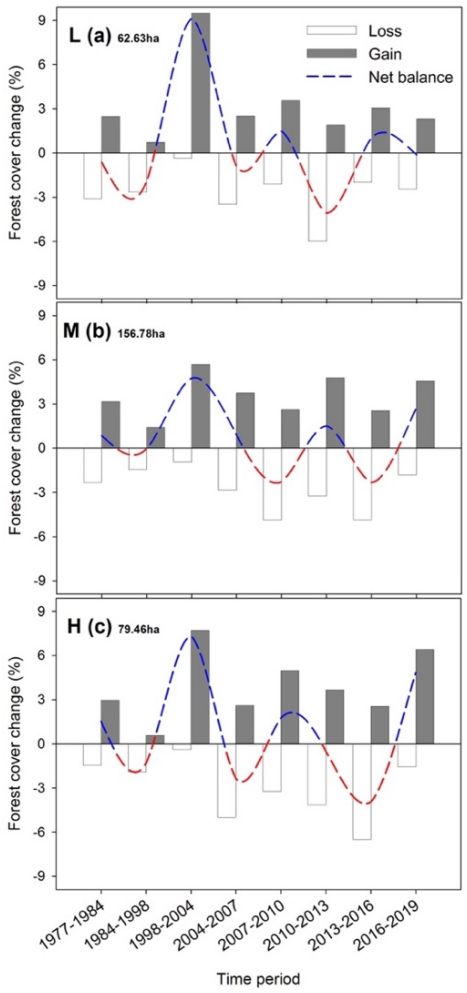

Figure 3.8. Annual rate of forest cover change is estimated as the loss (empty bars) and gain (gray bars) of forest surface (ha) between the dates of sequential aerial orthophotographs, divided by the number of years included in that period. The net balance was estimated as the difference between gains and losses in each period, depicting forest surface increases (blue dashed line) or decreases (red dashed line). Estimates were performed for low (880-1150 m a.s.l.; graph A), mid (1150-1350 m a.s.l.; graph B), and high (1350-1550 m a.s.l.; graph C) altitudinal bands. The total area (ha) for each band is also shown to understand the scale of the forest cover change.

3.4. Discussion

Abies pinsapo is known to have traits that suggest its capability to cope with Mediterranean summer conditions even in the absence of phenophasical plasticity (Latorre & Cabezudo, 2012).

However, previous studies (Linares *et al.*, 2011) indicated that, compared with other coexisting tree species, *A. pinsapo* shows a limited drought adaptive capacity in its main distribution area. For instance, in contrast with *Pinus halepensis* Mill. individuals in the same stands, *A. pinsapo* ones showed more acute growth reduction trends in the last decades, sudden growth reductions, and less responsive water use efficiency in the face of drought spells (Linares *et al.*, 2011). In fact, severe symptoms of stand stagnation and forest decline during the last decades, associated with regional trends of climate aridification, have been reported in some of the most important *A. pinsapo* populations (Linares *et al.*, 2009c).

These effects are synergistically amplified by increasing levels of intraspecific competition linked to rural abandonment and strict conservation policies that led to an absence of low intensity disturbances —no forest management nor herbivore activity (Linares *et al.*, 2010a). The consequence has been an extensive forest dieback and gap opening process (Fig. 3.9; Fig. S3.6), with the severe 1994-95 drought acting as a tipping point, so that very bad prospects had been forecasted for *A. pinsapo* (e.g., rapid rear-edge retraction, one of the highest vulnerabilities to climate change among circum-Mediterranean fir species; Linares *et al.*, 2010a; Sánchez-Salguero *et al.*, 2017).

Severe decline and dieback processes for other forest species in the Mediterranean region have been reported (e.g., Camarero *et al.*, 2018). Drought and heat-induced tree mortality are currently ubiquitous worldwide, affecting forest biomes from temperate to tropical regions (Allen *et al.*, 2010). Moreover, it has been proposed that current knowledge and models might even be underestimating global forest vulnerability to climate change, so the impact could be even worse (Allen *et al.*, 2015).

In this study, we observe similar climatic trends of rising temperature (Fig. S3.2A) and aridification (Fig. S3.2C, SPEI), which have worsened compared to previous research based on times series ending in 2005 (Linares *et al.*, 2009a; Linares *et al.*, 2011). The 2003 versus 2020 field-survey data also demonstrate the persistence of high mortality rates nowadays (tree classes 4 to 6 accounted for over 20% of the stands basal area in 2020; Fig. 3.2). These observations are congruent with recent reports of the *A. pinsapo* dieback process based on field survey data (Navarro-Cerrillo *et al.*, 2022).

Figure 3.9. Forest gap caused by the dieback process ant its recolonization and vegetation. Picture taken in the 2020 field survey.

However, the multiscale approach and longer time frame since initial mortality events applied in the present work has yielded results that indicate an unexpected resilience of *A. pinsapo* forests to dieback, thus not confirming the bad prospects forecasted by previous studies. Nevertheless, observations of recovery trends in *A. pinsapo* populations have been reported by Gutiérrez-Hernández *et al.* (2018), who also described an increasing tendency of NDVI values in *A. pinsapo* forests and an earlier start of the green up.

In our study, the fact that predicted NDVI based solely on climatic data is systematically above observations from the mid- 1990s to mid-2000s (Fig. 3.7) can be explained by concomitant high mortality (but still low recovery). However, NDVI time series indicate a sharp recovery of

forest cover and biomass in the late 2000s, and stable levels in the last decade which are maximums within the whole 1984-2020 time series, at all altitudes independently of SI (Fig. 3.5). Similarly, multi-temporal analysis of classified orthoimages showed a synchronic maximum of canopy gain across altitudes for the 1998 vs 2004 comparison (Fig. 3.8). The NDVI returned to be adequately modeled by climatic conditions in the LMEM analysis during the last decade of the studied time series (Fig. 3.7).

Ecologists are generally inclined to expect regime shifts when studying community dynamics against disturbance, since the latter is considered when it causes visible changes in biomass or species density and composition (Connell & Ghedini, 2015). However, there is increasing evidence of somewhat hidden compensatory mechanisms, triggered early as short-term responses, that adjust the system dynamics to counter the otherwise unchecked effects of disturbance, which are important in explaining apparently unexpected long-term processes of recovery (Lloret *et al.*, 2012; Loreau & de Mazancourt, 2013). In our study case, dieback is acting as a continuous background process that opens forest gaps.

However, the present net balance in *A. pinsapo* forest status seems positive, which may have resulted from the following compensation phenomena that might be involved: (i) recruitment of new *A. pinsapo* individuals; (ii) facilitative effects on such recruitment mediated by revegetation with other tree species and shrub species; and (iii) a 'release effect' in which surviving *A. pinsapo* trees can thrive with fewer resource competition.

Several of our results support this compensation phenomena hypothesis. First, the mean alive *A. pinsapo* basal area was not significantly different between the 2003 and the 2020 field surveys (Fig. 3.3A, B). Second, by the end of the considered time frame, NDVI values were maximum (> 0.5) at the lowest altitudinal band and in positions with the highest SI values (Fig. 3.5A). Low altitude and high irradiance mean drier conditions, which might have promoted the colonization of mortality gaps by thermophile vegetation (*Pinus halepensis*, *Juniperus sp*, *Cistus sp*, *Ulex sp*), through dispersal from below the *A. pinsapo* lower ecotone. Mortality gap invasion by thermophile shrubs has been recently evidenced in the area through the characterization of recent changes in fuel models (vegetation structure) in a study on fire risks (Cortés-Molino *et al.*, 2020). Encroachment of thermophile shrubs and bushes in open gaps would facilitate the understory establishment of shade-tolerant *A. pinsapo* saplings, whose growth would over time exceed the height of the bushes. Third, the recovery of NDVI values during the mid-1990s and 2000s showed steeper slopes at mid and high altitudes than at low altitude (Fig. 3.5B), which suggest a stronger contribution of

the 'release effect' at the former elevations. This steeper slope in NDVI is especially clear for the mid altitudinal band, which showed a rapid response in

less than a decade (~2005-2010). Consequently, the aforementioned gap recolonization process should not have time enough to fully develop at mid altitudes. This band was also the one with the least negative canopy balance (<1 ha· year $^{-1}$; Fig. 3.8) during the 1984-98 period. Evidence of growing crowns can be observed from aerial orthoimages (Fig. S3.7). The combination of all these three effects could explain the rebound effect in NDVI following the 1994-95 drought. However, compensation mechanisms have recently been shown to commonly fail in marginal tree populations in the long term, as has been reported in a study comprising more than fifty North American tree species (Yang *et al*., 2022).

Other effects, such as CO_2 fertilization should not be discarded. Indeed, vegetation greenness has been increasing globally, at least since the early 1980s (Piao *et al*., 2020). Despite vegetation models suggest that CO_2 fertilization is the main driver of greening on the global scale, other factors might be significant at the regional scale. In our case, further research is needed to disentangle the extent to which the observed rising NDVI (Fig. 3.7) also indicates an increasing carbon sink. Rising atmospheric N deposition may be also hypothesized a process involved in the increasing NDVI (Mao *et al*., 2012). Notwithstanding, this explanation lacks substantial support in our study site, as these *A. pinsapo* stands present limited N deposition (Blanes *et al*., 2013).

This positive recovery alleviates initial warnings about the dieback process in an endemic species with high conservation value. However, this resilience also implies risks derived from side effects that should be accounted for in management plans. The increasing fire risk due to the rising flammability of fuel models associated with the vegetation recovery dynamics is particularly relevant (Cortés-Molino *et al*., 2020). At the local scale, dead wood accumulation in recent mortality gaps, and fuel structures with overlap between shrubs, bushes, and tree crowns in revegetating gaps, increase flammability and spread probability. These changes in the fuel models highlight the need for a strategy of proactive management to limit fire risks; otherwise, the good news of high resiliency of *A. pinsapo* forest to drought-induced dieback might turn into bad news of wildfires. It has been demonstrated that the Spanish fir shows no resilience to wildfires, being the worst threat to their populations (Silva, 1996). This message is also valid for other tree species with wider distribution, which are relevant in terms of economic value and ecosystem services provision such as *Abies cephalonica* Loud. (Ganatsas *et al*., 2012) or *Cedrus atlantica* Endl. (Abel-Schaad *et al*., 2018).

We might be underestimating the resilience of the circum- Mediterranean firs to climate change, despite wide evidence about their drought sensitivity (Sánchez-Salguero *et al*., 2017). Indeed, recent studies suggest that silver fir (*Abies alba* Mill.) can grow and regenerate under Mediterranean conditions, forming mixed stands with evergreen (e.g., *Quercus ilex* L.) and deciduous Mediterranean tree species, while its drought sensitivity was also stated (Walder *et al*., 2021).

3.5. Conclusions of the study

Despite decades of persistent drought-induced decline and mortality in *A. pinsapo* forests, the results presented here, based on multitemporal and multiscale data from field surveys, orthoimages, and satellite imagery showed: (i) a rising photosynthetic activity since mid-2000s (ii) an almost steady alive basal area of *A. pinsapo* stands between 2003 and 2020 and (iii) an increase in forest canopy gains in the last years at mid and high elevation bands.

These results support the hypothesis of an *A. pinsapo* forests resilience to climate change events, perhaps, greater than expected. However, further research is needed to understand the scope of these compensation mechanisms, which other processes could be involved in this recovery and what role will they play in future climate change scenarios.

References

Abel-Schaad, D., Iriarte, E., López-Sáez, J.A., Pérez-Dıáz, S., SabariegoRuiz, S., Cheddadi, R., *et al.* (2018). Are *Cedrus atlantica* forests in the Rif mountains of Morocco heading towards local extinction? *Holocene* 28 (6), 1023–1037. https://doi.org/10.1177/0959683617752842

Acácio, V., Holmgren, M., Rego, F., Moreira, F., and Mohren, M. J., G. (2009). Are drought and wildfires turning Mediterranean cork oak forests into persistent shrublands? *Agroforestry Systems*. 76, 389–400. https://doi.org/10.1007/s10457-008-9165-y

Allen, C. D., Breshears, D. D., and McDowell, N. G. (2015). On underestimation of global vulnerability to tree mortality and forest die-off from hotter drought in the Anthropocene. *Ecosphere* 6 (8), 1–55. https://doi.org/10.1890/ES15-00203.1

Allen, C. D., Macalady, A. K., Chenchouni, H., Bachelet, D., McDowell, N., Vennetier, M., Kitzberger, T., Rigling, A., Breshears, D. D., Hogg, E. H. (Ted), Gonzalez, P., Fensham, R., Zhang, Z., Castro, J., Demidova, N., Lim, J. H., Allard, G., Running, S. W., Semerci, A., & Cobb, N. (2010). A global overview of drought and heat-induced tree mortality reveals emerging climate change risks for forests. *Forest Ecology and Management*, 259(4), 660–684. https://doi.org/10.1016/j.foreco.2009.09.001

Anderegg, W. R. L., Kane, J. M., and Anderegg, L. D. L. (2013). Consequences of widespread tree mortality triggered by drought and temperature stress. *Nature Climate Change* 3 (1), 30–36. https://doi.org/10.1038/nclimate1635

Arista, M., Knees, S., and Gardner, M. (2011). *Abies pinsapo* var. pinsapo. *IUCN Red List Threatened Species* 2011. doi: 10.2305/IUCN.UK.2011- 2.RLTS.T42295A10679577.en

Attiwill, P. M. (1994). The disturbance of forest ecosystems: the ecological basis for conservative management. *Forest Ecology and Management.* 63 (2–3), 247–300. https://doi.org/10.1016/0378-1127(94)90114-7

Baguskas, S. A., Peterson, S. H., Bookhagen, B., and Still, C. J. (2014). Evaluating spatial patterns of drought-induced tree mortality in a coastal California pine forest. *Forest Ecology and Management.* 315, 43–53. https://doi.org/10.1016/j.foreco.2013.12.020

Beguería, S., Vicente-Serrano, S. M., Reig, F., and Latorre, B. (2014). Standardized precipitation evapotranspiration index (SPEI) revisited: parameter fitting, evapotranspiration models, tools, datasets, and drought monitoring. *International Journal of Climatology.* 34 (10), 3001–3023. https://doi.org/10.1002/joc.3887

Blanes, M. C., Viñegla, B., Merino, J., and Carreira, J. A. (2013). Nutritional status of *Abies pinsapo* forests along a nitrogen deposition gradient: do C/N/P stoichiometric shifts modify photosynthetic nutrient use efficiency? *Oecologia.* 171 (4), 797–808. https://doi.org/10.1007/s00442-012-2454-1

Boletín Oficial de la Junta de Andalucía (2011). Plan de recuperación del pinsapo. Available at: https://www.juntadeandalucia.es/boja/2011/25/1

Breshears, D. D., Myers, O. B., Meyer, C. W., Barnes, F. J., Zou, C. B., Allen, C. D., *et al.* (2009). Tree die-off in response to global change-type drought: mortality insights from a decade of plant water potential measurements. *Frontiers in Ecology and the Environment*. 7, 185–189. https://doi.org10.1890/080016

Burnham, K. P., and Anderson, D. R. (2002). "Springer-verlag," in *Model selection and multimodel inference: A practical information-theoretic approach (2nd ed.)* (New York: Springer City). https://doi.org10.1007/b97636

Camarero, J. J., Gazol, A., Sangüesa-Barreda, G., Cantero, A., Sánchez-Salguero, R., Sánchez-Miranda, A., *et al.* (2018). Forest growth responses to drought at short- and long-term scales in Spain: Squeezing the stress memory from tree rings. *Frontiers in Ecology and the Environment* 6 (9). https://doi.org10.3389/fevo.2018.00009

Camarero, J. J., Gazol, A., Sangüesa-Barreda, G., Oliva, J., and Vicente-Serrano, S. M. (2015). To die or not to die: early warnings of tree dieback in response to a severe drought. *Journal of Ecol*ogy. 103 (1), 44–57. https://doi.org/10.1111/1365-2745.12295

Campo-Bescós, M., Muñoz-Carpena, R., Southworth, J., Zhu, L., Waylen, P., and Bunting, E. (2013). Combined spatial and temporal effects of environmental controls on long-term monthly NDVI in the southern Africa savanna. *Remote sensing*. 5 (12), 6513–6538. https://doi.org/10.3390/rs5126513

Connell, S. D., and Ghedini, G. (2015). Resisting regime-shifts: The stabilizing effect of compensatory processes. *Trends in Ecology and Evolution* 30 (9), 513–515. https://doi.org/10.1016/j.tree.2015.06.014

Coop, J. D., Parks, S. A., Stevens-Rumann, C. S., Crausbay, S. D., Higuera, P. E., Hurteau, M. D., Tepley, A., Whitman, E., Assal, T., Collins, B. M., Davis, K. T., Dobrowski, S., Falk, D. A., Fornwalt, P. J., Fulé, P. Z., Harvey, B. J., Kane, V. R., Littlefield, C. E., Margolis, E. Q., … Rodman, K. C. (2020). Wildfire-Driven Forest Conversion in Western North American Landscapes. *BioScience*, 70(8). https://doi.org/10.1093/biosci/biaa061

Cortés-Molino, Á., Aulló-Maestro, I., Fernandez-Luque, I., Flores-Moya, A., Carreira, J. A., and Salvo, A. E. (2020). Using ForeStereo and LIDAR data to assess fire and canopy structure-related risks in relict *Abies pinsapo* Boiss. forests. *PeerJ* 8, e10158. https://doi.org/10.7717/peerj.10158

DeSoto, L., Cailleret, M., Sterck, F., Jansen, S., Kramer, K., Robert, E. M. R., *et al.* (2020). Low growth resilience to drought is related to future mortality risk in trees. *Nature Communications*. 11 (1), 545. https://doi.org/10.1038/s41467-020-14300-5

Dorman, M., Svoray, T., Perevolotsky, A., and Moshe, Y. (2015). What determines tree mortality in dry environments? a multi-perspective approach. *Ecological Applications*. 25 (4), 1054–1071. https://doi.org/10.1890/14-0698.1

Fortini, L., Schubert, O. (2017) Beyond exposure, sensitivity, and adaptive capacity: a response based ecological framework to assess species climate change vulnerability. *Climate Change Responses* 4, 2. https://doi.org/10.1186/s40665-017-0030-y

Ganatsas, P., Daskalakou, E., and Paitaridou, D. (2012). Firstresultsonearly post-fire succession in an *Abies cephalonica* forest (Parnitha national park, Greece). iForest 5 (1), 6–12. https://doi.org/10.3832/ifor0600-008

Gazol, A., Camarero, J. J., Sangüesa-Barreda, G., and Vicente-Serrano, S. M. (2018b). Post-drought resilience after forest die-off: Shifts in regeneration, composition, growth, and productivity. *Frontiers in Plant Science* 9. https://doi.org/10.3389/fpls.2018.01546

Gazol, A., Camarero, J. J., Vicente-Serrano, S. M., Sánchez-Salguero, R., Gutiérrez, E., de Luis, M., *et al.* (2018a). Forest resilience to drought varies across biomes. *Global Change Biology*. 24 (5), 2143–2158. https://doi.org/10.1111/gcb.14082

Gonçalves, J., Pôças, I., Marcos, B., Mücher, C. A., and Honrado, J. P. (2019). SegOptim–a new r package for optimizing object-based image analyses of high- spatial resolution remotely-sensed data. *International Journal of Applied Earth Observation and Geoinformation* 76, 218–230. https://doi.org/10.1016/J.JAG.2018.11.011

González-Alonso, F., Merino-De-Miguel, S., Roldán-Zamarrón, A., Garcıá-Gigorro, S., and Cuevas, J. M. (2006). Forest biomass estimation through NDVI composites. the role of remotely sensed data to assess Spanish forests as carbon sinks. *International Journal of Remote Sensing*. 27 (24), 5409–5415. https://doi.org/10.1080/01431160600830748

Guerrero, J. J., Hernández, M., Cáceres, F., Giménez de Azcárate, F., and Moreira, J. M. (2014). Ecuación de la evapotranspiración de Pennman-Monteith modificada con la variable

fisiográfica de la incidencia solar.' *Red de Información Ambiental de Andalucía (REDIAM). Consejería de Medio Ambiente y Ordenación del Territorio la Junta Andalucía.*

Gunderson, L. H. (2000). Ecological resilience–in theory and application. *Annual Review of Ecology and Systematics* 31, 425–439. https://doi.org/10.1146/annurev.ecolsys.31.1.425

Guo, F., Lenoir, J., and Bonebrake, T. C. (2018). Land-use change interacts with climate to determine elevational species redistribution. *Nature* 9, 1315. https://doi.org/10.1038/s41467-018-03786-9

Gutiérrez-Hernández, O., Cámara Artigas, R., and Garcıá, L. (2018). Regeneración de los pinsapares béticos. análisis de tendencia interanual y estacional del NDVI. *Pirineos* 173, 035. https://doi.org/10.3989/pirineos.2018.173002

Hampe, A., and Jump, A. S. (2011). Climate relicts: Past, present, future. *Annual Review of Ecology Evolution and Systematics* 42 (1), 313–333. https://doi.org/10.1146/annurev-ecolsys-102710-145015

Haylock, M. R., Hofstra, N., Klein Tank, A. M. G., Klok, E. J., Jones, P. D., and New, M. (2008). A European daily high-resolution gridded data set of surface temperature and precipitation for 1950–2006. *Journal of Geophysical Research*. 113, D20119. https://doi.org/10.1029/2008JD010201

Jentsch, A., and Beierkuhnlein, C. (2008). Research frontiers in climate change: Effects of extreme meteorological events on ecosystems. *Comptes Rendus Geosciencie*. 340 (9–10), 621–628. https://doi.org/10.1016/j.crte.2008.07.002

Kennedy, R. E., Yang, Z., and Cohen, W. B. (2010). Detecting trends in forest disturbance and recovery using yearly Landsat time series: 1. LandTrendr — temporal segmentation algorithms. *Remote Sensing of Environment*. 114 (12), 2897–2910. https://doi.org/10.1016/j.rse.2010.07.008

Kuuluvainen, T., Angelstam, P., Frelich, L., Jõgiste, K., Koivula, M., Kubota, Y., *et al.* (2021). Natural disturbance-based forest management: Moving beyond retention and continuous-cover forestry. *Frontiers in Forests and Global Change* 4. https://doi.org/10.3389/ffgc.2021.629020

Latorre, A. V. P., and Cabezudo, B. (2012). Phenomorphology and ecomorphological traits in *Abies pinsapo*. a comparison to other Mediterranean species. *Phytocoenologia* 42 (1–2), 15–27. https://doi.org10.1127/0340-269X/2012/0042-0517

Linares, J. C., Camarero, J. J., and Carreira, J. A. (2009a). Interacting effects of changes in climate and forest cover on mortality and growth of the southernmost European fir forests. *Global Ecology and Biogeography* 18 (4), 485–497. https://doi.org/10.1111/j.1466-8238.2009.00465.x

Linares, J. C., Camarero, J. J., and Carreira, J. A. (2009b). Plastic responses of *Abies pinsapo* xylogenesis to drought and competition. *Tree Physiology*. 29 (12), 1525– 1536. https://doi.org/10.1093/treephys/tpp084

Linares, J. C., Camarero, J. J., and Carreira, J. A. (2010a). Competition modulates the adaptation capacity of forests to climatic stress: Insights from recent growth decline and death in relict stands of the Mediterranean fir *Abies pinsapo*. *Journal of Ecology*. 98 (3), 592–603. https://doi.org/10.1111/j.1365-2745.2010.01645.x

Linares, J. C., Camarero, J. J., and Carreira, J. A. (2010b). Stand-structural effects on *Heterobasidion abietinum*-related mortality following drought events in *Abies pinsapo*. *Oecologia* 164, 1107–1119. https://doi.org/10.1007/s00442-010-1770-6

Linares, J. C., and Carreira, J. A. (2009). Temperate-like stand dynamics in relict Mediterranean-fir (*Abies pinsapo* Boiss.) forests from southern Spain. *Annals of Forest Science*. 66, 610. https://doi.org/10.1051/forest/2009040

Linares, J. C., Delgado-Huertas, A., Camarero, J. J., Merino, J., and Carreira, J. A. (2009c). Competition and drought limit the response of water-use efficiency to rising atmospheric carbon dioxide in the Mediterranean fir *Abies pinsapo*. *Oecologia* 161, 611–624. https://doi.org/10.1007/s00442-009-1409-7

Linares, J.C., Delgado-Huertas, A., and Carreira, J.A. (2011). Climatic trends and different drought adaptive capacity and vulnerability in a mixed *Abies pinsapo- Pinus halepensis* forest. *Climatic Change* 105, 67–90. https://doi.org/10.1007/s10584-010- 9878-6

Lindner, M., Maroschek, M., Netherer, S., Kremer, A., Barbati, A., Garcia- Gonzalo, J., *et al.* (2010). Climate change impacts, adaptive capacity, and vulnerability of European forest ecosystems. *Forest Ecology and Management*. 259 (4), 698– 709. https://doi.org/10.1016/j.foreco.2009.09.023

Lloret, F., Escudero, A., Iriondo, J.M., Martıńez-Vilalta, J., and Valladares, F. (2012). Extreme climatic events and vegetation: the role of stabilizing processes. *Global Change Biology* 18 (3), 797–805. https://doi.org/10.1111/j.1365-2486.2011.02624.x

Lloret, F., Siscart, D., and Dalmases, C. (2004). Canopy recovery after drought dieback in holm-oak Mediterranean forests of Catalonia (NE Spain). *Global Change Biology* 10 (12), 2092–2099. https://doi.org/10.1111/j.1365-2486.2004.00870.x

Loreau, M., and de Mazancourt, C. (2013). Biodiversity and ecosystem stability: a synthesis of underlying mechanisms. *Ecology Letters*. 16, 106–115. https://doi.org/10.1111/ele.12073

Mao, J., Shi, X., Thornton, P. E., Piao, S., and Wang, X. (2012). Causes of spring vegetation growth trends in the northern mid-high latitudes from 1982 to 2004. *Environmental Research letters*. 7, 14010. https://doi.org/10.1088/1748-9326/7/1/014010

McGaughey, R. J., and Carson, W. W. (2003). *Fusing LIDAR data, photographs and other data using 2D and 4D visualization techniques,* pp. 16–24. Charleston, South Carolina.

Navarro-Cerrillo, R.M., Duque-Lazo, J., Ríos-Gil, N., Guerrero-Álvarez, J.J., López-Quintanilla, J., and Palacios-Rodríguez, G. (2021). Can habitat prediction models contribute to the restoration and conservation of the threatened tree *Abies pinsapo* Boiss. in southern Spain? *New Forests* 52, 89–112. https://doi.org/10.1007/s11056- 020-09784-4

Navarro-Cerrillo, R. M., González-Moreno, P., Ruiz-Gómez, F. J., Sánchez- Cuesta, R., Gazol, A., and Camarero, J. J. (2022). Drought stress and pests increase defoliation and mortality rates in vulnerable *Abies pinsapo* forests. *Forest Ecology and Management* 504, 119824. https://doi.org/10.1016/j.foreco.2021.119824

Navarro-Cerrillo, R. M., López-Quintanilla, J., Blanco-Oyonate, P., Sánchez-Salguero, R., Guzmán Álvarez, J. R., Calzado Martínez, C., *et al.* (2013). Distribución actual y potencial del pinsapo (*Abies pinsapo* Boiss). *Los pinsapares en Andalucía: Conservación y sostenibilidad.* Junta de Andalucía,149–183.

Nikinmaa, L., Lindner, M., Cantarello, E., Jump, A. S., Seidl, R., Winkel, G., *et al.* (2020). Reviewing the use of resilience concepts in forest sciences. *Current Forestry Reports* 6, 61–80. https://doi.org/10.1007/s40725-020-00110-x

Ogle, D. H. (2018). *Introductory fisheries analyses with R* (1st ed.) (Chapman and Hall/CRC: New York). https://doi.org/10.1201/9781315371986

Piao, S., Wang, X., Park, T., Chen, C., Lian, X., He, Y., *et al.* (2020). Characteristics, drivers, and feedbacks of global greening. *Nature Reviews Earth & Environment*. 1, 14–27. https://doi.org/10.1038/s43017-019-0001-x

Picket, S., and White, P. (1985). *The ecology of natural disturbance and patch dynamics* (Elsevier). https://doi.org/10.1016/C2009-0-02952-3

Restaino, C., Young, D. J. N., Estes, B., Gross, S., Wuenschel, A., Meyer, M., *et al.* (2019). Forest structure and climate mediate drought-induced tree mortality in forests of the Sierra Nevada, USA. *Ecological Applications* 29 (4), e01902. https://doi.org/10.1002/eap.1902

Sánchez-Pinillos, M., Leduc, A., Ameztegui, A., Kneeshaw, D., Lloret, F., and Coll, L. (2019). Resistance, resilience or change: Post-disturbance dynamics of Boreal forests after insect outbreaks. *Ecosystems* 22, 1886–1901. https://doi.org/10.1007/s10021-019-00378-6

Sánchez-Salguero, R., Camarero, J. J., Carrer, M., Gutiérrez, E. A., Andreu-Hayles, L., Hevia, A., Koutavas, A., Martínez-Sancho, E., Nola, P., Papadopulos, A., Pasho, E., Toromani, E., Carreira, J. A. and Linares, J. C. (2017). Climate extremes and predicted warming threaten Mediterranean Holocene firs forests refugia. *Proceedings of the National Academy of Sciences*. https://doi.org/10.1073/pnas.1708109114

Sánchez-Salguero, R., Ortíz, C., Covelo, F., Ochoa, V., García-Ruíz, R., Seco, J. I., Carreira, J. A., Merino, J. ángel, & Linares, J. C. (2015). Regulation of water use in the southernmost European fir (*Abies pinsapo* Boiss.): Drought Avoidance Matters. *Forests*, 6(6), 2241–2260. https://doi.org/10.3390/f6062241

Seidl, R., Fernandes, P. M., Fonseca, T. F., Gillet, F., Jönsson, A. M., Merganičová, K., *et al.* (2011). Modelling natural disturbances in forest ecosystems: A review. *Ecological Modelling.* 222 (4), 903–924. https://doi.org/10.1016/j.ecolmodel.2010.09.040

Rodríguez y Silva, F. (1996). '*Protección y defensa de los pinsapares ante los incendios forestales. jornadas técnicas internacionales sobre recuperación de pinsapares.*'. Jornadas Técnicas Internacionales Sobre Recuperación Pinsapares 95, 0–9.

Suarez, M. L., and Lloret, F. (2018). Self-replacement after small-scale partial crown dieback in austral *Nothofagus dombeyi* forests affected by an extreme drought. *Canadian Journal of Forest Research*. 48 (4), 412–420. https://doi.org/10.1139/cjfr-2017-0305

Swain, D. L., Singh, D., Touma, D., and Diffenbaugh, N. S. (2020). Attributing extreme events to climate change: A new frontier in a warming world. *One Earth* 2 (6), 522–527. https://doi.org/10.1016/j.oneear.2020.05.011

Vaglio Laurin, G., Pirotti, F., Callegari, M., Chen, Q., Cuozzo, G., Lingua, E., *et al.* (2016). 'Potential of ALOS2 and NDVI to estimate forest above-ground biomass, and comparison with lidar-derived estimates'. *Remote Sensing* 9 (1), 18. https://doi.org10.3390/rs9010018

Vicente-Serrano, S. M., Begueriá, S., and López-Moreno, J. I. (2010). A multiscalar drought index sensitive to global warming: The standardized precipitation evapotranspiration index. *Journal of Climate* 23 (7), 1696–1718. https://doi.org/10.1175/2009JCLI2909.1

Vilà-Cabrera, A., Martıń ez-Villalta, J., Galiano, L., and Retana, J. (2012). Patterns of forest decline and regeneration across Scots pine populations. *Ecosystems* 16, 323–335. https://doi.org/10.1007/s10021-012-9615-2

Walder, D., Krebs, P., Bugmann, H., Manetti, M. C., Pollastrini, M., Anzillotti, S., *et al.* (2021). Silver fir (*Abies alba* Mill.) is able to thrive and prosper under meso-Mediterranean conditions. Forest Ecol. Manage. 498, 119537. https://doi.org/10.1016/j.foreco.2021.119537

Wang, Q., and Tenhunen, J. D. (2004). Vegetation mapping with multitemporal NDVI in North-Eastern China transect (NECT). *International Journal of Applied Earth Observation and Geoinformation* 6 (1), 17–31. https://doi.org/10.1016/J.JAG.2004.07.002

Williams SE, Shoo LP, Isaac JL, Hoffmann AA, Langham G (2008). Towards an Integrated Framework for Assessing the Vulnerability of Species to Climate Change. *PLoS Biology* 6(12): e325. https://doi.org/10.1371/journal.pbio.0060325

Xu, P., Zhou, T., Yi, C., Fang, W., Hendrey, G., and Zhao, X. (2018). Forest drought resistance distinguished by canopy height. *Environmental Research Letters* 13 (7), 075003. https://doi.org/10.1088/1748-9326/aacadd

Yang, X., Angert, A. L., Zuidema, P. A., He, F., Huang, S., Li, S., *et al.* (2022). The role of demographic compensation in stabilising marginal tree populations in North America. *Ecological Letters*. 25 (7), 1676–1689. https://doi.org/10.1111/ele.14028

Yu, Z., Sun, G., Cai, T., Hallema, D. W., and Duan, L. (2019). Water yield responses to gradual changes in forest structure and species composition in a subboreal watershed in northeastern china. *Forests* 10 (3), 211. https://doi.org10.3390/f10030211

Zuur, A. F., Ieno, E. N., and Smith, G. M. (2007). *Analyzing ecological data* (New York: Springer New York). https://doi.org/10.1007/978-0-387-45972-1

Zuur, A. F., Ieno, E. N., Walker, N., Saveliev, A. A., and Smith, G. M. (2009). *Mixed effects models and extensions in ecology with r* (New York: Springer New York). https://doi.org/10.1007/978-0-387-87458-6

Zuur, A. F., Tuck, I. D., and Bailey, N. (2003). Dynamic factor analysis to estimate common trends in fisheries time series. *Canadian Journal of Fisheries and Aquatic Sciences* 60 (5), 542–552. https://doi.org/10.1139/f03-030

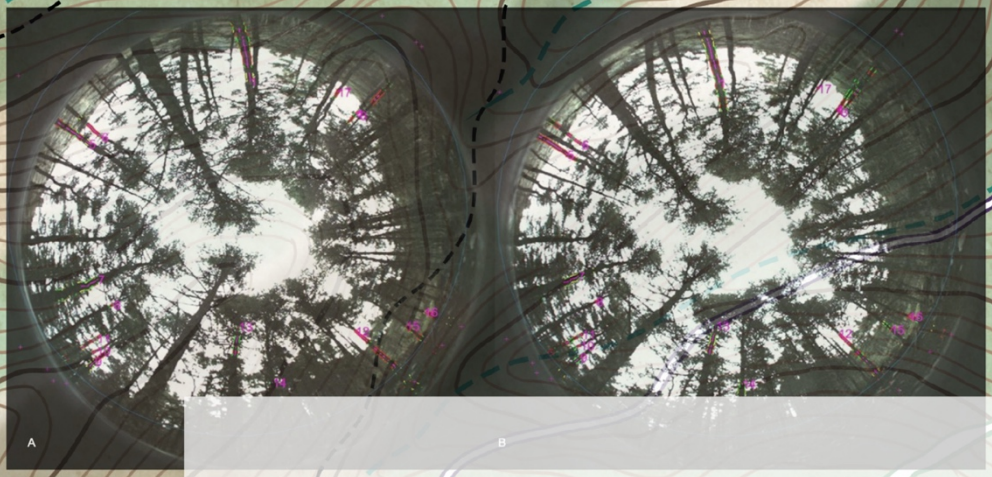

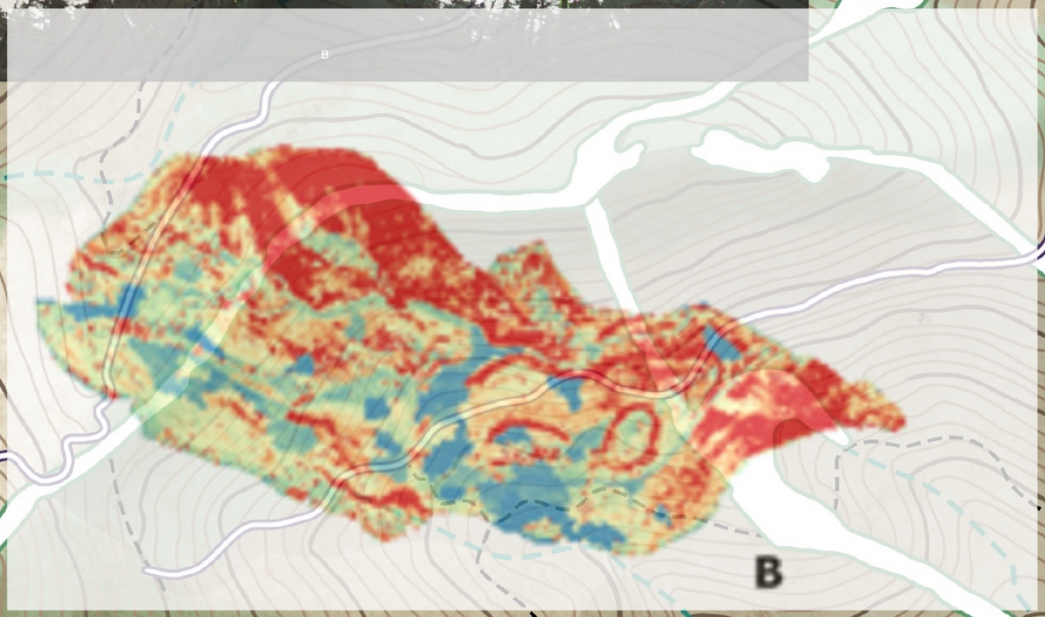

CHAPTER 4

STUDY 3

Using ForeStereo and LIDAR data to assess fire and canopy structure-related risks in relict *Abies pinsapo* Boiss forest

4

Abstract

We combined information from aerial LIDAR and hemispherical images taken in the field with ForeStereo, a forest inventory device, to assess the vulnerability and to design conservation strategies for endangered Mediterranean fir forests based on the mapping of fire risk and canopy structure spatial variability. We focused on the largest continuous remnant population of the endangered tree species *Abies pinsapo* Boiss, covering 252 ha in Sierra de las Nieves National Park (South Andalusia, Spain). We established 49 sampling plots over the study area. Stand structure variables were derived from a ForeStereo device, a sensing technology for approximate tree diameter, height, and crown dimensions. Stand crown cover and basal area were derived from stereoscopic hemispherical images photogrammetry. With this information, we developed regression models with airborne LIDAR data (spatial resolution of 0.5 points·m^{-2}). Thereafter, six fuel models were fitted to the plots according to the UCO40 classification criteria, and then the entire area was classified using the Nearest Neighbor algorithm on Sentinel imagery (overall accuracy of 0.56 and a KIA-Kappa Coefficient of 0.46). FlamMap software was used for fire simulation scenarios based on fuel models, stand structure, and terrain data. Besides the fire simulation, we analyzed canopy structure to assess the status and vulnerability of this fir population. The assessment shows a secondary growth forest that has an increasing presence of fuel models with the potential for high fire spread rate and burn probability. Our methodological approach has the potential to be integrated as a support tool for the adaptive management and conservation of *A. pinsapo* across its entire distribution area (<4000 ha), as well as for other endangered circum-Mediterranean fir forests, such as. *A. numidica* de Lannoy and *A. marocana* Trab. in North Africa.

Cortés-Molino Á, Aulló-Maestro I, Fernández-Luque I, Flores-Moya A, Carreira JA, Salvo AE. (2020). Using ForeStereo and LIDAR data to assess fire and canopy structure-related risks in relict *Abies pinsapo* Boiss. forests. *PeerJ* 8:e10158 https://doi.org/10.7717/peerj.10158

4.1. Introduction

Endemic conifer species are more numerous in Mediterranean-type climate regions in the Northern Hemisphere than in the Southern Hemisphere, which has been linked to the selective pressure of cold and/or drought conditions that led to the development of ecophysiological advantages for conifers over angiosperms on oligotrophic soils. Meanwhile, the Mediterranean-type climate regions of South Africa and Southwestern Australia have been more climatically and tectonically stable, which resulted in lower diversity and persistence of ancient lineages of conifers. The Mediterranean Basin has 32 endemic conifer species, accounting for more than 25% of the total conifer flora of 122 species (Rundel, 2019). In particular, the genus *Abies* Mill. experienced extensive speciation from the late Neogene that gave rise to nine species and one natural hybrid in the Mediterranean Basin (Linares, 2011). Past climate changes have led to population migrations, and to shrinkage and fragmentation of ancestral Mediterranean fir populations, further exacerbated by human impacts. This resulted in circum-Mediterranean endemic firs of high paleogeographic interest, since they are established in relict restricted-range populations with relevant vulnerability to global warming effects (Liepelt, *et al.*, 2010). Adaptive management of these forests to protect them from the increasing fire risk is essential for their survival.

Extreme climate events, such as severe droughts, mega-fires, and disease infestations threaten these relict Mediterranean fir populations (Sánchez-Salguero, *et al.*, 2017). It is well known that fire has influenced the landscape and terrestrial life as far back as the beginning of land plants (Bowman, *et al.*, 2009; Pausas & Keeley, 2009; He, *et al.*, 2012). Although many conifers have developed adaptive traits to live in fire-prone environments, this is not the case for the genus Abies. The firs developed traits appropriate for the humid areas where they thrive, which has rendered them neither resistant (thin bark) nor resilient (recruitment failure in open spaces) to fires (Furyaev, *et al.*, 1983; Vega, 1999).

Remote sensing is useful for assessment and development of measures for mitigation of the effects of global warming in relict Mediterranean fir forests. Spectral imagery has been employed for the early detection of forest pathogen infestations (Immitzer & Atzberger, 2014), to estimate evapotranspiration (Dzikiti, *et al.*, 2019), and to study photosynthetic activity (de Sousa, *et al.*, 2017). Meanwhile, 3D point cloud data from laser scanning (LIDAR) have been employed in fire management (Chuvieco & Kasischke, 2007) and to assess forest volume, biomass (Van Ardt, *et al.*, 2008), and canopy structure (Adamic, *et al.*, 2017) (Mura, *et al.*, 2015). Also, the point cloud can be used for ecological purposes, such as assessing light availability for species distribution modelling (Wüest, *et al.*, 2020) and forest changes in

ecotones (Wang, *et al.*, 2020). Airborne LIDAR has shown better suitability for mapping crown and canopy heights (Wang & Glenn, 2008), although in high density forests the point cloud may not reach the ground, and thus mapping understory vegetation may be inaccurate. However, terrestrial LIDAR has a great potential for estimating shrub and understory biomass, although there are insufficient points for a precise estimation of crown heights when the canopy cover is high (Hilker, *et al.*, 2012).

Mapping fire risk with the support of remote sensing tools is becoming essential for landscape planning in the Mediterranean Basin. High-precision fuel moisture and flammability spatial modelling is achieved by combining satellite and meteorological data into radiative transfer models (Chuvieco, *et al.*, 2006; Yebra, *et al.*, 2018). Burn probability is then assessed through algorithms such as the Minimum Travel Time (MTT) based on the Huygens' principle (Finney, 2002). Several studies have previously applied MTT through FlamMap software on fuel spatial models to assess fire risk in Mediterranean-type ecosystems of Greece (Mitsopoulos *et al.* 2015; Mallinis *et al.* 2016), Italy (Salis *et al.* 2015) and Spain (Molina *et al.*, 2017; Alcasena *et al.* 2019). In this last study, fire risk and highly vulnerable areas were mapped for the whole Catalonia region by applying the Scott & Burgan (2005) fuel model classification on vegetation structure data and running MTT through FlamMap to obtain 150 m resolution fire scenarios. Alternatively, fire spread from specific ignition events can be forecasted, for example, Salis *et al.* (2016) used the FARSITE software to derive fire spread simulations for several Euro-Mediterranean countries along an east-west gradient. All these studies agree that accurate and customized fuel models are key for assessing burn probability and fire risk.

In this respect, airborne LIDAR technology provides an unprecedented tool for fuel and canopy structure characterization in forest ecosystems. However, several studies highlighted limitations of this technology for accurate understory fuel mapping due to the lack of points reaching the ground (González-Olabarria, *et al.* 2012; Botequim, *et al.* 2019). Therefore, LIDAR data need to be implemented in regression models supported by field sampling to eventually characterize the forest structure. For this purpose, hemispherical images are an alternative to traditional field sampling. This technique has been used in forest ecology for more than 50 years, but its widespread adoption was limited due to constraints related to image processing capacity (Chianucci, 2019). However, technical improvements allowed reducing the time for image processing as well as better image quality acquisition. The widespread proliferation of digital cameras has increased the ease of obtaining and storing hemispherical images, which have become an important tool for fieldwork (Hall, *et al.*, 2017). ForeStereo, a forest inventorying device patented by the Forest Research Centre of the Spanish

National Institute for Agriculture and Food Research and Technology (CIFOR-INIA), allows one to obtain stand and tree variables in a cost-effective way by processing pairs of stereoscopic hemispherical images taken at a sampling location (Rodriguez García *et al.* 2014).

Most studies applying LIDAR to circum-Mediterranean fir forests have focused on the most widely distributed Abies alba Mill., whereas those focusing on other species such as the relicts *A. pinsapo* Boiss and *A. numidica* de Lannoy, which are becoming increasingly vulnerable to global change impacts (Liepelt, *et al.*, 2010), are very scant. Aragón *et al.* (2019) and Cortés-Molino *et al.* (2017) studied *A. pinsapo* Boiss forests using LIDAR, but only for basic tree identification and vegetation landscape analysis, respectively. Now, the combination of remote sensing technology such as laser scanning and proximal sensing (e.g., ForeStereo) can contribute to the monitoring of these relict forests through the acquisition of high-precision stand structure data.

Abies pinsapo is restricted to a few areas in southern Spain (*A. pinsapo*), totaling less than 8000 ha (Linares, 2008). Forest fires have markedly reduced the size of populations of this fir; in some localities the longest timespan without fires in the period 1817-1997 was just 34 years (Vega, 1999). Thus, fire is considered the most important threat for the conservation and survival of this endangered species (López-Quintanilla *et al.* 2013). *A. pinsapo* shows a very low resistance to fire due to its thin bark, despite its relatively low fuel flammability and low fire spread rates in dense stands, due to sparse understory and relatively humid conditions (Rodríguez y Silva 1996). Additionally, acute symptoms of tree growth decline and forest dieback due to stand stagnation and climate change have already been reported in some populations (Linares & Carreira, 2009), where *Pinus halepensis* Mill is increasing in abundance, turning previously pure *A. pinsapo* stands into mixed ones (Linares, *et al.*, 2011a).

Our work aimed to combine the use of LIDAR and hemispherical images to study one of the most significant *A. pinsapo* populations, located in a protected area in Málaga (Spain), to assess vulnerability through (i) mapping fire risk and (ii) analyzing canopy structure variability and its possible links to reported declining growth symptoms.

4.2. Materials & methods

4.2.1. Study site

The study location is a steep valley of about 250 ha in area in the municipality of Yunquera, in Sierra de las Nieves National Park (Fig 1.), in a transition between the upper and lower Mesomediterranean bioclimatic band. The annual rainfall is around 1500 mm and the average daily maximum temperature of the warmest month (August) is 33.6 ºC (S.Rivas-Martínez & Rivas-Saenz, 1996-2020). At the southern border of the valley there is a crest that was the limit of a severe wildfire in 1991 that burned 9000 ha (Narváez, 1991). The eastern part is bordered by crop fields. This, together with summer weather conditions and significant touristic pressure in Sierra de las Nieves National Park, makes the risk of wildfire especially high. This forest belongs to the *Paeonio broteroi-Abietetum pinsapo* (Asensi & Rivas-Martínez, 1976) vegetation association composed mainly of pinsapo fir, forming single-species stands in the upper and shaded parts of the valley. The incidence of the root-rot fungus *Heterobasidion abietinum* Niemelä & Korhonen is very high (Linares, *et al*., 2010). In sunny and low-altitude spots, the forest includes *Pinus halepensis* and shrubs of *Juniperus spp* and *Cistus spp*.

4.2.2. Fieldwork: ForeStereo inventory

The purpose of the fieldwork was to classify local fuel models and collect forest structure data, mainly canopy cover, and crown and stand heights. The valley was sampled in Spring 2018 with 49 plots of 8 m radius (201.06 m^2), using stereoscopic hemispherical images for obtaining tree metrics such as stand height (Ho), Canopy Base Height (CBH), Canopy Cover (CC), Canopy Bulk Density (CBD) and basal area (G). Shrub cover and height were also assessed by the line-intersect method to support the classification of the fuel models. Each sampling plot was accurately geolocated using a high precision GNSS receiver, supported by an RTK terrestrial station deployed in the upper part of the valley. We assumed a maximum error of 1m in each plot, due to the difficulty of getting GNSS signal in high dense canopy.

Access to field sites was approved by the Andalusian Regional Government (Consejería de Medio Ambiente y Ordenación del Territorio) with the approval code: *PNSN/AU/10-2018*.

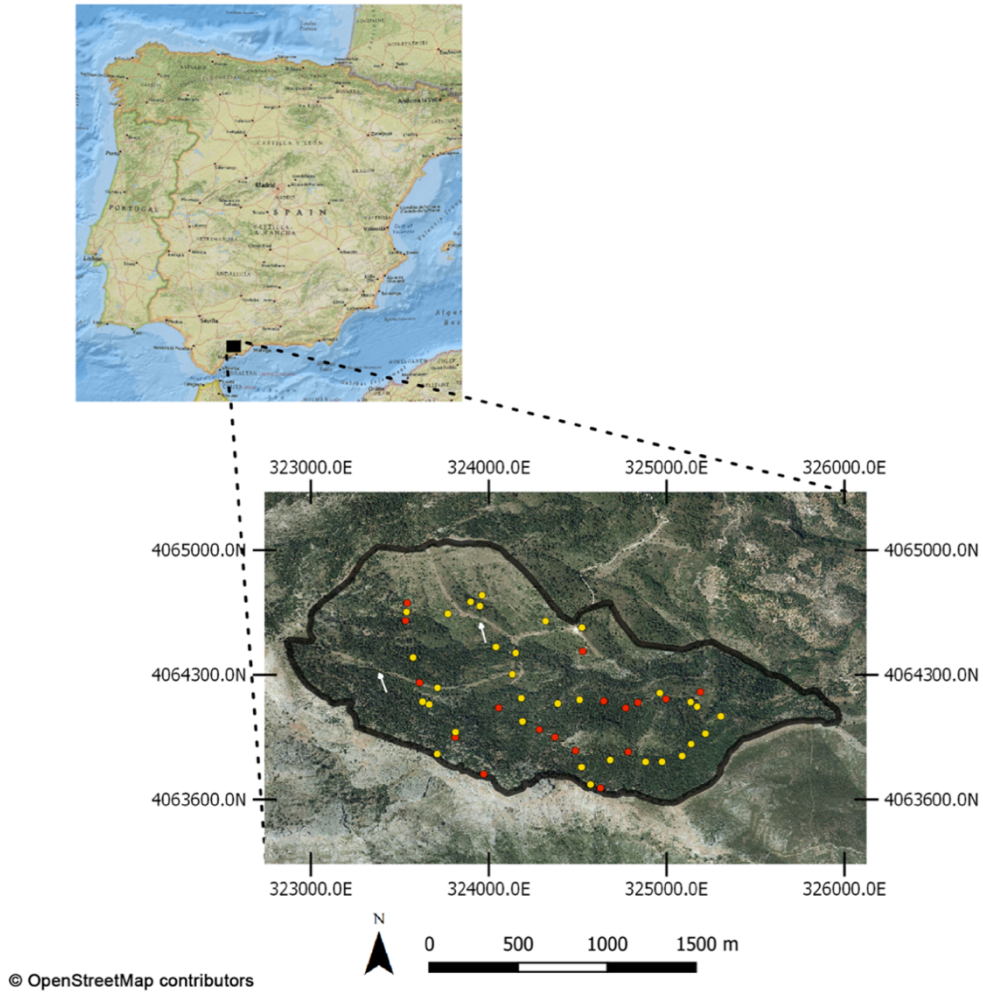

Figure 4.1. Study area location in the National Park of Sierra de las Nieves (Andalusia, Spain). Forty-nine plots were used in the field-based sampling for calibration purposes using ForeStereo device. Yellow points are training plots, red ones are validation plots. White arrows indicate the firewalls opened on the area. Base map and data from OpenStreetMap and OpenStreetMap Foundation.

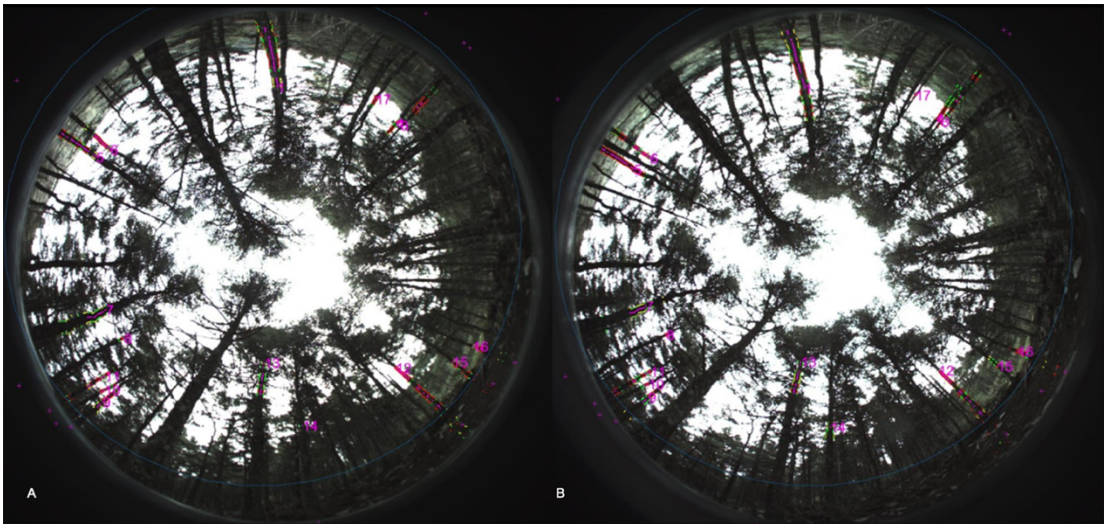

Figure 4.2. Example of hemispherical pair images obtained with ForeStereo to characterize forest stand canopy structure and the field sampling plots. (A) and (B) are both stereoscopic images obtained at the same time in each plot.

Forest inventory was derived using ForeStereo, a device developed by the Forest Research Centre of the Spanish National Institute for Agriculture and Food Research and Technology (INIA-CIFOR). ForeStereo is equipped with two upward-looking fish-eye cameras. At each sampling location three pairs of hemispherical stereoscopic images (Fig. 4.2*)* with different exposures are taken. The matching process, compiled in a MatLab® software package, consists of four main steps as detailed in Sánchez-González (2016): (i) a supervised segmentation of tree stems and crowns; (ii) correspondence of features between the two images and photogrammetric retrieval of tree dimensions; (iii) tree variable modelling and (iv) stand variable estimation, which requires correction of instrumental bias and occlusions *(*Montes, 2019*)*. ForeStereo was used to estimate tree height, crown base height, crown volume and diameter at breast height (DBH) for each tree, number of stems per hectare and crown cover (CC) and stand basal area (G). Tree metrics from the hemispherical images were compared with airborne LIDAR output data to develop regression models. Thirty-two of the plots were randomly chosen to adjust the models, and the remaining seventeen plots were used to assess the models' predictive capability.

Because the geometry of the ForeStereo system and image projections is known, no additional data calibration is needed to carry out photogrammetric retrieval of tree variables. Accuracy of ForeStereo estimated through the Root Mean Squared Error (RMSE) ranges from 0.015 to 0.057 m for DBH (Rodríguez-García, *et al.*, 2014; Sánchez-González, et al., 2016), 2.59 to 6.4 m for tree height (Rodríguez-García, *et al.*, 2014; Marino *et al.* 2018) and 3.1 and 0.6 m for crown base height and crown diameter respectively (Marino *et al*, 2018), and 11.6 m2/ha for G (Sánchez-González, 2016).

With the ForeStereo data we were able to estimate stand height at each plot following the Assman's criteria (Assman, 1970), whereas the canopy cover was obtained directly from the hemispherical images, and the Canopy Base Height (CBH) was averaged for each plot. The calculation of the Canopy Bulk Density (CBD) was based on equations reported by Ruiz-Peinado, *et al.*, (2011) for *A. pinsapo*, in which tree height and stem diameter are used to calculate thin branch and needle biomass. Therefore, CBD is estimated by dividing biomass by crown volume (which is obtained from ForeStereo estimates). with the results from this analysis.

4.2.3. LIDAR data

The LIDAR data were obtained in 2015 by the Spanish National Geographic Institute, through the "Plan Nacional de Ortofotografía Aérea (PNOA)" project. The point cloud density is 0.5 points·m^{-2}. FUSION software was employed for point cloud processing and data extraction (McGaughey & Carson, 2003). A correlation matrix between ForeStereo tree data and all LIDAR metrics obtained with FUSION was useful to detect which LIDAR metric was most suitable to build the regression models in 32 random plots. We selected the best correlation results ($R<0.5$, p-value < 0.05) to test linear, power, and exponential regression models. The models with less root-mean-square error (RMSE) and higher adjusted-R in the remaining 17 plots were chosen to predict ForeStereo tree metrics from the LIDAR point cloud. Height break for LIDAR metrics was 4 m, whereas it was 0.25 m for the total vegetation height to avoid high shrubs influence and ground points, respectively. These two height breaks were tested to inquire which one was the better to fit the models.

General canopy structure traits such as canopy cover and height were analysed from the regression models obtained to detect symptoms of declining growth in this *A. pinsapo* forest. These variables were chosen because airborne LIDAR can estimate them accurately

(Ahmed, *et al.*, 2015; Arumäe & Lang, 2018). Also, we tested whether canopy bulk density was consistent with the results from this analysis.

4.2.4. Fuel models and fire scenarios

To simulate fire risk, we first classified field plots according to the UCO40 fuel models, which use specific criteria and traits appropriate for Mediterranean environments and thus perform better than the widely used Prometheus or Rothermel models (Rodríguez y Silva & Molina Martínez, 2010; 2012). We identified a total of 6 fuel models across the plots (Table 4.1, Fig. 4.3). The UCO4 procedure is based on the fuel models classification of Scott & Burgan, (2005), but adapted for southern Spain climate conditions through providing hybrid model types that represent fuel traits and their evolution. Shrub and climate characteristics have shown different behaviours between American and Mediterranean fuel models, so parameters such as fuel load and fuel bed depth must be adjusted (Rodríguez y Silva & Molina Martínez, 2012).

Ecognition® software was used to segment the place of study using the Nearest Neighbour algorithm in an Object-Based Image Analysis (OBIA) (Gao, *et al.*, 2007). To carry out this segmentation, we used the raster layers resulting from the regression models validated previously (CBD, CBH, G, Hv) along with NDVI data from Sentinel-2 images (2015) and terrain models obtained from the LIDAR point cloud (topography, aspect, and slope). Later, a confusion matrix was calculated to evaluate the accuracy of the fuel model classification.

The following raster layers generated from the regression models were incorporated: terrain elevation, aspect, slope, Ho, CBH, CBD, CC, and fuel models.

The initial fuel moisture file (.FMD) used was based on Scott & Burgan (2005) suggestions. We assumed a low moisture content (two-third cured) for the fuel more commonly found in north-facing slopes (fuel models M8, HR7 and R4; see Table 4.1) and very low moisture content (fully cured) for the fuel models more frequently found in south-facing slopes (M3, M9 and HPM4). A Weather Stream file (.WXS) with typical values of circadian change under summer weather conditions in the area was used for dead fuel moisture conditioning (Table 4.2). This file modifies initial dead fuel moisture based on changes during a given

period in weather variables such as temperature, relative humidity, cloud cover and hourly precipitation.

Conditioning also implies adjusting initial dead fuel moisture to site factors (elevation, slope, aspect, and canopy cover), based on the corresponding raster layers previously uploaded in FlamMap (Finney, 2006). The .WXS file was built from meteorological data that are continuously recorded in situ by the University of Jaén (values of temperature, precipitation, and relative humidity) and from records of the Spanish Meteorological Agency-AEMET (values of wind and cloud cover). We chose the warmest day of 2014 (available recorded data) for the conditioning period between the 10:00 to 19:00 hours without precipitations or any cloud cover. The conditioned fuel moistures at the end of this period were the final fuel moistures used for the simulations.

Table 4.1. Fuel model classification obtained following the UCO40 criteria (Rodríguez y Silva & Molina-Martínez, 2012), based on Scott & Burgan (2005). Dead fuel models are classified by the time lag: the time required for the moisture content of a fuel to respond within 2/3 of the new equilibrium moisture content. Larger diameter fuels have longer time lags, so they respond slower to environmental changes (Anderson, 1982). LiveH: Live herbaceous fuel, LiveW, Live wood fuel. Moisture of extinction (%): moisture content that prevents flame from propagating.

Fuel type	Fuel loading (tn/ha)					Moisture of extinction (%)	Fuel bed depth (cm)
	Time lag			LiveH	LiveW		
	1h	10h	100h				
Predominance of shrubs							
M3	11.47	2.88	3.37	0	6.10	15	82.29
M8	11.23	6.10	3.47	0	7.27	30	121.92
M9	34.71	9.86	4.93	0	18.89	15	182.88
Pine-needle litter with shrubs and/or grassland under forest canopy							
HPM4	17.63	13.23	1.17	0	11.13	20	76.2
Predominance of pine-needle with branches and other canopy debris							
HR7	0.73	3.76	3.47	0	0	25	18.28
Predominance of canopy debris accumulation							
R4	1.57	5.16	6.29	0	0	25	82

We obtained three different datasets as model outputs: (i) Burn probability based on 200 random ignition points using the MTT algorithm, (ii) flame length and (iii) flame spread

rate, calculated for each cell. The purpose of simulating fire scenarios was to detect vulnerable areas and to assess for conservation planning how exposed the pinsapo forest is to this risk. For this reason, we did not simulate specific events or spotfires using Farsite software.

Instead, FlamMap software is more appropriate, because it calculates spread rate and flame length for each landscape cell without a temporal component and uses MTT to simulate 200 random fires to predict the probability of a point to be burned (Finney, 2006; González-Olabarria, *et al*., 2012). The simulations were set under two prevailing wind conditions: west winds (locally called "Ponent") and east winds (called "Levant"), both for a typical speed of 13 $km \cdot h^{-1}$.

Table 4.2. Dead fuel moisture conditioning. Weather stream file (.WXS) showing typical summer weather circadian change in the area, used as input to FlamMap software for quantifying the moisture of dead fuel.

Date	T (ºC)	RH (%)	PP (mm)	Wind SP (m/s)	Wind dir. (º)	Cloud (%)
08/27/14 10:00	28	33	0	2	180	0
08/27/14 11:00	29	32	0	2	180	0
08/27/14 12:00	30	29	0	1	180	0
08/27/14 13:00	31	27	0	2	180	0
08/27/14 14:00	30	27	0	2	180	0
08/27/14 15:00	29	28	0	2	180	0
08/27/14 16:00	29	29	0	2	180	0
08/27/14 17:00	28	30	0	1	180	0
08/27/14 18:00	27	31	0	2	180	0
08/27/14 19:00	26	32	0	2	180	0

4.3. Results

We found that the LIDAR metrics that best fit the ForeStereo data were (Table 4.3): Percentage of first returns above 4 m (x), Percentage of all returns above 4 m (y), Percentage of all returns above mean (z) and Percentage of first returns above 0.25 m (d). All the significant regression models were obtained with 95% confidence in the seventeen validation plots. Basal Area (G) was the only variable with an acceptable fit using a height break of 0.25 m. The rest of the variables were better modelled above 4 m. Canopy Cover (CC) had the best fitting model with an RMSE less than 20%, while the greatest error was found in modelling the Canopy Base Height (CBH) with an RMSE of 83.3%. This high difference could be due to low point cloud density (minimum 0.5 points·m^{-2} guaranteed) as well as the fact that airborne LIDAR produces better accuracy for variables related to the top of the canopy (Hilker, *et al*., 2012), such as canopy cover or canopy height, than variables under the canopy. Results for dominant height were acceptable (RMSE of 0.55), because finding the top of the crowns with ForeStereo in high-density forests can be difficult.

The error matrix for the fuel model classification using the Nearest Neighbour algorithm shows an overall accuracy of 0.56 and a Kappa Coefficient (KIA) of 0.46 (Table 4.4). The most frequent fuel model in the study area was M9 (30.5% of land cover), followed by M3 with 27.4% and M8 with 23%. In all the fuel models, shrubs play a predominant role in the fire behaviour. The least frequent fuel models were HPM4 (7.19% of land cover; fire behaviour mainly controlled by needle litter together with understory shrubs and/or grasses), HR7 (6.12% of land cover; conifer-needles and branches and other canopy debris play a predominant role) and R4 (5.73% of land cover; predominance of canopy debris accumulation in fire behaviour).

Figure 4.3. Example of the six fuel models identified in the plots based on Rodríguez y Silva & Molina Martínez's (2010) handbook. (A) R4 model: Predominance of canopy debris accumulation (B) HR7 model: Predominance of pine needle with branches (C) HPM4 model: Pine-needle with shrubs and grass (D) M3 model: Predominance of shrubs with a fuel bed close to 1 m (E) M8 model: Predominance of shrubs with grass with a fuel bed of 120 m. (F) M9 model: Predominance of thick shrubs with a fuel bed over 175 m.

Table 4.3. Best regression models between LIDAR data (independent variable) and field-based ForeStereo data (dependent variable), used to map spatial distribution of the main forest structure variables. To find which LIDAR data best suit to each field data, a correlation matrix was done. The best results (R> 0.5 and p-value < 0.05) were tested by using linear, power, and exponential regression models. The models with highest R^2 and lower RMSE were selected. CC: canopy cover; Ho: stand height; CBH; canopy base height; CBD; canopy bulk density; G: basal area, x: Percentage of LIDAR first returns above 4 m, y: Percentage of all returns above 4 m, z: Percentage of all returns above mean, d: Percentage of first returns above 0.25 m.

Dependent variable	Predictive model	R^2	RMSE (%)
CC	$x \cdot 0.92023$	0.84	17.7
Ho	$0.1469 \cdot y$	0.61	55.7
CBH	$x^{0.013839}$	0.43	83.3
CBD	$z \cdot 0.007893$	0.64	59.5
G	$d \cdot 9.28 \cdot 10^{-8}$	0.61	67.3

Table 4.4 Confusion matrix of the Nearest Neighbour classification for the fuel models. User accuracy: how often the class on the map will actually be present on the ground. Produce accuracy: how often are real features on the ground correctly shown on the classified map.

	Predicted classes						
		M3	**M8**	**M9**	**HPM4**	**HR7**	**R4**	**Sum**
Actual classes	Fuel type observed in field							
	M3	2	0	0	1	2	0	5
	M8	0	5	1	0	0	0	6
	M9	3	0	3	0	0	0	6
	HPM4	0	0	0	2	2	1	5
	HR7	0	1	0	0	0	1	2
	R4	0	0	0	0	0	3	3
	Sum	5	6	4	3	4	5	
	Accuracy							
	Producer	0.4	0.83	0.75	0.7	0	0.6	
	User	0.4	0.83	0.5	0.4	0	1	
	Overall accuracy				KIA			
	0.56				0.46			

Once the corresponding layers were created based on the regression models, the fuel model classification, and the terrain elevation data (Fig.4.4), fire simulations under two wind conditions were obtained from FlamMap (Fig.4.5). The final landscape file keeps the same pixel resolution of the input data (10 m). We found higher burn probabilities and spread rate under Levant wind conditions, but similar flame length scenarios under both Levant and Ponient winds. Burn probability was higher under Levant winds, with a mean value of 0.078, than under Ponent winds, with a mean value of 0.061. Fire spread rate showed a mean value of 41.82 m· min^{-1} under Levant wind conditions, and more than 50% of the landscape showed spread rates ≥50 m·min^{-1}. In contrast, Ponent winds resulted in lower fire spread rates (mean value of 33.34 m· min^{-1}) and a considerably lower fraction of the landscape (36%) was affected by spread rates ≥50 m· min^{-1}. Flame length values were similar for the fire simulations under both wind directions.

Regarding the canopy structure analysis to detect symptoms of forest decline and dieback, the estimated variables CBH and G were not considered due to RMSEs far above 60%. Instead, we use Ho and CC (Fig. 4.6), as well as CBD, for such assessment. The following results were estimated only in the landscape cells with a vegetation height above 4 m, in order to exclude non-forest patches of shrubs, as well as forest gaps recently opened due to tree mortality (Fig.4.7). Canopy heights (Ho) ranged from 4 to 18 m, with a mean value of 9.1 m and a standard deviation (SD) of 3.28. It is remarkable that the mode of canopy heights falls below 5 m in this forest area not affected by fire since the mid-20th century and under long-term, no management policy. On the other hand, canopy height classes between 7 and 12 m showed similar frequencies (high equitability). Lastly, canopy heights higher than 15 m were present, but with rather low frequency.

Canopy cover had a mean value of 64.5% and an SD of 18. We found low frequencies for values between 0-30% (<2% of the area) because most areas with low CC corresponded to land covered by shrubs with less than 4 m heights. Almost 25% of the land showed CC values above 80%, which means that areas with near to full cover are relatively common. Also, 66% of the area had a CC of 40-80%. Lastly, CBD mean value was 0.16 kg·m^{-3} with a SD of 0.1. Our results showed a high canopy density because >60% of the area had values over 0.1 kg·m^{-3} and >30% was over 0.3 kg·m^{-3}.

4.4. Discussion

Endangered circum-Mediterranean firs are highly vulnerable to climate change effects in the isolated areas where they remain (Sánchez-Salguero, *et al.*, 2017). *Abies nebrodensis* Mattei is currently the rarest conifer in the European flora, with only 34 mature trees able to reproduce sexually in the wild (Pasta, *et al.*, 2019). The recovery of this species and the protection of the other ones to avoid a similar decrease is an urgent matter that demands the best techniques available to support the traditional field survey.

We propose a methodology that combines the use of LIDAR with ForeStereo, UCO40 fuel models, and FlamMap simulations to significantly reduce the effort and time required for fieldwork, increasing the efficiency of the massive data capture required in forest management.

The application of this methodology in the study area obtained fire simulations that showed that east wind conditions ("Levant") resulted in worse fire scenarios than west winds ("Ponent") as illustrated in Fig. 345. Spread rate appears to be more influenced by topography and wind conditions (Salis, *et al.*, 2016) than by flame length, which appears to be more influenced by fuel characteristics. Low spread rate and flame length were found in areas with HR7 and R4 models because they correspond to high-density *A. pinsapo* stands, consistent with the findings of Rodríguez y Silva (1996).

Similar results can be found in the Euro-Mediterranean study of Salis *et al.*, (2016), in which the maximum spread rates simulated in the Attica region (Greece), Budoni (Italy), and Fresnedoso de Ibor and Navalmoral (Spain) are between 50-110 m· min^{-1}. In their study, the worst flame length scenarios are located in Fresnedoso de Ibor (Spain) and Penteli (Greece) with a range between 25-50 m. They also found a higher spread rate and low flame length mainly in areas with herbaceous vegetation, but also in forest and shrublands in steep mountains exposed to wind (as in our study). In these areas flame length is also higher than in lands with herbaceous vegetation.

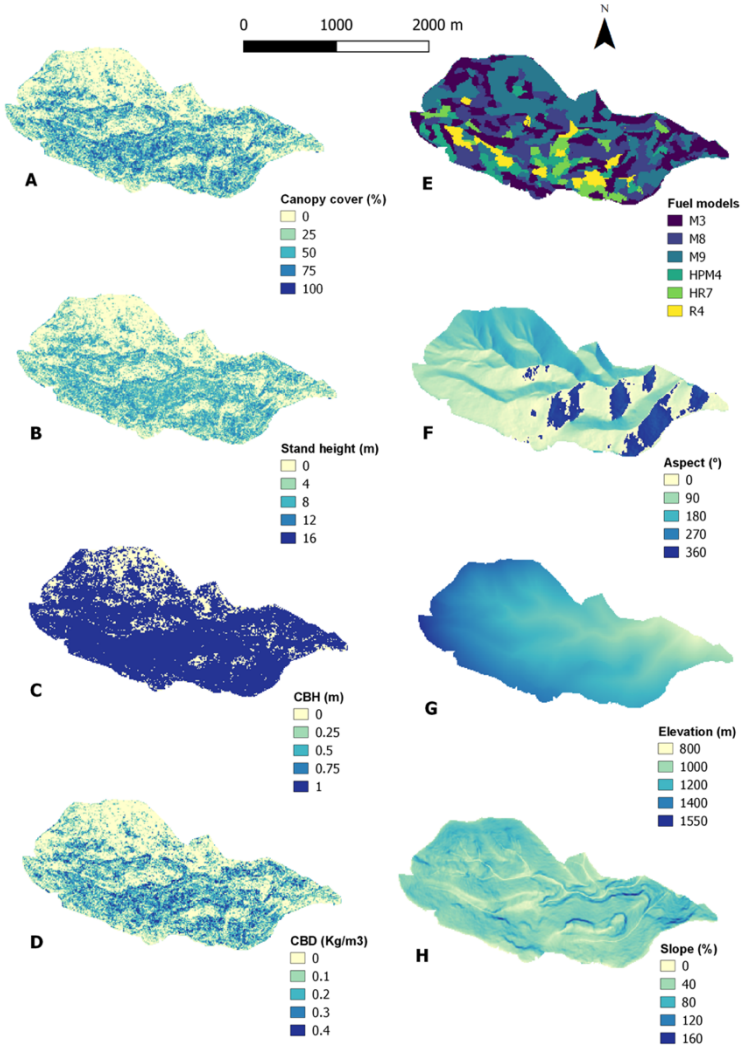

Figure 4.4 LIDAR raster layers produced to run FlamMap. A) Canopy cover (%). (B) Stand height (m). (C) CBH (m). (D) CBD (Kg/m³). (E) Fuel models. (F) Aspect (°). (G) Elevation (m). (H) Slope (%).

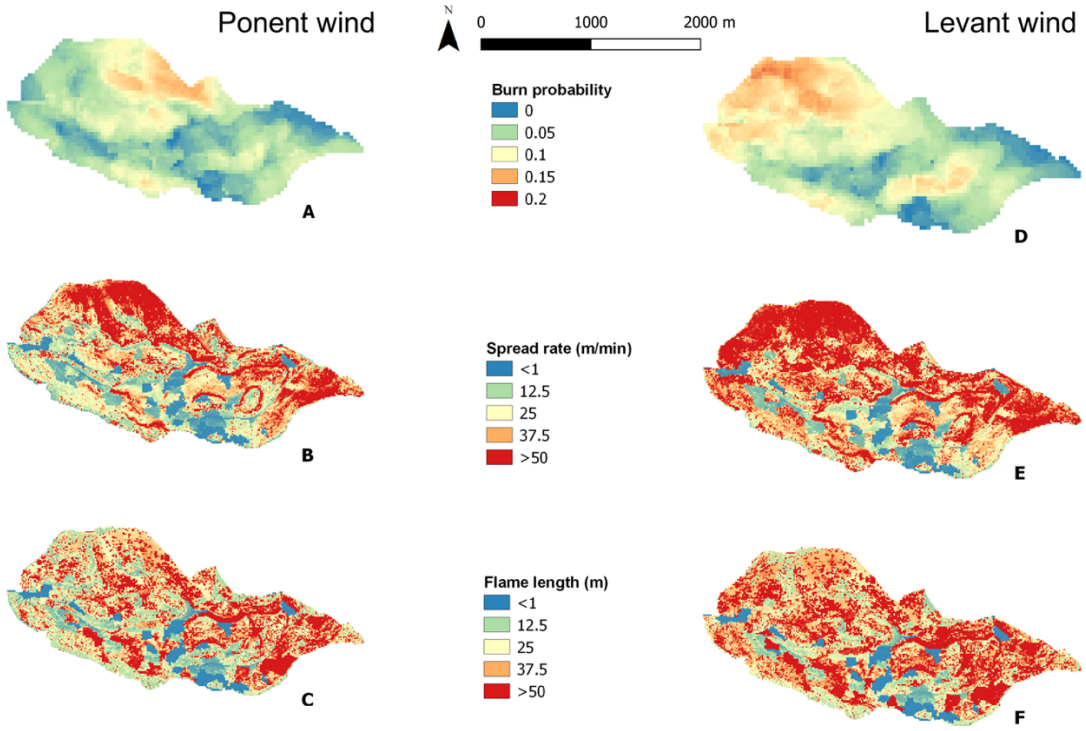

Figure 4.5. Fire simulations obtained from FlamMap for Ponent wind (West) and Levant wind (East) conditions. A) Burn probability in Ponent wind. (B) Spread rate in Ponent wind (m·min^{-1}). (C) Flame length in Ponent wind (m). (D) Burn probability in Levant wind. (E) Spread rate in Levant wind (m/min). (F) Flame length in Ponent wind (m).

However, both wind conditions generate two remarkable foci of fire risk, well highlighted in the burn probability map (Fig 4.5). One is in the north-west part of the valley, on south-facing slopes (180º N) where very dense and tall (>1.80 m) patches of the shrub *Juniperus spp* on steep terrain represent ideal conditions for a high fire spread rate (>50 m·min^{-1}), whereas the flame length will depend more on the wind (Ponent >15 m, Levant >30 m). It is not surprising that this condition corresponds to the M9 fuel model (Table 4.1), in which massive shrub formations dominate the fire behavior. The other focus is in the eastern part of the valley, due to the occurrence of fuel models for which fire behavior is mainly determined by the combination of dense shrub cover and very steep slopes (>75º).

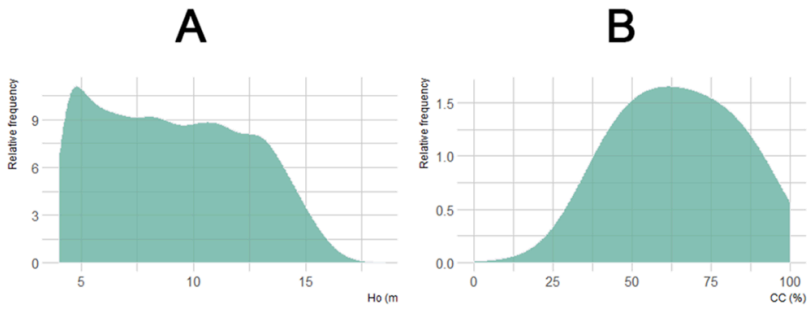

Figure 4.6. Frequency histograms for canopy height (Ho, A), and canopy cover (CC, B) values as derived from regressions between ForeStereo and LIDAR data, in the studied *A. pinsapo* forest.

González-Olabarria (2012) observed a lower fire risk landscape in a carefully managed even-aged forest of *Pinus nigra*. and *P. pinaster*, whereas our study corresponds to a non-managed forest of pinsapo firs. This contrast strengthens the argument for the urgent need for adaptive management of these endemic fir forests, abandoning the traditional paradigm of non-management in biological conservation. The kind of prevailing fuel model appears to be determinant for the fire scenarios obtained, and the current "don't touch" management strategy, together with the invasion by shrubs into forest mortality gaps, seem to promote high fire risk fuel models in the area.

The distribution of canopy structure features depicted in Fig. 4.6 highlights: (i) that the most frequent stand height barely reaches 5 m, the mean value is just 9.1 m and figures higher than 12-15 m are rare despite the fact that *A. pinsapo* can reach up to 30-35 m in height (López-Quintanilla, *et al*., 2013); (ii) that canopy cover has an average value of 64.5%, well below the full-cover criterion under a 'set aside' and 'no management' strategy since the late 1960s, and patches with 90%-100% cover account for less than 10% of the whole area; and (iii) that there is an overall very high variability for both stand height and canopy cover values across the landscape, with a relatively high evenness in both variable distributions, especially regarding tree height. All these results indicate a lack of old growth stands in the study area, and the predominance of secondary forests, which is consistent with previous studies based on field surveys (Linares, *et al*, 2011b; 2013).

We found considerably high values of canopy density (CBD: Fig. 4.4), which can increase the risk of severe crown fires (Arellano, 2017). These canopy density values in a well

below full-cover area, together with low Ho suggests two possible explanations: (i) the high CBD values correspond to full-cover patches with older stands where gaps are still not open and/or (ii) shrub strata are increasing their height above 4 m, interlocking with the canopy. Both are compatible with different phases of forest decline and the gap opening process.

The low stand height values we found, even in the patches with older stands and high cover values, could indicate symptoms of stand stagnation in such patches. A multi-temporal comparison (1957-2007) and fractal analysis of digital panchromatic aerial photographs of the same area (Linares, *et al.* 2006; 2009), revealed a process of simultaneous stand densification and expansion of *A. pinsapo* at the landscape level in the last decades. This is a consequence of strict protection since the 1960s of an area mostly covered at the time by bare soils and open scrublands, with a few sparsely distributed and small stands and isolated trees of *A. pinsapo*. Increasing competition due to the densification of these regenerating even-aged stands led to stand stagnation in the 1980s, which acted as a predisposing factor for the climate change-induced forest decline symptoms reported since 1994-95, associated with a series of very intense drought spells that acted as an inciting factor (Linares & Carreira, 2009). Finally, tree growth decline and loss of vigour led to the expansion of the root-rot fungus pathogen *Heterobasidion abietinum*, (Linares, *et al.*, 2010), which acted as a contributing factor (Manion, 1981) causing widespread mortality and extensive formation of forest-gaps in the last two decades (> 1/3 of the previous basal area lost). This multifactorial forest decline and dieback process increases the production of HR7 and R4 fuel models, as shown in Fig. 4.7. Under the prevalent 'no-management' policy, these new open areas are, eventually, being invaded by dense shrubs, as supported by our LIDAR and ForeStereo data. This increases their importance in the fire behaviour and promotes fuel models with high fire spread rate such as the UCO M9 fuel type. The fuel model classification revealed a remarkable contribution of M9 (Fig.4.4), covering 30.5% of the study area. This suggests that shrub invasion is taking place and is already in an advanced phase. Also, the CBD values point to a high exposure to crown fires (Arellano, *et al.*, 2017) and could explain the forecasted high flame length in some areas.

As explained in the Introduction section, fire intensity in pinsapo forests is known to be low, but the above-mentioned current invasion into the mortality gaps by the surrounding dense shrubs could invert this tendency.

However, it must be highlighted that the efficacy of employing fire simulations in risk management strongly depends on input data of high accuracy and precision, due to the complex heterogeneity of forest landscapes (Rodríguez y Silva & Molina-Martínez, 2012).

Although we precisely determined shrub composition and structure in a set of training field plots, the low LIDAR point cloud density available hindered reliable mapping of understory vegetation, which thus may restrict the accuracy of the obtained fire risk simulations. The combined use of LIDAR, both terrestrial and airborne, could be the best option to map fuel models and canopy data such as Canopy Base Height and Canopy Bulk Density, for increased accuracy. Nevertheless, ForeStereo was shown to be a useful alternative to terrestrial LIDAR for calculating stand structure. Our study attempts to set a precedent as the first approach to fire risk analysis in *Abies pinsapo* forests using LIDAR. Also, it demonstrates the significant potential of this method for study of the ecological structure of populations of endangered fir species, and to broaden the understanding of their conservation status. Most of the current work with LIDAR data focuses on forests with commercial interest, and few studies have employed this technology to understand the structure of the populations of endangered species forests and their vulnerability to fire risk.

Figure 4.7. Photograph showing the widespread decline and dieback processes (stand stagnation, tree mortality, forest gap opening) that *A. pinsapo* forests are experiencing in the study area. The dieback process of *A. pinsapo* forests stimulates the production of R4 fuel model (abundant dead wood and debris accumulation).

4.5. Conclusions of the study

Our results show a high fire risk for the largest remaining continuous forest of the relict and endangered *A. pinsapo* tree species. Such risk, especially under east wind conditions (Levant), was found to be associated with a remarkable presence of shrub-dominated fuel models (M9). Using aerial LIDAR and ForeStereo data to assess stand structure spatial variability in the area, we found symptoms of stand stagnation and forest decline under the current no-management conservation policy. This process together with climate change trends triggers the formation of mortality-gaps that are eventually invaded by shrubs, increasing the production of the M9 fuel model, which in turn worsen fire risk. These findings stress the need for proactive adaptive management of *A. pinsapo* forests, including: (i) the creation of bare patches through shrub clearing, (ii) a reinforcement of the firewalls in the west part of the valley and (iii) promotion of grazing and trampling levels by wild ungulates (or domestic livestock if they were insufficient) to reduce shrub fuel load without compromising *A. pinsapo*. We also support the efficacy of thinning treatments for canopy structural diversity enhancement as an essential tool to avoid stand stagnation (Linares *et al.*, 2009a), (Linares, *et al.*, 2009b), (Lechuga, *et al.*, 2017; 2019) and high CBD values, to reduce the probability of crown fires and thus increase resilience to wildfires (Koontz, *et al*, 2020), as well as to reduce climate change-induced tree mortality (Linares, *et al.*, 2009a).

The importance of the *A. pinsapo* populations in Sierra de las Nieves is one of the main reasons that inspired Spanish national policy to upgrade this protected area into a National Park. Although the models obtained have low accuracy due to technical limitations, our study provides a preliminary estimate, a first step to assess pinsapo forest risk factors using remote and proximal sensing as essential tools to support conservation management. These methods can also be extended to the monitoring of other endangered Western Mediterranean relict fir forests such as those of *A. numidica* De Lannoy and *A. marocana* in North Africa and can be implemented in their conservation strategies.

References

Adamic, M., Diaci, J., Rozman, A., & Hladnik, D. (2017). Long-term use of uneven-aged silviculture in mixed mountain Dinaric forests: A comparison of old-growth and managed stands. *Forestry*, 90(2), 279-291. https://doi.org/10.1093/forestry/cpw052

Ahmed, O. S., E., F. S., Wulder, M. A., & White, J. C. (2015). Characterizing stand-level forest canopy cover and height using Landsat time series, samples of airborne LIDAR, and the Random Forest algorithm. *ISPRS Journal of Photogrammetry and Remote Sensing*, 101, 89-101. https://doi.org/10.1016/j.isprsjprs.2014.11.007

Alcasena, F. J., Ager, A. A., Bailey, J. D., Pineda, N., Vega-García, C. (2019). Towards a comprehensive wildfire management strategy for Mediterranean areas: Framework development and implementation in Catalonia, Spain. *Journal of Environmental Management*. 231 303–320 https://doi.org/10.1016/j.jenvman.2018.10.027

Anderson, H.E. (1982). *Aids to determining fuel models for estimating fire behavior*. General Technical Report INT-122, United States Department of Agriculture, Forest Service, Intermountain Forest and Range Experiment Station, Ogden, UT. 26 p

Aragón, J. F., Navarro Cerrillo, R., & Mesas Carrascosa, F. (2019). Validación de un paratrike como plataforma para la captación de imágenes de alta resolución en formaciones de *Abies pinsapo* Boiss. *Cuadernos de la Sociedad Española de Ciencias Forestales*, 45(2), 171-204. https://doi.org/10.31167/csecfv5i45.19875

Arellano Pérez, S., González Álvarez, J. G., Vega Hidalgo, J. A., Ruiz González, A. D. (2017). *Modelos de estimación de la distribución vertical de combustibles finos de copas en masas de pinar a partir de datos del IV Inventario Forestal Nacional.* 7º Congreso Forestal Español. Plasencia (Cáceres, Spain).

Arumãe, T., & Lang, M. (2018). Estimation of canopy cover in dense mixed-species forests using airborne lidar data. *European Journal of Remote Sensing*, 51(1), 132-141. https://doi.org/10.1080/22797254.2017.1411169

Asensi, A., & Rivas-Martínez, S. (1976). *Contribución al conocimiento fitosociológico de los pinsapares de la Serranía de Ronda*. Anales Instituto Botánico Cavanilles, 33, 239-247.

Assman, E. (1970). *The principles of forest yield study*. Ofxord: Pergamon Press, 506. ISBN: 9781483150932

Botequim, B., Fernandes, P. M., Borges, J. G., González-Ferreiro, E., Guerra-Hernández, J. (2019). Improving silvicultural practices for Mediterranean forests through fire behavior modelling using LiDAR-derived canopy fuel characteristics. *International Journal of Wildland Fire*. 28, 823–839 https://doi.org/10.1071/WF19001

Bowman, D., Balch, J. K., Artaxa, P., Bond, W. J., Carlson, J. M., Cochrane, M. A., D'Antonio C. S., De Fries R. (2009). Fire in the earth system. *Science*, 324, 481-484. https://doi.org/10.1126/science.1163886

Chianucci, F. (2019). An overview of in situ digital photographic approaches to estimate forest canopy attributes. *Canadian Journal of Forest Research*. https://doi.org/10.1139/cjfr-2019-0055

Chuvieco, E., Riaño, D., Danson, F. M., Martin, P. (2006). Use of a radiative transfer model to simulate the postfire spectral response to burn severity. *Journal of Geophysical Research: Biogeosciences*, 111 (G4).

Chuvieco, E., & Kasischke, E. S. (2007). Remote sensing information for fire management and fire effects assessment. *Journal of Geophysical Research: Biogeosciences*, 112 (G1). https://doi.org/10.1029/2006JG000230

Cortés-Molino, A., Melero Jiménez, I. J., Fernández Luque, I., Flores-Moya, A., & Salvo Tierra, A. E. (2017). *Análisis de la estructura de la vegetación del poljé de la Nava de los Pinsapos mediante tecnología LIDAR*. Murcia: Asociación Española de Teledetección. ISBN: 978-84-9048-650-4

De Sousa, C. H., Hilker, T., Waring, R., de Moura, Y. M., & Lyapustin, A. (2017). Progress in remote sensing of photosynthetic activity over the Amazon Basin. *Remote Sensing* (Basel), 9(1). https://doi.org/10.3390/rs9010048

Dzikiti, S., Jovanovic, N. Z., Bugan, R. D., Majozi, N. P., Nickless, A., Cho, M. A., . . . Pienaar, H. H. (2019). Comparison of two remote sensing models for estimating evapotranspiration: algorithm evaluation and application in seasonally arid ecosystems in South Africa. *Journal of Arid Land*, 11, 495-512. https://doi.org/10.1007/s40333-019-0098-2

Finney M (2002). Fire growth using minimum travel time methods. *Canadian Journal of Forest* Research 32:1420–1424

Finney, M. A. (2006). *An overview of FlamMap fire modelling capabilities*. USDA Forest Service Proceedings, 41, 213-220.

Furyaev, V., Wein, W. R., & MacLean, D. A. (1983). Fire influences in Abies-dominated forests. In R. W. MacLean (Ed.), *The role of fire in Northern Circumpolar Ecosystems* (pp. 221-234). John Wiley & Sons Ltd. Chinchester

Gao, Y., Mas, J. M., Niemeyer, I., Marpu, P. R., & Palacio, J. L. (2007). *Object-based image analysis for mapping land-cover in a forest area*. Enschede: International Symposium for Spatial Date Quality (ISSDQ).

González-Olabarria, J. R., Rodríguez, F., Fernández-Landa, A., & Yudego-Mola, B. (2012). Mapping fire risk in the Model Forest of Urbión (Spain) based on airborne LIDAR measurements. *Forest Ecology and Management*, 282, 149-156. https://doi.org/10.1016/j.foreco.2012.06.056

Hall, R. J., Fournier, A. F., & Rich, P. (2017). *Introduction. In Hemispherical Photography in Forest Science: Theory, Methods, and Applications* (Vol. 28, p. 313). Springer. ISBN 978-94-024-1098-3.

He, T., Pausas, J. G., Belcher, C. M., Schwilk, W. D., & B., L. B. (2012). Fire adapted traits of Pinus arose in the fiery Cretaceous. *New Phytologist*, 194, 751-759. https://doi.org/10.1111/j.1469-8137.2012.04079.x

Hilker, T., N., C. C., Newnham, G. J., van Leeuwen, M., Wulder, M. A., Stewart, J., & Culvenor, D. S. (2012). Comparison of terrestrial and airborne LIDAR in describing stand structure of a thinned lodgepole pine forest. *Journal of Forestry*, 110(2), 97-104. https://doi.org/10.5849/jof.11-003

Immitzer, M., & Atzberger, C. (2014). Early detection of bark beetle infestation in Norway Spruce (*Picea Abies*, L.) using WorldView-2 Data. *Photogrammetrie - Fernerkundung - Geoinformation*, 2014(5), 351-367. https://doi.org/10.1127/1432-8364/2014/0229

Lechuga, V; V. Carraro, B. Viñegla, J.A. Carreira, J.C. Linares. (2017). Managing drought-sensitive forests under global change. Low competition enhances long-term growth and

water uptake in *Abies pinsapo*. *Forest Ecology and Management* 406: 72-82. https://doi.org/10.1016/j.foreco.2017.10.017

Lechuga, V.; V. Carraro, B. Viñegla, J.A. Carreira, J.C. Linares. (2019). Carbon limitation and drought sensitivity at contrasting elevation and competition of *Abies pinsapo* Forests. Does experimental thinning enhance water supply and carbohydrates? *Forests* 10 (12): 1132 (17 pp.). https://doi.org/10.3390/f10121132

Liepelt, S., Mayland-Quellhorst, E., Lahme, M., & Ziegenhagen, B. (2010). Contrasting geographical patterns of ancient and modern genetic lineages in Mediterranean Abies species. *Plant Systematics and Evolution*, 284(3-4), 141–151. https://doi.org/10.1007/s00606-009-0247-8

Linares J.C., F.J. Esteban, B. Viñegla & J.A. Carreira. (2006). A computational analysis of multi-temporal vegetation changes using the fractal dimension spectrum. *Harmonic and Fractal Image Analysis*, e-journal 1: 97-100.

Linares, J. C. (2008). Effects of global change overpopulation dynamic and ecophysiology of *Abies pinsapo* Boiss relictian forests. Ph.D. Thesis. University of Jaén.

Linares, JC; Camarero, JJ; Carreira, JA. (2009). Interacting effects of changes in climate and forest cover on mortality and growth of the southernmost European fir forests. *Global Ecology and Biogeography* 18 (4): 485-497.

Linares, J. C., & Carreira, J. A. (2009). Temperate-like stand dynamics in relict Mediterranean-fir (*Abies pinsapo*, Boiss.) forests from southern Spain. *Annals of Forest Sciences*, 66. https://doi.org/10.1051/forest/2009040

Linares, J. C., Camarero, J. J., and Carreira, J. A. (2009a). Plastic responses of *Abies pinsapo* xylogenesis to drought and competition. *Tree Physiology*. 29 (12), 1525– 1536. https://doi.org/10.1093/treephys/tpp084

Linares, J. C., Delgado-Huertas, A., Camarero, J. J., Merino, J., & Carreira, J. A. (2009b). Competition and drought limit the response of water-use efficiency to rising atmospheric carbon dioxide in the Mediterranean fir *Abies pinsapo*. *Oecologia*. https://doi.org/10.1007/s00442-009-1409-7

Linares, J. C., Camarero, J. J., and Carreira, J. A. (2010). Stand-structural effects on *Heterobasidion abietinum*-related mortality following drought events in *Abies pinsapo*. *Oecologia* 164, 1107–1119. https://doi.org/10.1007/s00442-010-1770-6

Linares J.C. (2011). Biogeography and evolution of Abies (Pinaceae) in the Mediterranean Basin. The roles of long-term climatic changes and glacial refugia. *Journal of Biogeography* 38: 619-630. https://doi.org/10.1111/j.1365-2699.2010.02458.x

Linares, J. C.; Carreira, JA.; Ochoa, V. (2011b). Human impacts drive forest structure and diversity. Insights from Mediterranean mountain forest dominated by *Abies pinsapo* (Boiss.) *European Journal of Forest Research* 130 (4): 533-542.

Linares, J. C., Delgado-Huertas, A., & Carreira, J. A. (2011a). Climatic trends and different drought adaptive capacity and vulnerability in a mixed *Abies pinsapo- Pinus halepensis* forest. *Climate Change*, 105, 67-90. https://doi.org/10.1007/s10584-010-9878-6

Linares J.C., J. J. Camarero, A. Delgado-Huertas & J.A. Carreira. (2013). Efectos de los cambios de clima y usos del territorio sobre la dinámica y el crecimiento de los bosques de *Abies pinsapo* en las últimas décadas. In: López-Quintanilla, J., R.M. Navarro, J.A. Carreira, M. Coca & C. Rodríguez, Los pinsapares (*Abies pinsapo* Boiss.) en Andalucía: Conservación y sostenibilidad en el siglo XXI., capítulo 24, pp. 401-412. Junta de Andalucía y Universidad de Córdoba. ISBN: 978-84-92807-74-1, 978-84-9927-137-8

López-Quintanilla, J.; Navarro, R.M., J.A. Carreira, M. Coca & C. Rodríguez (eds.) (2013). *Los pinsapares (Abies pinsapo Boiss.) en Andalucía: Conservación y sostenibilidad en el siglo XXI.* 576 pp. Junta de Andalucía y Universidad de Córdoba. ISBN: 978-84-92807-74-1, 978-84-9927-137-8

Mallinis, G., Mitsopoulos, I., Beltran, E., Goldamer, J. G. (2016). Assessing Wildfire Risk in Cultural Heritage Properties Using High Spatial and Temporal Resolution Satellite Imagery and Spatially Explicit Fire Simulations: The Case of Holy Mount Athos, Greece. *Forests*. 7, 46; https://doi:10.3390/f7020046

Manion P (1981) Tree Disease Concepts. Oxford: Prentice-Hall, Englewood Cliffs, NJ

Marino, E., Montesa, F., Tomé, J.L., Navarro, J.A., Hernando, C. (2018). Vertical forest structure analysis for wildfire prevention: Comparing airborne laser scanning data and stereoscopic hemispherical images. *Int J Appl Earth Obs Geoinformation* 73: 438–449 https://doi.org/10.1016/j.jag.2018.07.015

McGaughey, R. J., & Carson, W. W. (2003). Fusing LIDAR data, photographs and other data using 2D, and 3D visualization techniques. *Proceedings of Terrain Data: Applications and Visualization-Making the Connection*, 16-24.

Mitsopoulos, I., Mallinis, G., Arianoutsu, M. (2015). Wildfire risk assessment in a typical Mediterranean wildland-urban interface of Greece. *Environmental Management*. 55:900–915 https://doi:10.1007/s00267-014-0432-6

Molina, J. R., Rodríguez y Silva, F., Herrera, M. A. (2017). Economic vulnerability of fire-prone landscapes in protected natural areas: application in a Mediterranean Natural Park. *European Journal of Forest Research* 136:609–624. https://doi:10.1007/s10342-017-1059-y

Montes, F., Rubio-Cuadrado, Á., Sánchez-González, M. de la O., Aulló-Maestro, I., Cabrera, M., & Gómez, C. (2019). Occlusion Probability in Operational Forest Inventory Field Sampling with ForeStereo. *Photogrammetric Engineering and Remote Sensing*, 85(7), 493–508. https://doi.org/10.14358/PERS.85.7.493

Mura, M., McRoberts, R. E., Chirice, G., & Marchetti, M. (2015). Estimating and mapping forest structural diversity using airborne laser scanning data. *Remote Sensing of Environment*, 170, 133-142. https://doi.org/10.1016/j.rse.2015.09.016

Narváez, D. (1991, August 13). Extinguido el incendio que ha arrasado 9.000 hectáreas en la Serranía de Ronda. El País.

Pasta, S., Sala, G., La Mantia, T., Bondi, C., Tinner, W. (2019). The past distribution of Abies nebrodensis (Lojac.) Mattei: results of a multidisciplinary study. *Vegetation History and Archaeobotany*. https://doi.org/10.1007/s00334-019-00747-0

Pausas, J. G., & Keeley, J. E. (2009). A burning story: The role of fire in the history of life. *BioScience*, 59(7), 593-601. https://doi.org/10.1525/bio.2009.59.7.10

Rivas-Martínez, S. & Rivas-Sáenz, S. (1996-2020). Worldwide Bioclimatic Classification System. Phytosociological Research Center, Spain. http://www.globalbioclimatics.org

Rodríguez y Silva, F. (1996). *Protección y defensa de los pinsapares ante los incendios forestales. Jornadas técnicas internacionales sobre recuperación de pinsapares*, Grazalema, 12, 13 y 14 de diciembre de 1996.

Rodríguez y Silva, F., & Molina Martínez, J. R. (2010). *Manual técnico para la modelización de la combustibilidad asociada a los ecosistemas forestales mediterráneos*. Córdoba: Forest Fire Lab Defence, University of Córdoba (Spain). ISBN: 978-84-693-2151-1.

Rodríguez y Silva, F., & Molina-Martínez, J. (2012). Modelling Mediterranean forest fuels by integrating field data and mapping tools. *European Journal of Forest Research*, 131, 571-582. https://doi.org/10.1007/s10342-011-0532-2

Rodríguez-García, C., Montes, F., Ruiz, F., Cañellas, I., & Pita, P. (2014). Stem mapping and estimating standing volume from stereoscopic hemispherical images. *European Journal of Forest Research*, 133, 895-904. https://doi.org/10.1007/s10342-014-0806-6

Ruiz-Peinado, R., del Río, M., & Montero, G. (2011). New models for estimating the carbon sink capacity of Spanish softwood species. *Forest Systems*, I(20), 176-188. https://doi.org/10.5424/fs/2011201-11643

Rundel, P. W. (2019). A Neogene Heritage: Conifer Distributions and Endemism in Mediterranean-Climate Ecosystems. *Frontiers in Ecology and Evolution*, 7. https://doi.org/10.3389/fevo.2019.00364

Salis, M., Ager, A. A., Alcasena, F. J., Arca, B., Finney, M. A., Pellizzaro, G., Spano, D. (2015). Analyzing seasonal patterns of wildfire exposure factors in Sardinia, Italy. *Environ Monit Assess* 187:4175 https://doi.org/10.1007/s10661-014-4175-x

Salis, M., Arca, B., Alcasena, F., Arianoutsou, M., Bacciu, V., Duce, P., Duguy, B., Koutsias, N., Mallinis, G., Mitsopoulos, I., Moreno, J. M., Pérez, J. R., Urbieta, I.R., Xystrakis, F., Zavala, G., Spano, D. (2016). Predicting wildfire spread and behavior in Mediterranean landscapes. *International Journal of Wildland Fire* 25, 1015–1032 http://dx.doi.org/10.1071/WF15081

Sánchez-González, M., Cabrera, M., Herrera, P. J., Vallejo, R., Cañellas, I., & Montes, F. (2016). Basal area and diameter distribution estimation using stereoscopic hemispherical images. *Photogrammetric Engineering & Remote sensing*, 82, 605 - 616. https://doi.org/10.14358/PERS.82.8.605

Sánchez-Salguero, R., Camarero, J. J., Carrer, M., Gutiérrez, E., Alla, A. Q., Andreu-Hayles, L., Hevia, A., Koutavas, A., Martínez-Sancho, E., Nola, P., Papadopoulos, A., Pasho, E., Toromani, E., Carreira, J. A., & Linares, J. C. (2017). Climate extremes and predicted warming threaten Mediterranean Holocene firs forests refugia. *Proceedings of the National Academy of Sciences*. https://doi.org/10.1073/pnas.1708109114

Scott, Joe H.; Burgan, Robert E. (2005). *Standard fire behavior fuel models: a comprehensive set for use with Rothermel's surface fire spread mode*l. Gen. Tech. Rep. RMRS-GTR-153. Fort Collins, CO: U.S. Department of Agriculture, Forest Service, Rocky Mountain Research Station. 72 p.

Van Ardt, J. A., Wynne, R., & Scrivani, J. (2008). Lidar-based mapping of forest volume and biomass by taxonomic group using structurally homogenous segments. *Photogrammetric Engineering and Remote Sensing*, 75(8), 1033-1044. https://doi.org/10.14358/PERS.74.8.1033

Vega Hidalgo, J. A. (1999). Historia del fuego de *Pinus pinaster* y *Abies pinsapo* en la carta norte de Sierra Bermeja (Málaga): 1817-1997. *Incendios históricos, una aproximación multidisciplinar*. Baeza. UNIA.

Wang C., &. N., Glenn (2008). A linear regression method for tree canopy height estimation using airborne lidar data. *Canadian Journal of Remote Sensing*, 34. https://doi.org/10.5589/m08-043

Wang, Z., Ginzler, C., & Waser, L. T. (2020). Assessing structural changes at the forest edge using kernel density estimation. *Forest Ecology and Management*, 456, 117639. https://doi:10.1016/j.foreco.2019.117639

Wüest, R. O., Bergamini, A., Bollmann, K., & Baltensweiler, A. (2020). LiDAR data as a proxy for light availability improve distribution modelling of woody species. *Forest Ecology and Management*, 456, 117644. https://doi:10.1016/j.foreco.2019.117644

Yebra, M. Quan, X., Riaño, D., Larraondo, P. R., Van Djik, A. I. J. M., Cary, G. J. (2018). A fuel moisture content and flammability monitoring methodology for continental Australia based on optical remote sensing. *Remote Sensing of Environment* 212 260–272 https://doi.org/10.1016/j.rse.2018.04.053

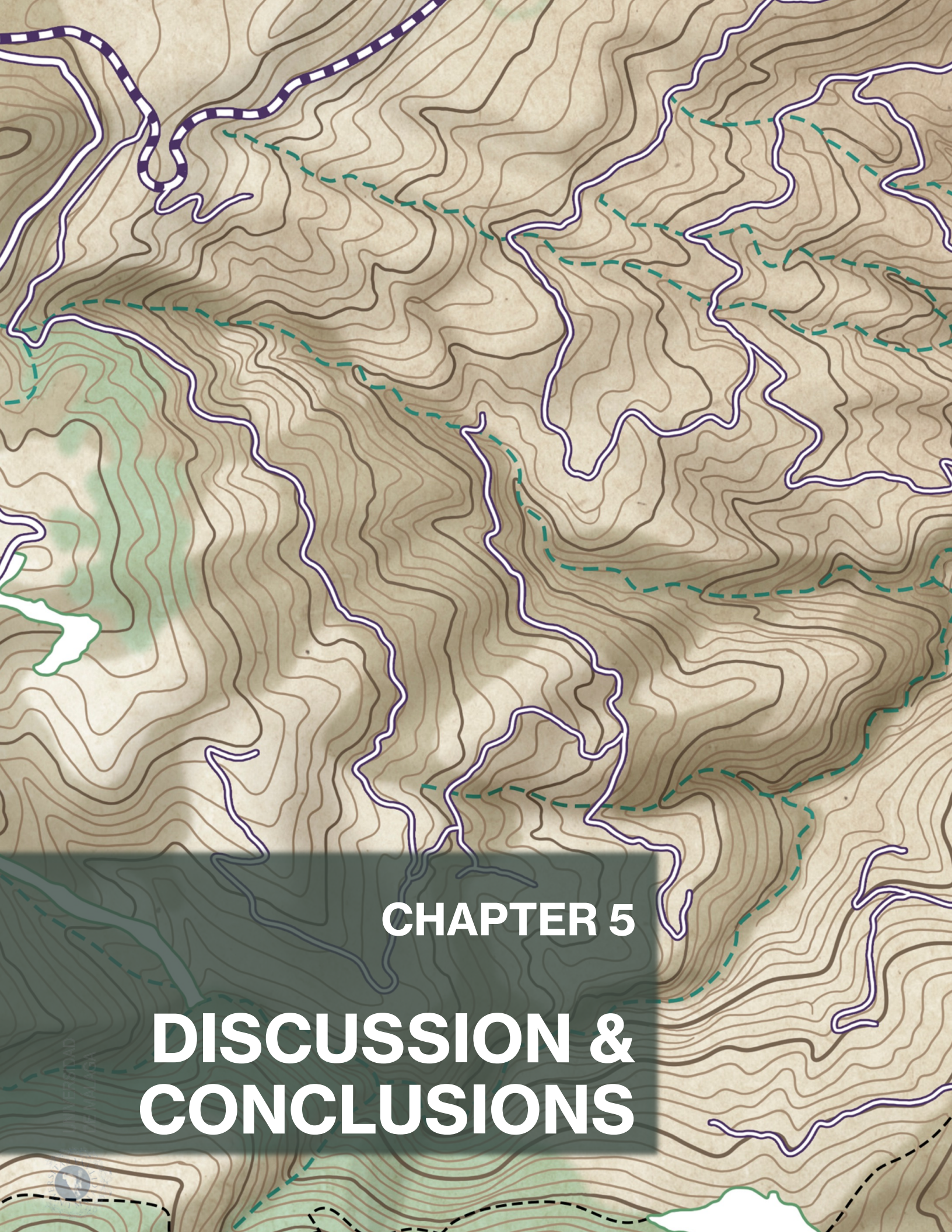

CHAPTER 5

DISCUSSION & CONCLUSIONS

General discussion & conclusions 5

Remote sensing is a powerful tool that enables the efficient acquisition of reliable spatio-temporal data, both in terms of time and cost, across extensive landscapes. The availability, quality, and volume of baseline information on forests ecosystems have always been a strong conditioning factor of forest management over the past decades. This information remains crucial in the present day and will continue to be so in the future, due to the ongoing and projected dynamics of global change. Such changes are expected to exacerbate known hazards and introduce new ones derived from climate change. Risk management has always been a cornerstone in forest management and has several components to be accounted for. Exposure refers to how much disturbance is likely to be experienced in a system. Sensitivity indicates how different exposures can impact the ecosystem (Roshani *et al.*, 2022). Vulnerability is the degree to which a system could be transformed as a consequence of its interaction with disturbance. Resilience is linked to ecosystem recovery after the impact (Fortini & Schubert, 2017). Lastly, adaptive capacity refers to evolutionary and ecological traits to manage and minimize impacts (Williams *et al.*, 2008).

This work explored how the integration of different sources of remote sensing data coupled with the development of pipelines that incorporates multiple approaches and processing algorithms, can enhance, and streamline the data acquisition necessary for managing the increasing risks in forest management. In this context, the decline of forests due to climate change, the recurrence of severe and large wildfires, and the ability of forests to recover after impacts associated to these risks are all matters of significant concern (An *et al.*, 2015; Bowman *et al.*, 2020). The predictive capabilities provided by remote sensing techniques enable the development of new tools to support preventive measures for forest risk management in the context of climate change (Botequim *et al.*, 2019; Yebra *et al.*, 2018).

Remote sensing techniques facilitate massive landscape data acquisition, processing, and modelling, which are essential for characterizing the main risk components in forest management under a climate change scenario: hazard, exposure, and vulnerability. (Fig. 5.1; IPCC, 2014).

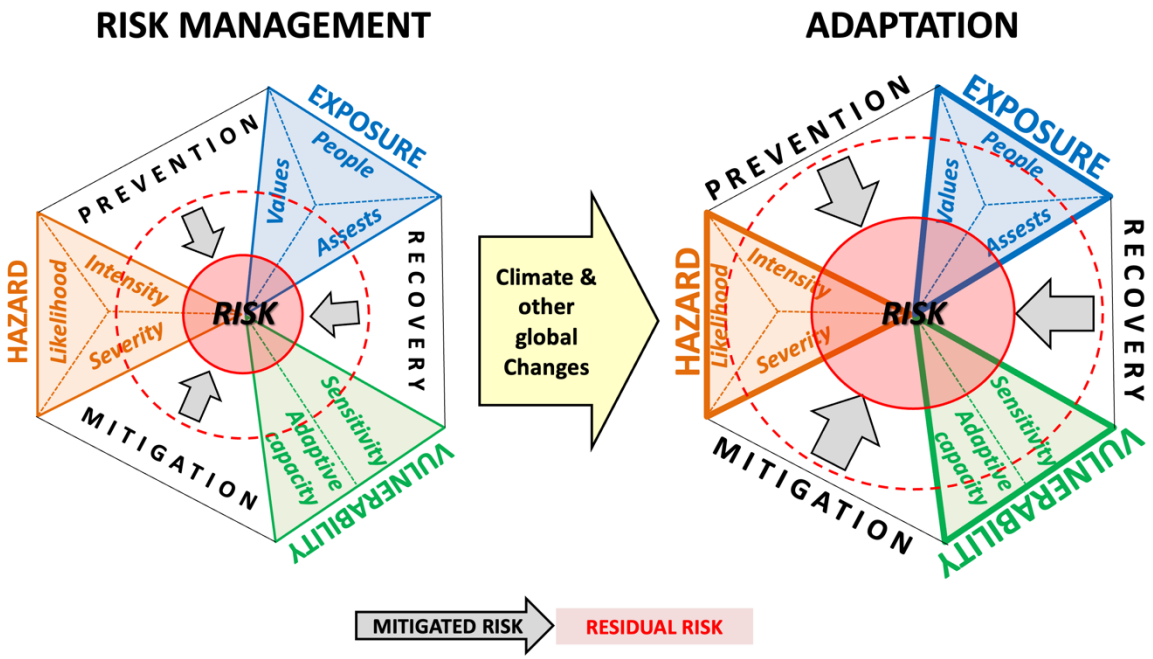

Figure 5.1. Differences between risk management and adaption. Adapted from IPCC, 2014. Risk is a consequence of the interaction between *hazard* (which also depends on likelihood, intensity, and severity), *exposure* (values, assets, and people susceptible to damage), and *vulnerability*, which relies on the sensitivity of the values, assets and people exposed, as well as their adaptive capacity to cope with damage. Risk managemenent is an anticipatory strategy to reduce and mitigate risk, which leads to a residual risk. In contrast, adaptation is a reaction to minimize the damage. Climate change will increase risks and challenge adaptation responses of forests ecosystems.

For instance, enhanced modelling of evapotranspiration can contribute to detect early signs of water stress in forests and their vulnerability to cavitation, which is the hazard component. Accurate and long-term monitoring, through the multitemporal analysis of post-drought mortality responses and recovery, can improve our understanding of resilience mechanisms, which is the vulnerability component. Lastly, simulating fire scenarios and spread in different fuel models landscape can enhance our capacity for anticipation and mitigation of fire risk, which is the exposure component.

In this respect, three studies were addressed to contribute to the field of forest risk management through remote sensing techniques. Each study employed a wide set of technologies, including several sensors and platforms. In Chapter 2 Unmanned Aerial Vehicle (UAV) were

used with photogrammetric and thermal sensors for modelling canopy evapotranspiration, a bioclimatic variable closely linked to water stress; Chapter 3 utilized multispectral imagery from satellites and aircraft derived orthoimages for monitoring post-drought responses of the forest through a time series approach; while Chapter 4 relied on aerial LIDAR and hemispherical images to assess wildfire risks and canopy related vulnerabilities by fuel model analysis. Due to the large amount of information obtained from these devices, data science and machine learning approaches were employed.

Two different ecosystems were chosen for this work. First, *A. pinsapo* forests (South Iberian Peninsula) were the main system analyzed, with two studies already published (Chapter 3 and 4). The reason to select these forests was motivated by the lack of previous studies in which novel remote sensing techniques were employed to characterize the conservation status of relict *A. pinsapo* stands at landscape scale. The other ecosystem is the Sumatran rainforest (Indonesia) to study canopy Evapotranspiration (ET) in Chapter 2. Water stress induced by droughts plays a key role in forest risk management, and monitoring ET enables to detect early issues in water usage by forests (Granier *et al.*, 1996; Waring *et al.*, 1979). Therefore, rainforests are ideal systems to study ET due to the relevant contribution of their transpiration to global climate (Schlesinger & Jasechko, 2014). The Sumatran rainforest, with its stable climate conditions and flat terrain that avoids topographical heterogeneity (Drescher *et al.*, 2016) is particularly suitable for this study.

5.1. Modelling canopy evapotranspiration

In most studies, ET is usually studied at the landscape level due to its relevant contribution to the hydrologic cycle (Schlesinger & Jasechko, 2014; Tabari, 2020). Returning water from soil and plants to air is mainly mediated by complex physical atmosphere dynamics, involving key variables such as wind speed, radiation, temperature, or vapor pressure deficit (Dimitriadou & Nikolakopoulos, 2021). Consequently, many studies have focused on the climatic implications in the ET modelling. Noce *et al.*, (2020) developed a global dataset of 35 bioclimatic indicators, in which potential evapotranspiration was estimated based on daily mean temperature. Allen *et al.*, (1998) developed an approach to calculate ET on crops based only in climatic variables that is still widely adopted (T R *et al.*, 2023; Wable *et al.*, 2021)

However, canopy features have received a modest attention in ET modelling, with LAI, canopy cover and tree height as the main variables studied (Liu *et al.*, 2022) and canopy resistance as a link between biological and meteorological factors (Perez *et al.*, 2006). LAI is

known to enhance evapotranspiration rates and canopy height is a key component of surface energy budget (Urrego *et al.*, 2021).

Few previous studies have focused on how microvariations in canopy features could influence ET at a pixel scale in forest ecosystems. Most of small-scale ET studies have been conducted in agricultural systems using ground-based measurements devices such as lysimeters, or eddy covariance towers (Liu *et al.*, 2016; Yang *et al.*, 2012). However, these systems capture data from specific points rather than providing spatial variability across the surface. Niu *et al.*, (2020) applied different UAV-based approaches for ET calculation, including machine learning and energy balance techniques, resulting on a high capability to detect water stress spatial variability. High precision data derived from UAV enable to get thermal, RGB and structural information about the forest canopy and broaden the opportunity to analyze such microvariations at the pixel level and how they could influence local ET. Ahongshangbam *et al.*, (2019) used an UAV SfM approach to study canopy transpiration at the crown level, finding high spatial variation in ET due to crown packing.

In this work, a pixel-based approach was employed to analyze canopy structure to explain ET spatial vaiabililty in a rainforest canopy through a machine learning approach (Chapter 2). Scale is a relevant factor to consider, as ecosystems exhibit emergent properties that cannot be understood as the sum of its parts (Gilber & Henry, 2015; Ponge, 2005). Subsequently, ET behavior might differ at such small scale compared to its behavior at the landscape level. ET is crucial in rainforests ecosystems since it substantially contributes to the amount of local rainfall (Staal *et al.*, 2020). In tropical rainforests, transpiration occurs in highly complex canopy structures (Kotowska *et al.*, 2021; Meinzer *et al.*, 2005), so a machine learning approach was used to better understand small-scale ET patterns. The approach developed in Chapter 2 for a Sumatran rainforest could be further tested in temperate forests as those dominated by conifers.

Adaptive management can benefit from this approach since ET is a key variable to understand forest hydraulics and to monitor potential water stress (Granier *et al.*, 1996; Waring *et al.*, 1979). A small-scale approach enables to manage forests at the stand level. Modelling ET canopy patterns is key to monitor local microclimate, since it is a bioclimatic variable related to water consumption on forests (Guerrieri *et al.*, 2016). Persistent decreases on ET rates can be interpreted as an early warning sign of aridification, especially in rainforests where ET play a significant role in water recycling. Thus, sensing water stress during drought events is crucial to detect water loss and vulnerabilities in adaptive forest management (González-Dugo *et al.*, 2021). Additionally, changes in forest water hydraulics could potentially

influence fuel moisture, and subsequently alter forest fire behavior through increased fuel flammability (Cawson *et al.*, 2020; Graham *et al.*, 2006).

5.2. Monitoring post-drought induced mortality dynamics

Ecologists tend to expect regime shifts after severe droughts, but this could overlook other processes that might be happening during the reorganization phase, such as replacement, restructuring, reassembly, or resilience (Seidl & Turner, 2022; see Fig. 1.1 in section 1.1). Understanding these complex mechanisms requires integrative procedures for obtaining multi-source data to create a comprehensive 'big picture' in risks and decisions management (Anderegg *et al.*, 2012; Italiano *et al.*, 2023).

Field-based approaches, such as proximal sensing or forest fieldsurveys allow for the acquisition of data about the phenological, physiological and dendrological status of forests. Despite the high value of this information, there are several limitations to consider. First, many field data are based on single observations from individuals or local stands (e.g., height, DBH or CBH). Some variables are obtained through subjective analysis, due to the difficulty in obtaining objective data, such as canopy transparency (Italiano *et al.*, 2023). Furthermore, installing sensors to cover large areas such as sap flux devices can be expensive.

Remote sensing technologies enable the study of forests at the landscape level through efficient and cost-effective data acquisition. Passive and active sensors can collect spectral reflectance, thermal and geometrical information that is employed for monitoring forest dynamics and health status. However, these approaches also exhibit technical limitations that hinder the capability to predict underlying ecological process. Pixel size from some satellite images is coarse (i.e., 30 m or 200 m); in these cases, spectral data might not be reliable in heterogenous, or sparse vegetation covers (Huang *et al.*, 2021; Italiano *et al.*, 2023). Also, the accuracy of LIDAR data will depend on whether the variables of interests are located above or below the canopy and whether the scanners are mounted on aerial or terrestrial platforms (Hilker *et al.*, 2012),

Despite new sensors and platforms are increasing the data quality and accuracy, a multiscale approach is still required to study post-drought dynamics and to overcome technical limitations caused by following single procedures in risk management (Italiano *et al.*, 2023; Fig 5.2.). In this work, a multi-proxy procedure is proposed (Chapter 3), which consists of combining NDVI from satellite imagery, forest cover from aerial orthoimages and DBH from

field surveys to integrate the data for a multitemporal analysis. This analysis aimed to study the effects of drought-induced dieback dynamics but could also be implemented to monitor other recovery process such as post-fire responses. While the NDVI calculated from satellite images is often associated with biomass (Vaglio Laurin *et al.*, 2016), its primary utility lies in analyzing photosynthetic activity and detecting early indicators of forest decay and dieback (Forzieri *et al.*, 2022). Estimation of canopy cover from aerial orthomosaic can show high accuracy in monospecific forests, especially when there is high spatial resolution (Sedykh, 1995). Collecting past and present data of NDVI and canopy cover offers a great potential for studying the dynamic evolution of forests. Furthermore, data acquisition by field surveys across decades is relevant for monitoring under-canopy processes and to integrate this information with remote sensing data through ecological modelling. This acquired knowledge allows to estimate the possible future forest dynamic pathways (Dakos *et al.*, 2015; Sturtevant & Fortin, 2021).

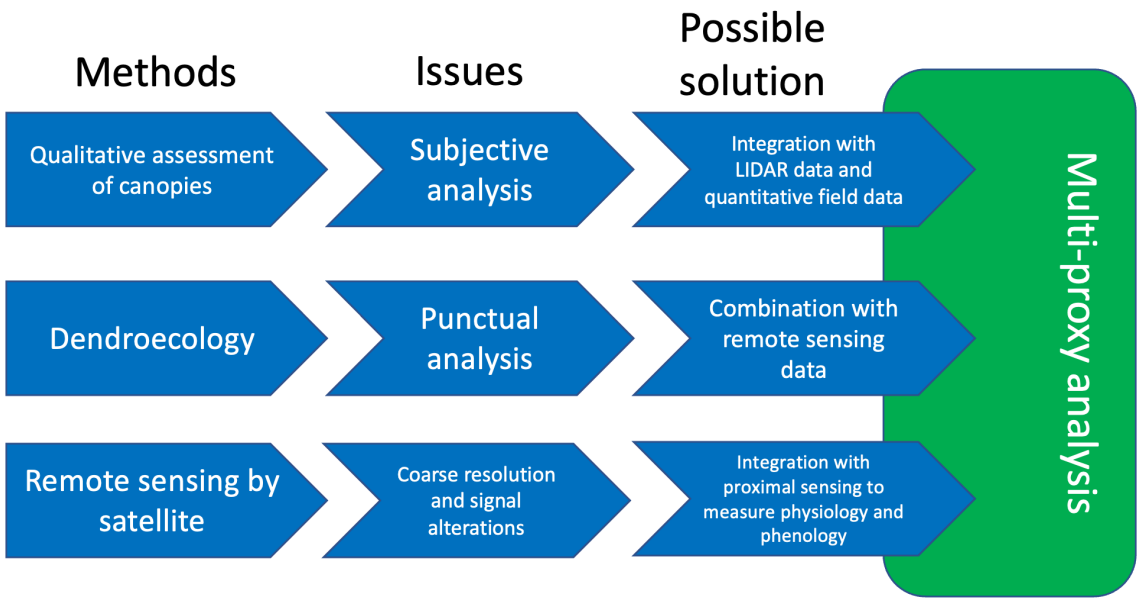

Figure 5.2. Justification for a multi-proxy approach, adapted from Italiano *et al.*, (2023). Weaknesses of the main methods employed for data acquirement in forestry and possible solutions to be integrated in the proposed approach

The multi-proxy approach proposed in this work, allowed to discover an unexpected resilience of relict *A. pinsapo* forests to diebacks induced by climate change. These findings contrast to previous studies that forecasted a continuous shrinking in *A. pinsapo* populations due to persistent mortality rate and gap opening process observed at their lower ecotone (Linares *et al.*, 2009; Sánchez-Salguero *et al.*, 2017). These resilience response to post-drought mortality are hypothesized to be due to compensation mechanisms. The results were unexpected since *A. pinsapo* is a drought-sensitive, endangered relict fir of Tertiary paleobiogeographic origin and its populations grow in restricted, shaded and humid locations (Alba-Sánchez *et al.*, 2019). However, recent studies have reported that some Eurosiberian species from cool and humid climates also showed unexpected responses to increasing Mediterranean conditions. Walder *et al.*, (2021) found that *Abies alba* Mill. can grow, develop, and regenerate in meso-Mediterranean conditions, even under extreme summer droughts. These results imply that *A. alba* could be less vulnerable to increasing temperatures than previously expected. Also, Pflug *et al.*, (2018) reported resilient leaf physiological response of *Fagus sylvatica* L. to drought events. In this case, physiological and ecological responses can enhance adaptive capacity and activate resilience responses.

However, despite these recent findings, drought-related mortality is spreading in many worldwide forests. In some cases, recurrent severe droughts are leading the ecosystems to a tipping point in which replacement of mesic communities by xeric ones is taking place (Anderegg *et a*l., 2021; Batllori *et al.*, 2020).

Forecasts of forest adaptive capacity responses to droughts and pests tend to carry a high degree of uncertainty since they rely on a complex set of physiological mechanisms (Anderegg *et al.*, 2020; Choat *et al.*, 2018; Reyer *et al.*, 2015). Consequently, monitoring post-disturbance responses, are key to modulate forest management strategies and anticipating future impacts. Additionally, studying resilience mechanisms may allow to detect side effects caused by the ecological succession, such as an increasing vulnerability to fire due to an encroachment of bushes and shrubs in forests gaps.

5.3. Sensing wildfire risk and canopy related vulnerability

There is a set of circumstances that are increasing the vulnerability to fires in many Mediterranean and temperate forests. First, rural abandonment has caused changes in land cover: numerous former agricultural fields are now high-density shrublands (Ustaoglu & Collier, 2018; Weissteiner *et al.*, 2011; Zhou *et al.*, 2020). Second, non-management practices were

supported in the last decades by policies based on letting the natural processes work without human intervention. Currently these management policies are being reinforced by a new management strategy called 'rewilding' (Lorimer *et al.*, 2015, Schulte to Bühne *et al.*, 2022).

Rewilding is a broad concept that can vary among different ecologists and managers, but essentially its promoters aim to restore ecological functions and connections (Ego *et al.*, 2021; Schulte to Bühne *et al.*, 2022). This initiative implies relevant opportunities to consider in land management and wildlife conservation (Perino *et al.*, 2019). However, rewilding promoters often overlook potential land issues since human intervention or current land occupation in these ecosystems is not accounted for (Schulte to Bühne *et al.*, 2022). Additionally, some rewilding supporters base their approach inspired on past environments that no longer exist in the present, and even less so in the next decades due to new climate change scenarios (Lorimer *et al.*, 2015).

Non-human intervention in ecosystems can provoke forest over-densification and stagnation, due to the lack of either natural or human low-intensity disturbances that dynamize ecological processes (Franklin *et al.*, 2007; Picket & White, 1985). However, even with the presence of ecological disturbances, such as drought events, mortality and recovery dynamics might lead to a high amount of dead fuel accumulation and to shrubs encroachment in forests mortality gaps. This process has the potential to promote dense, vertical, and horizontal continuum forest landscapes (Fig. 5.3).

Figure 5.3. Shrubs encroachment can interlock tree crowns and create high-dense vegetal continuum that leads to higher flammability

Management policies that allow these landscapes are increasing canopy vulnerability to drought-derived mortality, but mostly to severe wildfires (Weissteiner *et al.*, 2011; Zhou *et al.*, 2020). This increase is characterized by high Canopy Bulk Density (CBD), low Canopy Base Height (CBH) —which interlock the growing shrubs and bushes in secondary forests and forest edges— and a high tree density that promotes Canopy Covers (CC) above 80%. These canopy structures facilitate ladder effect during a fire, stimulating the transition from surface to crown fires (Arellano, 2017; Brown *et al.*, 2004). The new climatic scenarios are promoting the extension of dry periods with lower values of fuel and air moisture and higher maximum temperatures. Under this environment, the spread rate and flame length from crown fires can extraordinarily increase, leading to large wildfires that surpass control capacity (Li *et al.*, 2023). Additionally, recurrent wildfires may exhaust post-fire recovery from serotinous species, and forest ecosystems might be pushed towards a regime shift to shrublands (Acácio *et al.*, 2009; Seidl & Turner, 2022). This process has positive feedback to fire risk, due to the stimulation of landscapes with more flammable structures.

Remote sensing techniques are increasing the capability to anticipate to large fires through the characterization of fuel structure and moisture. Structure is classified in fuel models, in which LIDAR technology shows a great capacity to acquire this information (González-Olabarria, *et al.* 2012; Botequim, *et al.* 2019). Meanwhile, satellite imagery is commonly employed for fuel moisture modelling (Yebra *et al.*, 2018).

In this work, canopy structure vulnerability and fire risk were assessed through a second multiapproach in Chapter 4, following the perspective used in the multitemporal analysis with Chapter 3. The purpose of this procedure was to acquire multisource data to be integrated in a fire risk simulation. Forest survey was conducted using ForeStereo, a field device based in hemispherical images for obtaining crown and canopy metrics. This technology provides a reliable solution for forest inventory as an alternative to Terrestrial Laser Scanning (TLS) systems. Since LIDAR approaches allow to study forest structure through high quality point cloud data, they are currently essential for fire risk management (Botequim *et al.*, 2019). ForeStereo data were employed to model Aerial Laser Scanning (ALS) point cloud information and to acquire landscape forest structure. Scott & Burgan (2005) fuel models has previously been adapted to Mediterranean ecosystems —UCO 40 classification from Rodríguez y Silva & Molina Martínez, (2012)— and this enabled a precise characterization of the fuel models. The data integration resulted in fire risk simulations under different wind scenarios.

The results of Chapter 4 suggest that the resilience response to drought-induced mortality observed in Yunquera's *A. pinsapo* forests is making the stands more vulnerable to fires. These findings are consistent with Ruthrof *et al.*, (2016) results, who reported fire spread rates 30% higher in drought-induced forest die-off plots, due to increasing fuel loadings.

Although resilience of *A. pinsapo* forest are good news for the conservation of this relict fir, fire occurrence could push the ecosystem towards a tipping point, resulting in a regime shift in which *A. pinsapo* populations might disappear. Previous fire events eliminated other pinsapo populations (García, 2006) and the current population in Sierra Bermeja (Málaga) —the third *A. pinsapo* biggest forest in the Iberian Peninsula— has been shaped by past fire events (Hidalgo, 1999). Considering that *A. pinsapo* lacks any fire-resistant traits, due to its thin bark and difficulty growing in open and exposed areas (Rodríguez y Silva, 1996), fire risk is the main threat to these relict fir populations. Consequently, conservation management strategies should address these concerns.

5.4. Contributions to the field of knowledge: Remote sensing & Forest conservation

This doctoral thesis introduces a novel method for modelling canopy ET at small scale employing thermal and RGB data derived from UAV orthomosaics and point clouds. ET was modelled as a function of micro-canopy structure variations following a Random Forest approach.

Multiapproach analysis, based on the combination of field surveys and several remote sensing techniques, was conducted to enable a broader understanding of forest dynamics and to improve risk simulations. The novel application of ForeStereo data to support the simulation of fire scenarios could open the opportunity to be used among fire risk surveyors as an alternative to TLS systems.

Previously, remote sensing techniques were scarcely used to analyze relict *A. pinsapo* forests. Before this doctoral thesis, LIDAR technology was never used to analyze canopy metrics of pinsapo forests. This is also the first time that historical and high-resolution satellite data combined with aerial orthomosaics were employed for analyzing pinsapo forest evolution through time series modelling. This multiapproach criteria enabled the obtention of novel information about the conservation status of a relict endangered fir. Furthermore, it was possible to examine the connection between post-drought mortality resilience

mechanisms of *A. pinsapo* forests and the increasing fire risk. These findings allow the application of novel information and procedures to climate risks management in forest conservation.

This synthesis is summarized in Fig.5.4 and aims to integrate and contrast the results obtained by the three studies, and to discuss their ecological and management implications in forest conservation within a climate change scenario.

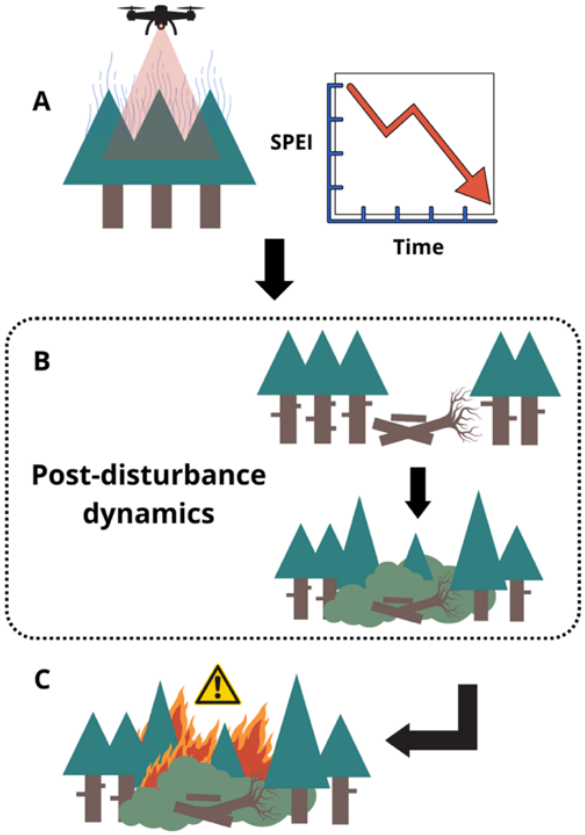

Figure 5.4. Summary of the contributions to the field of forest conservation. UAV-derived data allowed to analyze evapotranspiration canopy controls at pixel level. Studying ET is relevant for monitoring drought events through indexes like SPEI (A). Droughts increase forest vulnerability, triggering post-disturbance effects (i.e., diebacks and resilience responses; B). The debris and dead wood accumulation in the mortality gaps, together with shrubs overgrow promotes very high fire risk and severity.

5.5. Contributions to the field of application: Adaptive Forest Management

In this doctoral thesis, several remote sensing approaches were employed to contribute to climate risks assessment in the context of forest conservation. The reported results could be implemented in forest management strategies through knowledge transference to foresters, environmental managers, and protected areas administrators.

Thus, monitoring ET at local scale is relevant to detect symptoms of canopy water stress at stand level (Bhattarai & Wagle, 2021), with potential to support the anticipation of drought-derived mortality; whereas the analysis of photosynthetic activity could detect early warning signs of forest decline through NDVI (Forzieri *et al.*, 2022).

SfM photogrammetry expands the availability of canopy 3D point cloud to a wider range of forest suveryors and managers, due to the significant differences in financial investments. However, convenience will depend mostly on the forest canopy closure and the target variables, since at certain level of vegetation density it is only possible to obtain top of the canopy data (Lim *et al.*, 2003).

The remote sensing techniques employed in this work are useful to assist the design and implementation of silvicultural practices representing a low-intensity disturbance regime, in order to enhance canopy structural diversity at the stand level and forest patch-dynamics at the landscape level (Pérez-Rodríguez *et al.*, 2020). Mapping fuel models and simulating fire risk can assist fuel control actions. Management strategy should also consider practices such as thinning (Sohn *et al.*, 2016), prescribed burning (Fernandes, 2015), regulation of herbivory activity, or shrubs clearing in key locations. Fig.5.2 shows a visual summary of structural differences between adaptive management vs no-management. The use of UAVs, satellites, ForeStereo device, ALS and UCO40 fuel models showed strong potential for forest structure analysis and for assessing the effects of these management practices. The techniques employed in this doctoral thesis could also be applied to assess the performance of new *A. pinsapo* recruitments and study further protection actions.

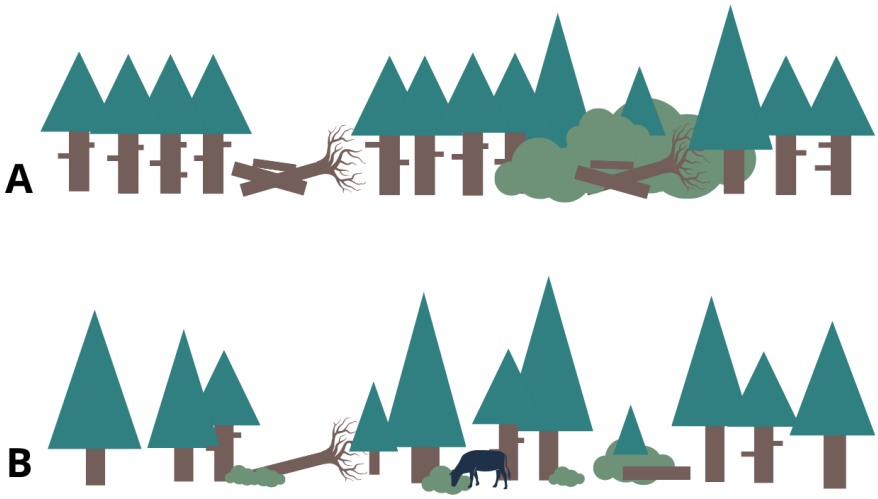

Figure 5.5. Structural differences between non-managed secondary forests (A) and managed secondary forests (B). In A, trees tend to be coetaneous, with similar low height and DBH values. There is also a high tree density which promotes less crown volume and a high number of dead branches. This structure increases vulnerability to post-disturbance diebacks, with subsequent fuel accumulation (i.e., dead wood falling and high-dense shrubs development which interlocks canopy). In B, forest management increase heterogeneity and structural diversity, and preserve natural traits (i.e., dead wood presence, shrubs growing, old growth development, saplings recruitment) while minimizing vulnerability to disturbances and fire severity.

5.6. Future perspectives

Over the last few years remote sensing has made great strides towards more affordable and on-demand multisource data acquisition and integration (Ghamisi *et al.*, 2018). The rise of SAR technology in satellites payload are opening new opportunities to study worldwide forests structure (Flores *et al.*, 2019). Internet of Things (IoT) devices will allow real-time acquisition of environmental variables and management performance in natural protected areas (Yu *et al.*, 2020). Tree species identification within forests has shown to be feasible using hyperspectral sensors (Shi *et al.*, 2018). Also, Artificial Intelligence algorithms are minimizing time of data processing and calculation efforts, simplifying remote sensing derived data to a broaden number of users, while improving calculation performance significantly (Nawaz *et al.*, 2022). Thus, in the future, all-in-one sensors will be used on new

generations of satellites, UAVs, or terrestrial devices, and most processing tasks would be performed by AI, making remote sensing easier for all levels users.

Since there is a high uncertainty regarding how much global temperature will rise, there is still a need for ecosystems monitoring to understand which are the resilience limits of the studied systems and which other forests could be resilient to climate change derived diebacks. Although some endangered ecosystems might be more resilient than previously hypothesized, only just the risk of extreme wildfire severity or the threat of invasive alien species should be enough to justify adaptive forest management (Alcasena *et al.*, 2019; Morri *et al.*, 2019), even in ecosystems already adapted to droughts. Lastly, adaptive management should be implemented in most threatened forest ecosystems to enhance and assist the resilience mechanisms to cope with climate change. Management strategies based on scientific criteria should also consider the livelihoods of local people and provide social rewards to ensure mutual benefits between forests and humans.

Conclusions

1. Remote sensing technologies have enabled the modelling of forest physiological variables closely related to microclimate alterations due to forest canopy variability.
   - ✓ In particular, modelling canopy ET at small scale through UAV sensors and a machine learning method has provided a consistent approach to monitor local variations of water usage and to anticipate drought effects on forests.
   - ✓ We have demonstrated that ET from a rainforest at small scale relies on microcanopy variations that interrelate in complex non-linear ways.

2. Multi-proxy criteria based on the integration of field surveys and different remote sensors have revealed a great potential for applications in climate risk management in forest conservation.
   - ✓ The combination of satellite images, aerial orthomosaics and periodic field surveys showed to be critical for multitemporal analysis to monitor forest dynamics.
   - ✓ The use of ForeStereo hemispherical images and aerial LIDAR point cloud data provided a consistent methodology to simulate fire risk and to analyze canopy structure-related vulnerabilities.

3. We have reported novel findings regarding the conservation status of relict *A. pinsapo*.
   - ✓ Based on the multiapproach criteria proposed, an unexpected resilience to drought and pest induced dieback due to climate change has been newly reported.
   - ✓ This resilience response to forest decline and dieback is hypothesized to be a consequence of compensation mechanisms that lead to an increase in photosynthetic activity and canopy gains that maintain a steady stand structure in *A. pinsapo* forests along decades despite continuous drought-induced mortality.

4. Although this resilient response to drought-induced mortality alleviates initial concerns about the conservation status of *A. pinsapo*, recovery dynamics are leading to increases in other risks.

- ✓ Compensation mechanisms have led to the overaccumulation of dead wood and debris, as well as to the high-density encroachment of shrubs that can, eventually, interlock with the forest canopy.
- ✓ This promotes high flammability fuel models and considerably increases the risk of severe and larger fires.

5. These findings can be applied to support *A. pinsapo* conservation strategies, as well as to general adaptive forest management policies and risk management under a climate change scenario, where drought spells and fire events are expected to increase significantly.

Conclusiones

1. Las técnicas de teledetección han permitido la modelización de variables fisiológicas forestales estrechamente relacionadas con alteraciones microclimáticas debidas a la variabilidad del dosel forestal.
    - ✓ En particular, la modelización de la evapotranspiración del dosel forestal a pequeña escala a través de sensores embarcados en UAV y técnicas de aprendizaje automático ha proporcionado un procedimiento consistente para monitorizar variaciones locales del consumo hídrico y anticipar los efectos de sequía en sistemas forestales.
    - ✓ Se ha demostrado que la evapotranspiración de una pluvisilva tropical a pequeña escala depende de pequeñas microvariaciones del dosel que se interrelacionan de una forma compleja y no linear.

2. El empleo de un procedimiento multicriterio basado en la integración de datos de campo y de diferentes sensores remotos demostrarion ser de gran de utilidad para la gestión de riesgos climáticos en conservación forestal.
    - ✓ La combinación de imágenes de satélite, ortoimágenes aéreas y campañas periódicas de muestreo de campo fue esencial para un análisis multitemporal para monitorizar la dinámica forestal.
    - ✓ El uso combinado de imágenes hemisféricas procedentes del ForeStereo y nube de puntos de LIDAR aéreo dio lugar a una metodología consistente para simular riesgo de incendio y analizar vulnerabilidad relacionadas con la estructura del dosel forestal.

3. Se han reportado hallazgos novedosos sobre el estado de conservación de la especie relicta *A. pinsapo*.
    - ✓ Basado en un criterio multienfoque, se constata una inesperada resiliencia al decaimiento originado por sequías y plagadas inducidas por el cambio climático.
    - ✓ Se hipotetiza que esta respuesta resiliente al fenómeno de decaimiento y mortalidad es una consecuencia de mecanismos de compensación que llevan a un aumento de la actividad fotosintética, de las ganancias de la cobertura forestal y una estructura estable del pinsapar a lo largo de décadas, a pesar de la persistente mortalidad inducida por eventos de sequía.

4. Aunque esta resiliencia pudiera aliviar la preocupación inicial sobre el estado de conservación de *A. pinsapo*, las dinámicas que genera la recuperación dan lugar al incremento en otros riesgos
    - ✓ Los mecanismos de compensación han llevado a una sobreacumulación de madera muerta, además de un proceso de sobrecrecimiento y densificación del matorral que terminarán por trabarse con el dosel forestal.
    - ✓ Este proceso promueve modelos de combustible de alta flamabilidad y por tanto aumentan de forma considerable el riesgo de grandes incendios.

5. Estos hallazgos pueden ser aplicados a estrategias para la conservación de *A. pinsapo*, así como apoyar políticas generales de gestión forestal adaptativa y gestión de riesgos en un escenario de cambio climático donde se espera que las sequías y los incendios forestales aumenten significativamente.

General references

Acácio, V., Holmgren, M., Rego, F., Moreira, F., and Mohren, M. J., G. (2009). Are drought and wildfires turning Mediterranean cork oak forests into persistent shrublands? *Agroforestry Systems*. 76, 389–400. https://doi.org/10.1007/s10457-008-9165-y

Aguilos, M., Stahl, C., Burban, B., Hérault, B., Courtois, E., Coste, S., Wagner, F., Ziegler, C., Takagi, K., & Bonal, D. (2018). Interannual and seasonal variations in ecosystem transpiration and water use efficiency in a tropical rainforest. *Forests*, 10(1). https://doi.org/10.3390/F10010014

Ahongshangbam, J., Khokthong, W., Ellsäßer, F., Hendrayanto, H., Hölscher, D., & Röll, A. (2019). Drone-based photogrammetry-derived crown metrics for predicting tree and oil palm water use. *Ecohydrology*, 12(6). https://doi.org/10.1002/eco.2115

Alba-Sánchez, F., López-Sáez, J. A., Abel-Schaad, D., Sabariego Ruiz, S., Pérez-Díaz, S., González-Hernández, A., & Linares, J. C. (2019). The impact of climate and land-use changes on the most southerly fir forests (*Abies pinsapo*) in Europe. *The Holocene*, 29(7), 1176–1188. https://doi.org/10.1177/0959683619838043

Albert, M., Nagel, R.-V., Nuske, R., Sutmöller, J., & Spellmann, H. (2017). Tree Species Selection in the Face of Drought Risk—Uncertainty in Forest Planning. *Forests*, 8(10), 363. https://doi.org/10.3390/f8100363

Alcasena, F. J., Ager, A. A., Bailey, J. D., Pineda, N., & Vega-García, C. (2019). Towards a comprehensive wildfire management strategy for Mediterranean areas: Framework development and implementation in Catalonia, Spain. *Journal of Environmental Management*, 231, 303–320. https://doi.org/10.1016/j.jenvman.2018.10.027

Allen, C. D., Breshears, D. D., and McDowell, N. G. (2015). On underestimation of global vulnerability to tree mortality and forest die-off from hotter drought in the Anthropocene. *Ecosphere* 6 (8), 1–55. https://doi.org/10.1890/ES15-00203.1

Allen, C. D., Macalady, A. K., Chenchouni, H., Bachelet, D., McDowell, N., Vennetier, M., Kitzberger, T., Rigling, A., Breshears, D. D., Hogg, E. H. (Ted), Gonzalez, P., Fensham, R., Zhang, Z., Castro, J., Demidova, N., Lim, J. H., Allard, G., Running, S. W., Semerci, A., & Cobb, N. (2010). A global overview of drought and heat-induced tree mortality reveals emerging climate change risks for forests. *Forest Ecology and Management*, 259(4), 660–684. https://doi.org/10.1016/j.foreco.2009.09.001

Allen, R., Pereira, L., Raes, D., & Smith, M. (1998). Crop evapotranspiration–Guidelines for computing crop water requirements. *Irrigation and Drainage*, 56.

An, H., Gan, J., & Cho, S. (2015). Assessing Climate Change Impacts on Wildfire Risk in the United States. *Forests*, 6(12), 3197–3211. https://doi.org/10.3390/f6093197

Anderegg, W. R. L., Kane, J. M., & Anderegg, L. D. L. (2013). Consequences of widespread tree mortality triggered by drought and temperature stress. *Nature Climate Change*, 3(1), 30–36. https://doi.org/10.1038/nclimate1635

Anderegg, W. R. L., Trugman, A. T., Badgley, G., Konings, A. G., & Shaw, J. (2020). Divergent forest sensitivity to repeated extreme droughts. *Nature Climate Change*, 10(12), 1091–1095. https://doi.org/10.1038/s41558-020-00919-1

Anderson, H.E. (1982). *Aids to determining fuel models for estimating fire behavior*. General Technical Report INT-122, United States Department of Agriculture, Forest Service, Intermountain Forest and Range Experiment Station, Ogden, UT. 26 p

Anyamba, A., & Tucker, C. J. (2012). *Historical Perspectives on AVHRR NDVI and Vegetation Drought Monitoring. In Remote Sensing of Drought: Innovative Monitoring Approaches* (pp. 23–51). Taylor & Francis Group LLC.

Arellano Pérez, S., González Álvarez, J. G., Vega Hidalgo, J. A., Ruiz González, A. D. (2017). *Modelos de estimación de la distribución vertical de combustibles finos de copas en masas de pinar a partir de datos del IV Inventario Forestal Nacional.* 7º Congreso Forestal Español. Plasencia (Cáceres, Spain).

Baker, J. C. A., Garcia-Carreras, L., Gloor, M., Marsham, J. H., Buermann, W., Da Rocha, H. R., Nobre, A. D., De Carioca Araujo, A., & Spracklen, D. V. (2021). Evapotranspiration in the Amazon: Spatial patterns, seasonality, and recent trends in observations, reanalysis, and climate models. *Hydrology and Earth System Sciences*, 25(4), 2279–2300. https://doi.org/10.5194/hess-25-2279-2021

Basso, B., & Antle, J. (2020). Digital agriculture to design sustainable agricultural systems. *Nature Sustainability*, 3(4), 254–256. https://doi.org/10.1038/s41893-020-0510-0

Bastin, J.-F., Finegold, Y., Garcia, C., Mollicone, D., Rezende, M., Routh, D., Zohner, C. M., & Crowther, T. W. (2019). The global tree restoration potential. *Science*, 365(6448), 76–79. https://doi.org/10.1126/science.aax0848

Batllori, E., Lloret, F., Aakala, T., Anderegg, W. R. L., Aynekulu, E., Bendixsen, D. P., Bentouati, A., Bigler, C., Burk, C. J., Camarero, J. J., Colangelo, M., Coop, J. D., Fensham, R., Floyd, M. L., Galiano, L., Ganey, J. L., Gonzalez, P., Jacobsen, A. L., Kane, J. M., … Zeeman, B. (2020). Forest and woodland replacement patterns following drought-related mortality. *Proceedings of the National Academy of Sciences*, 117(47), 29720–29729. https://doi.org/10.1073/pnas.2002314117

Beguería, S., Vicente-Serrano, S. M., Reig, F., & Latorre, B. (2014). Standardized precipitation evapotranspiration index (SPEI) revisited: Parameter fitting, evapotranspiration models, tools, datasets, and drought monitoring. *International Journal of Climatology*, 34(10), 3001–3023. https://doi.org/10.1002/joc.3887

Belcher, C. M. (2013). *Fire Phenomena and the Earth System: An Interdisciplinary Guide to Fire Science*, First Edition. Wiley-Blackwell ISBN: 978-0-470-65748-5

Bennett A.C., McDowell N.G., Allen C.D., Anderson-Teixeira K.J. (2015). Larger trees suffer most during drought in forests worldwide. *Nature Plants*. 1(10):15139. https://doi.org/10.1038/nplants.2015.139

Bhattarai, N., & Wagle, P. (2021). Recent Advances in Remote Sensing of Evapotranspiration. *Remote Sensing*, 13(21), 4260. https://doi.org/10.3390/rs13214260

Bolte, A., Ammer, C., Löf, M., Nabuurs, G.-J., Schall, P., & Spathelf, P. (2009). *Adaptive Forest Management: A Prerequisite for Sustainable Forestry in the Face of Climate Change*. Managing Forest Ecosystems, vol 19. Springer, Dordrecht. https://doi.org/10.1007/978-90-481-3301-7_8

Bonal, D., Burban, B., Stahl, C., Wagner, F., & Hérault, B. (2016). The response of tropical rainforests to drought—Lessons from recent research and future prospects. *Annals of Forest Science*, 73(1), 27–44. https://doi.org/10.1007/s13595-015-0522-5

Boon, M. A., Drijfhout, A. P., & Tesfamichael, S. (2017). Comparison of a fixed-wing and multirotor UAV for environmental mapping applications: A case study. *The International Archives of the Photogrammetry, Remote Sensing and Spatial Information Sciences*, XLII-2/W6, 47–54. https://doi.org/10.5194/isprs-archives-XLII-2-W6-47-2017

Botequim, B., Fernandes, P. M., Borges, J. G., González-Ferreiro, E., & Guerra-Hernández, J. (2019). Improving silvicultural practices for Mediterranean forests through fire behaviour modelling using LiDAR-derived canopy fuel characteristics. International Journal of Wildland Fire, 28(11), 823–839. https://doi.org/10.1071/WF19001

Bowman, D. M. J. S., Kolden, C. A., Abatzoglou, J. T., Johnston, F. H., van der Werf, G. R., & Flannigan, M. (2020). Vegetation fires in the Anthropocene. Nature Reviews Earth & Environment, 1(10), 500–515. https://doi.org/10.1038/s43017-020-0085-3

Bowman, D. M., O'Brien, J. A., & Goldammer, J. G. (2013). Pyrogeography and the global quest for sustainable fire management. *Annual Review of Environment and Resources*, 38, 57-80.

Bradstock, R. A. (2010). A biogeographic model of fire regimes in Australia: Current and future implications: A biogeographic model of fire in Australia. *Global Ecology and Biogeography*, 19(2), 145–158. https://doi.org/10.1111/j.1466-8238.2009.00512.x

Brown, K., & Pearce, D. W. (Eds.). (1994). *The causes of tropical deforestation: The economic and statistical analysis of factors giving rise to the loss of the tropical forests*. UBC Press.

Brown, R. T., Agee, J. K., & Franklin, J. F. (2004). Forest Restoration and Fire: Principles in the Context of Place. *Conservation Biology*, 18(4), 903–912. https://doi.org/10.1111/j.1523-1739.2004.521_1.x

Burrows, N., & McCaw, L. (2013). Prescribed burning in southwestern Australian forests. *Frontiers in Ecology and the Environment*, 11(s1). https://doi.org/10.1890/120356

Camarero, J. J. (2021a). The drought-dieback-death conundrum in trees and forests. *Plant Ecology and & Diversity*, 14:1-2, 1-12. https://doi.org/10.1080/17550874.2021.1961172

Camarero, J. J. (2021b). Within versus between species size effects on drought-induced dieback and mortality. *Tree Physiology*, 41(5), 679–682. https://doi.org/10.1093/treephys/tpaa167

Camarretta, N., Harrison, P. A., Bailey, T., Potts, B., Lucieer, A., Davidson, N., & Hunt, M. (2020). Monitoring forest structure to guide adaptive management of forest restoration: A review of remote sensing approaches. *New Forests*, *51*(4), 573–596. https://doi.org/10.1007/s11056-019-09754-5

Cawson, J.G. & Hemming, V., Ackland, A. (2020). Exploring the key drivers of forest flammability in wet eucalypt forests using expert-derived conceptual models. *Landscape Ecology* 35, 1775–1798 https://doi.org/10.1007/s10980-020-01055-z

Chakravarty, S., Ghosh, S. K., Suresh, C. P., Dey, A. N., & Shukla, G. (2012). Deforestation: Causes, Effects and Control Strategies. In C. A. Okia (Ed.), *Global perspectives on Sustainable Forest Management*. InTech.

Chapin, F. S., Torn, M. S., & Tateno, M. (1996). Principles of Ecosystem Sustainability. *The American Naturalist*, *148*(6), 1016–1037. https://doi.org/10.1086/285969

Choat, B., Brodribb, T. J., Brodersen, C. R., Duursma, R. A., López, R., & Medlyn, B. E. (2018). Triggers of tree mortality under drought. *Nature*, 558(7711), 531–539. https://doi.org/10.1038/s41586-018-0240-x

Choi, & Park. (2019). Monitoring, Assessment and Management of Forest Insect Pests and Diseases. *Forests*, 10(10), 865. https://doi.org/10.3390/f10100865

Chuvieco, E. (2010). *Teledetección ambiental: La observación de la tierra desde el espacio* (Tercera edición). Ariel. ISBN 9788434434981

Clements, F. (1916). *Plant succession; an analysis of the development of vegetation*. Carnegie Institution of Washington.

Colangelo, M., Camarero, J. J., Borghetti, M., Gazol, A., Gentilesca, T., & Ripullone, F. (2017). Size Matters a Lot: Drought-Affected Italian Oaks Are Smaller and Show Lower Growth Prior to Tree Death. *Frontiers in Plant Science*, 8. https://doi.org/10.3389/fpls.2017.00135

Coop, J. D., Parks, S. A., Stevens-Rumann, C. S., Crausbay, S. D., Higuera, P. E., Hurteau, M. D., Tepley, A., Whitman, E., Assal, T., Collins, B. M., Davis, K. T., Dobrowski, S., Falk, D. A., Fornwalt, P. J., Fulé, P. Z., Harvey, B. J., Kane, V. R., Littlefield, C. E., Margolis, E. Q., … Rodman, K. C. (2020). Wildfire-Driven Forest Conversion in Western North American Landscapes. *BioScience*, 70(8). https://doi.org/10.1093/biosci/biaa061

Corlett, R. T. (2016). The Impacts of Droughts in Tropical Forests. *Trends in Plant Science*, 21(7), 584–593. https://doi.org/10.1016/j.tplants.2016.02.003

Crawford, R. M. M. (2008). *Plants at the Margin: Ecological Limits and Climate Change* (1st ed.). Cambridge University Press. https://doi.org/10.1017/CBO9780511754906

Dakos, V., Carpenter, S. R., Van Nes, E. H., & Scheffer, M. (2015). Resilience indicators: Prospects and limitations for early warnings of regime shifts. *Philosophical Transactions of the Royal Society B: Biological Sciences*, 370(1659), 20130263. https://doi.org/10.1098/rstb.2013.0263

Dale, V.H. (1997). The relationship between land use change and climate change. *Ecological applications*, 7(3) 753-769.

Dalponte, M., Bruzzone, L., & Gianelle, D. (2008). Fusion of Hyperspectral and LIDAR Remote Sensing Data for Classification of Complex Forest Areas. *IEEE Transactions on Geoscience and Remote Sensing*, 46(5), 1416–1427. https://doi.org/10.1109/TGRS.2008.916480

D'Amato, A. W., Bradford, J. B., Fraver, S., & Palik, B. J. (2013). Effects of thinning on drought vulnerability and climate response in north temperate forest ecosystems. *Ecological Applications*, 23(8), 1735–1742. https://doi.org/10.1890/13-0677.1

Dassot, M., Constant, T., & Fournier, M. (2011). The use of terrestrial LiDAR technology in forest science: Application fields, benefits and challenges. *Annals of Forest Science*, 68(5), 959–974. https://doi.org/10.1007/s13595-011-0102-2

Davis, B. H. (2011). *Retrospective fire modelling: quantifying the impacts of fire suppression*. Gen. Tech. Rep. RMRS-GTR-236WWW. Fort Collins, CO: US. Department of Agriculture, Forest Service, Rocky Mountain Research Station.

del Campo, A. D., Otsuki, K., Serengil, Y., Blanco, J. A., Yousefpour, R., & Wei, X. (2022). A global synthesis on the effects of thinning on hydrological processes: Implications for forest management. *Forest Ecology and Management*, 519, 120324. https://doi.org/10.1016/j.foreco.2022.120324

Dey, N., Bhatt, C., & Ashour, A. S. (Eds.). (2019). *Big Data for Remote Sensing: Visualization, Analysis and Interpretation*. Springer International Publishing. https://doi.org/10.1007/978-3-319-89923-7

Dimitriadou, S., & Nikolakopoulos, K. G. (2021). Evapotranspiration trends and interactions in light of the anthropogenic footprint and the climate crisis: A review. *Hydrology*, 8(4). https://doi.org/10.3390/hydrology8040163

Din, S., Ghayvat, H., Paul, A., Ahmad, A., Rathore, M. M., & Shafi, I. (2015). An architecture to analyze big data in the Internet of Things. 2015 9th *International Conference on Sensing Technology* (ICST), 677–682. https://doi.org/10.1109/ICSensT.2015.7438483

Doğmuş-Lehtijärvi, H. T., Lehtijärvi, A., & Korhonen, K. (2006). *Heterobasidion abietinum* on *Abies* species in western Turkey: *Heterobasidion abietinum* in western Turkey. *Forest Pathology*, *36*(4), 280–286. https://doi.org/10.1111/j.1439-0329.2006.00456.x

Drescher, J., Rembold, K., Allen, K., Beckschäfer, P., Buchori, D., Clough, Y., Faust, H., Fauzi, A. M., Gunawan, D., Hertel, D., Irawan, B., Jaya, I. N. S., Klarner, B., Kleinn, C.,

Knohl, A., Kotowska, M. M., Krashevska, V., Krishna, V., Leuschner, C., … Scheu, S. (2016). Ecological and socio-economic functions across tropical land use systems after rainforest conversion. *Philosophical Transactions of the Royal Society B: Biological* Sciences, 371(1694), 20150275. https://doi.org/10.1098/rstb.2015.0275

Egoh, B. N., Nyelele, C., Holl, K. D., Bullock, J. M., Carver, S., & Sandom, C. J. (2021). Rewilding and restoring nature in a changing world. *PLOS ONE*, 16(7), e0254249. https://doi.org/10.1371/journal.pone.0254249

Ehsani, R., & Mari Maja, J. (2013). The Rise of Small UAVs in Precision Agriculture. Resource Magazine, 20(4), 18–19. https://elibrary.asabe.org/abstract.asp?aid=44296&t=11

Eloy, L., A. Bilbao, B., Mistry, J., & Schmidt, I. B. (2019). From fire suppression to fire management: Advances and resistances to changes in fire policy in the savannas of Brazil and Venezuela. *The Geographical Journal*, 185(1), 10-22.

Escuin, S., Navarro, R., & Fernández, P. (2008). Fire severity assessment by using NBR (Normalized Burn Ratio) and NDVI (Normalized Difference Vegetation Index) derived from LANDSAT TM/ETM images. *International Journal of Remote Sensing*, 29(4), 1053–1073. https://doi.org/10.1080/01431160701281072

Fernandes, P. M. (2015). Empirical Support for the Use of Prescribed Burning as a Fuel Treatment. *Current Forestry Reports*, 1(2),118–127. https://doi.org/10.1007/s40725-015-0010-z

Fernandes, P. M., Davies, G. M., Ascoli, D., Fernández, C., Moreira, F., Rigolot, E., Stoof, C. R., Vega, J. A., & Molina, D. (2013). Prescribed burning in southern Europe: Developing fire management in a dynamic landscape. *Frontiers in Ecology and the Environment*, 11(s1). https://doi.org/10.1890/120298

Fidelis, A., Zanzarini, V., Camargos, L., Silva, N., Rosalem, P., & Martins, A. (2017). Flowering after fire in the Cerrado: And example of *Bulbostylis paradoxa*. https://www.sanparks.org/assets/docs/conservation/scientific_new/savanna/ssnm2017/flowering-after-fire.pdf

Finney, M. A. (2006). *An overview of FlamMap fire modelling capabilities. Fuels Management—How to Measure Succes*s: Conference Proceedings, 213–220.

Flannigan, M. D., Stocks, B. J., & Wotton, B. M. (2000). Climate change and forest fires. *Science* of The Total Environment, 262(3), 221–229. https://doi.org/10.1016/S0048-9697(00)00524-6

Flores, A., K. Herndon, Rajesh Thapa, & Emil Cherrington. (2019). *Synthetic Aperture Radar (SAR) Handbook: Comprehensive Methodologies for Forest Monitoring and Biomass Estimation*. https://doi.org/10.25966/NR2C-S697

Fortini, L., Schubert, O. (2017) Beyond exposure, sensitivity, and adaptive capacity: a response based ecological framework to assess species climate change vulnerability. *Climate Change Responses* 4, 2. https://doi.org/10.1186/s40665-017-0030-y

Forzieri, G., Dakos, V., McDowell, N. G., Ramdane, A., & Cescatti, A. (2022). Emerging signals of declining forest resilience under climate change. *Nature*, 608(7923), 534–539. https://doi.org/10.1038/s41586-022-04959-9

Franklin, J. F., Mitchell, R. J., & Palik, B. J. (2007). *Natural disturbance and stand development principles for ecological forestry* (NRS-GTR-19; p. NRS-GTR-19). U.S. Department of Agriculture, Forest Service, Northern Research Station. https://doi.org/10.2737/NRS-GTR-19

García, D. H. (2022). Analysis of Urban Heat Island and Heat Waves Using Sentinel-3 Images: A Study of Andalusian Cities in Spain. *Earth Systems and Environment*, 6(1), 199–219. https://doi.org/10.1007/s41748-021-00268-9

García, D. S. (2006). *Núcleos residuales de pinsapo perdidos en Andalucía en el siglo XX*. Invest Agrar: Sist Recur For

Garcia, M., Saatchi, S., Ferraz, A., Silva, C. A., Ustin, S., Koltunov, A., & Balzter, H. (2017). Impact of data model and point density on aboveground forest biomass estimation from airborne LiDAR. *Carbon Balance and Management*, 12(1), 4. https://doi.org/10.1186/s13021-017-0073-1

Gaulton, R., & Malthus, T. J. (2010). LiDAR mapping of canopy gaps in continuous cover forests: A comparison of canopy height model and point cloud-based techniques LiDAR mapping of canopy gaps in continuous cover forests**.** International *Journal of Remote Sensing*, 31(5), 1193–1211. https://doi.org/10.1080/01431160903380565

Gely, C., Laurance, S. G. W., & Stork, N. E. (2020). How do herbivorous insects respond to drought stress in trees? *Biological Reviews*, 95(2), 434–448. https://doi.org/10.1111/brv.12571

Gens, R. (2008). Oceanographic Applications of SAR Remote Sensing. *GIScience & Remote Sensing*, 45(3), 275–305. https://doi.org/10.2747/1548-1603.45.3.275

Ghamisi, P., Rasti, B., Yokoya, N., Wang, Q., Hofle, B., Bruzzone, L., Bovolo, F., Chi, M., Anders, K., Gloaguen, R., Atkinson, P. M., & Benediktsson, J. A. (2018). Multisource and Multitemporal Data Fusion in Remote Sensing (arXiv:1812.08287). arXiv. http://arxiv.org/abs/1812.08287

Gibson, D. J. (1996). Textbook Misconceptions: The Climax Concept of Succession. *The American Biology Teacher*, 58(3), 135–140. https://doi.org/10.2307/4450101

Gilbert, J.A. and Henry, C. (2015), Predicting ecosystem emergent properties at multiple scales. *Environmental Microbiology Reports*, 7: 20-22. https://doi.org/10.1111/1758-2229.12258

Goodrich, Sherel (1983) "Utah flora: Salicaceae," *Great Basin Naturalist*: Vol. 43: No. 4, Article 2. Available at: https://scholarsarchive.byu.edu/gbn/vol43/iss4/2

González-Alonso, F., Merino-De-Miguel, S., Roldán-Zamarrón, A., García-Gigorro, S., & Cuevas, J. M. (2006). Forest biomass estimation through NDVI composites. The role of remotely sensed data to assess Spanish forests as carbon sinks. *International Journal of Remote Sensing*, 27(24). https://doi.org/10.1080/01431160600830748

González-Dugo, M. P., Chen, X., Andreu, A., Carpintero, E., Gómez-Giraldez, P. J., Carrara, A., & Su, Z. (2021). Long-term water stress and drought assessment of Mediterranean oak savanna vegetation using thermal remote sensing. *Hydrology and Earth System Sciences*, 25(2), 755–768. https://doi.org/10.5194/hess-25-755-2021

Graham, J.B., McCarthy, B.C. (2021). Effects of fine fuel moisture and loading on small scale fire behavior in mixed-oak forests of Southeastern Ohio. *Fire ecology* 2, 100–114. https://doi.org/10.4996/fireecology.0201100

Granier, A. & Breda, N. (1996). Modelling canopy conductance and stand transpiration of an oak forest from sap flow measurements. *Annales des Sciences Forestières* 53(2) https://doi.org/10.1051/forest:19960233

Gregory, S. C., & Petty, J. A. (1973). Value Action of Bordered Pits in Conifers. *Journal of Experimental Botany*, 24(4), 763–765. https://doi.org/10.1093/jxb/24.4.763

Gu, Y., Wylie, B. K., Howard, D. M., Phuyal, K. P., & Ji, L. (2013). NDVI saturation adjustment: A new approach for improving cropland performance estimates in the Greater Platte River Basin, USA. *Ecological Indicators*, 30, 1–6. https://doi.org/10.1016/j.ecolind.2013.01.041

Guerrieri, R., Lepine, L., Asbjornsen, H., Xiao, J., & Ollinger, S. V. (2016). Evapotranspiration and water use efficiency in relation to climate and canopy nitrogen in U.S. forests. *Journal of Geophysical Research: Biogeosciences*, 121(10), 2610–2629. https://doi.org/10.1002/2016JG003415

Gunderson, L. H., & Holling, C. S. (2002). *Resilience and adaptive cycles. In Panarchy. Understanding Transformations in Human and Natural Systems*. Island Press.

Guo, F., Lenoir, J., & Bonebrake, T. C. (2018). Land-use change interacts with climate to determine elevational species redistribution. *Nature*. https://doi.org/10.1038/s41467-018-03786-9

Gurevitch, J., & Padilla, D. (2004). Are invasive species a major cause of extinctions? *Trends in Ecology & Evolution*, 19(9), 470–474. https://doi.org/10.1016/j.tree.2004.07.005

Hidalgo, J. A. V. (1999). *Historia del fuego de Pinus pinaster y Abies pinsapo en la carta norte de Sierra Bermeja (Málaga)*: 1817-1997. In Incendios históricos, una aproximación multidisciplinar.

Hilker, T., N., C. C., Newnham, G. J., van Leeuwen, M., Wulder, M. A., Stewart, J., & Culvenor, D. S. (2012). Comparison of terrestrial and airborne LIDAR in describing stand structure of a thinned lodgepole pine forest. *Journal of Forestry*, 110(2), 97-104. https://doi.org/10.5849/jof.11-003

Hill, D. J., Tarasoff, C., Whitworth, G. E., Baron, J., Bradshaw, J. L., & Church, J. S. (2017). Utility of unmanned aerial vehicles for mapping invasive plant species: A case study on yellow flag iris (*Iris pseudacorus* L.). *International Journal of Remote Sensing*, 38(8–10), 2083–2105. https://doi.org/10.1080/01431161.2016.1264030

Hobbie, S.E.; Villeger, S. (2015). Interactive effects of plants, decomposers, herbivores, and predators on nutrient cycling. In Hanley, T.C., Pierre, K.J.L. (Eds.), *Trophic Ecology: Bottom-Up and Top-Down Interactions across Aquatic and Terrestrial System* (Ecological Reviews pp. 233-259). Cambridge: Cambridge University Press. https://doi.org/10.1017/CBO9781139924856.010

Hörl, J., Keller, K., & Yousefpour, R. (2020). Reviewing the performance of adaptive forest management strategies with robustness analysis. *Forest Policy and Economics*. 119 https://doi.org/10.1016/j.forpol.2020.102289

Huang, T., Ding, X., Zhu, X., Chen, S., Chen, M., Jia, X., Lai, F., & Zhang, X. (2021a). Assessment of Poplar Looper (*Apocheima cinerarius* Erschoff) Infestation on Euphrates (Populus euphratica) Using Time-Series MODIS NDVI Data Based on the Wavelet Transform and Discriminant Analysis. *Remote Sensing*, 13(12), 2345. https://doi.org/10.3390/rs13122345

Huang, S., Tang, L., Hupy, J. P., Wang, Y., & Shao, G. (2021b). A commentary review on the use of normalized difference vegetation index (NDVI) in the era of popular remote sensing. *Journal of Forestry Research*, 32(1), 1–6. https://doi.org/10.1007/s11676-020-01155-1

Hulcr, J., & Dunn, R. R. (2011). The sudden emergence of pathogenicity in insect–fungus symbioses threaten naive forest ecosystems. *Proceedings of the Royal Society B: Biological Sciences,* 278(1720), 2866–2873. https://doi.org/10.1098/rspb.2011.1130

Hulme, P. E. (2009). Trade, transport and trouble: Managing invasive species pathways in an era of globalization. *Journal of Applied Ecology*, 46(1), 10–18. https://doi.org/10.1111/j.1365-2664.2008.01600.x

Iglhaut, J., Cabo, C., Puliti, S., Piermattei, L., O'Connor, J., & Rosette, J. (2019). Structure from Motion Photogrammetry in Forestry: A Review. *Current Forestry Reports*, 5(3), 155–168. https://doi.org/10.1007/s40725-019-00094-3

Italiano, S. S. P., Camarero, J. J., Colangelo, M., Borghetti, M., Castellaneta, M., Pizarro, M., & Ripullone, F. (2023). Assessing Forest Vulnerability to Climate Change Combining Remote Sensing and Tree-Ring Data: Issues, Needs and Avenues. *Forests*, 14(6), 1138. https://doi.org/10.3390/f14061138

IPCC, 2014. Summary for Policymakers., in: *Contribution of Working Group II to the Fifth Assessment Report of the Intergovernmental Panel on Climate Change*. Cambridge University Press, Cambridge, UK. Reisinger, Andy, Mark Howden, Carolina Vera, et al. (2020) *The Concept of Risk in the IPCC Sixth Assessment Report: A Summary of Cross-Working Group Discussions*. Intergovernmental Panel on Climate Change, Geneva, Switzerland. pp15.

IUCN. (2021). Forests and climate change [Issues brief]. International Union for Conservation of Nature. https://www.iucn.org/sites/default/files/2022-04/forests_and_climate_change_issues_brief_2021.pdf

Jactel, H. *et al.* (2015). *Insect – Tree Interactions in* Thaumetopoea pityocampa . In: Roques, A. (eds) Processionary Moths and Climate Change: An Update. Springer, Dordrecht. https://doi.org/10.1007/978-94-017-9340-7_6

Jactel, H., Koricheva, J., & Castagneyrol, B. (2019). Responses of forest insect pests to climate change: Not so simple. *Current Opinion in Insect Science*, 35, 103–108. https://doi.org/10.1016/j.cois.2019.07.010

Jandl, R., Spathelf, P., Bolte, A., & Prescott, C. E. (2019). Forest adaptation to climate change—Is non-management an option? *Annals of Forest Science*, 76(2), 48. https://doi.org/10.1007/s13595-019-0827-x

Jones, M. W., Abatzoglou, J. T., Veraverbeke, S., Andela, N., Lasslop, G., Forkel, M., Smith, A. J. P., Burton, C., Betts, R. A., van der Werf, G. R., Sitch, S., Canadell, J. G., Santín, C., Kolden, C., Doerr, S. H., & Le Quéré, C. (2022). Global and Regional Trends and Drivers of Fire Under Climate Change. *Reviews of Geophysics*, 60(3). https://doi.org/10.1029/2020RG000726

Joseph, G. (2011). *Fundamentals of remote sensing* (2. ed., reprinted). Universities Press.

Jump AS, Ruiz-Benito P, Greenwood S, Allen CD, Kitzberger T, Fensham R, Martínez-Vilalta J, Lloret F. (2017). Structural overshoot of tree growth with climate variability and the global spectrum of drought-induced forest dieback. *Global Change Biology* 23(9):3742–3757. https://doi.org/10.1111/gcb.13636

Kausrud, K., Økland, B., Skarpaas, O., Grégoire, J.-C., Erbilgin, N., & Stenseth, N. Chr. (2012). Population dynamics in changing environments: The case of an eruptive forest pest species. *Biological Reviews*, 87(1), 34–51. https://doi.org/10.1111/j.1469-185X.2011.00183.x

Keeley, J. E., Pausas, J. G., Rundel, P. W., Bond, W. J., & Bradstock, R. A. (2011). Fire as an evolutionary pressure shaping plant traits. *Trends in Plant Science*, 16(8), 406–411. https://doi.org/10.1016/j.tplants.2011.04.002

Keeley, J. E., & Rundel, P. W. (2005). Fire and the Miocene expansion of C4 grasslands: Miocene C4 grassland expansion. *Ecology Letters*, 8(7), 683–690. https://doi.org/10.1111/j.1461-0248.2005.00767.x

Kelly, D. (1994). The evolutionary ecology of mast seeding. *Trends in Ecology & Evolution*, 9(12), 465–470. https://doi.org/10.1016/0169-5347(94)90310-7

Kent Shannon, D., Clay, D. E., & Kitchen, N. R. (Eds.). (2018). *Precision Agriculture Basics*. American Society of Agronomy and Soil Science Society of America. https://doi.org/10.2134/precisionagbasics

Khani P., H., Sadeghian, S., & Riahi Bakhtiari, H. R. (2018). Production of Digital Terrain Model (DTM) in Dense Forest Areas with Combined Airborne LiDAR Data Filtering Algorithms. *Geospatial Engineering Journal*, 9(1), 53–62. http://gej.issge.ir/article-1-237-en.html

Kimmerer, R.W., Lake F.K. (2001). The role of indigenous burning in land management. *Journal of Forestry*, 99 (11), 36–41. https://doi.org/10.1093/jof/99.11.36

Klein T, Di Matteo G, Rotenberg E, Cohen S, Yakir D. (2012). Differential ecophysiological response of a major Mediterranean pine species across a climatic gradient. *Tree Physiology*. 33(1):26–36. https://doi.org/10.1093/treephys/tps116.

Kotowska, M. M., Link, R. M., Röll, A., Hertel, D., Hölscher, D., Waite, P.-A., Moser, G., Tjoa, A., Leuschner, C., & Schuldt, B. (2021). Effects of Wood Hydraulic Properties on Water Use and Productivity of Tropical Rainforest Trees. *Frontiers in Forests and Global Change*, 3, 598759. https://doi.org/10.3389/ffgc.2020.598759

Kuklina, V., Sizov, O., Rasputina, E., Bilichenko, I., Krasnoshtanova, N., Bogdanov, V., & Petrov, A. N. (2022). Fires on Ice: Emerging Permafrost Peatlands Fire Regimes in Russia's Subarctic Taiga. *Land*, 11(3), 322. https://doi.org/10.3390/land11030322

Krawchuk, M. A., Moritz, M. A., Parisien, M. A., Van Dorn, J., & Hayhoe, K. (2009). Global pyrogeography: the current and future distribution of wildfire. *PloS one*, 4(4), e5102.

Lamont, B. B., Pausas, J. G., He, T., Witkowski, E. T. F., & Hanley, M. E. (2020). Fire as a Selective Agent for both Serotiny and Nonserotiny Over Space and Time. *Critical Reviews in Plant Sciences*, 39(2), 140–172. https://doi.org/10.1080/07352689.2020.1768465

Law, B. E., Hudiburg, T. W., & Luyssaert, S. (2013). Thinning effects on forest productivity: Consequences of preserving old forests and mitigating impacts of fire and drought. *Plant Ecology & Diversity*, 6(1), 73–85. https://doi.org/10.1080/17550874.2012.679013

Lawrence, D., & Vandecar, K. (2015). Effects of tropical deforestation on climate and agriculture. Nature Climate Change, 5(1), 27–36. https://doi.org/10.1038/nclimate2430

Lenton, T. M. (2001). The role of land plants, phosphorus weathering and fire in the rise and regulation of atmospheric oxygen**.** *Global Change Biology*, 7(6), 613–629. https://doi.org/10.1046/j.1354-1013.2001.00429.x

Li, T., Cui, L., Liu, L., Chen, Y., Liu, H., Song, X., & Xu, Z. (2023). Advances in the study of global forest wildfires. *Journal of Soils and Sediments*, 23(7), 2654–2668. https://doi.org/10.1007/s11368-023-03533-8

Li, X., Zhao, N., Jin, R., Liu, S., Sun, X., Wen, X., Wu, D., Zhou, Y., Guo, J., Chen, S., Xu, Z., Ma, M., Wang, T., Qu, Y., Wang, X., Wu, F., & Zhou, Y. (2019). Internet of Things to network smart devices for ecosystem monitoring. *Science* Bulletin, 64(17), 1234–1245. https://doi.org/10.1016/j.scib.2019.07.004

Lim, K., Treitz, P., Wulder, M., St-Onge, B., & Flood, M. (2003). LiDAR remote sensing of forest structure. https://doi.org/10.1191/0309133303pp360ra

Linares, J. C., Delgado-Huertas, A., Camarero, J. J., Merino, J., and Carreira, J. A. (2009). Competition and drought limit the response of water-use efficiency to rising atmospheric carbon dioxide in the Mediterranean fir *Abies pinsapo*. *Oecologia* 161, 611–624. https://doi.org/10.1007/s00442-009-1409-7

Liu, C., Chen, Z., Shao, Y., Chen, J., Hasi, T., & Pan, H. (2019). Research advances of SAR remote sensing for agriculture applications: A review. *Journal of Integrative Agriculture*, 18(3), 506–525. https://doi.org/10.1016/S2095-3119(18)62016-7

Liu, S., Xu, Z., Song, L., Zhao, Q., Ge, Y., Xu, T., Ma, Y., Zhu, Z., Jia, Z., & Zhang, F. (2016). Upscaling evapotranspiration measurements from multi-site to the satellite pixel scale over heterogeneous land surfaces. *Agricultural and Forest Meteorology*, 230–231, 97–113. https://doi.org/10.1016/j.agrformet.2016.04.008

Liu, Y., He, K., & Qin, F. (2021). Remote Sensing Big Data Analysis of the Lower Yellow River Ecological Environment Based on Internet of Things. *Journal of Sensors*, 2021, 1–11. https://doi.org/10.1155/2021/1059517

Liu, Z., Wang, Y., Yu, P., Xu, L., & Yu, S. (2022). Environmental and canopy conditions regulate the forest floor evapotranspiration of larch plantations. *Forest Ecosystems*, 9, 100058. https://doi.org/10.1016/j.fecs.2022.100058

Logan, J. A., Régnière, J., & Powell, J. A. (2003). Assessing the impacts of global warming on forest pest dynamics. *Frontiers in Ecology and the Environment*, 1(3), 130–137. https://doi.org/10.1890/1540-9295(2003)001[0130:ATIOGW]2.0.CO;2

Lorimer, J., Sandom, C., Jepson, P., Doughty, C., Barua, M., & Kirby, K. J. (2015). Rewilding: Science, Practice, and Politics. Annual Review of Environment and Resources, 40(1), 39–62. https://doi.org/10.1146/annurev-environ-102014-021406

Lovelock, C. E., Feller, I. C., Reef, R., Hickey, S., & Ball, M. C. (2017). Mangrove dieback during fluctuating sea levels. *Scientific Reports*, 7(1), 1680. https://doi.org/10.1038/s41598-017-01927-6

Manrique-Alba, À., Beguería, S., & Camarero, J. J. (2022). Long-term effects of forest management on post-drought growth resilience: An analytical framework. *Science of The Total Environment*, 810, 152374. https://doi.org/10.1016/j.scitotenv.2021.152374

Marchin, R. M., Stout, A. T., Davis, A. A., & King, J. S. (2017). Transgenically altered lignin biosynthesis affects photosynthesis and water relations of field-grown *Populus trichocarpa*. *Biomass and Bioenergy*, 98, 15–25. https://doi.org/10.1016/j.biombioe.2017.01.013

Maxwell, A. E., Warner, T. A., & Fang, F. (2018). Implementation of machine-learning classification in remote sensing: An applied review. *International Journal of Remote Sensing*, 39(9), 2784–2817. https://doi.org/10.1080/01431161.2018.1433343

McAlpine, C. A., Johnson, A., Salazar, A., Syktus, J., Wilson, K., Meijaard, E., Seabrook, L., Dargusch, P., Nordin, H., & Sheil, D. (2018). Forest loss and Borneo's climate. *Environmental Research Letters*, 13(4), 044009. https://doi.org/10.1088/1748-9326/aaa4ff

McDowell N.G, Allen C.D. (2015). Darcy's law predicts widespread forest mortality under climate warming. *Nature Climate Change*. 5(7):669–672. https://doi.org/10.1038/nclimate2641

McDowell, N., Pockman, W. T., Allen, C. D., Breshears, D. D., Cobb, N., Kolb, T., Plaut, J., Sperry, J., West, A., Williams, D. G., & Yepez, E. A. (2008). Mechanisms of plant survival and mortality during drought: Why do some plants survive while others succumb to drought? *New Phytologist*, 178(4), 719–739. https://doi.org/10.1111/j.1469-8137.2008.02436.x

McFeeters, S. K. (1996). The use of the Normalized Difference Water Index (NDWI) in the delineation of open water features. *International Journal of Remote Sensing*, 17(7), 1425–1432. https://doi.org/10.1080/01431169608948714

McGaughey, R. (2018). FUSION/LDV: software for LIDAR data analysis and visualization.

McGranahan, D. A., & Wonkka, C. L. (2021). *Ecology of Fire-Dependent Ecosystems; Wildland Fire Science*, Policy, and Management. Taylor & Francis Group LLC.

Means, J. E., Acker, S. A., Fitt, B. J., Renslow, M., Emerson, L., & Hendrix, C. J. (2000). *Predicting Forest Stand Characteristics with Airborne Scanning Lidar*. http://www.sbgmaps.com/lidar_technologies.htm

Meinzer, F. C., Bond, B. J., Warren, J. M., & Woodruff, D. R. (2005). Does water transport scale universally with tree size? *Functional Ecology*, 19(4), 558-565. https://doi.org/10.1111/j.1365-2435.2005.01017.x

Minnich, R. A. (1988). *The biogeography of fire in the San Bernardino Mountains of California: a historical study* (Vol. 28). Univ of California Press.

Moore, G. K. (1979). What is a picture worth? A history of remote sensing / Quelle est la valeur d'une image? Un tour d'horizon de télédétection. *Hydrological Sciences Bulletin*, 24(4), 477–485. https://doi.org/10.1080/02626667909491887

Morri, C., Montefalcone, M., Gatti, G., Vassallo, P., Paoli, C., & Bianchi, C. N. (2019). An Alien Invader is the Cause of Homogenization in the Recipient Ecosystem: A Simulation-Like Approach. *Diversity*, 11(9), 146. https://doi.org/10.3390/d11090146

Nawaz, S. A., Li, J., Bhatti, U. A., Shoukat, M. U., & Ahmad, R. M. (2022). AI-based object detection latest trends in remote sensing, multimedia, and agriculture applications. *Frontiers in Plant Science*, 13, 1041514. https://doi.org/10.3389/fpls.2022.1041514

Nielsen, D. C. (1990). Scheduling irrigations for soybeans with the Crop Water Stress Index (CWSI). *Field Crops Research*, 23(2), 103–116. https://doi.org/10.1016/0378-4290(90)90106-L

Niering, W. A. (1987). Vegetation Dynamics (Succession and Climax) in Relation to Plant Community Management. *Conservation Biology*, 1(4), 287–295. https://doi.org/10.1111/j.1523-1739.1987.tb00049.x

Niu, H., Hollenbeck, D., Zhao, T., Wang, D., & Chen, Y. (2020). Evapotranspiration Estimation with Small UAVs in Precision Agriculture. *Sensors*, 20(22), 6427. https://doi.org/10.3390/s20226427

Noce, S., Caporaso, L., & Santini, M. (2020). A new global dataset of bioclimatic indicators. *Scientific Data*, 7(1), 398. https://doi.org/10.1038/s41597-020-00726-5

Nolan, R. H., Collins, L., Leigh, A., Ooi, M. K. J., Curran, T. J., Fairman, T. A., Resco de Dios, V., & Bradstock, R. (2021). Limits to post-fire vegetation recovery under climate change. *Plant, Cell & Environment*, 44(11), 3471–3489. https://doi.org/10.1111/pce.14176

O'Brien, K. L. (1996). Tropical deforestation and climate change. *Progress in Physical Geography: Earth and Environment,* 20(3), 311–335. https://doi.org/10.1177/030913339602000304

González-Olabarria, J. R., Rodríguez, F., Fernández-Landa, A., & Yudego-Mola, B. (2012). Mapping fire risk in the Model Forest of Urbión (Spain) based on airborne LIDAR measurements. *Forest Ecology and Management*, 282, 149-156. https://doi.org/10.1016/j.foreco.2012.06.056

Othman, M. A., Ash'aari, Z. H., Aris, A. Z., & Ramli, M. F. (2018). *Tropical deforestation monitoring using NDVI from MODIS satellite: A case study in Pahang, Malaysia*. IOP Conference Series: Earth and Environmental Science, 169, 012047. https://doi.org/10.1088/1755-1315/169/1/012047

Pallardy, S. G., & Kozlowski, T. T. (2008). *Physiology of woody plants* (3rd ed). Elsevier.

Pausas, J. G. (2022). Pyrogeography across the western Palaearctic: A diversity of fire regimes. *Global Ecology and Biogeography*, 31(10), 1923-1932.

Pausas, J. G., & Keeley, J. E. (2009). A burning story: The role of fire in the history of life. *BioScience*, 59(7), 593–601. https://doi.org/10.1525/bio.2009.59.7.10

Penman, T. D., Christie, F. J., Andersen, A. N., Bradstock, R. A., Cary, G. J., Henderson, M. K., Price, O., Tran, C., Wardle, G. M., Williams, R. J., & York, A. (2011). Prescribed burning: How can it work to conserve the things we value? *International Journal of Wildland Fire*, 20(6), 721. https://doi.org/10.1071/WF09131

Perez, P. J., Lecina, S., Castellvi, F., Martínez-Cob, A., & Villalobos, F. J. (2006). A simple parameterization of bulk canopy resistance from climatic variables for estimating hourly

evapotranspiration. *Hydrological Processes*, 20(3), 515–532. https://doi.org/10.1002/hyp.5919

Pérez-Rodríguez, L. A., Quintano, C., Marcos, E., Suarez-Seoane, S., Calvo, L., & Fernández-Manso, A. (2020). Evaluation of Prescribed Fires from Unmanned Aerial Vehicles (UAVs) Imagery and Machine Learning Algorithms. *Remote Sensing*, 12(8), 1295. https://doi.org/10.3390/rs12081295

Perino, A., Pereira, H. M., Navarro, L. M., Fernández, N., Bullock, J. M., Ceauşu, S., Cortés-Avizanda, A., Van Klink, R., Kuemmerle, T., Lomba, A., Pe'er, G., Plieninger, T., Rey Benayas, J. M., Sandom, C. J., Svenning, J.-C., & Wheeler, H. C. (2019). Rewilding complex ecosystems. *Science*, 364(6438), eaav5570. https://doi.org/10.1126/science.aav5570

Pflug, E. E., Buchmann, N., Siegwolf, R. T. W., Schaub, M., Rigling, A., & Arend, M. (2018). Resilient Leaf Physiological Response of European Beech (Fagus sylvatica L.) to Summer Drought and Drought Release. *Frontiers in Plant Science*, 9, 187. https://doi.org/10.3389/fpls.2018.00187

Phillips, O. L., Aragão, L. E. O. C., Lewis, S. L., Fisher, J. B., Lloyd, J., López-González, G., Malhi, Y., Monteagudo, A., Peacock, J., Quesada, C. A., van der Heijden, G., Almeida, S., Amaral, I., Arroyo, L., Aymard, G., Baker, T. R., Bánki, O., Blanc, L., Bonal, D., … Torres-Lezama, A. (2009). Drought Sensitivity of the Amazon Rainforest. *Science*, 323(5919), 1344–1347. https://doi.org/10.1126/science.1164033

Picket, S., & White, P. (1985). *The Ecology of Natural Disturbance and Patch Dynamics* (S. Picket & P. White, Eds.). Elsevier. https://doi.org/10.1016/C2009-0-02952-3

Pickett, S. T. A., & McDonnell, M. J. (1989). Changing perspectives in community dynamics: A theory of successional forces. *Trends in Ecology & Evolution*, 4(8), 241–245. https://doi.org/10.1016/0169-5347(89)90170-5

Polle, A., Chen, S. L., Eckert, C., & Harfouche, A. (2019). Engineering Drought Resistance in Forest Trees. *Frontiers in Plant Science*, 9, 1875. https://doi.org/10.3389/fpls.2018.01875

Ponge, J. (2005). Emergent properties from organisms to ecosystems: Towards a realistic approach. *Biological Reviews*, 80(3), 403-411. https://doi.org/10.1017/S146479310500672X

Prakash, A. (2000). *Thermal remote sensing: Concepts, issues and applications*. International Archives of Photogrammetry and Remote Sensing, XXXIII.

Pureswaran, D. S., Roques, A., & Battisti, A. (2018). Forest Insects and Climate Change. *Current Forestry Reports*, 4(2), 35–50. https://doi.org/10.1007/s40725-018-0075-6

Quintas-Soriano, C., Buerkert, A., & Plieninger, T. (2022). Effects of land abandonment on nature contributions to people and good quality of life components in the Mediterranean region: A review. *Land Use Policy*, 116, 106053. https://doi.org/10.1016/j.landusepol.2022.106053

Ramsfield, T. D., Bentz, B. J., Faccoli, M., Jactel, H., & Brockerhoff, E. G. (2016). Forest health in a changing world: Effects of globalization and climate change on forest insect and pathogen impacts. *Forestry*, 89(3), 245–252. https://doi.org/10.1093/forestry/cpw018

Raven, P. H. (1988). *Our diminishing tropical forests.* In E. O. Wilson, F. M. Peter, National Academy of Sciences (U.S.), & Smithsonian Institution (Eds.), Biodiversity. National Academy Press.

Raymond Hunt, E., Daughtry, C. S. T., Eitel, J. U. H., & Long, D. S. (2011). Remote sensing leaf chlorophyll content using a visible band index. *Agronomy Journal*, 103(4), 1090–1099. https://doi.org/10.2134/agronj2010.0395

Reyer, C. P. O., Brouwers, N., Rammig, A., Brook, B. W., Epila, J., Grant, R. F., Holmgren, M., Langerwisch, F., Leuzinger, S., Lucht, W., Medlyn, B., Pfeifer, M., Steinkamp, J., Vanderwel, M. C., Verbeeck, H., & Villela, D. M. (2015). Forest resilience and tipping points at different spatio-temporal scales: Approaches and challenges. *Journal of Ecology*, 103(1), 5–15. https://doi.org/10.1111/1365-2745.12337

Rodríguez y Silva, F., & Molina-Martínez, J. (2012). Modelling Mediterranean forest fuels by integrating field data and mapping tools. *European Journal of Forest Research*, 131, 571-582. https://doi.org/10.1007/s10342-011-0532-2

Roshani; Sajjad, H.; Kumar, P.; Masroor, M.; Rahaman, M.H.; Rehman, S.; Ahmed, R.; Sahana, M. (2022) Forest Vulnerability to Climate Change: A Review for Future Research Framework. *Forests*, 13, 917. https://doi.org/10.3390/f13060917

Ruthrof, K. X., Fontaine, J. B., Matusick, G., Breshears, D. D., Law, D. J., Powell, S., & Hardy, G. (2016). How drought-induced forest die-off alters microclimate and increases fuel loadings and fire potentials. *International Journal of Wildland Fire*, 25(8), 819. https://doi.org/10.1071/WF15028

Saatchi, S., Longo, M., Xu, L., Yang, Y., Abe, H., André, M., Aukema, J. E., Carvalhais, N., Cadillo-Quiroz, H., Cerbu, G. A., Chernela, J. M., Covey, K., Sánchez-Clavijo, L. M., Cubillos, I. V., Davies, S. J., De Sy, V., De Vleeschouwer, F., Duque, A., Sybille Durieux, A. M., … Elmore, A. C. (2021). Detecting vulnerability of humid tropical forests to multiple stressors. *One Earth*, 4(7), 988–1003. https://doi.org/10.1016/j.oneear.2021.06.002

Saeed, A. S., Younes, A. B., Islam, S., Dias, J., Seneviratne, L., & Cai, G. (2015). A review on the platform design, dynamic modelling, and control of hybrid UAVs. 2015 *International Conference on Unmanned Aircraft Systems (ICUAS)*, 806–815. https://doi.org/10.1109/ICUAS.2015.7152365

Sánchez-Salguero, R., Camarero, J. J., Carrer, M., Gutiérrez, E., Alla, A. Q., Andreu-Hayles, L., Hevia, A., Koutavas, A., Martínez-Sancho, E., Nola, P., Papadopoulos, A., Pasho, E., Toromani, E., Carreira, J. A., & Linares, J. C. (2017). Climate extremes and predicted warming threaten Mediterranean Holocene firs forests refugia. *Proceedings of the National Academy of Science*s, 201708109. https://doi.org/10.1073/pnas.1708109114

Sanderson, J. E. (1974). The role of fire suppression in fire management. *Proceedings of the 14th Tall Timbers fire ecology conference*, Missoula, MT. Tall Timbers Research Station, Tallahassee, FL, 19-31.

Sannikov, S. N. (1994). Evolutionary pyroecology and pyrogeography of the natural regeneration of Scots Pine. *Forest Fire Research* (pp. 961-968).

Saunier, S., Northrop, A., Lavender, S., Galli, L., Ferrara, R., Mica, S., Biasutti, R., Goryl, P., Gascon, F., Meloni, M., Desclee, B., & Altena, B. (2017). *European Space agency (ESA) Landsat MSS/TM/ETM+/OLI archive: 42 years of our history*. 2017 9th International Workshop on the Analysis of Multitemporal Remote Sensing Images (MultiTemp), 1–9. https://doi.org/10.1109/Multi-Temp.2017.8035252

Sedykh, V.N. (1995). Using Aerial Photography and Satellite Imagery to Monitor Forest Cover in Western Siberia. In: Apps, M.J., Price, D.T., Wisniewski, J. (eds) *Boreal Forests and Global Change*. Springer, Dordrecht. https://doi.org/10.1007/978-94-017-0942-2_47

Schelhaas, M.-J., Nabuurs, G.-J., & Schuck, A. (2003). Natural disturbances in the European forests in the 19th and 20th centuries**.** *Global Change Biology*, 9(11), 1620–1633. https://doi.org/10.1046/j.1365-2486.2003.00684.x

Schlesinger, W. H., Dietze, M. C., Jackson, R. B., Phillips, R. P., Rhoades, C. C., Rustad, L. E., & Vose, J. M. (2016). Forest biogeochemistry in response to drought. Global Change Biology, 22(7), 2318–2328. https://doi.org/10.1111/gcb.13105

Schlesinger, W. H., & Jasechko, S. (2014). Transpiration in the global water cycle. *Agricultural and Forest Meteorology*, 189–190, 115–117. https://doi.org/10.1016/j.agrformet.2014.01.011

Schmidt, J. P., Dellinger, A. E., & Beegle, D. B. (2009). Nitrogen Recommendations for Corn: An On-The-Go Sensor Compared with Current Recommendation Methods. *Agronomy Journa*l, 101(4), 916–924. https://doi.org/10.2134/agronj2008.0231x

Schulte To Bühne, H., Pettorelli, N., & Hoffmann, M. (2022). The policy consequences of defining rewilding. *Ambio*, 51(1), 93–102. https://doi.org/10.1007/s13280-021-01560-8

Schultz, M., Clevers, J. G. P. W., Carter, S., Verbesselt, J., Avitabile, V., Quang, H. V., & Herold, M. (2016). Performance of vegetation indices from Landsat time series in deforestation monitoring. *International Journal of Applied Earth Observation and Geoinformation*, 52, 318–327. https://doi.org/10.1016/j.jag.2016.06.020

Scott, A. C. (2000). The Pre-Quaternary history of fire. In *Palaeogeography, Palaeoclimatology, Palaeoecology* (Vol. 164, pp. 281–329). www.elsevier.nl/locate/palaeo

Scott, A. C., Bowman, D. M. J. S., Bond, W. J., Pyne, S. J., & Alexander, M. E. (2014). *Fire on earth: An introduction*. John Wiley & Sons Ltd. Chichester.

Scott, J. H., & Burgan, R. E. (2005). *Standard Fire Behavior Fuel Models: A Comprehensive Set for Use with Rothermel's Surface Fire Spread Model*. United States Department of Agriculture, Forest Service. http://www.fs.fed.us/rm/publications

Seidl, R., & Turner, M. G. (2022). Post-disturbance reorganization of forest ecosystems in a changing world. *Proceedings of the National Academy of Sciences*, 119(28). https://doi.org/10.1073/pnas.2202190119

Shen, X., & Cao, L. (2017). Tree-species classification in subtropical forests using airborne hyperspectral and LiDAR data. *Remote Sensing*. https://doi.org/10.3390/rs9111180

Shi, Y., Skidmore, A. K., Wang, T., Holzwarth, S., Heiden, U., Pinnel, N., Zhu, X., & Heurich, M. (2018). Tree species classification using plant functional traits from LiDAR and

hyperspectral data. *International Journal of Applied Earth Observation and Geoinformation*, 73, 207–219. https://doi.org/10.1016/j.jag.2018.06.018

Singh, R., Gehlot, A., Vaseem Akram, S., Kumar Thakur, A., Buddhi, D., & Kumar Das, P. (2022). Forest 4.0: Digitalization of forest using the Internet of Things (IoT). *Journal of King Saud University - Computer and Information Sciences*, 34(8), 5587–5601. https://doi.org/10.1016/j.jksuci.2021.02.009

Smith, C., Baker, J. C. A., & Spracklen, D. V. (2023). Tropical deforestation causes large reductions in observed precipitation. *Nature*, 615(7951), 270–275. https://doi.org/10.1038/s41586-022-05690-1

Sohn, J. A., Saha, S., & Bauhus, J. (2016). Potential of forest thinning to mitigate drought stress: A meta-analysis. *Forest Ecology and Management*, 380, 261–273. https://doi.org/10.1016/j.foreco.2016.07.046

Staal, A., Fetzer, I., Wang-Erlandsson, L., Bosmans, J. H. C., Dekker, S. C., Van Nes, E. H., Rockström, J., & Tuinenburg, O. A. (2020). Hysteresis of tropical forests in the 21st century. *Nature Communications*, 11(1), 4978. https://doi.org/10.1038/s41467-020-18728-7

Steel, Z. L., Safford, H. D., & Viers, J. H. (2015). The fire frequency-severity relationship and the legacy of fire suppression in California forests. *Ecosphere*, 6(1), 1-23.

Stott, P. (1988). The forest as Phoenix: towards a biogeography of fire in mainland South-East Asia. *Geographical Journal*, 337-350.

Sturtevant, B. R., & Fortin, M.-J. (2021). Understanding and Modelling Forest Disturbance Interactions at the Landscape Level. *Frontiers in Ecology and Evolution*, 9, 653647. https://doi.org/10.3389/fevo.2021.653647

Su, Y., Guo, Q., Jin, S., Guan, H., Sun, X., Ma, Q., Hu, T., Wang, R., & Li, Y. (2021). The Development and Evaluation of a Backpack LiDAR System for Accurate and Efficient Forest Inventory. *IEEE Geoscience and Remote Sensing Letters*, 18(9), 1660–1664. https://doi.org/10.1109/LGRS.2020.3005166

Sun, W., & Liu, X. (2020). Review on carbon storage estimation of forest ecosystem and applications in China. *Forest Ecosystems*, 7(1), 4. https://doi.org/10.1186/s40663-019-0210-2

T R, J., Reddy, N. S., & Acharya, U. D. (2023). Modelling Daily Reference Evapotranspiration from Climate Variables: Assessment of Bagging and Boosting Regression Approaches.

Water *Resources Management*, 37(3), 1013–1032. https://doi.org/10.1007/s11269-022-03399-4

Tabari, H. (2020). Climate change impact on flood and extreme precipitation increases with water availability. *Scientific Reports*, 10(1), 13768. https://doi.org/10.1038/s41598-020-70816-2

Tansley, A. G. (1935). The Use and Abuse of Vegetational Concepts and Terms. *Ecology*, 16(3), 284–307. https://doi.org/10.2307/1930070

Timmermans, W. J., Kustas, W. P., & Andreu, A. (2015). Utility of an Automated Thermal-Based Approach for Monitoring Evapotranspiration. *Acta Geophysica*, 63(6), 1571–1608. https://doi.org/10.1515/acgeo-2015-0016

Miłosz Tkaczyk (2023). Worldwide review of bacterial diseases of oaks (*Quercus* sp.) and their potential threat to trees in Central Europe, *Forestry: An International Journal of Forest Research*, Volume 96, Issue 4, Pages 425–433, https://doi.org/10.1093/forestry/cpac048

Torresan, C., Berton, A., Carotenuto, F., Di Gennaro, S. F., Gioli, B., Matese, A., Miglietta, F., Vagnoli, C., Zaldei, A., & Wallace, L. (2017). Forestry applications of UAVs in Europe: A review. *International Journal of Remote Sensing*, 38(8–10), 2427–2447. https://doi.org/10.1080/01431161.2016.1252477

Trugman, A. T., Anderegg, L. D. L., Anderegg, W. R. L., Das, A. J., & Stephenson, N. L. (2021). Why is Tree Drought Mortality so Hard to Predict? *Trends in Ecology & Evolution*, 36(6), 520–532. https://doi.org/10.1016/j.tree.2021.02.001

Uchida, K., & Ushimaru, A. (2014). Biodiversity declines due to abandonment and intensification of agricultural lands: Patterns and mechanisms. *Ecological Monographs*, 84(4), 637–658. https://doi.org/10.1890/13-2170.1

Urrego, J. P. F., Huang, B., Næss, J. S., Hu, X., & Cherubini, F. (2021). Meta-analysis of leaf area index, canopy height and root depth of three bioenergy crops and their effects on land surface modelling. *Agricultural and Forest Meteorology*, 306, 108444. https://doi.org/10.1016/j.agrformet.2021.108444

Ursino, N., & Romano, N. (2014). Wild forest fire regime following land abandonment in the Mediterranean region. *Geophysical Research Letters*, 41(23), 8359–8368. https://doi.org/10.1002/2014GL061560

Ustaoglu, E., & Collier, M. J. (2018). Farmland abandonment in Europe: An overview of drivers, consequences, and assessment of the sustainability implications. *Environmental Reviews*, 26(4), 396–416. https://doi.org/10.1139/er-2018-0001

Vaglio Laurin, G., Pirotti, F., Callegari, M., Chen, Q., Cuozzo, G., Lingua, E., *et al.* (2016). 'Potential of ALOS2 and NDVI to estimate forest above-ground biomass, and comparison with lidar-derived estimates'. *Remote Sensing* 9 (1), 18. https://doi.org10.3390/rs9010018

Wable, P. S., Chowdary, V. M., Panda, S. N., Adamala, S., & C. S. Jha. (2021). Potential and net recharge assessment in paddy dominated Hirakud irrigation command of eastern India using water balance and geospatial approaches. *Environment, Development and Sustainability*, 23(7), 10869–10891. https://doi.org/10.1007/s10668-020-01092-3

Waite, C. E., van der Heijden, G. M. F., Field, R., & Boyd, D. S. (2019). A view from above: Unmanned aerial vehicles (UAVs) provide a new tool for assessing liana infestation in tropical forest canopies. *Journal of Applied Ecology*, May 2018. https://doi.org/10.1111/1365-2664.13318

Walvoord M. A., Kurylyk B. L. (2016) Hydrologic Impacts of Thawing Permafrost—A Review. *Vadose Zone Journal*; 15 (6). https://doi.org/10.2136/vzj2016.01.0010

Walder, D., Krebs, P., Bugmann, H., Manetti, M. C., Pollastrini, M., Anzillotti, S., & Conedera, M. (2021). Silver fir (*Abies alba* Mill.) is able to thrive and prosper under meso-Mediterranean conditions. *Forest Ecology and Management*, 498. https://doi.org/10.1016/j.foreco.2021.119537

Waring, R. H., & Running, S. W. (1978). Sapwood water storage: Its contribution to transpiration and effect upon water conductance through the stems of old-growth Douglas-fir. *Plant, Cell and Environment*, 1(2), 131–140. https://doi.org/10.1111/j.1365-3040.1978.tb00754.x

Waring, R. H., Whitehead, D., & Jarvis, P. G. (1979). The contribution of stored water to transpiration in Scots pine. *Plant, Cell and Environment*, 2(4), 309–317. https://doi.org/10.1111/j.1365-3040.1979.tb00085.x

Weissteiner, C. J., Boschetti, M., Böttcher, K., Carrara, P., Bordogna, G., & Brivio, P. A. (2011). Spatial explicit assessment of rural land abandonment in the Mediterranean area. *Global and Planetary Change*, 79(1–2), 20–36. https://doi.org/10.1016/j.gloplacha.2011.07.009

Westoby, M. J., Brasington, J., Glasser, N. F., Hambrey, M. J., & Reynolds, J. M. (2012). 'Structure-from-Motion' photogrammetry: A low-cost, effective tool for geoscience applications. *Geomorphology*, 179, 300–314. https://doi.org/10.1016/j.geomorph.2012.08.021

Whittaker, R. H. (1953). A Consideration of Climax Theory: The Climax as a Population and Pattern. *Ecological Monographs*, 23(1), 41–78. https://doi.org/10.2307/1943519

Woodward, F. I. (1987). *Climate and plant distribution*. Cambridge University Press.

Wu, Z., Dijkstra, P., Koch, G. W., Peñuelas, J., & Hungate, B. A. (2011). Responses of terrestrial ecosystems to temperature and precipitation change: A meta-analysis of experimental manipulation. *Global Change Biology*, 17(2), 927–942. https://doi.org/10.1111/j.1365-2486.2010.02302.x

Wulder, M. A., Bater, C. W., Coops, N. C., Hilker, T., & White, J. C. (2008). The role of LiDAR in sustainable forest management. *The Forestry Chronicle*, 84(6). https://doi.org/10.5558/tfc84807-6

Wulder, M. A., & Franklin, S. E. (Eds.). (2003). *Remote Sensing of Forest Environments*. Springer US. https://doi.org/10.1007/978-1-4615-0306-4

Rodríguez y Silva, F. R. (1996). *Protección y defensa de los pinsapares ante los incendios forestales. Jornadas técnicas internacionales sobre recuperación de pinsapares*. Jornadas Técnicas Internacionales Sobre Recuperación de Pinsapares, 95, 0–9.

Yang, Y., Shang, S., & Jiang, L. (2012). Remote sensing temporal and spatial patterns of evapotranspiration and the responses to water management in a large irrigation district of North China. *Agricultural and Forest Meteorology*, 164, 112–122. https://doi.org/10.1016/j.agrformet.2012.05.011

Yebra, M., Quan, X., Riaño, D., Rozas Larraondo, P., van Dijk, A. I. J. M., & Cary, G. J. (2018). A fuel moisture content and flammability monitoring methodology for continental Australia based on optical remote sensing. *Remote Sensing of Environment*, 212, 260–272. https://doi.org/10.1016/j.rse.2018.04.053

Yu, E., Cui, N., Quan, Y., Wang, C., Jia, T., Wu, D., & Wu, G. (2020). Ecological protection for natural protected areas based on landsenses ecology: A case study of Dalinor National Nature Reserve. *International Journal of Sustainable Development & World Ecology*, 27(8), 709–717. https://doi.org/10.1080/13504509.2020.1727585

Zhou, T., Koomen, E., & Ke, X. (2020). Determinants of Farmland Abandonment on the Urban–Rural Fringe. *Environmental Management*, 65(3), 369–384. https://doi.org/10.1007/s00267-020-01258-9

Supplementary Materials

Chapter 2

Table S2.1 UAV flight characteristics across the four study plots. Time and date of flight, mean air temperature (T^a) and short-wave (SW) radiation during the flight and number of images per sensor (thermal infrared, TIR, and red-green-blue, RGB).

Time	Date	Plot ID	T^a(ºC)	SW radiation ($W \cdot m^{-2}$)	Images TIR	Images RGB
12:00:00	09/08/17	HF1	31.54	703.46	366	295
13:00:00	13/09/17	HF2	36.54	935.96	371	290
13:00:00	12/09/17	HF3	32.15	857.61	329	222
12:00:00	11/09/17	HF4	38.45	893.09	336	298

Table S2.2. Regression model output. The relationship between the target variable small-scale evapotranspiration (ET) and the 16 available single predictor variables were examined with simple linear regression models, separately for each of the four study sites.

Variable category	Variable	HF1		HF2		HF3		HF4	
		R^2	*p*	R^2	*p*	R^2	*p*	R^2	*p*
RGB related	GLI	0.002	< 0.01	0.0010	< 0.01	0	0.013	0	< 0.01
	VARI	0.0038	< 0.01	0	< 0.01	0	< 0.01	0	0.619
Vegetation height	Height_abs_max	0	< 0.01	0.0422	< 0.01	0.0232	< 0.01	0.0438	< 0.01
	Height_abs_min	0.0011	< 0.01	0.0057	< 0.01	0.0023	< 0.01	0.0029	< 0.01
	Height_abs_sm	0.002	< 0.01	0.040	< 0.01	0.0221	< 0.01	0.0430	< 0.01
	Height_rel	0.002	< 0.01	0.0405	< 0.01	0.0221	< 0.01	0.0430	< 0.01
	P25	0.002	< 0.01	0.0197	< 0.01	0.0062	< 0.01	0.008	< 0.01
	P50	0.0003	< 0.01	0.029	< 0.01	0.0207	< 0.01	0.005	< 0.01
	P75	0.001	< 0.01	0.0320	< 0.01	0.0184	< 0.01	0.0056	< 0.01
	P90	0.0011	< 0.01	0.0437	< 0.01	0.0219	< 0.01	0.0421	< 0.01
Vegetation height variability	CRR	0	< 0.01	0.0008	< 0.01	0	< 0.01	0.0017	< 0.01
	CV_height	0.0011	< 0.01	0.0024	< 0.01	0.0009	< 0.01	0.0011	< 0.01
Vegetation density	Cover10	0.0025	< 0.01	0.0008	< 0.01	0.0081	< 0.01	0.0014	< 0.01
	LAD	0.0034	< 0.01	0	0.693	0.0010	< 0.01	0.0028	< 0.01
	PCD	0.0032	< 0.01	0.0021	< 0.01	0	< 0.01	0.0066	< 0.01
	PM	0	< 0.01	0	< 0.01	0	< 0.01	0.0018	< 0.01

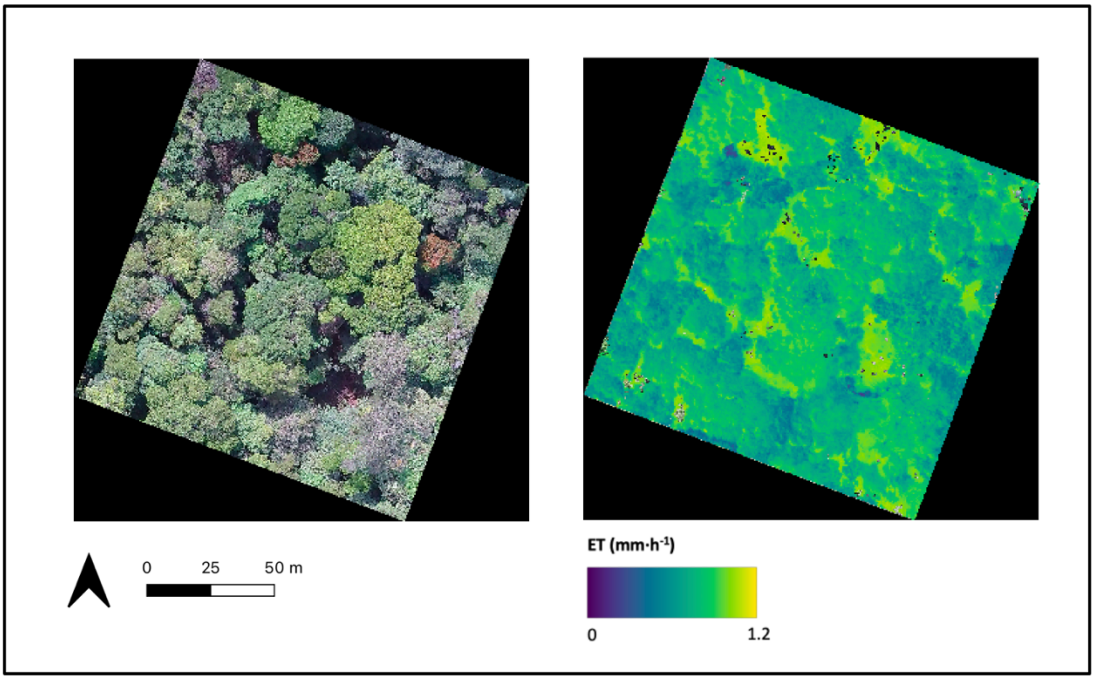

Figure S2.1 Large-sized RGB (left) and evapotranspiration (ET) orthomosaic (right) for the study plot HF2. Hourly ET ($mm \cdot h^{-1}$) as indicated in the legend was derived from UAV-based thermal images with the plugin QWaterModel (Ellsäßer, *et al*., 2020b). Air temperature at the time of flight was 36.5°C, short-wave radiation was at 936 $W\ m^{-2}$

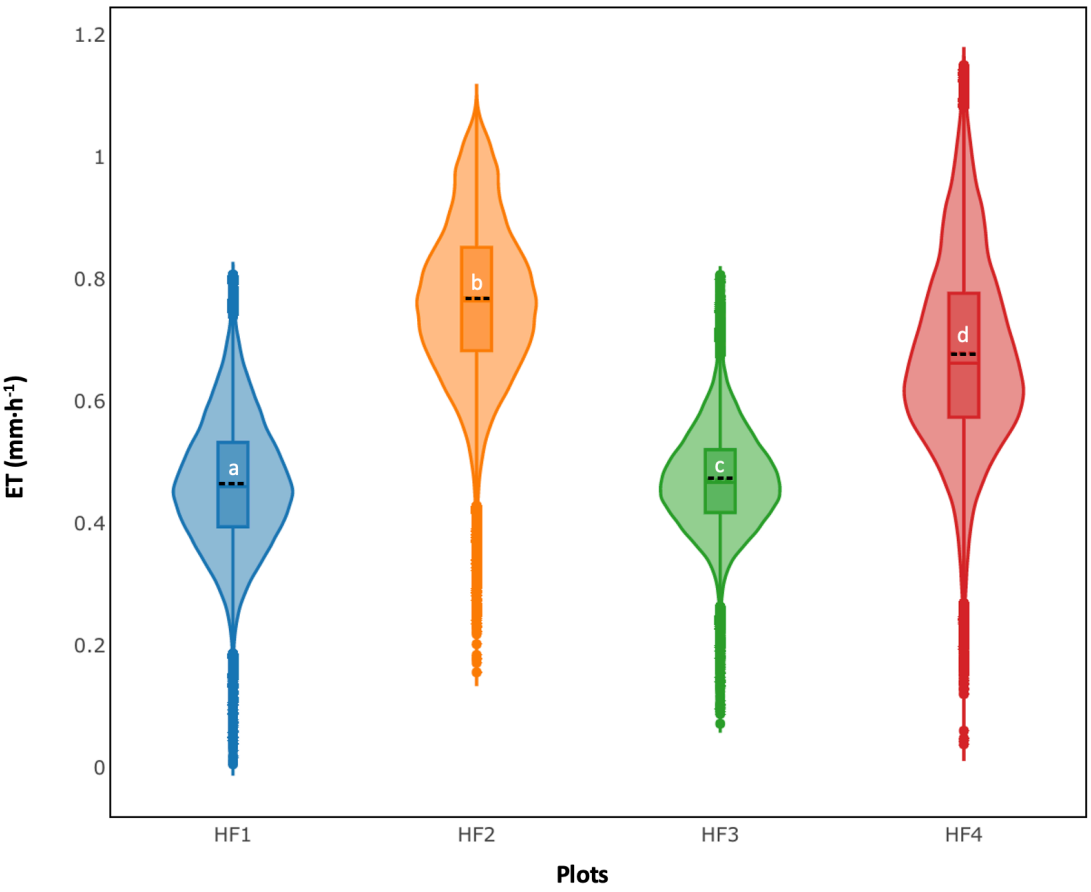

Figure S2.2 Pixel-level evapotranspiration (ET, mm·h^{-1}) distribution across the four study plots. Sample sizes (i.e., the number of pixels per plot) ranged from 218,000- 226,000 pixels. Significant differences ($p <$ 0.05) among plot means as based on ANOVA with a Scheffe post-hoc test is indicated by different letters. The flights were carried out close to noon on successive days in August 2017. Air temperatures at the respective times of flight were 31.5°C (HF1), 36.5°C (HF2), 32.2°C (HF3) and 38.4°C (HF4), short-wave radiation was at 704 W m^{-2} (HF1), 936 W m^{-2} (HF2), 858 W m^{-2} (HF3) and 893 W m^{-2} (HF4).

Chapter 3

Table S3.1. Results from the ANOVA of tree classes. *p*-values for Year in all classes were $p > 0.05$. (see Fig. 2).

Class 1_2					
Factor	**DF**	**Sum Sq**	**Mean Sq**	**Fvalue**	***p*-values**
Intercept	1	39234.96	9234.96	166.26	$< 1 \cdot 10^{-15}$
Year	1	216.61	216.61	0.92	0.342
Error	53	12742.81	235.98		
Class 3					
Factor	**DF**	**Sum Sq.**	**Mean Sq.**	**Fvalue**	***p*-values**
Intercept	1	113.77	113.77	7.12	0.010
Year	1	19.54	19.54	1.22	0.273
Error	54	862.18	15.96		
Class 4					
Factor	**DF**	**Sum Sq.**	**Mean Sq.**	**Fvalue**	***p*-values**
Intercept	1	37.94	37.94	37.94	$9.36 \cdot 10^{-4}$
Year	1	1.22	1.22	0.39	0.532
Error	54	167.11	3.09		
Class 5					
Factor	**DF**	**Sum Sq.**	**Mean Sq.**	**Fvalue**	***p*-values**
Intercept	1	262.17	262.17	17.45	$1.08 \cdot 10^{-4}$
Year	1	0.50	0.50	0.03	0.854

Error	54	810.96	15.01		
			Class 6		
Factor	**DF**	**Sum Sq.**	**Mean Sq.**	**Fvalue**	***p*-values**
Intercept	1	334.23	334.23	6.06	$1.08 \cdot 10^{-4}$
Year	1	79.18	79.18	1.43	0.234
Error	54	2976.23	55.11		

Table S3.2. Results from the ANOVAs performed on BAI per altitudinal bands, obtained from the two surveys -2003 and 2020- (see Fig. 3.3). Tukey post-hoc test only showed significant higher mortality in 2020 mid elevation band comparing to 2003 high elevation band (*p*-value = 0.042).

Alive trees					
Factor	**DF**	**Sum Sq**	**Mean Sq**	**Fvalue**	***p*-values**
Intercept	1	39128.72	39128.72	176.85	-
Year	5	1896.94	379.39	1.71	0.148
Error	50	11062.49	221.25	-	-
Dead trees					
Intercept	1	1126.86	1126.86	39.22	-
Year	5	349.93	69.78	2.49	0.047
Error	50	1436.53	28.73	-	-
Stumps					
Intercept	1	328.79	328.79	5.91	0.018
Year	5	274.97	54.99	0.98	0.433

Error	50	2780.45	55.60	-
Residuals	603400	1305.6	0.00	

Table S3.3. Results from the repeated measures ANOVA performed on NDVI time series and Bonferroni pairwise comparison. *p*-values in all factors were $< 1 \cdot 10^{-15}$, except for the Time*Elevation ($2.35 \cdot 10^{-4}$) and Time*SI ($2.29 \cdot 10^{-7}$).

Factor	**DF**	**Sum Sq**	**Mean Sq**	**Fvalue**
Time	35	243.2	6.95	3211.10
Elevation	2	86.7	43.37	20044.77
SI	2	33.9	16.96	7839.37
Elevation*SI	4	14.4	3.59	1659.78
Time*Elevation	70	9.5	0.14	62.96
Time*SI	70	7.6	0.11	49.97
Time*SI*Elevation	140	3.0	0.02	9.91
Residuals	603400	1305.6	0.00	

Pairwise comparison using Bonferroni test		
NDVI and Elevation *p*-values		
Levels	1150	1350
1350	$< 1 \cdot 10^{-15}$	$< 1 \cdot 10^{-15}$
1550	$< 1 \cdot 10^{-15}$	
NDVI and SI *p*-values		

Levels	46	130
46	$< 1 \cdot 10^{-15}$	$< 1 \cdot 10^{-15}$
175	$< 1 \cdot 10^{-15}$	

Table S3.4. Factor loadings of the nine "altitude by solar incidence" NDVI time series on the common trends detected by Dynamic Factor Analysis (DFA). The low, mid, and high altitudinal bands are denoted by their upper limits ("1150", "1350" and "1550", respectively); the same apply for the solar incidence value ranges ("46", "130" and "175", respectively).

Time series	**DFA 1 (absolute NDVI data)**	**DFA 2 (normalized NDVI data)**	
	Trend 1	**Trend 1**	**Trend 2**
NDVI_1150_46	0.010	-0.234	-0.225
NDVI_1150_130	0.010	-0.112	-0.185
NDVI_1150_175	0.011	0.161	-0.534
NDVI_1350_46	0.008	-0.275	0.309
NDVI_1350_130	0.007	0.014	0.478
NDVI_1350_175	0.008	-0.116	-0.101
NDVI_1550_46	0.007	-0.058	0.440
NDVI_1550_130	0.006	0.138	-0.007
NDVI_1550_175	0.006	0.482	-0.173

Table S3.5. Confusion matrixes from the orthoimages classification. Class 1: Shrubs / Class 2: Pinsapo Canopy / Class 3: Bare ground – grassland

1977			
Predicted	Observed		
	1	2	3
1	409	108	22
2	161	651	1
3	18	1	167
Kappa	PSS	GSS	Accuracy
0.6739486	0.6739486	0.7381568	0.8088582
1998			
Predicted	Observed		
	1	2	3
1	457	167	16
2	163	646	0
3	13	0	25
Kappa	PSS	GSS	Accuracy
0.5989007	0.5993758	0.7033439	0.7712775
2002			
Predicted	Observed		
	1	2	3
1	177	98	20
2	166	952	4
3	20	1	122
Kappa	PSS	GSS	Accuracy
0.5893727	0.5631768	0.6138216	0.8102564
2004			
Predicted	Observed		
	1	2	3
1	143	19	17
2	51	1453	7
3	18	5	106
Kappa	PSS	GSS	Accuracy
0.7758212	0.7360288	0.6968384	0.9312914
2007			
Predicted	Observed		
	1	2	3
1	153	17	6
2	27	1398	1
3	8	3	105
Kappa	PSS	GSS	Accuracy
0.8651735	0.8582546	0.8462251	0.9598329

2010			
Predicted	Observed		
	1	2	3
1	118	41	6
2	102	1304	6
3	1	4	125
Kappa	PSS	GSS	Accuracy
0.6894445	0.6423380	0.6877799	0.8980638
2013			
Predicted	Observed		
	1	2	3
1	179	24	8
2	59	1543	1
3	4	0	146
Kappa	PSS	GSS	Accuracy
0.8544705	0.8254044	0.8342646	0.9516280
2016			
Predicted	Observed		
	1	2	3
1	623	130	43
2	161	2355	8
3	18	9	722
Kappa	PSS	GSS	Accuracy
0.8147459	0.8084766	0.7954032	0.8976528
2019			
Predicted	Observed		
	1	2	3
1	239	48	18
2	95	1405	2
3	6	0	165
Kappa	PSS	GSS	Accuracy
0.7909352	0.7582873	0.7733844	0.9155747

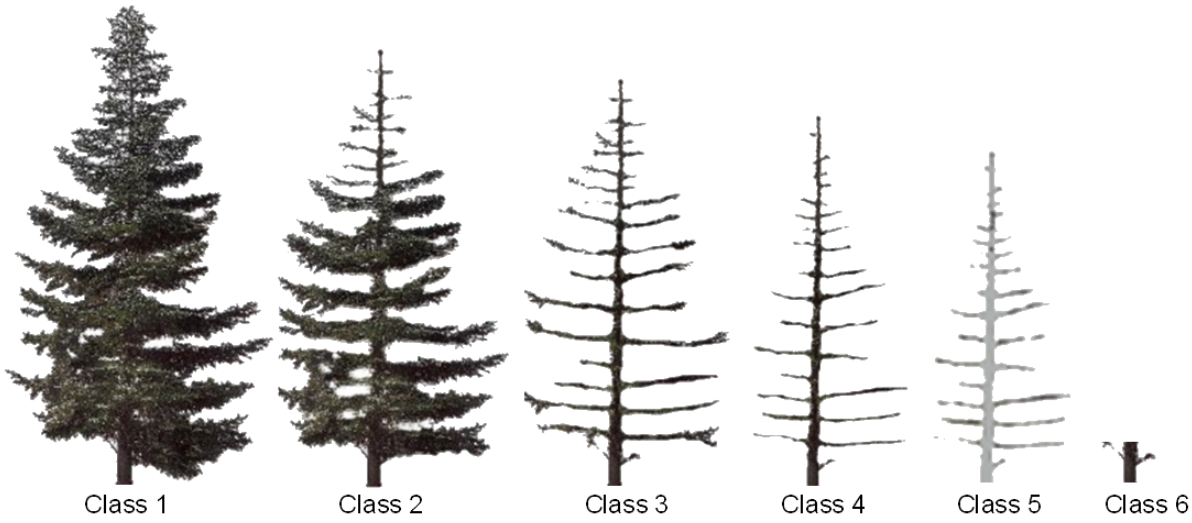

Figure S3.1. Dieback classes defined according to defoliation and wood decay states. Class 1 was assigned to healthy trees showing more than 2/3 of the crown green and retaining a significant number of needles cohorts (>5 years old needles; needle longevity reaches up to 10-15 years in *A. pinsapo*). Class 2 corresponds to declining trees showing dieback and severe defoliation in at least 1/3 of the crown; defoliation is very severe in the older needles cohorts (more than five years old needles are almost absent). Class 3 contained trees that died recently (i.e., in the current or the prior year); they are characterized by severe defoliation and brown needles. Class 4 was assigned to trees that died likely 3 - 10 years ago; they are characterized by a total loss of needles and thin branches, while bark is still present in medium and coarse branches and the stem. Class 5 corresponds to trees dead likely more than 10 years ago; they are characterized by a total loss of medium branches and bark is almost absent. Class 6 was assigned to stumps, where species identification was based on bark and wood morphology when possible.

a)

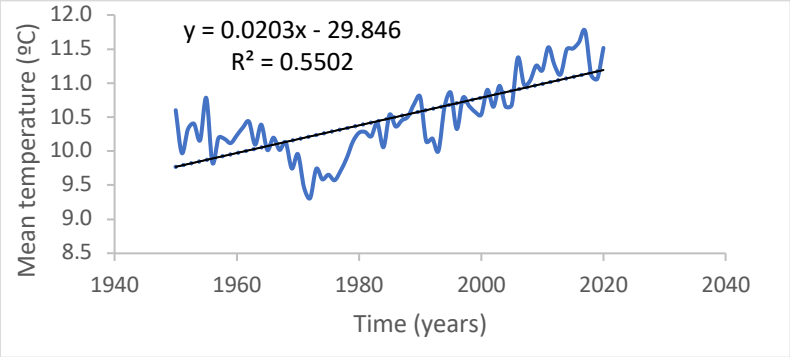

b)

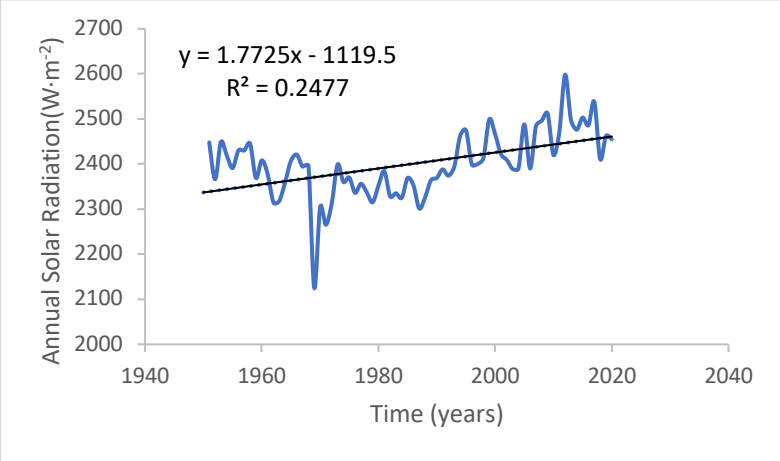

c)

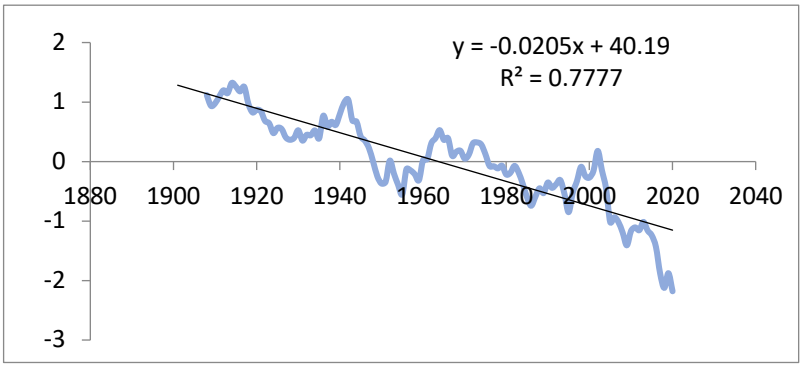

Figure S3.2. Climatic trends in the study area showing an increase in solar radiation (a) and, specially, in annual mean temperature (b). The SPEI drought index (c) shows an increasing trend to drier years, with a special dry period in the late years (2018-2020).

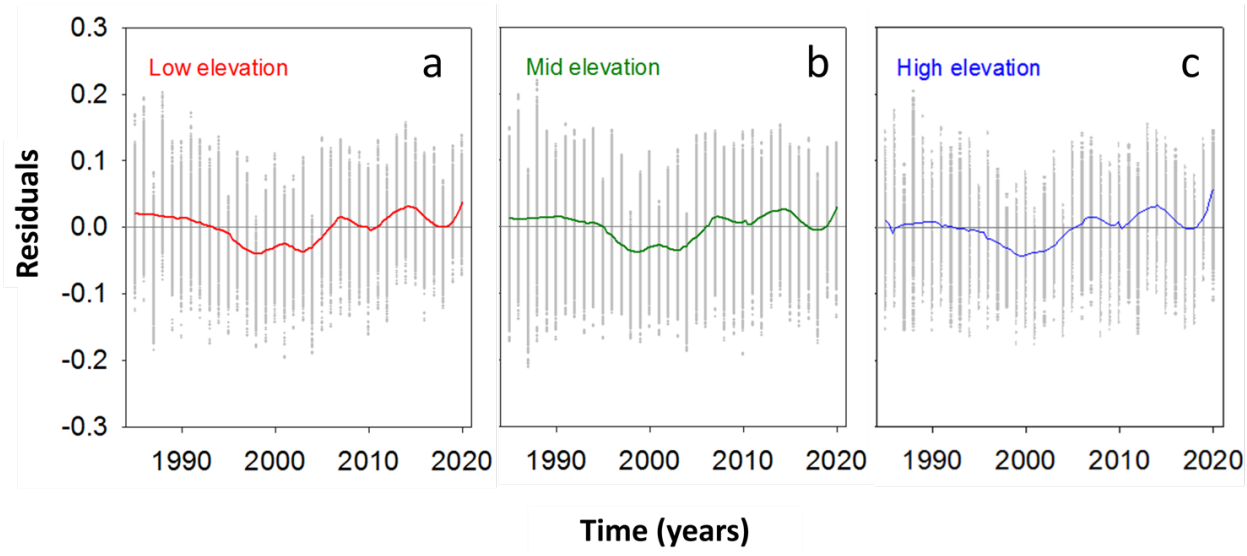

Figure S3.3. Temporal pattern of residuals obtained for 1985-2020 NDVI values al low elevation (a), mid elevation (b) and high elevation (c) of *Abies pinsapo*-dominated forests. Temporal trends were modeled by the Loess smoothing method using a polynomial weight function of degree 3.

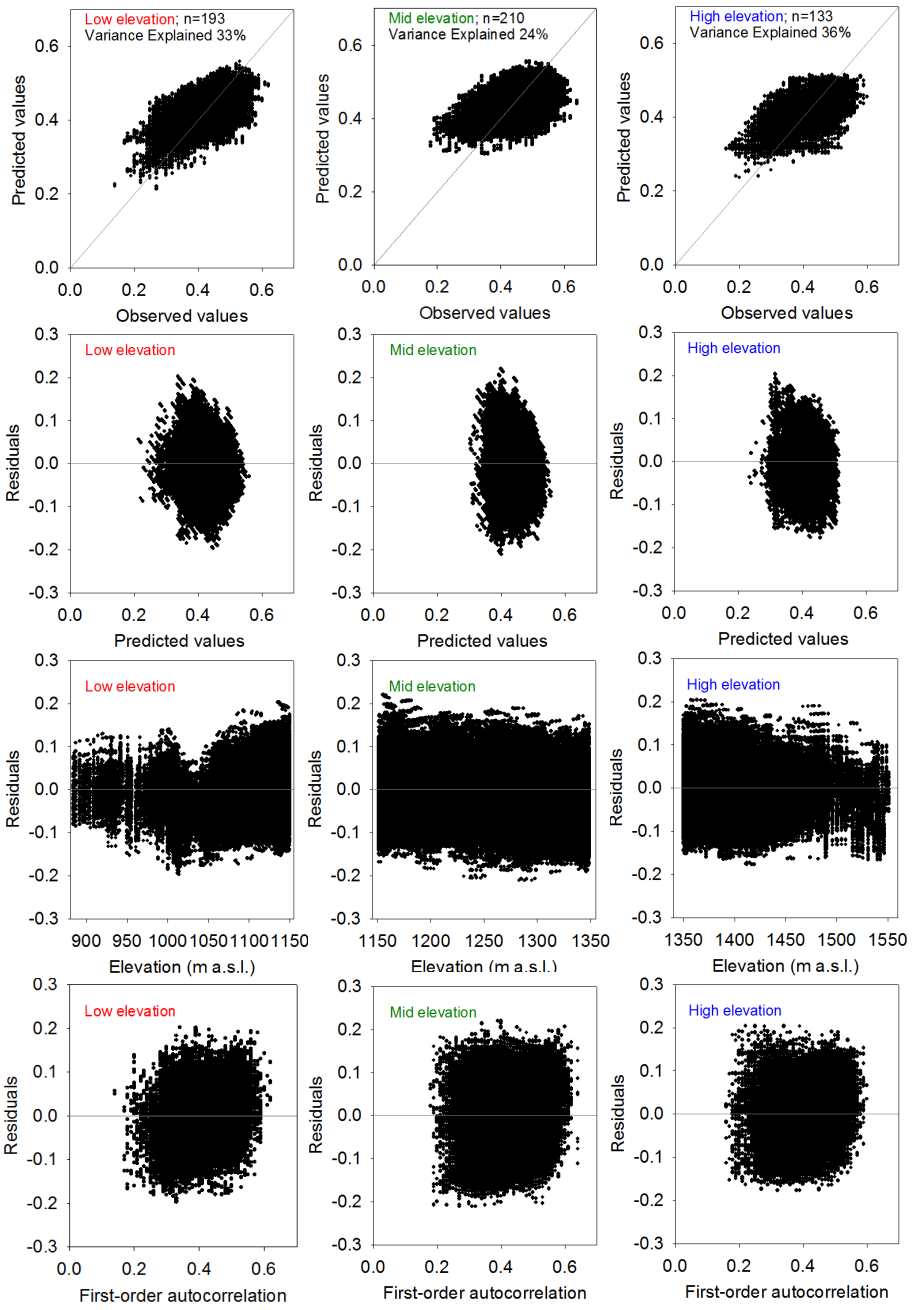

Figure S3.4. Model fitting and residuals pattern obtained for 1985-2020 NDVI values al low elevation (left column), mid elevation (central column), and high elevation (right column) of *Abies pinsapo*-dominated forests.

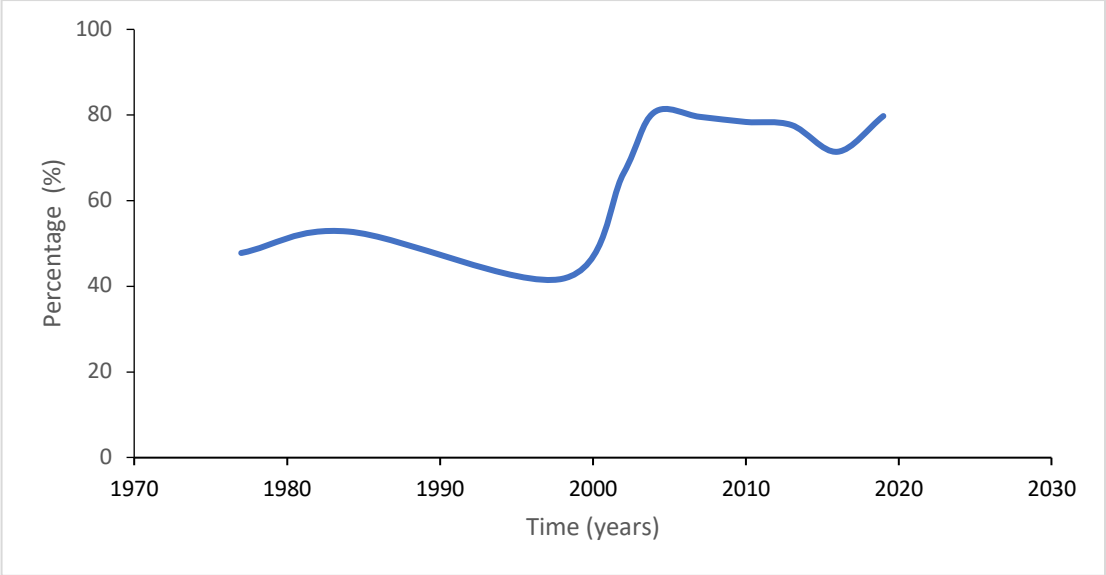

Figure S3.5. Temporal change in the percentage of pixels classified as canopy. The proportion of canopy pixels dropped between 1984 and 1998, (extreme drought in 1994-95). Then, it increased between 1998 and 2004. Since 2004 the amount of canopy pixels has remained stable, with a small drop between 2013 and 2016 (2012 drought).

Figure S3.6. 2007 orthoimage. Widely spread mortality from the severe 2005 drought can be observed across the whole 2007 orthoimage. Dark pixels are dead trees in the opening gaps process.

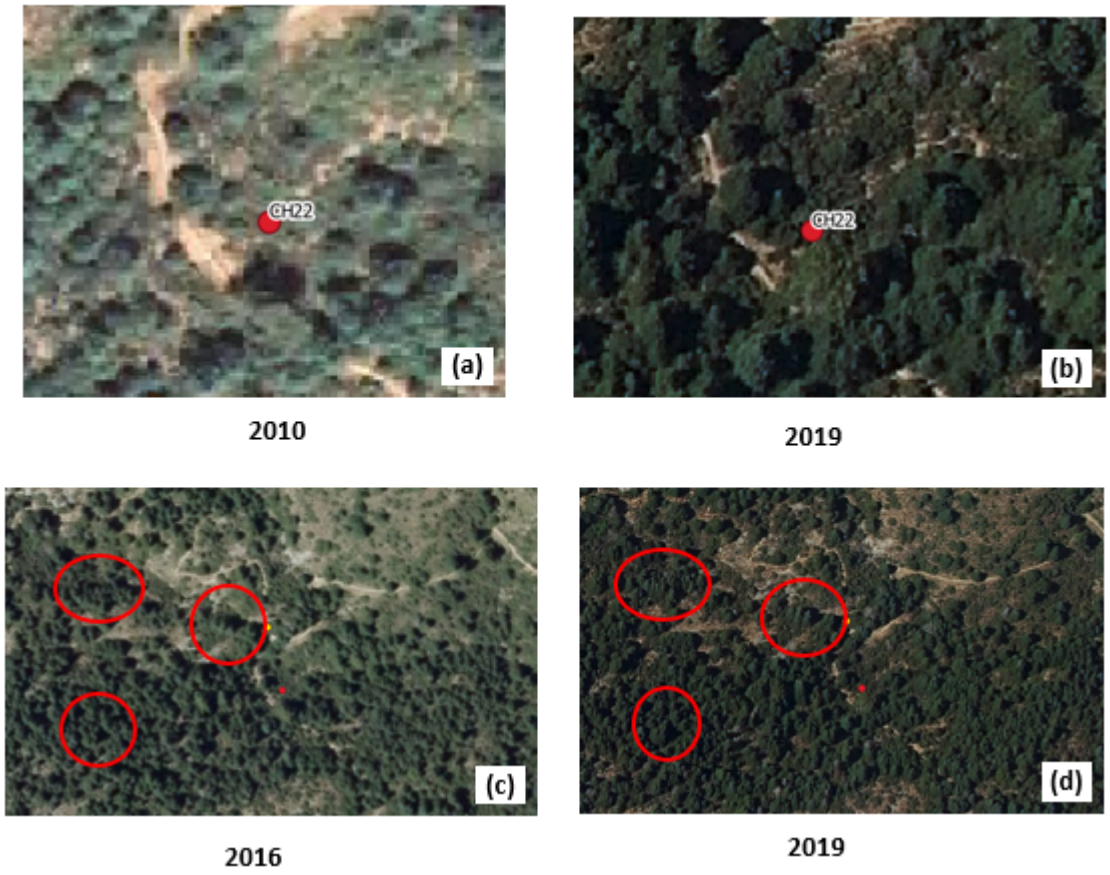

Figure S3.7. Two examples of pinsapo tree growth visual evidence. In (a) and (b) nine years of difference meant bigger crowns and more shrubs in 2019 than in 2010. Meanwhile, in only three years (2016-2019) the rapid crown development between (c) and (d) is evident. All paired images have same scale and, in the pair, (c) and (d) is noticeable this crown development since both orthoimages the same light angle.

Agradecimientos

Los comienzos de esta tesis doctoral fueron difíciles y tortuosos, como imagino que el de muchos doctorandos españoles a la hora de hacerse un hueco en el mundo académico. Es por ello por lo que este apartado cobra especial relevancia, puesto que somos el resultado de la influencia y del conjunto de personas que nos rodea. Hacer buena ciencia empieza por asumir que se avanza y se progresa a hombros de gigantes, a partir del trabajo de otros y del trabajo desinteresado de la comunidad científica, en la que se generan redes de apoyo mutuo.

En primer lugar, agradecer eternamente a Enrique Salvo Tierra por la apuesta que hizo por mí, desde antes del comienzo de la tesis, ya con el trabajo fin de máster del Máster de Análisis y Gestión Ambiental, en 2016. Aún recuerdo cuando rechacé todas las propuestas sobre la mesa y me diste un ultimátum para poder elegir tema antes de cuarenta y ocho horas. Yo quería hacer un trabajo fin de máster relacionado con la temática forestal, puesto que andaba con deseos de llevar el bagaje y el trasfondo del ambientólogo al mundo de la gestión forestal y había recibido formación complementaria por parte de grandes ingenieros forestales como Pedro Tíscar y Miguel Ángel Ruiz, del Centro de Capacitación Forestal Vadillo-Castril. Fue entonces, cuando me colé en una clase del máster que ni siquiera me había matriculado por ser optativa y entró Ismael Fernández Luque en escena, presentándonos las potencialidades de la tecnología LIDAR a multitud de aplicaciones, entre ellas la gestión forestal. Fue terminar esa clase que me acerqué a Ismael para que me dirigiera el trabajo fin de máster junto con Enrique, aprovechando los datos LIDAR que había a disposición pública de toda España y que nadie había trabajado previamente con esta tecnología en pinsapar. Al poco, una reunión entre los tres definió los objetivos iniciales del trabajo. Terminado el máster empecé con la tesis doctoral, a ella se incorporó como tutor Antonio Flores Moya, que fue crucial en el planteamiento de los diseños experimentales que se hicieron posteriormente. Por tanto, en primer lugar, me gustaría agradecer a Enrique por su apuesta por mí y la gran labor que ha hecho aportando facilidades y recursos para poder progresar en la tesis, a Ismael por abrirme todo un campo de conocimiento y a Antonio por enseñarme las verdaderas implicaciones de lo que supone pensar y analizar de forma científica. De las primeras cosas que hice al empezar la tesis fue llevar el trabajo fin de máster al XVII Congreso de la Asociación Española de Teledetección en Murcia, ya en 2017. Hubo dos cosas que me llevé de esta experiencia. La primera, el conocer a Isabel Aulló Maestro, también doctoranda, que

presentó el ForeStereo, el dispositivo de medición forestal que sería clave para el primer trabajo de la tesis. Gracias a ella y a Fernando Montes por facilitar la posterior cesión del dispositivo de forma atenta y desinteresada para realizar el trabajo de campo en el pinsapar de Yunquera. La segunda experiencia que me llevé fue al alojarme con mi primo Antonio Molino (Totó) y Nati, con sus hijas Elena e Irene. Fue una gran oportunidad para reconectar y pasar tiempo juntos, disfrutando de buenos momentos de tertulia, paseos y cerveza murciana.

Posteriormente se incorporó a los trabajos Jose A. Carreira de la Universidad de Jaén, que vio de interés el ForeStereo y ayudó de forma bastante desinteresada en la ejecución de los trabajos de campo y la posterior redacción del manuscrito. A raíz de esto seguimos trabajando juntos y era de recibo que participase como director de tesis, coincidiendo con que Ismael estaba en un periodo más volcado en la cooperativa que fundó, 3DGeospace. Agradecer eternamente a Pepe por hacerme partícipe de sus proyectos, canalizar mi motivación y empujar en la dirección adecuada. Y con Pepe a todo el equipo que hay con él, que tanto han aportado a esta tesis y los buenos momentos de trabajo de campo que hemos pasado: Juan Carlos Linares de la UPO y del resto de compañeros de la UJA: Víctor Lechuga, Benjamín Viñegla, Jaime Lechuga, Sergio Esparcia, Juan, Antonio Román y demás personas con las que he coincidido ya sea durante mi estancia en la UJA o en muestreos realizados.

También a Jose Luis López Quintanilla, Juanjo Jiménez y Rafael Haro, responsables tanto de la gestión del pinsapo como del Parque Nacional de Sierra de las Nieves. Gracias por facilitar los estudios dentro del parque y mostrar un interés activo en los resultados derivados.

Thanks to Dirk Hölscher for accepting the internship in Göttingen, he gave me the chance to meet a great city and a great team with Alex Röll, Medha Bulusu, Alejandra Valdés, Florian… I strongly appreciate the time spent in Göttingen, the project derived from the internship, and the time you worked on this (Chapter 2).

Thanks to Alistair Jump and Lahcen Taiqui for the time they employed to carefully review this doctoral thesis. Their detailed suggestions greatly improved the quality of the final manuscript.

Also, thanks to Andy Marshall for accept an initial internship in Sunshine Coast (Australia) and to Emma, Catherine Waite, and Liz Sousa for providing support during my attempt to go. A shame that pandemic happened, cancelling this internship. Hopefully, we could meet during my post PhD experience.

Agradecer por supuesto a todos mis compañeros de departamento, no todo el mundo tiene la suerte de que los compañeros de trabajo además sean amigos, buenos amigos. Agradecer

a: Jose García del Herbario, Federico, María Altamirano, Andrés, María del Mar, Marta, Mayca, Mamen, Antonio Picornell, Kike, Andros, Jesús, Marianela, Jaime, Rocío, Ángel, Isidro, Raquel, Noelia, Elena, Pedro Guerrero, Miguel Ángel Quesada, José Ángel, Rafael Sesmero, Alberto Jiménez… Me da miedo seguir mencionando nombres porque por mucho que me esfuerce en recordar es probable que me deje alguno en el tintero. A todos vosotros os tengo que agradecer vuestro tiempo, vuestro ánimo y que es un gran lujo teneros como compañeros y como amigos. Las horas de comer en la Venta del Túnel alegran el día a cualquiera que haya tenido un mal día y decida pasarse a la biblioteca para comer. Mención especial también a mi antiguo profesor de Derecho Ambiental, Juan Manuel Ayllón Díaz-González, siendo uno de mis grandes referentes docentes. He aprendido mucho de vuestra sabiduría, mi experiencia de teneros de compañeros me ha hecho crecer mucho profesionalmente y me he sentido muy lleno todo este tiempo. Ojalá poder mantener este espíritu tan sano de honestidad, cooperación y entusiasmo que hemos logrado construir en el departamento, que nada nos frene. Incluyo también en este párrafo a Antonio Martín, Juan Antonio Casanova, Juan Antonio Báez, Susana Ávila y a Luis Alberto Díaz y Juan (arbolista), compañeros de trabajo que hemos establecido una gran conexión durante los proyectos que hemos trabajado juntos en el sector de la empresa.

A toda mi familia, en especial a mis padres Josefina Molino y José Antonio Cortés, por ofrecer todo el apoyo moral que requiere una persona ante retos como una tesis doctoral, ayudar en los comienzos y por garantizar los medios materiales en los peores momentos de este viaje. La precariedad es frecuente, indignante y dolorosa en España, no todo el mundo hubiera podido continuar una tesis doctoral sin un apoyo como el de mis padres. También dedicar este párrafo al resto de mi familia: mis hermanos JB y Ana, toda mi familia de Granada, de Murcia… Gracias por vuestra comprensión y apoyo en los momentos que hemos podido estar juntos, sólo espero poder pasar más tiempo con vosotros después de este periodo.

A todos mis amigos, imposible no agradecerles que hayan estado ahí todo este tiempo. No mencionaré nombres, pero ellos saben quiénes son perfectamente: hemos pasado grandes momentos con juegos de mesa, rol, senderismo y aventuras en el campo, en la Sauceda, en las jornadas Tierra de Nadie, de casa rural, viendo las estrellas fugaces, en conciertos y festivales, en la piscina, manteniendo grandes conversaciones sobre política, historia y ciencia, o simplemente tomando algo en una tetería, en una cervecería o incluso mandarnos memes a cuál más

absurdamente *accurate,* retroalimentándonos en ocurrencias estúpidas. Además de estar presentes siempre para los momentos más duros. Estoy bastante orgulloso de mis amistades, me hacéis sentirme lleno y pleno, espero poder compartir nuevas experiencias con vosotros a partir de ahora.

A los miembros de la comunidad de Voluntarios de la Sierra de las Nieves, por esos domingos de trabajo físico y buen humor que tan bien sientan para desconectar y los vínculos tan sanos que forjamos mientras quitamos protectores o desbrozamos a golpe de azada.

También es de recibo agradecer a las comunidades online tuiteras y mastodonteras de las que he formo parte, he aprendido muchísimo con el intercambio de conocimiento y pensamiento crítico, alzándose por encima de todo el ruido que es la red. Por un lado a compañeros del sector ambiental, forestal y bichero: @HJorvik (Pedro), @Fuegolab (Javier Madrigal), @JavierMartos99 (Javier Martos), @quecoak (Jose Luís Tomé), @BIOEAF (Eneko Arrondo), @enochmm (Enoch Martínez), @eforestal (Celso), @rescodedios (Víctor), @jgpausas (Juli), además de @AndreuEscriva (Andreu Escrivá), @maria_smur (María), @Ipathia_ (Nessa), @i_ameztoy (Iban), @txaverius (Javier Martín), @AlvaroLuna87 (Álvaro Luna), @Abies_gabriel (Gabriel), @ferrandalmau78 (Ferrán), @FenixCanarias, @WildlandFirefig (Ignacio Villaverde), @jorge_seo (Jorge Orueta), @forelenapg (Elena)… y un larguísimo etcétera. Todos vosotros con vuestros hilos. los interesantes debates y el contenido compartido me han hecho pensar, aprender, cuestionarme ideas y cambiar de opinión en determinadas ocasiones. He crecido mucho con vosotros. Incluyo también aquí al profesor Rafael Serrada por compartir su gran sabiduría forestal ya no sólo en redes, si no también material docente y libros, además de formar a muchos de los que acabaron formándome a mí. También a @gemagoldie, que, sin pertenecer a estos sectores, me ha generado las mismas sensaciones que los demás cuando interactúo con ella sobre otros temas.

A todo el equipo de Hablando de Ciencia, gracias por alojarme en esta comunidad de divulgación científica y a toda la gran labor de comunicación y sensibilización que se viene realizando con actividades enormemente enriquecedoras como Desgranando Ciencia. A Jaime de la Torre Naharro por ilustrar la portada de la tesis y los pinsapitos que decoran estos agradecimientos. Ha hecho un gran trabajo y recomiendo encarecidamente visitar su porfolio: https://www.jaimedelatorreart.com.

Primero va la ciencia, el conocimiento científico con su rigor crítico con el propósito de señalar los objetivos a cumplir para resolver los principales problemas en medio ambiente. Luego, aportar a la causa. La ciencia ha de tener vocación social, no puede limitarse a trabajar para justificarse a sí misma, tal y como nos empuja el sistema académico. Necesitamos ciencia que nos aporte conocimiento crítico y riguroso que pueda contribuir para orientar la vocación social de aquellos que persisten en tener la vista puesta en un futuro mejor. Agradecer, por tanto, a los camaradas que han servido de inspiración en este sentido: Jónathan Moriche, Javier Martínez, Xan López, Emilio Santiago Muin, Jorge Moruno, Hectór Tejero, Kate Raworth, Thomas Piketty, Yayo Herrero, al colectivo Contra el Diluvio... Y también a los antiguos compañeros que trabajaron de forma destacada tanto en Fridays For Future como en la Alianza Malagueña para la Emergencia Climática y Ecológica durante el periodo 2018-2019. Conseguimos poner la cuestión ambiental sobre la mesa, de forma repentina y con un apoyo inédito y abrumador en una ciudad como es Málaga.

Y por último agradecer a Rocío, quien es actualmente mi pareja desde 2019. Gracias por todo tu tiempo revisando mi *rusty English* en correos y cartas, por toda la compañía que me das mientras trabajo, por tu comprensión y paciencia en momentos difíciles, y por todo el torrente de cariño que recibo de ti todos los días. Espero que una vez terminada la tesis podamos marcar un nuevo hito en nuestra relación.

Gracias a todos por ser mi contexto.